Feynman integrals and the three-loop Higgs boson self-energy

JG|U

JOHANNES GUTENBERG UNIVERSITÄT MAINZ

Dissertation

zur Erlangung des Grades
„Doktor der Naturwissenschaften"
am Fachbereich Physik, Mathematik und Informatik
der Johannes Gutenberg-Universität in Mainz

Ina Hönemann

geb. in Mainz

Mainz, den 08.02.2023

Datum der mündlichen Prüfung: 11.05.2023

Hiermit versichere ich gemäß §12 Abs. 3e der Promotionsordnung des Fachbereichs 08, Physik, Mathematik und Informatik der Johannes Gutenberg-Universität Mainz vom 02.12.2013:

a) Ich habe die jetzt als Dissertation vorgelegte Arbeit selbständig verfasst. Es wurden ausschließlich die angegebenen Quellen und Hilfsmittel verwendet. Von der Ordnung zur Sicherung guter wissenschaftlicher Praxis in Forschung und Lehre und vom Verfahren zum Umgang mit wissenschaftlichem Fehlverhalten habe ich Kenntnis genommen.

b) Ich habe oder hatte die jetzt als Dissertation vorgelegte Arbeit nicht schon als Prüfungsarbeit für eine andere Prüfung eingereicht.

c) Ich hatte weder die jetzt als Dissertation vorgelegte Arbeit noch Teile davon an einer anderen Stelle als Dissertation eingereicht.

Mainz, den 08.02.2023

Ina Hönemann

Institut für Physik
Staudingerweg 7
Johannes Gutenberg-Universität D-55128 Mainz
`ihoenem@uni-mainz.de`

ZUSAMMENFASSUNG

Das Standard Modell und insbesondere die Eigenschaften des Higgs Boson auf die Probe zu stellen ist eine zentrale Aufgabe der modernen Teilchenphysik, wobei präzise theoretische Vorhersagen eine wesentliche Rolle spielen. Feynman-Integrale sind essentielle Bausteine quantenfeldtheoretischer Präzisionsberechnungen, da sie in der Berechnung höherer Ordnungen innerhalb der Störungstheorie auftreten. In dieser Arbeit behandle ich einerseits drei-Schleifen zwei-Punkt Feynman-Integrale, welche zwei unterschiedliche Massen beinhalten [1], andererseits betrachte ich eine phänomenologische Anwendung dieser Integrale[1]. Die Integrale bilden die vollständige Menge der Masterintegrale, die zu der Selbstenergie des Higgs Bosons in der Ordnung $\mathcal{O}\left(\alpha^2\alpha_s\right)$ gehören, welche W-Bosonen und Top Quarks beinhalten. Die Masterintegrale, also Basisintegrale, werden in drei Systeme aufgeteilt: Integrale relevant für Feynman-Diagramme proportional zu dem Produkt der Yukawakopplungen $y_b y_t$, Integrale relevant für Feynman-Diagramme die HW^+W^- Vertices beinhalten und Integrale relevant für Feynman-Diagramme proportional zu dem Produkt der Yukawakopplungen $y_b y_b$. Innerhalb jedes Systems entstehen unterschiedliche Wurzeln. Wir behandeln Feynman-Integrale mit der Methode der Differentialgleichungen. Wir erstellen und lösen Differentialgleichungssysteme für jedes Set von Masterintegrale, indem wir die Gleichungen in ϵ-Form bringen. Dabei konstruieren wir Integrale mit einheitlichem transzendentem Gewicht. Alle auftretenden Wurzeln werden rationalisiert und wir drücken die resultierenden Basisintegrale durch multiple Polylogarithmen aus. Das optische Theorem verknüpft den Imaginärteil der Higgs Boson Selbstenergie mit dessen Zerfallsrate. Daher haben wir alle Integrale bestimmt, die für die NNLO (next-to-next-to-leading order) QCD-elektroschwache Korrektur mit W-Bosonen oder geladenen Goldstone Bosonen zur Zerfallsrate $\Gamma\left(H \to b\bar{b}\right)$ benötigt werden.

---

[1]Noch nicht veröffentlicht.

ABSTRACT

Probing the standard model and especially properties of the Higgs boson is a central task of modern particle physics, whereby precise theoretical predictions play a crucial role. Feynman integrals are essential building blocks of quantum field theoretical precision calculations, since they emerge in higher-order calculations within perturbation theory. In this thesis, I derive three-loop two-point Feynman integrals involving two different kinds of internal masses [1] and consider a phenomenological application of them[2]. These Feynman integrals amount to the full set of master integrals associated to the Higgs boson self-energy at $\mathcal{O}\left(\alpha^2 \alpha_s\right)$ with internal W-bosons and top quarks. The master integrals, i.e. basis integrals, are split into three systems: Integrals relevant to the Feynman diagrams proportional to the product of Yukawa couplings $y_b y_t$, integrals relevant to Feynman diagrams containing an HW^+W^- vertex and integrals relevant to the Feynman diagrams proportional to the product of Yukawa couplings $y_b y_b$. Each system gives rise to different combinations of square roots. We handle the Feynman integrals with the method of differential equations. We set up and solve systems of differential equations for each set of master integrals by transforming to an ϵ-form. We thereby construct Feynman integrals of uniform weight. All emerging square roots are rationalised and we express the resulting basis integrals in terms of multiple polylogarithms. The optical theorem links the imaginary part of the Higgs boson self-energy directly to its decay rate. We therefore determined all integrals required for the NNLO (next-to-next-to-leading order) QCD-electroweak correction involving W-bosons or charged Goldstone bosons to the decay rate $\Gamma\left(H \rightarrow b\bar{b}\right)$.

---

[2]Not yet published.

CONTENTS

LIST OF FIGURES

LIST OF BOXES

INTRODUCTION

The journey of particle physics started in ancient times. Already during the 5th century BC, Demokrit postulated atoms as fundamental building blocks of everything. In the beginning of the 19th century, this hypothesis was reinforced by Dalton's atomic theory, which states that elements are made from inseparable atoms. The discovery of electrons and protons in the 19th and 20th century uncovered an even deeper structure of matter. The prediction [2, 3] as well as the experimental proof [4, 5] of the existence of quarks in the second half of the 20th century led the way to our modern understanding of the constituents of nature. Today, strong, weak and electromagnetic interactions are united within a quantum field theory with

$$SU(3)_c \times SU(2) \times U(1)_Y,$$

as underlying gauge groups: *The Standard Model of particle physics*. Solely one fundamental force, namely gravity is described through classical general relativity instead. The Standard Model is an extraordinarily successful theory, even though it has limitations, like not incorporating gravity, dark matter and dark energy. However, phenomena like the baryon asymmetry problem or the neutrino oscillations as well as recent measurements regarding the muon's anomalous magnetic moment [6] or the W-boson mass [7][1] hint at physics beyond the Standard Model.

The Standard Model consists of fermions, divided into leptons and quarks, and bosons, i.e. gauge bosons and the scalar Higgs boson. Gauge bosons are force carriers of the fundamental interactions. *The Higgs boson* plays a special role. The Higgs field has a non-zero vacuum expectation value, giving mass to fermions and the W and Z gauge bosons through spontaneous symmetry breaking. Postulated in 1964 [9], the Higgs boson was finally discovered in 2012 by ATLAS [10] and CMS [11], completing the mathematical theory of the Standard Model. Consequently, Higgs precision physics became the centrepiece of the experimental LHC program. Furthermore, future colliders like the high-luminosity (HL-)LHC [12], the ILC [13, 14] or the FCC-hh [15] will enable groundbreaking experimental work. However, only the interplay between precision measurements and precise theoretical predictions drives the the development of particle physics forward. Accurate predictions of Standard Model attributes and studying in

---

[1]In disagreement with other measurements [8].

particular the properties of the Higgs boson are the foundation for future experimental efforts [16–20].

A way to handle quantum field theories describing interactions is perturbation theory, where solutions are expressed as power series in coupling constants. Precise theoretical predictions require higher-order calculations in perturbation theory. The essential theoretical building block of measurable cross sections or decay rates are scattering amplitudes. A scattering amplitude corresponds to a sum over *Feynman diagrams*. These diagrams, developed by Richard Feynman [21, 22] and interpreted by Freeman Dyson [23, 24], are pictorial representations of particle interactions. Whereas the lowest order in perturbation theory is usually represented by tree-level diagrams, higher orders require the derivation of Feynman diagrams involving internal loops. The translation of loop diagrams into mathematical expressions leads to *Feynman integrals*; they are integrals over the momenta flowing inside the loops. Feynman integrals are therefore essential building blocks of quantum field theoretical precision calculations. Understanding and deriving them enables not only the evaluation of measurable quantities, but provides insights into their underlying mathematical structures. It comes as no surprise that Feynman integrals are an interesting topic of active research.

The complexity of Feynman integrals depends on two main aspects: The number of loops, which corresponds directly to the order in perturbation theory; and the number of kinematic variables defined by external kinematics and the masses of internal particles. Beyond one-loop advanced solution methods are crucial. A set of Feynman integrals may be reduced to a basis with the help of integration by parts relations [25, 26]. The basis integrals are called master integrals. The standard method for the analytic calculation of master integrals is *the method of differential equations* [27–30], which requires the construction and solution of their system of differential equations with respect to kinematic variables. The ϵ-form of differential equations [31] thereby simplifies the evaluation of Feynman integrals as expansions in the dimensional regularisation parameter ϵ drastically. In this context, an important and well understood class of functions are multiple polylogarithms [32–34]. For specific values of the arguments, they evaluate to multiple zeta values. There exist Feynman integrals that are not expressible in terms of multiple polylogarithms, like elliptic Feynman integrals (see for example [35–44]). However, in this thesis we are able to express all results in terms of multiple polylogarithms. Hence, we do not address other classes of Feynman integrals.

The main work of this thesis is the derivation of Feynman integrals corresponding to the three-loop Higgs boson self-energy involving internal W-boson and top-quark propagators. Not only three loop integrations, but also two different kinds of internal masses are involved. Hence, these integrals are an intricate contribution to the Higgs boson self-energy. The Higgs boson self-energy is a key ingredient for many Standard Model observables. It enters the Higgs mass definition via renormalisation. In addition to the derivation of the master integrals, we address one of their phenomenological applications: the Higgs boson decay rate of its predominant decay mode $\Gamma\left(H \to b\bar{b}\right)$, which is linked to the imaginary part of the self-energy via the optical theorem. The determination of the three-loop Feynman integrals enables the analytic evaluation of the mixed

QCD-electroweak correction to $\Gamma\left(H \to b\bar{b}\right)$. Previously, this computation was not accomplished analytically but only with the help of Padé approximations [45].

We start this thesis with a review of some important properties of the Standard Model in chapter 2 and a detailed discussion about Feynman integrals evaluating to multiple polylogarithms in chapter 3. Sections 2.1, 2.2 will clarify the emergence of Feynman diagrams and section 3.1 the ensuing emergence of Feynman integrals within precision calculations. Section 2.3 and section 3.1-3.3 deal with the structure and basic properties of Feynman integrals. The method of differential equations is elaborated in sections 3.5 and 3.6. It builds upon the techniques considered in sections 3.3 and 3.4.

The foundations covered in these two chapters allow us to formulate a strategy for the evaluation of the master integrals as well as for the calculation of the decay rate, which is sketched in chapter 4. Chapter 4 serves equally as guide and framework for this thesis: As guide, it helps locating sections on specific topics and connects sections on theoretical background to sections on calculations. As framework it clarifies the overall workflow of this thesis as well as the positioning of each section within the workflow. Furthermore, we specify the content of each chapter and required sections on theoretical background at the beginning of each chapter.

In chapter 5, the full set of master integrals for the three-loop Higgs boson self-energy involving internal W-boson and top-quarks is derived. We generate pre-canonical master integrals and construct their system of differential equations with respect to kinematic variables in section 5.3. In section 5.4, we transform the master integrals to a basis of Feynman integrals with uniform transcendental weight zero. This builds upon section 5.2, which introduces so-called auxiliary topologies enabling the utilisation of maximal cuts in Baikov representation. We demonstrate in section 5.4.4 that maximal cuts are an essential tool for the derivation of Feynman integrals with uniform weight zero. The variable transformation in section 5.5.1 allows to represent the system of differential equations via differential one-forms (section 5.5.2). After evaluating boundary values in section 5.5.3, the found basis integrals (section 5.5) are expressible in terms of multiple polylogarithms, as described in section 5.5.4.

In chapter 6, we consider the mixed QCD-electroweak correction to the Higgs boson decay rate into a bottom-quark pair. Chapter 6 presents the evaluation of scattering amplitudes and Feynman diagrams in quantum field theoretical calculations up to the point where Feynman integrals enter the game. We demonstrate the application of the optical theorem in section 6.2 and the translation of Feynman diagrams to mathematical expressions in sections 6.3, 6.4. Furthermore, we address the handling of divergences in section 6.5. Eventually, the diagrams depend on the three-loop Feynman integrals evaluated in chapter 5. We close this thesis with final conclusions in chapter 7.

THE STANDARD MODEL OF PARTICLE PHYSICS

Particle physics deals with the most fundamental particles and their interactions. Three out of the four fundamental forces of nature the strong, the weak and the electromagnetic interaction are united within the Standard Model of particle physics. The Standard Model is, therefore, one of the most successful theories of physics. It is based on quantum field theory, a formalism combining classical field theory, quantum mechanics and relativity. Its defining element is a Lagrangian (or Hamiltonian), which may be separated into a part describing free fields $\mathcal{L}_0 \left(\mathcal{H}_0 \right)$ and a part consisting of non-linear terms accounting for interactions $\mathcal{L}_{int} \left(\mathcal{H}_{int} \right)$,

$$\mathcal{L} = \mathcal{L}_0 + \mathcal{L}_{int},$$
$$\mathcal{H} = \mathcal{H}_0 + \mathcal{H}_{int},$$
$$\mathcal{H}_{int} = -\mathcal{L}_{int}.$$

More details on the Standard Model Lagrangian will be given in section 2.2. Field equations can be derived from the Lagrangian, utilising Hamilton's principle of least action which leads to the Euler-Lagrange equations. However, nonlinear field equations arising out of interacting parts are not solvable beyond two space-time dimensions (except in some special cases) [46]. A physical four space-time dimensional quantum field theory describing interactions is not exactly solvable by currently known methods! An important method addressing this issue is perturbation theory. The interacting parts of a Hamiltonian are proportional to coupling constants,

$$\mathcal{H}_{int} = \lambda \mathcal{H}'_{int}.$$

If λ is sufficiently small, the interacting part can be viewed as a small perturbation relative to the free part $\mathcal{H}_0$ and expansions with respect to λ yield practical series approximations. The perturbative series has even a pictorial representation in terms of Feynman graphs.

This chapter provides by no means a somewhat complete overview of the Standard Model of particle physics, but just a slight insight. For more details we refer to the main references of this chapter [46–50]. We only address topics relevant for our purposes. Along that line, we briefly introduce the scattering matrix and the decay rate

in the following section. We derive the optical theorem in section 2.1.1. In section 2.2, we discuss the Standard Model Lagrangian, which leads to Feynman rules listed in section 2.2.1. The last section of this chapter explains the necessity of regularisation and introduces the dimensional regularisation parameter ϵ. The next chapter provides a theoretical background of the main subject of this thesis, Feynman integrals.

2.1 The scattering matrix

In this thesis we are dealing with Feynman diagrams and the integrals arising therefrom. In this section we define the object, which is calculated by a sum of Feynman diagrams expressed through Feynman rules: the scattering amplitude, which emerges out of the scattering or S-matrix. The S-matrix is a key object within quantum field theories describing interactions. It encapsulates all information about the evolution of states in time. The S-matrix is a rather abstract object. However, we may relate it to quantities, which are actually measurable in scattering experiments.

Before we define the S-matrix, we recall from quantum field theory: States, which may be represented by wave packets, are just mathematical objects. Physical quantities are given by the expectation values of operators. Consequently, states can be considered within different pictures. A state in Schrödinger picture is time-dependent,

$$|X, t\rangle = \exp\left(-i\hat{H}(t - t_0)\right)|X, t_0\rangle, \tag{2.1}$$

where

$$\hat{H} = \int d^3x\, \mathcal{H}.$$

The norm of a state is always time-independent,

$$\langle a, 0|a, 0\rangle \overset{!}{=} \langle a, t \neq 0|a, t \neq 0\rangle \overset{(2.1)}{\Leftrightarrow} \langle a, 0|a, 0\rangle \overset{!}{=} e^{i(H^\dagger - H)t}\langle a|a\rangle \Rightarrow H = H^\dagger.$$

An important property of $\hat{H}$ follows, it has to be hermitian. We may transfer from Schrödinger picture to Heisenberg picture, where the time-dependence is shifted to operators, via

$$|X\rangle = \exp\left(i\hat{H}(t - t_0)\right)|X, t\rangle. \tag{2.2}$$

The **scattering matrix** transfers states into each other. Assuming interactions happen within a finite time, we may consider an initial state constructed in the far past $|i, -\infty\rangle$ evolving into a final state in the far future $\langle f, \infty|$, and define the scattering matrix S by

$$\langle f| S |i\rangle = \langle f, \infty|i, -\infty\rangle = \lim_{T \to \infty} \langle f, T|i, -T\rangle \overset{(2.2)}{=} \lim_{T \to \infty} \langle f| \exp\left(-i\hat{H}(2T)\right)|i\rangle$$

$$\Rightarrow S = \lim_{T \to \infty} \exp\left(-i\hat{H}(2T)\right). \tag{2.3}$$

The S-matrix is unitary

$$S^\dagger S = \mathbb{1},$$

because $\hat{H}$ is hermitian. The scattering matrix can be related to Green functions. The n-point Green function is defined by

$$G_n(x_1, \ldots, x_n) = \langle \Omega | \, \mathrm{T}\Phi(x_1) \ldots \Phi(x_n) \, | \Omega \rangle, \tag{2.4}$$

with $|\Omega\rangle$ being the ground state of the full theory and T the time-ordering operator. Wicks theorem states that (2.4) is given by the sum of all Feynman diagrams with n external particles, excluding diagrams which are disconnected from all external points [47].

The S-matrix can be separated into a non-interaction part, i.e. $\mathbb{1}$ and a part describing interactions, the so-called transfer matrix T,

$$S = \mathbb{1} + iT. \tag{2.5}$$

The matrix element of T between a final $|f\rangle$ and an initial state $|i\rangle$,

$$\langle f | \, T \, | i \rangle = (2\pi)^4 \delta^4(p_i - p_f) \mathcal{A}(i \to f), \tag{2.6}$$

consists of an overall momentum conservation $p_i \overset{!}{=} p_f$ and the **scattering amplitude**

$$\mathcal{A}(i \to f). \tag{2.7}$$

The scattering amplitude is given by the truncated n-point Green function in momentum space. Consequently, we calculate it as we sum up all contributing Feynman diagrams in the respective orders in coupling constants. Feynman diagrams are then evaluated through Feynman rules (see section 2.2.1).

The S-matrix and therefore the scattering amplitude is the building block needed to theoretically calculate measurable quantities from scattering experiments. An important measurable quantity is the cross section. It is intrinsic to the colliding particles under consideration and related to the likelihood of a particular final state. It can be calculated through phase space integration over squared scattering amplitudes. In this thesis, we consider another measurable quantity, the decay rate. **The decay rate** Γ of an unstable particle A is defined as [47]

$$\Gamma = \frac{\text{Number of decays per unit time}}{\text{Number of A particles present}}.$$

More formally it can be shown, that the decay rate of a one-particle state $|A\rangle$ to a state $|X\rangle$ is given by

$$\Gamma(A \to X) = \frac{1}{2m_A} \int d\varphi^{(X)} (2\pi)^4 \delta^4(p_A - p_X) |\mathcal{A}(A \to X)|^2, \tag{2.8}$$

with m_A being the mass of particle A and

$$d\varphi^{(X)} = \prod_{i \in X} \frac{d^3 p_i}{(2\pi)^3 2E_i} \tag{2.9}$$

the phase space integration measure. The lifetime of a particle is the inverse of its total decay rate, i.e. the sum of its decay rates into all possible final states.

2.1.1 The optical theorem

The optical theorem relates cross sections or decay rates, to the imaginary part of forward scattering amplitudes. It thereby creates an alternative theoretical approach to the calculation of measurable cross sections and decay rates. In this section, we derive a version of the optical theorem addressing decay rates as required in this thesis (see chapter 6) (cf.[48]).

The optical theorem is based on the unitarity of the S-matrix, we encountered in section 2.1,

$$S^\dagger S = \mathbb{1}. \tag{2.10}$$

The unitarity of the S-matrix leads to a relation between transfer matrix elements. Inserting (2.5) into (2.10) and embedding the outcome between final and initial state, we find

$$S^\dagger S = \mathbb{1} \overset{(2.5)}{\Leftrightarrow} (\mathbb{1} - iT^\dagger)(\mathbb{1} + iT) = \mathbb{1} \Leftrightarrow i(T^\dagger - T) = T^\dagger T$$
$$\Rightarrow \langle f | i(T^\dagger - T) | i \rangle = \langle f | T^\dagger T | i \rangle. \tag{2.11}$$

The matrix element on the left hand side of (2.11) is given by

$$\langle f | i(T^\dagger - T) | i \rangle \overset{(2.6)}{=} i(2\pi)^4 \delta^4(p_i - p_f) \Big[\mathcal{A}^\dagger(i \to f) - \mathcal{A}(i \to f) \Big].$$

Into the right hand side of (2.11), we may insert a resolution of identity in terms of a complete set of states $|X\rangle$ and find

$$\langle f | T^\dagger T | i \rangle = \langle f | T^\dagger \mathbb{1} T | i \rangle = \sum_X \int d\varphi^{(X)} \langle f | T^\dagger | X \rangle \langle X | T | i \rangle$$
$$\overset{(2.6)}{=} (2\pi)^8 \sum_X \int d\varphi^{(X)} \delta^4(p_i - p_X) \delta^4(p_X - p_f) \mathcal{A}^\dagger(X \to f) \mathcal{A}(i \to X).$$

Consequently, **the generalised optical theorem** emerges out of (2.11) expressed in terms of matrix elements of M via (2.6),

$$\mathcal{A}^\dagger(i \to f) - \mathcal{A}(i \to f) = -i(2\pi)^4 \sum_X \int d\varphi^{(X)} \delta^4(p_i - p_X) \mathcal{A}^\dagger(X \to f) \mathcal{A}(i \to X). \tag{2.12}$$

The generalised optical theorem relates the difference of a matrix element between final and initial state and its adjoint on the left hand side to a momentum conservation and a product of matrix elements on the right hand side. Additionally, the right hand side is summed over all possible intermediate states X and integrated over phase space (2.9). The right hand side is quadratic in matrix elements, contrary to the left hand side. Furthermore, (2.12) has to hold for any order in perturbation theory. Implying, for example, that tree level matrix elements on the right hand side correspond to one-loop level elements on the left hand side.

A case significant for this thesis occurs if initial and final state are given by the same one-particle state $|A\rangle$. Replacing initial and final state in (2.12) with $|A\rangle$, we obtain

$$\underbrace{\mathcal{A}^\dagger(A \to A) - \mathcal{A}(A \to A)}_{=-2i\mathrm{Im}(\mathcal{A}(A \to A))} = -i(2\pi)^4 \sum_X \int d\varphi^{(X)} \delta^4(p_A - p_X) \underbrace{\mathcal{A}^\dagger(X \to A)\mathcal{A}(A \to X)}_{=|\mathcal{A}(A \to X)|^2}$$

$$\Leftrightarrow \mathrm{Im}(\mathcal{A}(A \to A)) = \frac{1}{2}(2\pi)^4 \sum_X \int d\varphi^{(X)} \delta^4(p_A - p_X)|\mathcal{A}(A \to X)|^2. \qquad (2.13)$$

We immediately recognise the decay rate of a one-particle state $|A\rangle$ to a state $|X\rangle$,

$$\Gamma(A \to X) = \frac{1}{2m_A} \int d\varphi^{(X)} (2\pi)^4 \delta^4(p_A - p_X)|\mathcal{A}(A \to X)|^2, \qquad (2.14)$$

with m_A being the mass of particle A. The decay rate is proportional to a phase space integral over the matrix element squared, the same holds for the imaginary part of the two-point amplitude in (2.13). Hence, combining (2.13) and (2.14) relates the imaginary part of the two-point function of particle A to the sum over its decay rates, i.e. its total decay rate $\Gamma_{A,total}$,

$$\mathrm{Im}(\mathcal{A}(A \to A)) = m_A \sum_X \Gamma(A \to X) = m_A \Gamma_{A,\mathrm{total}}. \qquad (2.15)$$

This version of the **optical theorem** (2.15) is the starting point of the calculations performed in chapter 6.

2.2 The Standard Model Lagrangian

The scattering amplitude, we encountered in the preceding section $\mathcal{A}(i \to f)$, corresponds to the sum over all required Feynman diagrams. A Feynman diagram is a graph describing elementary particles. To translate Feynman diagrams into mathematical expressions, we require Feynman rules describing the propagation of particles (propagators) as well as interactions among them (vertex rules). All Feynman rules required in this thesis will be provided in section 2.2.1. The Feynman rules of a theory arise from its Lagrangian. Propagators arise from terms bilinear in the corresponding field and vertices from non-linear terms. We, therefore, start this section with a presentation of the Standard Model Lagrangian. In order to keep this presentation short, we do not describe intermediate calculations in detail. For more information we refer to [46], [49] and [50].

The underlying gauge group of the Standard Model is

$$\underbrace{SU(3)_c}_{\mathrm{QCD}} \times \underbrace{SU(2) \times U(1)_Y}_{\mathrm{electroweak\ theory}}.$$

$SU(3)_c$ gives rise to eight gauge fields G_μ^b with gauge coupling g_s. Within the quantised theory, these gauge fields correspond to gluons, the gauge bosons of quantum chromo-dynamics (QCD). The fermions participating in strong interactions are quarks. They carry colour charge c in addition to electric charge. The gauge fields of $SU(2) \times U(1)$ are W_μ^a, where $a \in \{1, 2, 3\}$, and B_μ with gauge couplings g and g'. The electric charge of fermions is $Q = I^3 + \frac{Y}{2}$. Y is the weak hypercharge. I^3 is the third of the weak isospin. $W_\mu^{a=1,2}$ are related to W-bosons, the charged mediators of weak interactions $W_\mu^\pm$, through the Weinberg transformation of gauge fields,

$$W_\mu^\pm = \frac{1}{\sqrt{2}}(W_\mu^1 \mp iW_\mu^2). \tag{2.16}$$

Additionally, we may define $I_\pm = \frac{1}{\sqrt{2}}(I^1 \pm iI^2)$ in order to obtain the equality

$$I_+W_\mu^+ + I_-W_\mu^- = I^1W_\mu^1 + I^2W_\mu^2. \tag{2.17}$$

The Standard Model Lagrangian may be decomposed into

$$\mathcal{L}_{SM} = \mathcal{L}_{Fermion} + \mathcal{L}_{Yukawa} + \mathcal{L}_{gauge} + \mathcal{L}_{Higgs} + \mathcal{L}_{fix} + \mathcal{L}_{Ghosts}. \tag{2.18}$$

$\mathcal{L}_{Fermion}$ (2.19) describes (massless) fermions and their interactions with gauge fields. Masses are obtained within $\mathcal{L}_{Yukawa}$ (2.21) as fermions couple to a field with non-zero vacuum expectation value, the Higgs field. The Higgs field, introduced in $\mathcal{L}_{Higgs}$ (2.27) causes spontaneous symmetry breaking

$$SU(2) \times U(1)_Y \to U(1)_{em},$$

and, thereby, yields masses for the vector bosons, originally constructed in $\mathcal{L}_{gauge}$ (2.26). The gauge fixing Lagrangian $\mathcal{L}_{fix}$ (2.28) and the ghost Lagrangian $\mathcal{L}_{Ghosts}$ are present if we work in general R_ξ gauge. In the following, we first combine $\mathcal{L}_{Fermion}$ and $\mathcal{L}_{Yukawa}$ to obtain a Lagrangian describing quarks and their interactions with the Higgs boson, charged W-bosons and charged Goldstone bosons. Afterwards we consider $\mathcal{L}_{gauge}$, $\mathcal{L}_{Higgs}$ and $\mathcal{L}_{fix}$, determining bosons and interactions among them. We do not need $\mathcal{L}_{Ghosts}$ here.

$\mathcal{L}_{Fermion}$ inherits the kinetic terms for fermions, including their interactions with gauge fields. We are only interested in the parts of $\mathcal{L}_{Fermion}$ describing quarks,

$$\mathcal{L}_{Fermion} = \sum_j \left(\bar{Q}_j^L i\gamma^\mu D_\mu Q_j^L + \bar{u}_j^R i\gamma^\mu D_\mu u_j^R + \bar{d}_j^R i\gamma^\mu D_\mu d_j^R \right) \tag{2.19}$$

$$+ \text{ leptonic parts.}$$

The Lagrangian inherits a sum over all three families. In correspondence, the left-handed quark field isospin doublets Q^L, and right-handed singlets q^R are

$$Q_j^L = \begin{pmatrix} u_j^L \\ d_j^L \end{pmatrix}, \ u_j = u_c, c_c, t_c, \ d_j = d_c, s_c, b_c,$$

$$q^L = \frac{1}{2}(1 - \gamma_5)q, \ q^R = \frac{1}{2}(1 + \gamma_5)q.$$

Ordinary partial derivatives account for the propagation of (massless) quarks. The covariant derivatives in (2.19) not only contain partial derivatives, but also gauge fields facilitating interactions with them. They are defined as

$$D_\mu Q^L = \left(\partial_\mu - ig T^a W^a_\mu - ig' \frac{Y}{2} B_\mu - ig_s T^b_s G^b_\mu \right) Q^L,$$

$$D_\mu q^R = \left(\partial_\mu - ig' \frac{Y}{2} B_\mu - ig_s T^b_s G^b_\mu \right) q^R,$$

with $T^b_s = \frac{\lambda^b}{2}$, $b \in \{1, ..., 8\}$, being the generators of $SU(3)_c$ represented by the Gell-Mann matrices λ_b and $T^a = \frac{\sigma^a}{2}$, $a \in \{1, 2, 3\}$, being the generators of $SU(2)$ represented by Pauli matrices σ_a.

The gauge bosons we encounter in this thesis are gluons and charged W-bosons. Whereas interactions of quarks with gluons G^b_μ arise more or less straightforwardly from the covariant derivative in $\mathcal{L}_{Fermion}$, we need to perform the Weinberg transformation (2.16) to find interactions with W-bosons. These correspond to the part of $\mathcal{L}_{Fermion}$ (2.19) containing charged currents. Performing the Weinberg transformation (2.16), using (2.17) and bringing the quarks into their mass basis, we find

$$(2.19) \stackrel{\text{basis change}}{\Rightarrow} \mathcal{L}^{CC}_{quarks} = \frac{g}{2\sqrt{2}} \left(\bar{d}, \bar{s}, \bar{b} \right) \gamma^\mu (1 - \gamma_5) V^\dagger \left(u, c, t \right)^T W^-_\mu$$

$$+ \frac{g}{2\sqrt{2}} \left(\bar{u}, \bar{c}, \bar{t} \right) \gamma^\mu (1 - \gamma_5) V \left(d, s, b \right)^T W^+_\mu. \qquad (2.20)$$

The coupling of quarks to W-bosons becomes off-diagonal, with V being the Cabibbo–Kobayashi–Maskawa-matrix (CKM-matrix).

To complete interactions of quarks and derive their mass terms, we introduce the complex Higgs doublet

$$\Phi(x) = \begin{pmatrix} \Phi^+(x) \\ \Phi^0(x) \end{pmatrix} = \begin{pmatrix} \Phi^+(x) \\ \frac{1}{\sqrt{2}}(v + H(x) + i\chi(x)) \end{pmatrix},$$

$$\Phi^\dagger(x) = \begin{pmatrix} \Phi^-(x) \\ \Phi^{0\,*}(x) \end{pmatrix} = \begin{pmatrix} \Phi^-(x) \\ \frac{1}{\sqrt{2}}(v + H(x) - i\chi(x)) \end{pmatrix},$$

with non-zero vacuum expectation value $v = 2\frac{m_W}{g}$. Quarks couple to the complex Higgs doublet via

$$\mathcal{L}_{Yukawa} = \sum_{jk} - \left[(\bar{u}_j, \bar{d}_j)^L \left(c^{(d)}_{jk} \begin{pmatrix} \Phi^+ \\ \Phi^0 \end{pmatrix} d^R_k + c^{(u)}_{jk} \begin{pmatrix} \Phi^{0*} \\ -\Phi^- \end{pmatrix} u^R_k \right) \right] + \text{h.c.} \qquad (2.21)$$

$$+ \text{ leptonic parts.}$$

We may diagonalise the coupling matrices $c^{(q)}$ within $\mathcal{L}_{Yukawa}$ (2.21) and shift the variables respectively, i.e. we bring the quarks into their mass basis. Finally, we obtain

mass terms for the quarks as well as interaction terms with the Higgs boson H from $\mathcal{L}_{Yukawa}$

$$(2.21) \overset{\text{basis change}}{\Rightarrow} \mathcal{L}_{Yukawa}^{Higgs-quarks} = - \left(1 + \frac{gH}{2m_W} \right) \sum_j \left[\bar{u}_j m_{u_j} u_j + \bar{d}_j m_{d_j} d_j \right]. \quad (2.22)$$

Furthermore, another off-diagonal coupling arises in the Yukawa Lagrangian (2.21), the coupling of quarks to charged Goldstone bosons Φ^+, Φ^-.

$$(2.21) \overset{\text{basis change}}{\Rightarrow}$$

$$\mathcal{L}_{Yukawa}^{ch.GB.-quarks} = \frac{g}{2\sqrt{2}} \Big[\Phi^+ \left((1 + \gamma_5) \frac{m_{d_j}}{m_W} - (1 - \gamma_5) \frac{m_{u_i}}{m_W} \right) \bar{u}_i V_{ij} d_j$$

$$+ \Phi^- \left((1 - \gamma_5) \frac{m_{d_j}}{m_W} - (1 + \gamma_5) \frac{m_{u_i}}{m_W} \right) u_i V_{ij}^* \bar{d}_j \Big], \quad (2.23)$$

with mass matrices $M_u = diag(m_u, m_c, m_t)$, $M_d = diag(m_d, m_s, m_b)$.

Collecting the first part of (2.19), as well as (2.22), (2.20) and (2.23) adds up to a Lagrangian, which describes quarks and their interactions needed for the calculation performed in this thesis,

$$\underbrace{\mathcal{L}_{Fermion} + \mathcal{L}_{Yukawa}^{Higgs-quarks}}$$
$$\downarrow$$

$$\mathcal{L}_{quarks} \equiv \bar{q} \left(i\gamma^\mu D_\mu - m_q \left(1 + \frac{gH}{2m_W} \right) \right) q + \mathcal{L}_{quarks}^{CC} + \mathcal{L}_{Yukawa}^{ch.GB.-quarks}$$

$$= \underbrace{\bar{q} \left(i\gamma^\mu \partial_\mu - m_q \right) q}_{\rightarrow \text{quark propagator}} \underbrace{-g_s \bar{q} \left(\gamma^\mu G_\mu^a T^a \right) q}_{\text{interaction with gluon}} \underbrace{- \frac{gm_q}{2m_W} H \bar{q} q}_{\text{interaction with Higgs}}$$

$$+ \underbrace{\frac{g}{2\sqrt{2}} \Big[\gamma^\mu (1 - \gamma_5) \left(u_i V_{ij}^* \bar{d}_j W_\mu^- + \bar{u}_i V_{ij} d_j W_\mu^+ \right)}_{\text{interaction with W-bosons}}$$

$$+ \Phi^+ \left((1 + \gamma_5) \frac{m_{d_j}}{m_W} - (1 - \gamma_5) \frac{m_{u_i}}{m_W} \right) \bar{u}_i V_{ij} d_j$$

$$+ \underbrace{\Phi^- \left((1 - \gamma_5) \frac{m_{d_j}}{m_W} - (1 + \gamma_5) \frac{m_{u_i}}{m_W} \right) u_i V_{ij}^* \bar{d}_j \Big].}_{\text{interactions with Goldstone bosons}} \quad (2.24)$$

We deduce, the Feynman rules of the quark propagator and the interaction vertices with a gluon, Higgs boson, W-boson as well as with the charged Goldstone bosons can be obtained from $\mathcal{L}_{quarks}$ (2.24). They will be listed in section 2.2.1. To give an example, we explicitly construct the quark propagator from

$$\mathcal{L}_{quarks} \rightarrow \bar{q} \underbrace{(i\gamma^\mu \partial_\mu - m_q)}_{\equiv P(x)} q. \quad (2.25)$$

The desired propagator in momentum space is given by the Fourier transform of the inverse of $P(x)$ times i, where the inverse is defined by

$$\sum_j P_{ij}(x)P_{jk}^{-1}(x-y) = \delta_{ik}\delta^4(x-y),$$

and its Fourier transform by

$$P_{jk}^{-1}(x-y) = \int \frac{d^4k}{(2\pi)^4}e^{-ik.x}\tilde{P}_{jk}^{-1}(k).$$

We construct

$$P(x)\int \frac{d^4k}{(2\pi)^4}e^{-ik.x}\tilde{P}^{-1}(k) \overset{!}{=} \int \frac{d^4k}{(2\pi)^4}e^{-ik.x},$$

$$\Leftrightarrow \int \frac{d^4k}{(2\pi)^4}(\slashed{k}-m_q)\,e^{-ik.x}\tilde{P}^{-1}(k) \overset{!}{=} \int \frac{d^4k}{(2\pi)^4}e^{-ik.x}, \quad (\slashed{k}=\gamma_\mu k^\mu),$$

$$\Rightarrow (\slashed{k}-m_q)\,\tilde{P}^{-1}(k) = 1,$$

$$\overset{\cdot(\slashed{k}+m_q)}{\Leftrightarrow} \tilde{P}^{-1}(k) = \frac{\slashed{k}+m_q}{k^2-m_q^2}.$$

The quark propagator follows,

$$i\frac{\slashed{k}+m_q}{k^2-m_q^2}.$$

We return to the Standard Model Lagrangian: The gauge field Lagrangian

$$\mathcal{L}_{gauge} = -\frac{1}{4}(\partial_\mu G_\nu^b - \partial_\nu G_\mu^b + g_s f^{bcd}G_\mu^c G_\nu^d)^2 - \frac{1}{4}(\partial_\mu W_\nu^a - \partial_\nu W_\mu^a + g\epsilon^{abc}W_\mu^b W_\nu^c)^2$$
$$-\frac{1}{4}(\partial_\mu B_\nu - \partial_\nu B_\mu)^2, \tag{2.26}$$

with transformations (2.16) and

$$\begin{pmatrix} B_\mu \\ W_\mu^3 \end{pmatrix} = \begin{pmatrix} \cos(\Theta_W) & -\sin(\Theta_W) \\ \sin(\Theta_W) & \cos(\Theta_W) \end{pmatrix}\begin{pmatrix} A_\mu \\ Z_\mu \end{pmatrix},$$

and the Higgs Lagrangian

$$\mathcal{L}_{Higgs} = (D_\mu\Phi)^\dagger(D_\mu\Phi) - \frac{\lambda}{4}(|\Phi|^2)^2 + \mu^2|\Phi|^2, \tag{2.27}$$

with

$$D_\mu\Phi = (\partial_\mu - igT^a W_\mu^a - ig'\frac{Y}{2}B_\mu)\Phi,$$

and furthermore the gauge fixing Lagrangian in R_ξ-gauges

$$\mathcal{L}_{fix} = -\frac{1}{2\xi_g}(\partial^\mu G_\mu^b)^2 - \frac{1}{2\xi_A}(\partial^\mu A_\mu)^2 - \frac{1}{2\xi_Z}(\partial^\mu Z_\mu - \xi_Z m_Z \chi)^2$$
$$-\frac{1}{\xi_W}(\partial^\mu W_\mu^+ - i\xi_W m_W \Phi^+)(\partial^\mu W_\mu^- + i\xi_W m_W \Phi^-), \tag{2.28}$$

13

give rise to boson propagators as well as interactions among them. We will not go into details here. However, we note that as above the Weinberg transformation of gauge fields (2.16) has to be performed. Afterwards, we uncover that the Higgs Lagrangian produces mass terms for the gauge bosons

$$(D_\mu\Phi)^\dagger(D_\mu\Phi) \to m_W^2 W_\mu^+ W^{-\mu} + \frac{1}{2}m_Z^2 Z_\mu Z^\mu,$$
$$m_Z = \frac{v}{2}\sqrt{g^2 + g'^2},\ m_W = g\frac{v}{2},\ m_A = 0.$$

Furthermore, the gauge fixing Lagrangian cancels mixed quadratic terms involving a gauge and a Goldstone field appearing in $\mathcal{L}_{Higgs}$ (2.27) at the cost of adding terms proportional to gauge fixing parameters ξ_A, ξ_Z, ξ_W,

$$\begin{aligned}
\mathcal{L}'_{fix} =& \mathcal{L}_{fix} + \text{mixed quadratic terms in } \mathcal{L}_{Higgs} \\
=& -\frac{1}{2\xi_g}(\partial^\mu G_\mu^a)^2 - \frac{1}{2\xi_A}(\partial^\mu A_\mu)^2 \\
& -\frac{1}{2\xi_Z}((\partial^\mu Z_\mu)^2 + (\xi_Z m_Z \chi)^2) - \frac{1}{\xi_W}(\partial^\mu W_\mu^- \partial^\mu W_\mu^+ + \xi_W^2 m_W^2 \Phi^- \Phi^+).
\end{aligned}$$

After inspecting the Standard Model Lagrangian, we are able to obtain all Feynman rules required in this thesis. They are listed in the following subsection.

2.2.1 Feynman rules

In this subsection, we list the Feynman rules obtainable from the Standard Model Lagrangian (2.18) discussed above. Feynman rules enable the translation of Feynman diagrams into mathematical expressions and therefore the calculation of scattering amplitudes. A Feynman diagram is a graph describing the propagation and interaction of elementary particles. A graph consists of edges connecting vertices. An edge is drawn as a line. The edge of a Feynman graph represents a propagating particle, hence, it carries its mass and momentum. Strictly speaking, also vertices only attached to one edge (external vertices) and vertices attached to two edges (dots) are vertices of a graph. Usually, we only call internal vertices connecting at least three edges "vertex", since those represent the interaction among particles. Feynman diagrams are translated into mathematical expressions as edges and vertices are expressed in Feynman rules. Correspondingly, each edge is associated with one propagator obtained from Feynman rules and each vertex with a vertex rule proportional to a coupling constant. In addition every vertex must obey momentum conservation. In this thesis we are dealing with Feynman diagrams containing closed loops as we consider higher orders in perturbation theory. These loops require special attention since they carry momenta, which are not determined by momentum conservation. Hence, these momenta are understood as integration variables. In this way Feynman integrals enter the game. We will discuss them in chapter 3. Note, within the context of Feynman rules the phrase "propagator" refers to the complete mathematical expression of an edge, whereas in the context of Feynman integrals (section 3.1) it solely refers to the part in the denominator.

In addition to the translation of edges and vertices the following rules have to be taken into account:

1) Momentum conservation at each vertex must hold.

2) There must be an integration over each loop-momentum k, i.e. each undetermined momentum,

$$\int \frac{d^D k}{(2\pi)^D}. \tag{2.29}$$

3) For each closed fermion loop an additional factor of (-1) appears and the trace has to be taken.

In (2.29) we consider a D-dimensional loop momentum as opposed to the physical four space-time dimensions. The shift to general D dimensions will be explained and verified in section 2.3. Now, we list all propagators and vertex-rules required in this thesis, they agree with the Feynman rules and conventions of [46–50] (for an overview on Feynman rules and sign conventions see [51]). For definitions/notations we refer to the preceding section.

Propagators:

- **The quark propagator** for a quark with momentum k and mass m_q,

$$i \frac{\not{k} + m_q}{k^2 - m_q^2}$$

- **The gluon propagator:**

$$\frac{i}{k^2} \left(-g^{\mu\nu} + (1 - \xi_g) \frac{k^\mu k^\nu}{k^2} \right) \delta_{ab}$$

- **The W-boson propagator:**

$$\frac{i}{k^2 - m_W^2} \left(-g^{\mu\nu} + (1 - \xi_W) \frac{k^\mu k^\nu}{k^2 - \xi_W m_W^2} \right)$$

- **The Goldstone-boson propagator:**
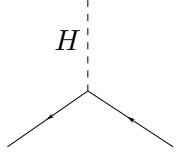
$$\frac{i}{k^2 - \xi_W m_W^2}$$

Vertex-rules:

- A gluon g and two quarks:

$$ig_s \gamma^\mu T^b_{s_{ij}} , \quad T^b_s = \frac{\lambda^b}{2}$$

15
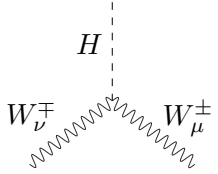
- A Higgs boson H and two quarks:
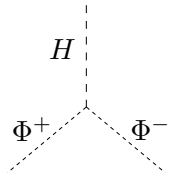
$$-i\frac{gm_q}{2m_W}$$

- A Higgs boson H and two W-bosons
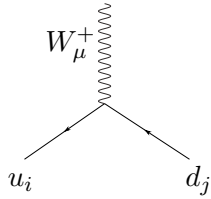
$$igm_W g^{\mu\nu}$$

- A Higgs boson H and two Goldstone-bosons
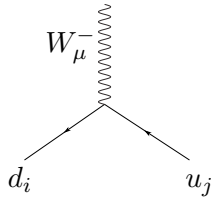
$$-i\frac{g}{2}\frac{m_H^2}{m_W}$$

- A W-boson $W^{+/-}$ and two quarks:
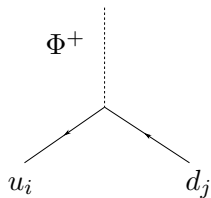
$$i\frac{g}{\sqrt{2}}\gamma^\mu\frac{1-\gamma_5}{2}V_{ij}$$
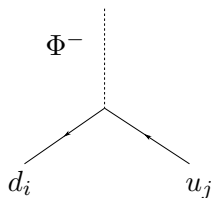
$$i\frac{g}{\sqrt{2}}\gamma^\mu\frac{1-\gamma_5}{2}V_{ji}^*$$

- A charged Goldstone-boson $\Phi^{+/-}$ and two quarks:

$$i\frac{g}{2\sqrt{2}}\left[(1+\gamma_5)\frac{m_{d_j}}{m_W}-(1-\gamma_5)\frac{m_{u_i}}{m_W}\right]V_{ij}$$

$$i\frac{g}{2\sqrt{2}}\left[(1-\gamma_5)\frac{m_{d_j}}{m_W}-(1+\gamma_5)\frac{m_{u_i}}{m_W}\right]V_{ji}^*$$

16

2.3 Divergences in quantum field theories

Now, we established how amplitudes are given by sums of Feynman diagrams, which may be expressed via Feynman rules. In this thesis we are interested in higher perturbative orders and, hence, in Feynman diagrams with loops. A certain Feynman rule deals with the emergence of loops: Undetermined loop momenta k must be integrated over $\frac{d^4k}{(2\pi)^4}$ (see (2.29)). A physical momentum has four dimensions, one time and three space dimensions. We have already mentioned how the physical four dimensions may be modified to general D dimensions, demanding us to take an integration measure $\frac{d^Dk}{(2\pi)^D}$ for every loop momentum. In the following we will provide an explanation for this procedure, known as dimensional regularisation. Dimensional regularisation [52–54] handles integrals which are divergent in four-dimensional space-time, through the modification of space-time itself.

We provide two examples to motivate regularisation given by the easiest types of Feynman diagrams with loops. Both of them will be investigated more carefully in section 3.2. For now we may take results thereof. The simplest example of a loop diagram is the one-loop tadpole diagram shown in fig.2.1. The tadpole diagram represents a single loop given by a single propagator without external influences. We may express it in the physical four-dimensional case by
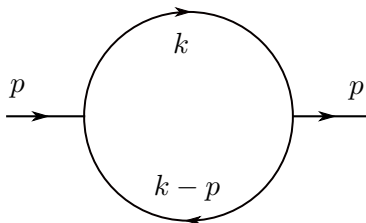
$$\sim \int \frac{d^4k}{(2\pi)^4} \frac{1}{(k^2 - m^2)^\nu}.$$

Figure 2.1: One-loop tadpole diagram.

k denotes the loop momentum and m the mass. We place an exponent $\nu \in \mathbb{N}$ in the denominator, whereas $\nu = 1$ gives fig.2.1, $\nu = 2$ implies an additional internal vertex attached to two edges only, i.e. a propagator with a dot, $\nu = 3$ implies two additional internal vertices, etc.

Attaching two external legs to a tadpole diagram results in the one-loop bubble diagram displayed in fig.2.2.

$$\sim \int \frac{d^4k}{(2\pi)^4} \frac{1}{(k^2)^{\nu_1} \left((k-p)^2\right)^{\nu_2}}.$$

Figure 2.2: One-loop bubble diagram.

All Feynman diagrams were created with `Inkscape` [55], unless stated otherwise.

The external momentum of the bubble diagram is denoted by p and similar to before ν_1, $\nu_2 \in \mathbb{N}$. Here, we take the bubble diagram as massless.

Now, we investigate the behaviour of both diagrams at $k^2 \to \infty$ and at $k^2 \to 0$. For large momentum the tadpole integral behaves like

$$\int \frac{d^4 k}{(2\pi)^4} \frac{1}{(k^2 - m^2)^{\nu}} \xrightarrow{k^2 \to \infty} \int \frac{d^4 k}{(2\pi)^4} \frac{1}{(k^2)^{\nu}}.$$

We see, that this integral diverges for $\nu \leq 2$. We call divergences appearing at $k^2 \to \infty$ **ultraviolet divergences**. The massless bubble diagram also develops an ultraviolet divergence if $\nu_1 + \nu_2 \leq 2$, since

$$\int \frac{d^4 k}{(2\pi)^4} \frac{1}{(k^2)^{\nu_1} ((k-p)^2)^{\nu_2}} \xrightarrow{k^2 \to \infty} \int \frac{d^4 k}{(2\pi)^4} \frac{1}{(k^2)^{\nu_1 + \nu_2}}.$$

A second kind of divergences appears in the massless case of the tadpole integral

$$\int \frac{d^4 k}{(2\pi)^4} \frac{1}{(k^2)^{\nu}}. \tag{2.30}$$

This integral not only diverges at large momenta if $\nu \leq 2$ but also at $k^2 \to 0$ if $\nu \geq 2$. We call the second kind of divergence **infrared divergence**. We note how the existence of a mass in the tadpole integral prevents infrared divergences. Similarly, we find for the massless bubble integral at small momenta an infrared divergence if $\nu_2 \geq 2$, since

$$\int \frac{d^4 k}{(2\pi)^4} \frac{1}{(k^2)^{\nu_1} ((k-p)^2)^{\nu_2}} \xrightarrow{k^2 \to 0} \int \frac{d^4 k}{(2\pi)^4} \frac{1}{(k^2)^{\nu_2}}.$$

We see how divergences may occur in the calculation of Feynman integrals. Regularisation provides a way of handling this problem, because it generates well defined integrals. In this thesis, we will utilise a standard regularisation method, namely dimensional regularisation [53, 54, 56]. In **dimensional regularisation** the four-dimensional vector space of momentum vectors is exchanged for a D-dimensional vector space, which is divided into an integer part D_0 and a non-integer part $D - D_0$,

$$\begin{aligned}
&4 \to D = D_0 - 2\epsilon, \\
&k = (k_0, k_1, k_2, k_3)^T \to k = (k_0, \dots, k_{D-1})^T, \\
&\frac{d^4 k}{(2\pi)^4} \to \frac{d^D k}{(2\pi)^D}.
\end{aligned} \tag{2.31}$$

We call

$$\epsilon = \frac{D - D_0}{2}$$

the dimensional regularisation parameter. We recover the physical case if we set $D_0 = 4$ and take the limit $\epsilon \to 0$, hence, we usually set

$$D = 4 - 2\epsilon.$$

Properties of integration like linearity, invariance under translation or rotation and scaling behaviour are preserved under the transition to D dimensions (see [57] section 2.4.2). The integration measure is normalised such that

$$\int d^D k\, e^{ak^2} = i \left(\frac{\pi}{a}\right)^{\frac{D}{2}}.$$

We may translate our investigations on the tadpole and the bubble integral to D dimensions and find

- $k^2 \to \infty$: The tadpole and bubble integral have an ultraviolet divergence if $D \geq 2\nu$ and $D \geq 2(\nu_1 + \nu_2)$, respectively.

- $k^2 \to 0$: The massless tadpole and massless bubble integral have an infrared divergence if $D \leq 2\nu$ and $D \leq 2\nu_2$, respectively.

- $(k - p)^2 \to 0$: The massless bubble integral has an infrared divergence if $D \leq 2\nu_1$.

We handle ultraviolet divergences with dimensional regularisation as we set $D < 2\nu$ ($D < 2(\nu_1 + \nu_2)$). Theoretically, infrared divergences are handled with the help of another regulator, for example through the introduction of small masses. After performing the integration in the ultraviolet convergent domain, we may analytically continue the result to all values of D and especially to $D > 2\nu$ ($D > 2(\nu_1 + \nu_2)$). Here, the integral is infrared finite and we remove the additional regulator. Both divergences, ultraviolet and infrared, are then regulated by dimensional regularisation.

A Feynman integral I in D dimensions has a Laurent expansion around $\epsilon = 0$

$$I_i = \sum_j I_i^{(j)} \epsilon^j.$$

In practice, ultraviolet and infrared divergences in four dimensions, therefore, become apparent as poles in ϵ in D dimensions. Ultraviolet divergences give rise to poles up to ϵ^{-l} and infrared divergences up to ϵ^{-2l}, where l denotes the number of loops, i.e. the number of integration variables. The tadpole integral with $\nu = 1$, for example, inherits a pole in ϵ as it amounts to (see (3.21) and (3.22))

$$\int \frac{d^D k}{(2\pi)^D} \frac{1}{(k^2 - m^2)} \stackrel{D=4-2\epsilon}{\sim} -\frac{1}{\epsilon} \left(m^2\right) + \left(\ln\left(m^2\right) - 1\right) \left(m^2\right) + \mathcal{O}(\epsilon).$$

We stress this point a bit further by looking at our second example. In section 3.3.1 (see 3.39) we will express the massless bubble diagram in terms of Euler's Gamma function Γ (3.16),

$$\int \frac{d^D k}{(2\pi)^D} \frac{1}{(k^2)^{\nu_1} ((k-p)^2)^{\nu_2}} \left(-p^2\right)^{-\frac{D}{2} + (\nu_1 + \nu_2)}$$

$$\sim \frac{\Gamma\left((\nu_1 + \nu_2) - \frac{D}{2}\right)}{\Gamma(\nu_1)\Gamma(\nu_2)} \frac{\Gamma\left(\frac{D}{2} - \nu_2\right)\Gamma\left(\frac{D}{2} - \nu_1\right)}{\Gamma\left(D - (\nu_1 + \nu_2)\right)}$$

$$\stackrel{D=4-2\epsilon}{=\!=} \frac{\Gamma\left((\nu_1 + \nu_2) - (2 - \epsilon)\right)}{\Gamma(\nu_1)\Gamma(\nu_2)} \frac{\Gamma\left((2 - \epsilon) - \nu_2\right)\Gamma\left((2 - \epsilon) - \nu_1\right)}{\Gamma\left((4 - 2\epsilon) - (\nu_1 + \nu_2)\right)}.$$

Here, we do not need to introduce Euler's gamma function in its full generality, it is sufficient to note that

$$\Gamma(\epsilon) = \frac{1}{\epsilon} - \gamma_E + \mathcal{O}(\epsilon).$$

For $\nu_1 = \nu_2 = 1$, i.e. $4 \geq 2(\nu_1 + \nu_2)$, the ultraviolet divergence becomes visible as pole in ϵ in the first gamma function of the numerator

$$\Gamma\left((\nu_1 + \nu_2) - (2 - \epsilon)\right) \stackrel{\nu_1 = \nu_2 = 1}{=\!=} \Gamma(\epsilon).$$

The pole in ϵ of the infrared divergence $\nu_2 \geq 2$ appears in the second gamma function of the numerator

$$\Gamma\left((2 - \epsilon) - \nu_2\right) \stackrel{\nu_2 = 2}{=\!=} \Gamma(-\epsilon).$$

Poles in ϵ are handled different regarding their origin in an infrared or an ultraviolet divergence. Infrared divergences are handled with the Kinoshita-Lee-Nauenberg theorem, ultraviolet divergences by renormalisation. Here, we will not describe the former in detail. We only note the following: A detector has a finite resolution, hence, two particles close to each other in phase space are indistinguishable and will be detected as if they were one particle. The Kinoshita-Lee-Nauenberg [58, 59] theorem assures that all infrared divergences cancel by summing over all degenerated states, i.e. by taking all virtual loops as well as real emitted particles into account.

Renormalisation redefines a finite number of parameters and fields in order to absorb occurring ultraviolet divergences. "Bare" fields and parameters are defined to be a renormalisation constant times a renormalised field/parameter. For instance, the quark field q and its mass m_q may be redefined as follows

$$q_{bare} = \sqrt{Z_2}q_{ren},$$
$$m_{q,bare} = Z_m m_{q,ren}.$$

The renormalisation constants Z_2, Z_m absorb ultraviolet divergences by construction, leaving a finite renormalised field/parameter $q_{ren}/m_{q,ren}$ behind. As a consequence, a Lagrangian may be separated into a part containing all physical parameters and fields of the theory $\mathcal{L}_{renormalised} = \mathcal{L}_{ren}$ and a part yielding the cancellation of divergences $\mathcal{L}_{CounterTerms} = \mathcal{L}_{CT}$,

$$\mathcal{L} \to \mathcal{L}_{bare} = \mathcal{L}_{ren} + \mathcal{L}_{CT}. \tag{2.32}$$

The part of the Standard Model Lagrangian yielding the quark propagator (2.25), for example, is separated like

$$\mathcal{L} = \bar{q}(i\gamma^\mu \partial_\mu - m_q)q \to \mathcal{L}_{bare} = Z_2 \bar{q}_{ren}(i\gamma^\mu \partial_\mu - Z_m m_{q,ren})q_{ren}$$
$$= \mathcal{L}_{ren} + \mathcal{L}_{CT},$$
$$\mathcal{L}_{ren} = \bar{q}_{ren}(i\gamma^\mu \partial_\mu - m_{q,ren})q_{ren},$$
$$\mathcal{L}_{CT} = \bar{q}_{ren}((Z_2 - 1)i\gamma^\mu \partial_\mu - (Z_2 Z_m - 1)m_{q,ren})q_{ren}.$$
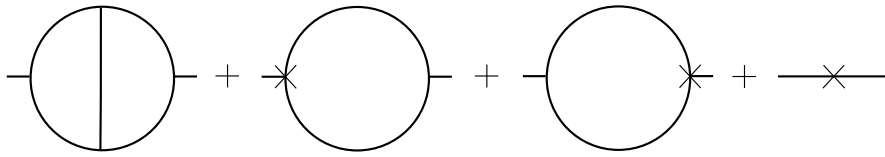
Figure 2.3: Illustrative example of two-loop Feynman diagram and corresponding diagrams with counterterm insertions.

We see, we gain additional Feynman rules from $\mathcal{L}_{CT}$ which may be utilised to express Feynman diagrams with counterterm insertions. Ultraviolet divergences, which arise in the calculation of a Feynman diagram with Feynman rules obtained from $\mathcal{L}_{bare}$, are cancelled by Feynman diagrams with appropriate counterterm insertions. Those are found as loops of the original diagram are pinched and counterterm insertions are placed instead. A counterterm insertion is indicated by a cross in the graph. We give an illustrative example of a not further specified two-loop graph, whose divergent parts may be cancelled through one-loop and tree graphs in fig.2.3.

The choice of renormalisation constants is not unique. Different renormalisation schemes reflect different choices. Within the **minimal subtraction** scheme renormalisation constants are designed to absorb nothing more than exactly the poles in ϵ. As Euler's constant γ_E and the logarithm $\ln(4\pi)$ accompany each pole in ϵ, the renormalisation constants within **modified minimal subtraction** absorb

$$\frac{1}{\epsilon} - \gamma_E + \ln(4\pi).$$

Within the **on-shell scheme**, renormalisation constants are defined via conditions found as particles are set on-shell $\left(p^2 = m^2\right)$.

We close this chapter with the conclusion that physical measurable quantities describing particle interactions like decay rates are theoretically derived from scattering amplitudes (see section 2.1). Scattering amplitudes correspond to sums of Feynman diagrams, which are calculated via Feynman rules (section 2.2.1). Feynman diagrams with loops yield integrations. Since Feynman integrals in four dimensions can be ill-defined, we apply dimensional regularisation and consider $D = (4 - 2\epsilon)$ space-time dimensions. Divergences become explicit as poles in the dimensional regularisation parameter. We are left with the question: How can we compute D-dimensional Feynman integrals? We address this question in the following chapters. Chapter 3 provides an introduction into the topic of Feynman integrals and develops methods for their calculation. Chapter 5 shows new results as integrals for the three-loop Higgs self-energy are found.

FEYNMAN INTEGRALS

Perturbation theory demands us to calculate scattering amplitudes and thereby measurable quantities describing particle interactions order by order in coupling constants. As a consequence, precision calculations in quantum field theory require the derivation of high orders in perturbation theory, represented by the calculation of Feynman diagrams with multiple loops. Loop diagrams create Feynman integrals, which are therefore essential building blocks of quantum field theoretical precision calculations. This chapter starts the discussion on Feynman integrals with an introduction, which demonstrates the emergence of Feynman integrals. Along the way, we define basic properties and concepts like scalar integrals, auxiliary topologies and the momentum representation of Feynman integrals. Section 3.2 can be considered as an extension to the introduction, since it investigates one-loop diagrams more closely. Sections 3.3 and 3.4 prepare the calculation of higher loop integrals. The former defines representations of Feynman integrals required in this thesis. The latter discusses ordering as well as relations between different integrals and thereby enables the construction of master integrals. Section 3.5 introduces a solution technique for loop integrals, the method of differential equations. Tools required to utilise this method successfully, like maximal cuts of Feynman integrals, will be given in section 3.6. The main references of this chapter are [57, 60] (see also [61, 62]), further references will be provided as needed.

3.1 Introduction

Feynman diagrams with loops naturally arise during the calculation of higher orders in perturbative quantum field theory. We acquired in section 2.2 the Feynman rules needed to translate those diagrams into mathematical expressions. Loops particularly give rise to integrations, namely integrations over the undetermined loop momenta. These integrals need to be regularised. As discussed in section 2.3, dimensional regularisation constitutes an appropriate regularisation scheme. Hence, momenta are taken to be D-dimensional. Expressing a Feynman diagram with l loops and n internal edges via Feynman rules leads to a Feynman integral of the following form:

$$I = \int \prod_{i=1}^{l} \frac{d^D k_i}{(2\pi)^D} \, \mathcal{N}(q_1^\mu, ..., q_n^\mu, m_1, ..., m_n) \prod_{j=1}^{n} \frac{1}{(q_j^2 - m_j^2)}, \qquad (3.1)$$

where k_i, $i = 1, ...l$ are the loop momenta, q_j, $j = 1, ...n$ are the internal momenta, which can be expressed in terms of loop momenta and external momenta due to momentum conservation, and m_j, $j = 1, ...n$ are the internal masses. In the context of Feynman integrals, we call $(q_j^2 - m_j^2)$ (internal) propagator. The numerator $\mathcal{N}$ in (3.1) gets determined through the internal edges and vertices of the diagram. It may contain vectors, axial-vectors and tensors in contrast to the denominator solely depending on scalars. Additionally, it absorbs any prefactors arising from Feynman rules.
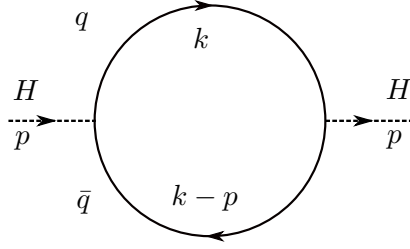
Figure 3.1: Two-point one-loop diagram $H \to q\bar{q} \to H$. The dotted line carries mass m_H and the solid line carries mass m_q.

To gain further insights into the possible structures of (3.1), we look at an example: $H \to q\bar{q} \to H$, a one-loop contribution to the Higgs-boson self-energy depicted in fig.3.1. The internal edges represent a quark q and an antiquark $\bar{q}$. The quark carries an undetermined loop momentum k and due to momentum conservation the antiquark carries momentum $(k - p)$ if p denotes the Higgs-boson's momentum. In correspondence, we may assign to the quark's edge $P_1 = (k^2 - m_q^2)$ which we call first propagator and to the other edge $P_2 = ((k - p)^2 - m_q^2)$ which we call second propagator. Both propagators form the topology corresponding to fig.3.1. The kinematic invariants are the quark mass m_q and the squared external momentum $p^2 = s$. Expressing figure 3.1 with the help of Feynman rules from section 2.2.1 yields

$$- \int \frac{d^D k}{(2\pi)^D} \frac{g^2 m_q^2}{4 m_W^2} \frac{Tr\left((\slashed{k} + m_q)(\slashed{k} - \slashed{p} + m_q)\right)}{\left(k^2 - m_q^2\right)\left((k - p)^2 - m_q^2\right)} \tag{3.2}$$

$$= - \int \frac{d^D k}{(2\pi)^D} \frac{g^2 m_q^2}{m_W^2} \frac{\left(k^2 - k \cdot p + m_q^2\right)}{\left(k^2 - m_q^2\right)\left((k - p)^2 - m_q^2\right)}. \tag{3.3}$$

The trace in (3.2) is evaluated using the following properties from Dirac algebra

$$\{\gamma^\mu, \gamma^\nu\} = 2g^{\mu\nu}, \ \slashed{k}\slashed{k} = k^2, \ Tr(1) = 4,$$
$$Tr\left(\gamma^\mu\right) = Tr\left(\gamma^{\mu_1} \ldots \gamma^{\mu_{2n+1}}\right) = 0, \ \forall n \in \mathbb{N}, \tag{3.4}$$

which leads to the following numerator

$$\mathcal{N} = -\frac{g^2 m_q^2}{m_W^2} \left(k^2 - k \cdot p + m_q^2\right) \sim \left(k^2 - k \cdot p + m_q^2\right).$$

We see, that numerators of Feynman integrals can depend on loop momenta. This type of loop integral is called **tensor integral**. We would like to deal with **scalar integrals**

only, i.e. integrals in which loop momenta solely appear as components of propagators, to enable the use of various techniques helpful for solving Feynman integrals. A scalar integral can be represented in the following way:

$$I \sim \int \prod_{i=1}^{l} \frac{d^D k_i}{(2\pi)^D} \prod_{j=1}^{n} \frac{1}{(q_j^2 - m_j^2)^{\nu_j}}, \quad \nu_j \in \mathbb{Z}, \tag{3.5}$$

To transfer (3.1) into a (sum of) scalar integrals, loop momenta inside scalar products as well as loop momenta appearing as vectors have to be eliminated from $\mathcal{N}$. Here, "elimination" of scalar products refers to expressing them in terms of propagators and kinematic invariants.

In the example (3.3) k^2 and $k \cdot p$ appear inside $\mathcal{N}$. The number of propagators and the number of independent scalar products involving loop momenta matches, as always in the case of one-loop diagrams. Since the first propagator depends on k^2 and the quark mass, k^2 can be expressed through P_1 and m_q. Similarly, $p \cdot k$ can be rewritten in terms of both propagators and s,

$$P_1 = k^2 - m_q^2 \Rightarrow k^2 = P_1 + m_q^2,$$
$$P_2 = (k - p)^2 - m_q^2 \Rightarrow k \cdot p = \frac{1}{2} \left(P_1 - P_2 + s \right). \tag{3.6}$$

Inserting those linear combinations into (3.3) gives

$$\int \frac{d^D k}{(2\pi)^D} \frac{\mathcal{N}}{P_1 P_2} \overset{(3.6)}{=} - \int \frac{d^D k}{(2\pi)^D} \frac{g^2 m_q^2}{m_W^2} \frac{\left(P_1 + m_q^2 - \frac{1}{2}\left(P_1 - P_2 + s \right) + m_q^2 \right)}{P_1 P_2}$$
$$= -\frac{g^2 m_q^2}{m_W^2} \left(\int \frac{d^D k}{(2\pi)^D} \frac{4m_q^2 - s}{2 P_1 P_2} + \int \frac{d^D k}{(2\pi)^D} \frac{1}{2 P_1} + \int \frac{d^D k}{(2\pi)^D} \frac{1}{2 P_2} \right)$$
$$= -\frac{g^2 m_q^2}{m_W^2} \left(\left(2m_q^2 - \frac{s}{2} \right) I_{11} + \frac{1}{2} I_{10} + \frac{1}{2} I_{01} \right). \tag{3.7}$$

In the last step, we introduced a notation

$$I_{\nu_1 \nu_2} \equiv \int \frac{d^D k}{(2\pi)^D} \frac{1}{P_1^{\nu_1} P_2^{\nu_2}}, \tag{3.8}$$

which identifies each scalar integral through the exponents of its propagators P_1 and P_2. Three scalar integrals remain. We will see their evaluation in section 3.2. The set of integrals $I_{\nu_1 \nu_2}$ with arbitrary exponents ν_1, ν_2 is called **integral family** (belonging to the diagram in fig.3.1).

In general, for l loop momenta k_i and e independent external momenta p_m, the scalar products

$$k_i \cdot k_j, \ k_i \cdot p_m, \ p_m \cdot p_n, \quad i, j = 1, \dots l, \quad m, n = 1, \dots e,$$

arise in the numerator of the Feynman integral. That amounts to

$$N_{scp} = \frac{l(l+1)}{2} + e \cdot l \tag{3.9}$$

independent scalar products involving loop momenta. If the number of internal edges and therefore the number of propagators equals N, each scalar product involving a loop momentum can uniquely be expressed through a linear combination of propagators and kinematic variables.

It follows, that we may replace scalar products inside the numerator with linear combinations of propagators. We cancel the propagators with the corresponding propagators in the denominator and obtain a sum of different scalar integrals (3.5). These integrals can be identified through the exponents of their propagators, which are at this stage either one or zero, as seen in (3.7) and (3.8). Diagrams with less propagators than required by (3.9) can be interpreted as sub-graphs of graphs with an appropriate number of edges. In this way an **auxiliary topology**, namely the topology belonging to the larger graph, can be found and utilised for each diagram. The auxiliary propagators that did not appear in the original diagram emerge in the denominators of integrals only with negative exponents. The construction of an auxiliary topology will be shown in practice in section 5.2.

The closed fermion loop in the above example led to a trace in the integral, hence, no vectors survived. In general, the numerator of (3.1) can contain vectors, which are not contracted. If each independent scalar product involving a loop momentum can uniquely be expressed by a linear combination of propagators, we can eliminate the dependencies on vector like loop momenta through the **Passarino-Veltman reduction technique** [63]. The evaluated integral of a scalar function times loop momenta carrying indices must be equal to a tensor structure carrying these respective indices. Furthermore, this tensor structure has to be constituted of the fixed external momenta and the metric tensor $g_{\mu\nu}$. In the case of one loop momentum k and one external momentum p follows

$$\int d^D k \ k^\mu f(k) = p^\mu \cdot B, \quad B \in \mathbb{C},$$

where $f(k)$ is an arbitrary scalar function. Through contraction with p_μ, the constant B can be rewritten,

$$\stackrel{p_\mu}{\Rightarrow} \int d^D k \ p_\mu k^\mu f(k) = p_\mu p^\mu \cdot B,$$

$$\Leftrightarrow \int d^D k \ p \cdot k \ f(k) = p^2 \cdot B,$$

$$\Leftrightarrow B = \frac{1}{p^2} \int d^D k \ p \cdot k \ f(k).$$

After inserting the result, we obtain for the original integral

$$\int d^D k \ k^\mu f(k) = \frac{p^\mu}{p^2} \int d^D k \ p \cdot k \ f(k).$$

Now, the integration is solely over scalars. We replace $p \cdot k$ with an appropriate linear combination of propagators and obtain a scalar integral. In a similar manner, integrals containing more vectors can be transformed to scalar integrals. We will see another

application of the Passarino-Veltman reduction technique in (6.17), section 6.4.

After obtaining scalar integrals out of (3.1), we are left with a set of integrals which can be written in the momentum representation of Feynman integrals. In D space-time dimensions, **the momentum representation of a Feynman integral** corresponding to an l-loop diagram with n internal edges is defined by

$$I_{\nu_1\nu_2...\nu_n} = e^{\epsilon l \gamma_E} \left(\mu^2\right)^{\nu - \frac{lD}{2}} \int \prod_{i=1}^{l} \frac{d^D k_i}{i\pi^{D/2}} \prod_{j=1}^{n} \frac{1}{P_j^{\nu_j}}, \quad P_j = (-q_j^2 + m_j^2), \qquad (3.10)$$

where k_i, $i = 1,...l$ are the loop momenta and q_j, $j = 1,...n$ is the internal momentum flowing through the edge j which carries mass m_j. Furthermore, $\nu_j \in \mathbb{Z}$ is the exponent of the propagator P_j, whereby

$$\nu = \sum_{j=1}^{n} \nu_j.$$

μ is an arbitrary parameter with mass dimension one, γ_E is Euler's constant and

$$\epsilon = \frac{D_0 - D}{2}, \quad D_0 \in \mathbb{N},$$

is the dimensional regularisation parameter. Note, that any scalar factors that emerged during the transformation from the original expression of the Feynman diagram (3.1) are written in front of the obtained integrals. Note further, that this transformation includes the compensation of the extra factor $e^{\epsilon l \gamma_E} \left(\mu^2\right)^{\nu - \frac{lD}{2}}$ and the replacement from $(2\pi)^D$ in (3.1) with $(i\pi^{D/2})$ as well as the change of the overall signs of propagators. We will justify the use of the latter conventions in section 3.2 (see especially (3.14) and (3.15)). The factor $e^{\epsilon l \gamma_E}$ removes Euler's constant from the evaluated integral (see (3.26)). The renormalisation scale μ is introduced to render the integrals dimensionless. Dimensional power counting,

$$\frac{d^D k_1 ... d^D k_l}{P_1^{\nu_1} ... P_n^{\nu_n}} \sim \frac{\left(m^D\right)^l}{(m^2)^\nu},$$

reveals a mass dimension of $Dl - 2\nu = -2(\nu - \frac{lD}{2})$ for an l-loop integral in D dimensions and, hence, verifies that the factor $\left(\mu^2\right)^{\nu - \frac{lD}{2}}$ ensures (3.10) to be dimensionless.

Due to the insertion of μ, the integral depends on scalar, dimensionless **kinematic variables**

$$\frac{p_i \cdot p_j}{\mu^2}, \quad \frac{m_q^2}{\mu^2}, \qquad (3.11)$$

where p_i, $i, j = 1, \ldots, e$ are linear independent external momenta and m_q are internal masses (see e.g. (3.19)). The products of external momenta in (3.11) are usually rewritten in terms of Mandelstam variables. One kinematic variable can be set to one, which

fixes μ^2 to be either a squared mass or a Mandelstam variable. As a consequence, the number of independent kinematic variables is given by

$$N_v = \frac{e\,(e-1)}{2} + n_m - 1, \tag{3.12}$$

where $n_m \leq n$ is the number of different internal masses.

Summarising, any Feynman graph G with loops gives rise to a certain Feynman integral (3.1). After evaluating its numerator, it is reduced to a sum of scalar Feynman integrals, thereby, an appropriate auxiliary topology is found if necessary. The number of edges of the auxiliary graph has to be equal to the number of independent scalar products containing a loop momentum N_{scp} (3.9). The remaining integrals are identified through the exponents of their propagators: $I_{\nu_1\nu_2...\nu_n}$. They can be expressed in the momentum representation of Feynman integrals (3.10). The set of integrals $I_{\nu_1\nu_2...\nu_n}$ with arbitrary exponents $\nu_1, \nu_2, \ldots, \nu_n$ is called family of Feynman integrals associated to G. The integral family includes sub-graphs of G which correspond to an integral $I_{\nu_1\nu_2...\nu_n}$ with one or more zero exponents $\nu_i = 0$. Here, the sub-graph is obtained from G through pinching the appropriate edge(s) i.

The Feynman integrals of a family are not independent, instead, linear relations among them can be found and used to obtain a basis of this family. The basis integrals are also called master integrals. We will learn more about master integrals and their evaluation in sections 3.4 and 3.5, but first we will look at the easiest type of Feynman integrals, namely integrals corresponding to one-loop diagrams.

3.2   One-loop diagrams

In this section we investigate one-loop diagrams and integrals. For this purpose, we return to the two-point one-loop example $H \to q\bar{q} \to H$ from fig.3.1. We encounter and solve two important one-loop integrals, namely, the tadpole (3.13) and the bubble integral (3.24) which are expressible through Euler's gamma (3.16) and beta function (3.20). On the way, we find a general procedure for calculating one-loop diagrams.

After expressing the one-loop diagram from fig.3.1 through scalar integrals (3.6), the calculation proceeds as we write it in terms of Feynman integrals in momentum representation (3.7).

$$-\int \frac{d^D k}{(2\pi)^D} \frac{g^2 m_q^2}{4m_W^2} \frac{Tr\left(({\not{k}} + m_q)({\not{k}} - {\not{p}} + m_q)\right)}{\left(k^2 - m_q^2\right)\left((k-p)^2 - m_q^2\right)}$$

$$= \frac{i e^{-\epsilon\gamma_E}}{2^D \pi^{\frac{D}{2}}} \frac{g^2 m_q^2}{m_W^2} \left(\left(\mu^2\right)^{\frac{D}{2}-2}\left(-2m_q^2 + \frac{s}{2}\right) I_{11} + \frac{1}{2}\left(\mu^2\right)^{\frac{D}{2}-1}\left(I_{10} + I_{01}\right)\right),$$

where the integrals are defined by

$$I_{\nu_1\nu_2} = e^{\epsilon\gamma_E} \left(\mu^2\right)^{\nu - \frac{D}{2}} \int \frac{d^D k}{i\pi^{D/2}} \frac{1}{P_1^{\nu_1} P_2^{\nu_2}},$$

$$P_1 = -k^2 + m_q^2, \quad P_2 = -(k-p)^2 + m_q^2.$$

Since I_{01} can be transformed into I_{10} through a variable transformation $k \to \tilde{k} = k - p$, two integrals I_{01}, I_{11} remain to be evaluated.
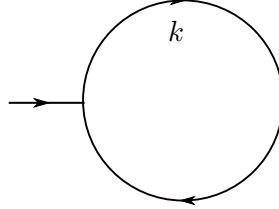
Figure 3.2: One-loop tadpole diagram.

We start with the easier integral I_{10} which is also known as **one-loop tadpole integral** T_1, due to its diagrammatic depiction (fig.3.2),

$$I_{10} = T_1 \left(D, m_q^2\right),$$

$$T_\nu \left(D, m^2\right) \equiv e^{\epsilon \gamma_E} \left(\mu^2\right)^{\nu - \frac{D}{2}} \int \frac{d^D k}{i \pi^{D/2}} \frac{1}{\left(-k^2 + m^2\right)^\nu}. \tag{3.13}$$

The tadpole integral depends on the loop momentum $k = (k_0, k_1, \ldots, k_{D-1})^T$ solely through its square. Note, it depends not only on the dimension D, but also explicitly on the dimensional regularisation parameter ϵ through the prefactor $e^{\epsilon \gamma_E}$. However, we write $T_\nu \left(D, m^2\right)$ instead of $T_\nu \left(D, \epsilon, m^2\right)$, since this prefactor is always the same by definition. As a first step in the evaluation of the tadpole integral, we change from Minkowski space,

$$k^2 = k_0^2 - k_1^2 - \ldots - k_{D-1}^2,$$

to Euclidean space,

$$K^2 = K_0^2 + K_1^2 + \ldots + K_{D-1}^2,$$

through a **Wick rotation** [64]. The integration contour of the Wick rotation is given by the closed contour in fig.3.3.
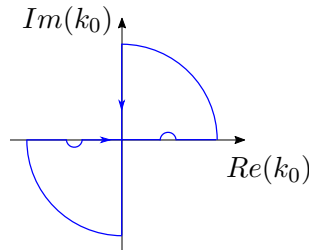
Figure 3.3: Integration contour of the Wick rotation. Small semicircles on the real axis circumvent the poles.

The poles of the propagator on that contour are bypassed by Feynman's $i\delta$-prescription,

$$\frac{i}{-k^2 + m^2 - i\delta},$$

which is usually not written down explicitly, but always implied. It follows, that the integration over the first component of the loop momentum k_0 along the closed contour vanishes. Additionally, the integrations along the quarter-circles at infinity vanish too if no singularities are on the quarter-circles. Hence, only the integration along the axes are left and we can find a relation among them,

$$0 = \oint dk_0 f(k_0) = \int_{-\infty}^{\infty} dk_0 f(k_0) + \int_{i\infty}^{-i\infty} dk_0 f(k_0),$$

$$\Rightarrow \int_{-\infty}^{\infty} dk_0 f(k_0) = -\int_{i\infty}^{-i\infty} dk_0 f(k_0).$$

Using this relation we obtain a loop momentum with Euclidean signature if we change the time component $k_0 = iK_0$ and leave the space components as they are $k_j = K_j$, for $0 < j \leq D - 1$,

$$k^2 = -K^2, \, d^D k = i d^D K,$$

$$\Rightarrow \frac{d^D k}{i\pi^{D/2}} \frac{1}{(-k^2 + m^2)^\nu} = \frac{d^D K}{\pi^{D/2}} \frac{1}{(K^2 + m^2)^\nu}. \tag{3.14}$$

Here, we see the reason for changing the signs of the propagators and placing an i in the denominator of the momentum representation of Feynman integrals (3.10).

In the next step, we introduce generalised spherical coordinates (see appendix A.1) to split the integration into an angular and a radial part, since the integration variable appears only squared. The measure is $d^D K = K^{D-1} dK d\Omega_D$. The angular integration,

$$\int d\Omega_D = \frac{2\pi^{\frac{D}{2}}}{\Gamma\left(\frac{D}{2}\right)}, \tag{3.15}$$

validates the convention $\frac{1}{\pi^{\frac{D}{2}}}$ in (3.10), since this factor cancels now. Here,

$$\Gamma(x) \equiv \int_0^\infty e^{-t} t^{x-1} dt \tag{3.16}$$

is **Euler's gamma function** which has various properties (see for example [57] section 2.4.2) such as

$$\Gamma(z + 1) = z\Gamma(z),$$
$$\Gamma(n + 1) = n!, \, n \in \mathbb{N},$$
$$\Gamma(\epsilon) = \frac{1}{\epsilon} - \gamma_E + \mathcal{O}(\epsilon).$$

The tadpole integral becomes

$$T_\nu \left(D, m^2\right) \stackrel{\text{Wick rot.}}{=} e^{\epsilon \gamma_E} \left(\mu^2\right)^{\nu - \frac{D}{2}} \int \frac{d^D K}{\pi^{D/2}} \frac{1}{\left(K^2 + m^2\right)^\nu} \tag{3.17}$$

$$\stackrel{\text{angular int.}}{=} e^{\epsilon \gamma_E} \left(\mu^2\right)^{\nu - \frac{D}{2}} \frac{2}{\Gamma \left(\frac{D}{2}\right)} \int dK \frac{\left(K^2\right)^{\frac{D-1}{2}}}{\left(K^2 + m^2\right)^\nu}. \tag{3.18}$$

Changing the variable,

$$K \to t = \frac{K^2}{m^2} \Rightarrow dK = dt \frac{m^2}{2K},$$

leads to

$$T_\nu \left(D, m^2\right) = e^{\epsilon \gamma_E} \left(\frac{m^2}{\mu^2}\right)^{\frac{D}{2} - \nu} \frac{1}{\Gamma \left(\frac{D}{2}\right)} \int dt \frac{t^{\frac{D}{2} - 1}}{(t+1)^\nu}$$

$$= e^{\epsilon \gamma_E} \left(\frac{m^2}{\mu^2}\right)^{\frac{D}{2} - \nu} \frac{1}{\Gamma \left(\frac{D}{2}\right)} B \left(\frac{D}{2}, \nu - \frac{D}{2}\right). \tag{3.19}$$

We see how the renormalisation scale μ yields a dimensionless integral. Furthermore, we recognise **Euler's beta function**

$$B(z_1, z_2) \equiv \int_0^\infty \frac{t^{z_1 - 1}}{(t+1)^{z_1 + z_2}} \, dt = \int_0^1 t^{z_1 - 1}(1 - t)^{z_2 - 1} dt = \frac{\Gamma(z_1)\Gamma(z_2)}{\Gamma(z_1 + z_2)}. \tag{3.20}$$

We are therefore able to express the tadpole integral in terms of gamma functions

$$T_\nu \left(D, \frac{m^2}{\mu^2}\right) = e^{\epsilon \gamma_E} \left(\frac{m^2}{\mu^2}\right)^{\frac{D}{2} - \nu} \frac{\Gamma(\nu - \frac{D}{2})}{\Gamma(\nu)}, \tag{3.21}$$

and obtain in $D = 4 - 2\epsilon$ dimensions

$$I_{10} = T_1 \left(4 - 2\epsilon, \frac{m_q^2}{\mu^2}\right) = e^{\epsilon \gamma_E} \left(\frac{m_q^2}{\mu^2}\right) e^{-\epsilon \ln\left(\frac{m_q^2}{\mu^2}\right)} \Gamma(\epsilon - 1) \tag{3.22}$$

$$= -\frac{1}{\epsilon} \left(\frac{m_q^2}{\mu^2}\right) + \left(\ln\left(\frac{m_q^2}{\mu^2}\right) - 1\right) \left(\frac{m_q^2}{\mu^2}\right) + \mathcal{O}(\epsilon).$$

In addition, we may set

$$\mu^2 = m_q^2,$$

and find

$$T_1 \left(4 - 2\epsilon\right) = e^{\epsilon \gamma_E} \Gamma(\epsilon - 1) \tag{3.23}$$

$$= -\frac{1}{\epsilon} - 1 - \left(1 - \frac{1}{2}\zeta_2\right) \epsilon + \left(\frac{1}{3}\zeta_3 - \frac{1}{2}\zeta_2 - 1\right) \epsilon^2 + \mathcal{O}(\epsilon^3).$$

We encounter the tadpole integral with a general mass and with a mass equal to μ^2 again in section 5.4.3 in (5.39) and (5.38). There, the tadpole is taken in $D = (2 - 2\epsilon)$-dimensions in order to find an integral of uniform weight (see section 3.5.1 and section 3.5.2 for definitions of weight properties).

The second integral of the two-point one-loop example $H \to q\bar{q} \to H$ is named **one-loop bubble** $B_{\nu_1 \nu_2}(p^2, m_1^2, m_2^2)$, again after its diagrammatic depiction (fig.3.4).
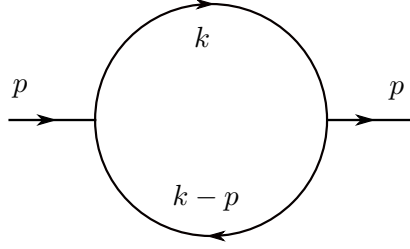
Figure 3.4: One-loop bubble diagram.

The one-loop bubble integral is defined by

$$I_{11} = B_{11}\left(D, p^2, m_q^2, m_q^2\right),$$

$$B_{\nu_1 \nu_2}\left(D, p^2, m_1^2, m_2^2\right) \equiv e^{\epsilon \gamma_E} \left(\mu^2\right)^{\nu - \frac{D}{2}} \int \frac{d^D k}{i\pi^{D/2}} \frac{1}{\left(-k^2 + m_1^2\right)^{\nu_1} \left(-(k-p)^2 + m_2^2\right)^{\nu_2}}.$$
(3.24)

As in the case of the tadpole integral, we do not point out the bubble integrals' dependence on ϵ. In contrast to the tadpole, the dependency of the one-loop bubble on the loop momentum is not solely through its square. Prior to performing a Wick rotation and shifting to spherical coordinates, we have to complete the square. We therefore have to find an appropriate integration variable. First, we convert the product of propagators in the denominator into a sum with the help of Feynman's trick, which will be given in its full generality in (3.37) in section 3.3. Here, we only need the special case of two propagators P_1, P_2,

$$\frac{1}{P_1 P_2} = \int_0^1 da \frac{1}{(aP_1 + (1-a)P_2)^2}.$$
(3.25)

Feynman's trick introduces a so-called Feynman parameter a. Unfortunately, the conversion to a product comes with an additional integration over a. Alternatively, Schwinger's trick could be utilised, which introduces additional integrations over Schwinger parameters. Applying (3.25) to the integrand of I_{11} and reordering the result such that k is placed inside a squared term gives

$$\frac{1}{\left(-k^2 + m_q^2\right)\left(-(k-p)^2 + m_q^2\right)} = \int_0^1 da \frac{1}{-\underbrace{(k - (1-a)p)^2}_{\tilde{k}^2} + a(a-1)p^2 + m_q^2},$$

$$\Rightarrow I_{11} = e^{\epsilon \gamma_E} \left(\mu^2\right)^{2 - \frac{D}{2}} \int_0^1 da \int \frac{d^D \tilde{k}}{i\pi^{D/2}} \frac{1}{-\tilde{k}^2 + a(a-1)p^2 + m_q^2}.$$

After shifting the integration variable to $\tilde{k}$, the integration over $\tilde{k}$ can be performed with the help of a Wick rotation and D-dimensional spherical coordinates, just as before. Looking at the definition of the tadpole (3.13) we can transfer its result (3.21) if we set $\tilde{m} = a\,(a-1)\,p^2 + m_q^2$. For $D = 4 - 2\epsilon$, we obtain

$$I_{11} = e^{\epsilon\gamma_E}\mu^{2\epsilon}\Gamma(\epsilon)\int_0^1 da\,\frac{1}{\left(a\,(a-1)\,p^2 + m_q^2\right)^{\epsilon}}.$$

In the massless case, we can identify Euler's beta function again

$$
\begin{aligned}
B_{11}\left(D, p^2, 0, 0\right) &= e^{\epsilon\gamma_E}\mu^{2\epsilon}\Gamma(\epsilon)\int_0^1 da\,\left(a\,(a-1)\,p^2\right)^{-\epsilon} \\
&= e^{\epsilon\gamma_E}\left(\frac{-p^2}{\mu^2}\right)^{-\epsilon}\Gamma(\epsilon)\underbrace{\int_0^1 da\,a^{-\epsilon}\,(1-a)^{-\epsilon}}_{B(1-\epsilon,1-\epsilon)} \\
&= e^{\epsilon\gamma_E}\left(\frac{-p^2}{\mu^2}\right)^{-\epsilon}\Gamma(\epsilon)\,\frac{\Gamma(1-\epsilon)\Gamma(1-\epsilon)}{\Gamma(2-2\epsilon)} \\
&= \frac{1}{\epsilon} - \ln\left(\frac{-p^2}{\mu^2}\right) + 2 + \mathcal{O}(\epsilon).
\end{aligned}
\tag{3.26}
$$

Here, we see how the series expansion of $e^{\epsilon\gamma_E}$ cancels γ_E coming from $\Gamma(\epsilon) = \frac{1}{\epsilon} - \gamma_E + \mathcal{O}(\epsilon)$. In section 3.3.1 we obtain an expression for the massless bubble depending on general indices ν_1, ν_2 (3.39). The calculation with non-zero masses will not be shown here, we simply give the result in the appendix A.2.

The massive bubble will occur again in section 5.4.3 (see (5.42)) together with the massive tadpole, both taken in $D = (2 - 2\epsilon)$-dimensions. There, we develop versions of the bubble and the tadpole integral, which are more suited within the context of differential equations of Feynman integrals (section 3.5).

In summary, the one-loop example $H \to q\bar{q} \to H$ from fig.3.1 becomes in $D = 4 - 2\epsilon$ dimensions

$$
\begin{aligned}
\frac{ie^{-\epsilon\gamma_E}}{2^4 - 2\epsilon\pi^{2-\epsilon}}\frac{g^2 m_q^2}{m_W^2} \\
\left(\left(\mu^2\right)^{-\epsilon}\left(-2m_q^2 + \frac{s}{2}\right)B_{11}\left(D, p^2, m_q^2, m_q^2\right) + \left(\mu^2\right)^{1-\epsilon}T_1\left(4 - 2\epsilon, m_q^2\right)\right),
\end{aligned}
\tag{3.27}
$$

where the tadpole is given by (3.22) and the bubble by (A.1).

The methods we used for the example can be transferred to general one-loop integrals as calculations of one-loop diagrams all follow the same pattern:

1. After translating the diagram via Feynman rules, the resulting tensor integrals are reduced to scalar integrals, for example through Passarino-Veltman reduction. Scalar products containing the loop momentum in the numerator can be replaced with appropriate linear combinations of propagators and kinematic invariants.

2. Independent integrals have to be evaluated. Utilising Feynman's or Schwinger's trick transforms the product of propagators in their denominators into a sum. The integration variable is shifted, such that the integrand only depends on its square.

3. After Wick rotation, D-dimensional spherical coordinates come into play. The angular integration is trivial and for the radial integration Euler's gamma and beta functions are recognised.

4. The integration over Feynman or Schwinger parameter's remains.

As the procedure for 3. is always the same, it can be summarised in a formula (cf. [57], eq.(2.133)),

$$\int \frac{d^D k}{i\pi^{D/2}} \frac{(-k^2)^a}{(-Uk^2 + V)^\nu} = \frac{\Gamma\left(\frac{D}{2} + a\right) \Gamma\left(\nu - \frac{D}{2} - a\right)}{\Gamma\left(\frac{D}{2}\right)} \frac{U^{-\frac{D}{2} - a}}{\Gamma(\nu)} \frac{U^{-\frac{D}{2}-a}}{V^{\nu - \frac{D}{2} - a}}, \qquad (3.28)$$

where a is a scalar and U, V are polynomials independent of k.

3.3   Representations of Feynman integrals

In the preceding section, we derived a strategy to calculate one-loop integrals. Unfortunately, the evaluation of higher loop integrals is trickier. In preparation for the discussion of a widely used solution strategy, namely the method of differential equations, we will first take a look at different representations of Feynman integrals.

We have already seen the momentum representation of Feynman integrals (3.10) which more or less arises out of the application of Feynman rules. It will be the starting point for each representation introduced here. Hence, we quickly recapitulate it and we will keep its accompanying notation. Accordingly, each representation introduced and utilised in the following will be equivalent to (3.10) (and (3.29)). We work with l loops, n internal edges and in $D = D_0 - 2\epsilon$ dimensions where $D_0 \in \mathbb{N}$. The momentum representation is given by

$$I_{\nu_1 \nu_2 \ldots \nu_n} = e^{\epsilon l \gamma_E} \left(\mu^2\right)^{\nu - \frac{lD}{2}} \int \prod_{i=1}^{l} \frac{d^D k_i}{i\pi^{D/2}} \prod_{j=1}^{n} \frac{1}{P_j^{\nu_j}}, \quad P_j = (-q_j^2 + m_j^2), \qquad (3.29)$$

where $k_i, \; i = 1, \ldots l$ are the loop momenta and $q_j, m_j, \; j = 1, \ldots n$ are the internal momenta and masses corresponding to the propagators P_j which carry exponents $\nu_j \in \mathbb{Z}$, whereby $\nu = \sum_{j=1}^{n} \nu_j$. Furthermore, μ is the renormalisation scale with mass dimension one and γ_E is Euler's constant.

Additionally, we already gained an insight into the Feynman parameter representation of integrals in the previous section. We treated the integration over the loop momentum for an integration over a Feynman parameter as we applied Feynman's trick and evaluated the simplified momentum integration. In the upcoming subsection we briefly introduce the Schwinger and Feynman parameter representation in their full generality. Along the way, we encounter the graph polynomials $\mathcal{U}$, $\mathcal{F}$, which play an essential role within the method of differential equations. The graph polynomial $\mathcal{U}$ enables the construction

of dimensional shift relations between integrals and $\mathcal{F}$ helps constructing derivatives of Feynman integrals. Afterwards, we deal with another important representation of Feynman integrals, namely the Baikov representation. The Baikov representation as well as dimensional shift relations play a crucial role in the method of differential equations, as we will see later.

3.3.1 Schwinger and Feynman parameter representation

Schwinger and Feynman parameter representation of Feynman integrals simplify the integration over loop momenta at the cost of introducing auxiliary integrations. Both can be obtained from the momentum representation (3.29) through the application of either Schwinger's or Feynman's trick. The trick is applied to every propagator $P_j = \left(-q_j^2 + m_j^2\right)$, trading the product of propagators in the denominator of (3.29) for a sum. In the case of **Schwinger's trick**

$$\frac{1}{P_j^{\nu_j}} = \frac{1}{\Gamma(\nu)} \int_0^\infty d\alpha \, \alpha^{\nu-1} e^{-\alpha P_j}, \tag{3.30}$$

which follows from the definition of Euler's gamma function (3.16), this sum of propagators emerges in an exponential,

$$I \stackrel{(3.30)}{\sim} \int_{\alpha_j \geq 0} d^n \alpha \prod_{j=1}^n \alpha_j^{\nu_j - 1} \int \prod_{i=1}^l \frac{d^D k_i}{i\pi^{\frac{D}{2}}} \exp\left(-\sum_j^n \alpha_j \left(-q_j^2 + m_j^2\right)\right). \tag{3.31}$$

Now, each propagator is accompanied by an auxiliary integration variable, called Schwinger parameters α_j, $j = 1, \ldots, n$. The sum in the exponential is sorted by the dependence on loop momenta creating an $l \times l$ -matrix M, an l-dimensional vector v with linear combinations of the d-dimensional external momenta as entries and a scalar J,

$$\sum_j^n \alpha_j \left(-q_j^2 + m_j^2\right) = -\sum_{i=1}^l \sum_{m=1}^l k_i M_{im} k_m + \sum_{i=1}^l 2k_i \cdot v_i + J. \tag{3.32}$$

This enables the use of (3.33) (cf. [57] eq.(2.158)), which simplifies the integration over loop momenta in (3.31),

$$\int_{-\infty}^\infty dy_1 ... dy_n \exp\left(-\vec{y}^T A \vec{y} + 2\vec{w}^T \vec{y} + c\right) = \pi^{\frac{n}{2}} \det A^{-\frac{1}{2}} \exp\left(\vec{w}^T A^{-1} \vec{w} + c\right), \tag{3.33}$$

where A is an $n \times n$ -matrix and $\vec{w}$ is an n-dimensional vector.

Before we give the resulting representation, we define the **graph polynomials** in terms of M, v and J found in (3.32),

$$\mathcal{U} = \det(M),$$
$$\mathcal{F} = \frac{\det(M)}{\mu^2} \left(J + v^T m^{-1} v\right). \tag{3.34}$$

$\mathcal{U}$, also called 1st Symanzik polynomial, is a homogeneous polynomial of degree l in the Schwinger parameter's, whereas $\mathcal{F}$, the 2nd Symanzik polynomial, is of degree $l + 1$.

Finally, the **Schwinger parameter representation** of a Feynman diagram with l loops and n internal edges is given by

$$I = \frac{e^{\epsilon l \gamma_E}}{\prod\limits_{j=1}^{n} \Gamma(\nu_j)} \int_{\alpha_j \geq 0} d^n \alpha \prod_{j=1}^{n} \alpha_j^{\nu_j-1} \, \mathcal{U}^{-\frac{D}{2}} \exp\left(-\frac{\mathcal{F}(\alpha)}{\mathcal{U}(\alpha)}\right), \qquad (3.35)$$

where α_j are the Schwinger parameters and, as before, ν_j is the exponent of the jth propagator, ϵ is the dimensional regularisation parameter and γ_E is Euler's constant.

The **Feynman parameter representation** of a diagram with l loops and n internal edges is defined by

$$I = \frac{e^{\epsilon l \gamma_E} \Gamma\left(\nu - \frac{lD}{2}\right)}{\prod\limits_{j=1}^{n} \Gamma(\nu_j)} \int_{a_j \geq 0} d^n a \, \delta\left(1 - \sum_{j=1}^{n} a_j\right) \prod_{j=1}^{n} a_j^{\nu_j-1} \, \frac{\mathcal{U}(a)^{\nu - \frac{(l+1)D}{2}}}{\mathcal{F}(a)^{\nu - \frac{lD}{2}}}, \qquad (3.36)$$

where a_j, $j = 1, .., n$ are called Feynman parameters. Similar to the Schwinger parameter representation, it can be derived from momentum representation (3.29) with the help of Feynman's trick

$$\prod_{j=1}^{n} \frac{1}{P_j^{\nu_j}} = \frac{\Gamma(\nu)}{\prod\limits_{j=1}^{n} \Gamma(\nu_j)} \int_{a_j \geq 0} d^n a \, \delta\left(1 - \sum_{j=1}^{n} a_j\right) \frac{\prod_{j=1}^{n} a_j^{\nu_j-1}}{\left(\sum_{j=1}^{n} a_j P_j\right)^{\nu}}. \qquad (3.37)$$

Alternatively, (3.36) can be constructed from Schwinger parameter representation through the insertion of $1 = \int_0^{\infty} \delta\left(t - \sum_{j=1}^{n} \alpha_j\right) dt$ and the variable substitution $a_j = \frac{\alpha_j}{t}$.

Alternative ways of constructing the Symanzik polynomials exist. We mention a graphical approach here (cf. [65]). The result reveals the structures of the polynomials. $\mathcal{U}$ can be obtained from the spanning trees and $\mathcal{F}$ from the spanning 2-forests of the respective graph. A spanning tree T is a connected sub-graph without loops, that contains all vertices of the original graph. If a graph has l loops, l edges must be removed to obtain a spanning tree. Removing l edges in all possible ways, such that no vertices are lost, gives the set of spanning trees $\mathcal{T}_1$. If the deletion of $l + 1$ internal edges results in two connected tree-graphs (instead of one), we call it a spanning 2-forest (T_1, T_2). The corresponding set of all spanning 2-forests is denoted by $\mathcal{T}_2$. The Symanzik polynomials are given by

$$\mathcal{U} = \sum_{T \in \mathcal{T}_1} \prod_{e_i \notin T} a_i,$$

$$\mathcal{F} = \sum_{(T_1, T_2) \in \mathcal{T}_2} \left(\prod_{e_i \notin (T_1, T_2)} a_i\right) \left(\frac{-s_{(T_1, T_2)}}{\mu^2}\right) + \mathcal{U}(a) \sum_{i=1}^{n} a_i \frac{m_i^2}{\mu^2}, \qquad (3.38)$$

where a_i is the Feynman parameter corresponding to the deleted edge e_i and $s_{(T_1,T_2)}$ gives the square of the momenta flowing through all deleted edges of the respective spanning 2-forest. Now, we clearly see, that $\mathcal{U}$ is a homogeneous polynomial of degree l in Schwinger/Feynman parameters and $\mathcal{F}$ one of degree $l+1$. Additionally, we see, that $\mathcal{U}$ depends linearly on each Schwinger/Feynman parameter. This property plays a role in the construction of dimensional shift operators (see section 5.3). $\mathcal{F}$ is linear in the kinematic variables $\frac{-s_{(T_1,T_2)}}{\mu^2}, \frac{m_i^2}{\mu^2}$, which plays a role in the construction of a differential equation (see section 5.3.1).

We complete this subsection with an example, namely the one-loop bubble (fig.3.4) we already investigated in the prior subsection,

$$B_{\nu_1\nu_2}(p^2, m_1^2, m_2^2) = e^{\epsilon\gamma_E} \left(\mu^2\right)^{\nu-\frac{D}{2}} \int \frac{d^D k}{i\pi^{D/2}} \frac{1}{\left(-k^2 + m_1^2\right)^{\nu_1} \left(-(k-p)^2 + m_2^2\right)^{\nu_2}}.$$

The Feynman parameter representation of the one-loop bubble is given by

$$B_{\nu_1\nu_2}(p^2, m_1^2, m_2^2) =$$
$$\frac{e^{\epsilon\gamma_E}\Gamma\left(\nu-\frac{D}{2}\right)}{\Gamma(\nu_1)\Gamma(\nu_2)} \int_0^\infty da_1 \int_0^\infty da_2 \, \delta\left(1-(a_1+a_2)\right) a_1^{\nu_1-1} a_2^{\nu_2-1} \frac{\mathcal{U}(a)^{\nu-D}}{\mathcal{F}(a)^{\nu-\frac{D}{2}}},$$
$$\mathcal{U} = a_1 + a_2,$$
$$\mathcal{F} = a_1 a_2 \left(\frac{-p^2}{\mu^2}\right) + (a_1 + a_2)\left(a_1 \frac{m_1}{\mu^2} + a_2 \frac{m_2}{\mu^2}\right).$$

Here, we found the graph polynomials $\mathcal{U}$ and $\mathcal{F}$ with the just described method. In the massless case, we easily calculate the Feynman representation of the bubble integral,

$$B_{\nu_1\nu_2}(p^2, 0, 0) = \frac{e^{\epsilon\gamma_E}\Gamma\left(\nu-\frac{D}{2}\right)}{\Gamma(\nu_1)\Gamma(\nu_2)} \left(\frac{-p^2}{\mu^2}\right)^{\frac{D}{2}-\nu} \int_0^\infty da_1 \, a_1^{\nu_1-1}(1-a_1)^{\nu_2-1} \frac{(a_1+1-a_1)^{\nu-D}}{a_1^{\nu-\frac{D}{2}}(1-a_1)^{\nu-\frac{D}{2}}}$$
$$= \frac{e^{\epsilon\gamma_E}\Gamma\left(\nu-\frac{D}{2}\right)}{\Gamma(\nu_1)\Gamma(\nu_2)} \left(\frac{-p^2}{\mu^2}\right)^{\frac{D}{2}-\nu} \underbrace{\int_0^\infty da_1 \, a_1^{\frac{D}{2}-1-\nu_2}(1-a_1)^{\frac{D}{2}-1-\nu_1}}_{B\left(\frac{D}{2}-\nu_2, \frac{D}{2}-\nu_1\right)}.$$

We recognise Euler's beta function (3.20) and, therefore, find a general solution for the massless one-loop bubble,

$$B_{\nu_1\nu_2}(p^2, 0, 0) = \left(\frac{-p^2}{\mu^2}\right)^{\frac{D}{2}-\nu} \frac{e^{\epsilon\gamma_E}\Gamma\left(\nu-\frac{D}{2}\right)}{\Gamma(\nu_1)\Gamma(\nu_2)} \frac{\Gamma\left(\frac{D}{2}-\nu_2\right)\Gamma\left(\frac{D}{2}-\nu_1\right)}{\Gamma(D-\nu)}. \tag{3.39}$$

3.3.2 Baikov representation of Feynman integrals

In addition to momentum, Feynman and Schwinger parameter representation, we introduce a last representation of Feynman integrals, the Baikov representation [66]. The Baikov representation may be utilised to determine the maximal cut of a Feynman integral, which plays a key role in the solution strategy within the method of differential

equations applied in this thesis. We will discuss the method of differential equations designed for calculating Feynman integrals in section 3.5 and maximal cuts in section 3.6.1.

The Baikov representation treats the integration over loop momenta for the integration over propagators. This transition is split into a change from momentum integration to integration over scalar products involving loop momenta and a subsequent change to integration over propagators to simplify the development of the Baikov representation. We summarise the independent scalar products involving loop momenta in

$$\sigma = (\sigma_1, \ldots, \sigma_{N_{scp}}) = (-k_1 \cdot k_1, -k_1 \cdot k_2, \ldots, -k_l \cdot k_l, -k_1 \cdot p_1, \ldots, -k_l \cdot p_e).$$

The number of scalar products N_{scp}, i.e. the length of σ was given in the beginning of this chapter in (3.9). A propagator belonging to edge i is given by

$$z_i = -q_i^2 + m_i,$$

where m_i denotes the mass of edge i and q_i its momentum. As we seek for an integration over propagators, we call z_i a **Baikov variable**. The number of Baikov variables is given by the number of internal edges n. We may summarise our strategy for the derivation of the Baikov representation as

$$d^D k_i \to d^{N_{scp}} \sigma \to d^n z.$$

The second transition requires a topology where every σ_i is uniquely expressible in terms of propagators (see (3.40)). The Baikov representation is, therefore, only applicable for topologies which have the same amount of propagators as independent scalar products involving loop momenta,

$$n \overset{!}{=} N_{scp}.$$

In the beginning of this chapter we discussed, how we may always find an auxiliary topology with appropriate propagators if the original number of edges deceeds N_{scp}. In this way we are always able to stretch our starting conditions and, thus, convert to the Baikov representation.

In the beginning of this chapter we also discussed how scalar products involving loop momenta are expressible in terms of propagators. In correspondence, we may write

$$z_i = C_{ij}\sigma_j + f_i, \tag{3.40}$$

with an invertible $n \times n$-dimensional matrix C and an n-dimensional vector f free of loop momenta.

Now, we are able to determine the Baikov representation for the one-loop case

$$\sigma = (-k \cdot k, -k \cdot p_1, \ldots, -k \cdot p_e).$$

The multi-loop case can then be obtained through iterative application of the one-loop procedure. To find the Baikov representation from an integral in momentum representation,

$$I \sim \int \frac{d^D k}{i\pi^{D/2}} \prod_{j=1}^{n} z_j^{-\nu_j},$$

we first seek for a transfer from the integration over loop momenta to an integration over σ. We decompose the loop momentum into a part parallel to the space spanned by external momenta and an orthogonal part,

$$k = k_{\parallel} + k_{\perp}, \quad k_{\parallel} \in \langle p_1, \ldots, p_e \rangle,$$

in order to treat them separately. Additionally, we go to Euclidean space, implying for the measure

$$d^D k = d^e k_{\parallel} d^{D-e} k_{\perp} = i d^e K_{\parallel} d^{D-e} K_{\perp},$$

where e is the number of independent external momenta and consequently the dimension of the parallel space. A scalar product of the orthogonal part of the loop momentum with external momenta vanishes by definition, hence, the orthogonal part survives only as a square in the integrand. Accordingly, it is natural to switch to spherical coordinates. The angular integrations in orthogonal space is then performed straightforwardly,

$$d^{D-e} K_{\perp} = \frac{\pi^{\frac{D-e}{2}}}{\Gamma\left(\frac{D-e}{2}\right)} \left(K_{\perp}^2\right)^{\frac{D-e-2}{2}} dK_{\perp}^2.$$

Additionally, we may trade the integration over $K_{\perp}^2$ for the integration over $\sigma_1 = K^2$,

$$dK_{\perp}^2 = d\sigma_1,$$

and express the squared orthogonal part in terms of scalar products,

$$K_{\perp}^2 = \frac{\det G^{eucl.}(K, P_1, \ldots, P_e)}{\det G^{eucl.}(P_1, \ldots, P_e)} = \frac{\det G(k, p_1, \ldots, p_e)}{\det G(p_1, \ldots, p_e)}.$$

Here, the **Gram determinant** $\det G$ and the Euclidean Gram determinant $\det G^{eucl.}$ are defined by

$$\det G(q_1, \ldots, q_e) = \det\left(-q_i \cdot q_j\right) = \det\left(Q_i \cdot Q_j\right) = \det G^{eucl.}(Q_1, \ldots, Q_e). \tag{3.41}$$

The parallel part remains. We may change integration variables in parallel space to $(\sigma_2, \ldots, \sigma_{e+1}) = (K \cdot P_1, \ldots, K \cdot P_e)$,

$$d^e K_{\parallel} = \det J^{-1} d\sigma_2 \ldots d\sigma_{e+1},$$

$$\det J = \det\left(\frac{\partial(\sigma_2, \ldots, \sigma_{e+1})}{\partial(K^0, \ldots, K^{e-1})}\right) = \sqrt{\det G(p_1, \ldots, p_e)}.$$

In the final step, we change variables from scalar products σ to Baikov variables z with the help of (3.40), which yields a Jacobian $\det C = \frac{\partial z}{\partial \sigma}$. For the complete measure we obtain

$$\frac{d^D k}{i\pi^{\frac{D}{2}}} = \frac{\det G(p_1, \ldots, p_e)^{\frac{-D+e+1}{2}}}{\pi^{\frac{e}{2}}(\det C)\Gamma\left(\frac{D-e}{2}\right)} \det G(k, p_1, \ldots, p_e)^{\frac{D-e-2}{2}} d^{N_{scp}} z. \tag{3.42}$$

In the one loop case, the number of Baikov variables is given by $N_{scp} = e + 1$. To emphasise, that Gram determinants are expressed in terms of Baikov variables, we replace

$$\mathcal{B}(z) = \det G(k_1, \ldots, k_l, p_1, \ldots, p_e) \tag{3.43}$$

and call $\mathcal{B}$ **Baikov polynomial**. The variable z represents all Baikov variables $z_1, \ldots, z_{N_{scp}}$.

The l-loop **Baikov representation** may be developed iteratively from (3.42), it amounts to

$$I_{\nu_1,\ldots,\nu_n} = \frac{e^{\epsilon l \gamma_E} \left(\mu^2\right)^{\nu - \frac{lD}{2}} \det G\left(p_1, \ldots, p_e\right)^{\frac{-D+e+1}{2}}}{\pi^{\frac{1}{2}(n-l)} \det(C) \prod_{i=1}^{l} \Gamma\left(\frac{D - e + 1 - i}{2}\right)} \int_{\mathcal{C}} d^n z \, \mathcal{B}(z)^{\frac{D-l-e-1}{2}} \prod_{j=1}^{n} z_j^{-\nu_j}. \quad (3.44)$$

The rather complicated integration domain is given by

$$\mathcal{C} = \mathcal{C}_1 \cap \mathcal{C}_2 \cap \ldots \cap \mathcal{C}_l,$$
$$\mathcal{C}_i = \left\{ \frac{\det G\left(k_j, \ldots, k_l, p_1, \ldots, p_e\right)}{\det G\left(k_{j+1}, \ldots, k_l, p_1, \ldots, p_e\right)} \geq 0 \right\}. \quad (3.45)$$

3.4 Master integrals and the Laporta algorithm

After the introduction of the graph polynomials (3.34),(3.38) and the Baikov representation (3.44), we proceed with the calculation of Feynman integrals beyond one-loop. We already discussed the concept of auxiliary topologies and the Passarino-Veltman reduction technique in the beginning of this chapter. Both are utilised in a first simplification step of the calculation process, namely the conversion of tensor integrals obtained from Feynman rules to scalar integrals. This conversion may generate a huge number of scalar integrals. We have seen in the one-loop example from the beginning of this chapter (fig.3.1), how one tensor integral gave rise to three scalar integrals (3.7). Beyond one-loop the numbers become far greater (see for example section 6.4, page 145).

Before we actually calculate any Feynman integrals we want to reduce their number. This can be achieved with the help of the Laporta algorithm [67], which starts with a set of scalar Feynman integrals and returns a smaller set of so-called master integrals. It constructs relations between integrals, such that "more complicated" integrals can be erased in favour of "simpler" integrals. To define simplicity in the context of Feynman integrals, we introduce some classifying variables in the following subsection. Afterwards, we discuss how integration by parts helps relating integrals to "simpler" integrals.

3.4.1 Sectors

We recall, that any scalar Feynman integral $I_{\nu_1 \nu_2 \ldots \nu_n}$ of a certain integral family is completely determined by its indices ν_i, which are the exponents of its n propagators. A set of integrals with common propagators in the denominator, i.e. with a common set $\{\nu_i > 0\}$, is called a **sector**. Each sector can be drawn as a graph consisting of all edges i that correspond to $\nu_i > 0$. In section 3.6, we will see how sectors appear as blocks inside the system of differential equations of master integrals. Integrals within a sector differ by their irreducible scalar products, i.e. propagators with negative exponents, and

the actual values of their positive indices. The **sector identity**

$$S_{ID} = \sum_{j=1}^{n} 2^{j-1} \Theta \left(\nu_j - \frac{1}{2} \right), \tag{3.46}$$

characterises each sector and simplifies the assignment of integrals. Θ is the Heaviside step-function. If we refer to a sector by a number we always talk about its sector identity. The number of propagators with positive powers

$$N_{\text{prop}} = \sum_{j=1}^{n} \Theta \left(\nu_j - \frac{1}{2} \right), \tag{3.47}$$

gives the length of the set $\{\nu_i > 0\}$. In the calculation of a Feynman diagram, the transition from tensor integrals to scalar integrals naturally gives rise to sub-sectors of the diagram of interest. The diagram of interest defines the **top sector**, possessing the largest set of positive indices,

$$N_{\text{prop,top sector}} = N_{\text{prop,max}},$$
$$S_{ID,\text{top sector}} = S_{ID,\text{max}}.$$

A **sub-sector** is obtained as propagators and thereby edges of the graph get pinched, manifested through zero indices in the integral representation. Every sub-sector is, therefore, defined through a subset $\{\nu_i > 0\}$ of the original set and corresponds to a sub-graph of the original graph.

The Laporta algorithm demands a sorting of integrals according to their simplicity. Hence, we have to define criteria for simplicity. Integrals with more propagators, i.e. a greater N_{prop}, are naturally more difficult. We deduce, that integrals from the top sector are most challenging. We further deduce, that N_{prop} gives a good first sorting criterion. Sectors with the same amount of propagators can be arranged according to their sector identity, where we choose to start with the smallest S_{ID}.

In order to be able to sort integrals within their sectors, we introduce the following variables:

$$r = \sum_{j=1}^{n} \nu_j \Theta \left(\nu_j - \frac{1}{2} \right), \tag{3.48}$$

$$s = \sum_{j=1}^{n} |\nu_j| \Theta \left(-\nu_j + \frac{1}{2} \right), \tag{3.49}$$

r sums all positive and s all negative indices. Integrals with smaller propagator powers within one sector give rise to smaller r or s and are considered simpler. It follows that integrals can be ordered lexicographically, for example with respect to

$$(N_{\text{prop}}, S_{ID}, r, s, \dots). \tag{3.50}$$

41

3.4.2 Integration by parts

The second main ingredient of Laporta's algorithm besides the classification of integrals are relations among the integrals, which can be found from integration by parts identities or symmetry relations. Integration by parts identities [25, 26] rely on the fact that the integral of a total derivative vanishes within dimensional regularisation,

$$\int d^D k \frac{\partial}{\partial k^\mu} v^\mu f(k, p_i) = 0, \tag{3.51}$$

where $v^\mu = k^\mu, p_i^\mu$ or any linear combination thereof, implying the absence of boundary terms. For Feynman integrals,

$$e^{\epsilon l \gamma_E} \left(\mu^2\right)^{\nu - \frac{lD}{2}} \int \prod_{i=1}^{l} \frac{d^D k_i}{i \pi^{D/2}} \frac{\partial}{\partial k_l^\mu} v^\mu \prod_{j=1}^{n} \frac{1}{(-q_j^2 + m_j^2)^{\nu_j}} = 0, \tag{3.52}$$

follows right away, with v^μ being any vector consisting of loop and external momenta. Inserting different sets $\{\nu_i\}$ and vectors v^μ into (3.52) yields various relations between integrals, which are then called **integration by parts identities**.

After obtaining all integration by parts identities (and symmetry relations) of a set of Feynman integrals, each integral can be replaced by combinations of simpler integrals according to the ordering relation (3.50). Only a small subset of integrals is left behind. These are called **master integrals**. The substitutions have the following structure,

$$I_i = \sum_{j}^{N_{MI}} c_{i,j} I'_j, \tag{3.53}$$

where I_i is the integral which gets expressed in terms of master integrals I'_j, and N_{MI} denotes the number of master integrals. The rational coefficients $c_{i,j}$ depend on products of masses, the invariant external momenta squared and the dimension D.

The master integrals form a basis, hence their number N_{MI} is fixed. However, the choice of basis is not unique. The numbering of edges as well as the specified order criteria influence the gained basis. For example, swapping r and s in (3.50) also leads to a possible order relation, but results into different master integrals. Viewing the ordered set of master integrals as a vector

$$\vec{I'} = \left(I'_1, \ldots, I'_{N_{MI}}\right)^T,$$

transformations between different bases are written as

$$\vec{I'} = U \vec{J}, \tag{3.54}$$

with U being an $N_{MI} \times N_{MI}$-dimensional transformation matrix. Some bases are easier to evaluate then others. Finding a suitable basis J of master integrals is one of the main tasks during the evaluation of Feynman diagrams. A canonical basis is particularly suited, as we will see in the following section. There, we will explore the method of differential equations. This method relies on the ability to reduce Feynman integrals to a small set of master integrals, i.e. it relies on integration by parts reduction techniques.

3.5 The method of differential equations

In the previous section we deduced that several scalar Feynman integrals, which emerged during the evaluation of Feynman diagrams, can be eliminated in favour of a minimal set of integrals. These master integrals are found with the help of the Laporta algorithm. The ordered set of master integrals is usually denoted by a vector

$$\vec{I} = (I_1, \ldots, I_{N_{MI}})^T \, .$$

The calculation of $\vec{I}$ remains to be done. A particularly efficient method of deriving master integrals is the method of differential equations [27–30], which circumvents the need of direct integration over loop momenta. As reflected by the method's name, a system of first order differential equations of master integrals with respect to kinematic variables is set up and solved.

The first step within the method of differential equations is clearly setting up differential equations with respect to kinematic variables. Each master integral kinematically depends on internal masses and products of external momenta. We remember from (3.10) and (3.11) that scaling the integrals with the renormalisation constant μ^2 yields dimensionless kinematic variables,

$$\frac{p_i \cdot p_j}{\mu^2}, \quad \frac{m_i^2}{\mu^2}.$$

μ^2 is set to be either an internal mass squared or a product of external momenta, more specifically a mandelstam variable, reducing the number of kinematic variables by one (see (3.12)). In the following we call the kinematic variables

$$x_1, \ldots, x_{N_v}.$$

A derivative with respect to a variable corresponding to a mass, like $x_i = \frac{m_i^2}{\mu^2}$, is derived as follows. We recall the momentum representation of Feynman integrals from (3.29),

$$I = I_{\nu_1 \nu_2 \ldots \nu_n} = e^{\epsilon l \gamma_E} \left(\mu^2 \right)^{\nu - \frac{lD}{2}} \int \prod_{r=1}^{l} \frac{d^D k_r}{i \pi^{D/2}} \prod_{j=1}^{n} \frac{1}{(-q_j^2 + m_j^2)^{\nu_j}}, \qquad (3.55)$$

where $\nu = \sum_j^n \nu_j$. If only one propagator carries m_i^2 we deduce

$$\begin{aligned}
\frac{\partial}{\partial x_i} I &= \mu^2 \frac{\partial}{\partial m_i^2} I_{\nu_1 \nu_2 \ldots \nu_n} \\
&= e^{\epsilon l \gamma_E} \left(\mu^2 \right)^{\nu + 1 - \frac{lD}{2}} \int \prod_{r=1}^{l} \frac{d^D k_r}{i \pi^{D/2}} \left(\frac{\partial}{\partial m_i^2} \frac{1}{(-q_i^2 + m_i^2)^{\nu_i}} \right) \prod_{j \neq i} \frac{1}{(-q_j^2 + m_j^2)^{\nu_j}} \\
&= e^{\epsilon l \gamma_E} \left(\mu^2 \right)^{\nu + 1 - \frac{lD}{2}} \int \prod_{r=1}^{l} \frac{d^D k_r}{i \pi^{D/2}} \left(\frac{-\nu_i}{(-q_i^2 + m_i^2)^{\nu_i + 1}} \right) \prod_{j \neq i} \frac{1}{(-q_j^2 + m_j^2)^{\nu_j}} \\
&= -\nu_i \, I_{\ldots (\nu_i + 1) \ldots} .
\end{aligned} \qquad (3.56)$$

43

We introduce the **raising operator** $\boldsymbol{j^+}$, which raises the power of the j-th propagator by one and multiplies by its previous power ν_j,

$$\boldsymbol{j^+} I_{...,\nu_j,...} = \nu_j \cdot I_{...,(\nu_j+1),...}. \tag{3.57}$$

Afterwards, equation (3.56) can be summarised as

$$\mu^2 \frac{\partial}{\partial m_i^2} I = -\boldsymbol{i^+} I.$$

The extension to multiple propagators carrying m_i^2 utilises the product rule. The derivative is expressed as a sum over all edges j which carry mass m_i^2. These edges are collected in the set $J_{m_i^2}$, and we obtain

$$\mu^2 \frac{\partial}{\partial m_i^2} I = - \sum_{j \in J_{m_i^2}} \boldsymbol{i^+} I.$$

This equation is true for every integral from the same family of Feynman integrals, hence, we write for the basis integrals $\vec{I} = (I_1, \ldots, I_{N_{MI}})^T$

$$\mu^2 \frac{\partial}{\partial m_i^2} \vec{I} = - \sum_{j \in J_{m_i^2}} \boldsymbol{j^+} \vec{I}. \tag{3.58}$$

If different topologies, i.e. different sets of propagators, are joined within one vector of master integrals the sets $J_{m_i^2}$ have to be chosen accordingly.

The integrals appearing in the sum on the right hand side of (3.58) have additional dots compared to the basis integrals, but they are again expressible as linear combinations of master integrals via the Laporta algorithm (see section 3.4). Equation (3.58) can be rewritten,

$$\mu^2 \frac{\partial}{\partial m_i^2} \vec{I} = A_{m_i^2} \vec{I}, \tag{3.59}$$

where $A_{m_i^2}$ is an $N_{MI} \times N_{MI}$- dimensional matrix, containing kinematic variables and the dimension D.

Setting up differential equations with respect to variables, which do not correspond to a mass, will be described as needed in section 5.3.1 (see especially (5.13)). In the end, any differential equation of the master integrals with respect to a variable x_i can be displayed as

$$\frac{\partial}{\partial x_i} \vec{I} = A_{x_i}(D, x_1, \ldots, x_{N_v}) \vec{I}, \tag{3.60}$$

with A_{x_i} being an $N_{MI} \times N_{MI}$- dimensional matrix, containing kinematic variables and the dimension D. The matrices A_{x_i} are lower block-triangular matrices if the master integrals are ordered according to the order relation (for example (3.50)) within the Laporta algorithm. The order relation primarily sorts integrals by their number of edges

and their sectors, such that the first few integrals in the vector $\vec{I}$ belong to the simplest sector. Hence, reductions of integrals and their derivatives within the lowest sector only generate integrals in the same sector. In other words, differential equations of the master integrals belonging to the first sector are homogeneous. This gives rise to a block matrix in the upper left corner of the differential equation of the full vector $\vec{I}$. In accordance, all sectors appear as blocks on the diagonal of A_{x_i}. The matrices become lower block-triangular, since the reductions of integrals in higher sectors include integrals of simpler sectors.

All differential equations (3.60) of the master integrals $\vec{I} = (I_1, \ldots, I_{N_{MI}})^T$ with respect to each kinematic variable $x_1, \ldots, x_{N_v}$ are combined into **the system of first-order differential equations**

$$d\vec{I} = A\vec{I}, \tag{3.61}$$

where the matrix-valued one-form A is defined by

$$A = \sum_i^{N_v} A_{x_i}(D, x_1, \ldots, x_{N_v}) \ dx_i, \tag{3.62}$$

and the total derivative is given by

$$dI_i = \sum_j^{N_v} \left(\frac{\partial I_i}{\partial x_j} \right) dx_j. \tag{3.63}$$

The system (3.61) is integrable, hence, the following **integrability condition** must hold,

$$\partial_{x_n} A_{x_m} - \partial_{x_m} A_{x_n} - [A_{x_n}, A_{x_m}] = 0, \quad n, m = 1, \ldots, N_v, \tag{3.64}$$

where $[,]$ denotes the commutator,

$$[A, B] = A \cdot B - B \cdot A.$$

A general solution to (3.61) can be written as an infinite series, where the j-th term is given by a j-fold iterated integral (cf. [31, 57]),

$$\vec{I} = \mathbb{P}\exp\left[\int_\gamma A \right] \vec{I}_0, \tag{3.65}$$

$\mathbb{P}$ denotes the path ordering operator with respect to an integration contour γ. $\vec{I}_0$ denotes the value of $\vec{I}$ at the boundary point determined by γ. However, due to the lack of a truncation criterion the infinite series in (3.65) yields no practical solution to (3.61). It follows, that we seek a solution strategy providing an appropriate truncation criterion.

Before we discuss such a solution strategy for (3.61) in the next subsection, we want to make a note on the dependence of the matrices A_x on kinematic variables x following [60] especially chapters 2.3&4.1 and [57] chapter 7.1.5. The differential equations

(3.60) are build up from Feynman integrals, hence, their properties put restrictions on A_x. Singular points x_k in the differential equation must arise from singularities of the original integrals. The leading behaviour of Feynman integrals is expected to grow like $\sim (x - x_k)^j$ for some j. In correspondence, the differential equations should only have regular singularities and the series expansion of Feynman integrals should only have a finite number of terms with negative exponent. If A_x depends rationally on x, we may write

$$A_x = \sum_{x_k \in S} \sum_{j}^{o_{x_k}} A_{x_k,j} \frac{1}{(x - x_k)^j} + \text{terms non-singular in } x, \qquad (3.66)$$

where $A_{x_k,j}$ denote matrices free of x and rational in the dimension, S the set of all singular points and o_{x_k} the order of the pole at x_k. Under conditions which are usually fulfilled in the context of Feynman integrals, the poles in (3.66) may be removed successively utilising Moser's algorithm [68–70]. Hence, the rational matrix A_x can be transformed to Fuchsian form,

$$A_x = \sum_{x_k \in S} A_{x_k,1} \frac{1}{(x - x_k)}. \qquad (3.67)$$

3.5.1 The canonical form of differential equations

Now, the first step of the method of differential equations, namely setting up a system of first-order differential equations with respect to kinematic variables (3.61), is completed. The second step consists of finding a solution for the system and, therefore, for the master integrals. In the following, we discuss a key method within the context of solving differential equations of Feynman integrals. The main idea is the conversion of differential equations into canonical differential equations, which are linear in the dimensional regularisation parameter [31]. The homogeneous solution of a canonical differential equation is trivial in the limit $\epsilon = \frac{4-D}{2} \to 0$. This reduces the problem of finding a solution to the problem of finding an appropriate basis of master integrals which transforms the differential equation accordingly. (Box 1 in section 3.6 provides a concise summary on the transformation to canonical differential equations.)

After starting this section with a short motivation, we bring a system of differential equations into ϵ-form via basis transformations and variable transformations. We define the ϵ-form, which is determined by its letters. Furthermore, we sketch a solution process leading to iterated integrals and give a first notion on weight properties.

We recall, that master integrals are functions of kinematic variables and the dimensional regularisation parameter ϵ. We may motivate the technique of canonical differential equations as we look at the general solution of (non-canonical) differential equations (3.58). The general solution consists of an infinite series of iterated integrals, which lacks an appropriate truncation criterion. However, under a conversion to a differential equation with linear dependence on ϵ,

$$A(\epsilon, x_1, \ldots, x_{N_v}) \to \epsilon \tilde{A}(x_1, \ldots, x_{N_v}),$$

the general solution transforms as

$$\vec{I} = \mathbb{P}\exp\left[\int_\gamma A\left(\epsilon, x_1, \ldots\right)\right]\vec{I}_0 \;\rightarrow\; \vec{J} = \mathbb{P}\exp\left[\int_\gamma \epsilon\tilde{A}\left(x_1, \ldots\right)\right]\vec{J}_0, \qquad (3.68)$$

again $\mathbb{P}$ denotes the path ordering operator with respect to an integration contour γ. $\vec{I}_0/\vec{J}_0$ denote values of $\vec{I}/\vec{J}$ at the boundary point determined by γ. The series becomes a series in ϵ, hence, an appropriate truncation criterion is determined by the required order in ϵ! Before we go into details, we already observe an important property of the transformed general solution. Each series coefficient consists of iterated integrals of same transcendental weight, i.e. iterated integrals of same depth.

Let us look at the details of such a transformation. We start with the set of N_{MI} master integrals $\vec{I}$ and their system of differential equations, that we found in the preceding section

$$d\vec{I} = A\vec{I},$$

$$A = \sum_i^{N_v} A_{x_i}(\epsilon, x_1, \ldots, x_{N_v})\; dx_i.$$

We apply a **basis transformation** given by a $N_{MI} \times N_{MI}$- dimensional matrix U, which depends (rationally) on ϵ and the kinematic variables,

$$\vec{I} = U\left(\epsilon, x_1, \ldots, x_{N_v}\right)\vec{J}$$
$$\Rightarrow d\left(U^{-1}\vec{J}\right) = A\left(U^{-1}\vec{J}\right)$$
$$\Rightarrow \left(UdU^{-1}\right)\vec{J} + d\vec{J} = \left(UAU^{-1}\right)\vec{J}$$
$$\Rightarrow d\vec{J} = A'\vec{J}, \qquad (3.69)$$

where the transformed matrix-valued one-form is given by

$$A' = UAU^{-1} - UdU^{-1}. \qquad (3.70)$$

In accordance with our motivation, we search for a transformation which yields a matrix A' purely linear in the dimensional regularisation parameter,

$$A'\left(\epsilon, x_1, \ldots, x_{N_v}\right) = \epsilon\tilde{A}\left(x_1, \ldots, x_{N_v}\right).$$

If $\tilde{A}$ additionally fulfils

$$\tilde{A} = \sum_i C_i\omega_i, \qquad (3.71)$$

where C_i are $N_{MI} \times N_{MI}$- dimensional matrices consisting of algebraic numbers and ω_i are differential one-forms containing only simple poles, we call $\vec{J}$ a **canonical basis** of master integrals. Furthermore, the non-zero boundary constants of $\tilde{A}$ have to be of uniform weight zero (description further on). The resulting system of differential equations

$$d\vec{J} = \epsilon\tilde{A}\left(x_1, \ldots, x_{N_v}\right)\vec{J} = \epsilon\sum_i C_i\omega_i\vec{J} \qquad (3.72)$$

is named a canonical or **ϵ-form of differential equations**.

The differential one-forms ω_i are called **letters** and the set of all independent letters sufficient to express $\tilde{A}$ is called alphabet. A simple but frequently occurring example of a letter is

$$\omega = \frac{dx}{x}.$$

It has only a single pole as required and can, therefore, be expressed in terms of a dlog-form

$$\omega = \text{dlog}\,(x)\,. \tag{3.73}$$

In general, we seek for an alphabet completely consisting of dlog-forms, i.e. letters of the form

$$\omega_i = \text{dlog}\,(f_i\,(x_1,\ldots,x_{N_v}))\,, \tag{3.74}$$

where f_i denotes rational functions depending on the kinematic variables.

It may happen, that only a non-rational basis transformation U (3.69) causing a linear dependence in ϵ can be found. This leads to square roots in arguments of some dlog-forms. The condition of differential one-forms which have only simple poles is not fulfilled. To solve this issue, a coordinate transformation must be applied. This **variable transformation** has to rationalise all square roots, i.e. it has to lead to a square under each square root. An example is given by

$$r = \sqrt{-x(4-x)} \;\;\longrightarrow\;\; x = \frac{-(1-x')^2}{x'} \;\;\longrightarrow\;\; r = \frac{1-x'^2}{x'}.$$

In section 3.6.2 we will obtain this example explicitly (see especially (3.96)), as we will describe a general method to find appropriate variable transformations.

The ϵ-form of differential equations is particularly nice, since it can be solved straightforwardly order by order in ϵ. For this purpose, the master integrals $\vec{J} = (J_1,\ldots,J_{N_{MI}})$ are expanded as a Laurent-series in ϵ,

$$J_i = \sum_{j=j_{\min}}^{\infty} J_i^{(j)}\epsilon^j = \epsilon^{j_{\min}} J_i^{(j_{\min})} + \ldots, \tag{3.75}$$

where $j_{\min}$ might be negative, but finite. The starting term is explicitly written to demonstrate, that we can force the expansion of any master integral to start with an ϵ^0-term, simply through a redefinition $J_i \to \epsilon^{-j_{\min}} J_i$. Now the set of canonical master integrals can be viewed as

$$\vec{J} = \begin{pmatrix} \epsilon^0 J_1^{(0)} + \epsilon J_1^{(1)} + \epsilon^2 J_1^{(2)} + \ldots \\ \ldots \\ \epsilon^0 J_{N_{MI}}^{(0)} + \epsilon J_{N_{MI}}^{(1)} + \epsilon^2 J_{N_{MI}}^{(2)} + \ldots \end{pmatrix}. \tag{3.76}$$

Inserting (3.76) into the differential equation (3.72), we find

$$
d\begin{pmatrix} \epsilon^0 J_1^{(0)} + \epsilon^1 J_1^{(1)} + \epsilon^2 J_1^{(2)} + ... \\ \dots \\ \epsilon^0 J_{N_{MI}}^{(0)} + \epsilon^1 J_{N_{MI}}^{(1)} + \epsilon^2 J_{N_{MI}}^{(2)} + ... \end{pmatrix} = \sum_i C_i \omega_i \begin{pmatrix} \epsilon^1 J_1^{(0)} + \epsilon^2 J_1^{(1)} + \epsilon^3 J_1^{(2)} + ... \\ \dots \\ \epsilon^1 J_{N_{MI}}^{(0)} + \epsilon^2 J_{N_{MI}}^{(1)} + \epsilon^3 J_{N_{MI}}^{(2)} + ... \end{pmatrix}.
$$
(3.77)

The resulting system of differential equations is solved order by order in ϵ, starting with ϵ^0. We see, that the right hand side of (3.77) has no ϵ^0-terms as opposed to the left hand side,

$$
d\vec{J}^{(0)} = 0.
$$

Hence, the integrations of $dJ_i^{(0)}$ yield constants. These are determined by **boundary conditions**, i.e. values of the master integrals at specific kinematic configurations: One kinematic variable is set to be a certain value, making the calculation of boundary conditions simpler. Next, we compare the terms proportional to ϵ on the left and right hand side of (3.77) and conclude

$$
d\vec{J}^{(q+1)} = \sum_i C_i \omega_i \, \vec{J}^{(q)}.
$$
(3.78)

Since we know $\vec{J}^{(0)}$, we can find $\vec{J}^{(1)}$ through integration. The result is an iterated integral of depth one plus an integration constant, which is again determined by boundary conditions (see for example (3.81)). Proceeding with the integration of $d\vec{J}^{(2)}$ using the result obtained for $\vec{J}^{(1)}$, we successively find solutions for all $\vec{J}^{(i)}$ in terms of iterated integrals of depth $\leq i$.

The **iterated integrals**, appearing in the solutions of $\vec{J}$, are specified by ordered sequences of letters ω_i,

$$
\int_{\gamma:[0,1]\to M} \omega_1 \dots \omega_n = \int_{0\leq t_1 \leq \dots \leq t_n \leq 1} f_1(t_1)\, dt_1 \dots f_n(t_n)\, dt_n,
$$
(3.79)

where M is a smooth manifold over $\mathbb{R}$, and $f_i(t_i)\, dt_i$ denotes the pull back of ω_i to the interval $[0, 1]$ (cf. [71]). n corresponds to the depth of the iterated integral. If $n = 0$ the integral equals 1 by definition. To give a simple example we return to (3.73)

$$
\omega_0 = \frac{dx}{x}.
$$

The iterated integral

$$
\int_\gamma \omega_0 = \log(x) - \log(x_0)
$$

solely depends on the endpoints of γ, namely $\gamma(0) = x_0$ and $\gamma(1) = x$. We elaborate

$$
\int_\gamma \underbrace{\omega_0 \dots \omega_0}_{r \text{ times}} = \frac{1}{r!}\left(\int_\gamma \omega_0\right)^r = \frac{1}{r!}\left(\log(x) - \log(x_0)\right)^r,
$$

which follows from the so-called shuffle product. A **shuffle product** for iterated integrals (3.79) is defined by

$$\int_\gamma \omega_1 \ldots \omega_i \int_\gamma \omega_{i+1} \ldots \omega_r = \sum_\sigma \int_\gamma \omega_{\sigma(1)} \ldots \omega_{\sigma(r)}, \tag{3.80}$$

where σ "shuffles" the sets $(1, \ldots, i)$ and $(i+1, \ldots, r)$, i.e. it permutes all indices without changing the internal order of $(1, \ldots, i)$ and $(i+1, \ldots, r)$, respectively. The shuffle product of a one-fold and a two-fold integral is, for example, given by

$$\int_\gamma \omega_1 \int_\gamma \omega_2 \omega_3 = \int_\gamma \omega_1 \omega_2 \omega_3 + \int_\gamma \omega_2 \omega_1 \omega_3 + \int_\gamma \omega_2 \omega_3 \omega_1.$$

One condition on the ϵ-form (3.72) requires the non-zero boundary constants to be of uniform weight zero. This condition originates from the observation we made earlier, the series coefficients of (3.68) consist of iterated integrals of same weight. We discussed that (solutions of) master integrals are series expansions in ϵ (3.76). The same holds for integrals on boundary points. The request for **uniform transcendental weight** zero puts a constraint on every term in the series, every term must have weight zero. Here, rational numbers are assigned weight zero as opposed to transcendental numbers like π, which has weight one, and **zeta values**

$$\zeta_n = \sum_{j=1}^\infty \frac{1}{j^n}, \quad \zeta_2 = \frac{\pi^2}{6},$$

which have weight n. Weights are summed if factors are multiplied. It follows, that weights can be balanced if ϵ is assigned weight -1. If a series starts at order ϵ^0, the parts proportional to ϵ^j must have weight j to produce uniform weight zero (see also end of section 3.5.2).

In the next section, we will derive the solution to a canonical differential equation in more details. We thereby present the solution in terms of a special class of functions, multiple polylogarithms, and put more emphasise on weight properties. Beforehand, we want to emphasise the advantages of the just described method. Verifying if a differential equation is in ϵ-form is straightforward, since the dependence on ϵ is easily checked. As demonstrated, the solution of the ϵ-form is easily determined. The only requirements are the existence of appropriate boundary terms. The tricky part within this method is, therefore, not solving a differential equation, but finding transformations. We seek for a basis transformation to a canonical basis (3.69), (3.70) and if necessary a variable transformation to rationalise appearing square roots. Unfortunately, no general method of finding such a canonical basis is known. We will explore a systematic approach, which utilises the properties of maximal cuts on Feynman integrals throughout this thesis (see section 5.4.4). Maximal cuts are usually found within the Baikov representation, which was described in section 3.3.2. We will define them in section 3.6.1.

3.5.2 Multiple polylogarithms in the solution of differential equations

Now, we explain an important class of iterated integrals, which are fundamental blocks of the solution of canonical differential equations, namely multiple polylogarithms [32–

34]. Subsequent to the previous subsection, we illustratively sketch their emergence in the solution of canonical differential equations. For simplicity, we look at a toy example consisting of one kinematic variable x and one master integral. The emergence of multiple polylogarithms in more complex cases proceeds similarly (see for example section 5.5.4, especially (5.105)). Afterwards, we will define multiple polylogarithms in detail.

In the preceding subsection we started with pre-canonical master integrals and, after applying a basis transformation, the system of differential equations became canonical (see (3.72)),

$$dJ = \epsilon \tilde{A}(x) J = C \omega J.$$

C is an algebraic number and the letter ω has only a simple pole. With regards to (3.67) we may consider

$$\omega = \frac{dx}{x - z} = \mathrm{dlog}(x - z),$$

where z is constant with respect to x. The master integral can be expanded in a Taylor series in ϵ (3.76),

$$J = \epsilon^0 J^{(0)} + \epsilon J^{(1)} + \epsilon^2 J^{(2)} + ...,$$

which is inserted into the canonical differential equation to find in correspondence with (3.78)

$$dJ^{(0)} = 0,$$

$$dJ^{(q+1)} = C \frac{dx}{x - z} J^{(q)}.$$

The solution for $J^{(0)}$ follows immediately,

$$\Rightarrow J^{(0)} = B^{(0)},$$

where $B^{(0)}$ and all $B^{(i)}$ that will appear in the following calculation are constants determined by boundary conditions. The next order in ϵ becomes

$$\Rightarrow dJ^{(1)} = B^{(0)} C \frac{dx}{x - z}.$$

Choosing integration boundaries from 0 to x,

$$\begin{aligned} J^{(1)} &= B^{(0)} C \int_0^x \frac{dx'}{x' - z} + B^{(1)}, \\ &= B^{(0)} C \underbrace{\log(x' - z)\big|_0^x}_{=\log\left(1 - \frac{x}{z}\right)} + B^{(1)}, \end{aligned} \tag{3.81}$$

we can simultaneously interpret $J^{(1)}$ as a logarithm and as a one-fold iterated integral. We set

$$G[z; x] = \int_0^x \frac{dx'}{x' - z} = \log\left(1 - \frac{x}{z}\right), \tag{3.82}$$

and write

$$J^{(1)} = B^{(0)} C \, G\,[z; x] + B^{(1)}.$$

The second order in ϵ follows

$$J^{(2)} = B^{(0)} C^2 \int_0^x \frac{dx'}{x' - z} \int_0^{x'} \frac{dx''}{x'' - z} + B^{(1)} C \int_0^x \frac{dx'}{x' - z} + B^{(2)}$$

$$\Leftrightarrow J^{(2)} = B^{(0)} C^2 \int_0^x \frac{dx' G\,[z; x']}{x' - z} + B^{(1)} C \, G\,[z; x] + B^{(2)}. \tag{3.83}$$

The solution to the second order contains a two-fold iterated integral. Similar to (3.82), we set

$$G\,[z_1, z_2; x] = \int_0^x \frac{dx'}{x' - z_1} \int_0^{x'} \frac{dx''}{x'' - z_2}, \tag{3.84}$$

and find

$$J^{(2)} = B^{(0)} C^2 \, G\,[z, z; x] + B^{(1)} C \, G\,[z; x] + B^{(2)}.$$

A pattern in the solution becomes visible, the j-th order gives rise to iterated integrals of depth $\leq j$, which can be written in terms of G-functions. Both G's we encountered (3.82), (3.84) belong to the same class of functions. The one-fold G-function (3.82) is equivalent to a logarithm. Accordingly, the class of functions is called **multiple polylogarithms**. As indicated in (3.83), a multiple polylogarithm of depth n is naturally defined recursively

$$G\,[z_1, z_2, \ldots, z_n; x] = \int_0^x \frac{dx_1}{x_1 - z_1} G\,[z_2, \ldots, z_n; x_1], \tag{3.85}$$

whereby

$$G[\underbrace{0, \ldots, 0}_{n \text{ times}}; x] = \frac{\ln(x)^n}{n!}. \tag{3.86}$$

For $z_n \neq 0$, we conclude

$$G\,[z_1, z_2, \ldots, z_n; x] = \int_0^x \frac{dx_1}{x_1 - z_1} \int_0^{x_1} \frac{dx_2}{x_2 - z_2} \ldots \int_0^{x_{n-1}} \frac{dx_n}{x_n - z_n}. \tag{3.87}$$

The depth of the iterated integral, which is n in the above equation, also defines the **weight** of a multiple polylogarithm. Multiple polylogarithms with $z_n \neq 0$ additionally fulfil a scaling relation

$$G\,[z_1, z_2, \ldots, z_n; x] = G\,[y z_1, y z_2, \ldots, y z_n; y x], \quad z_n, y \in \mathbb{C} \backslash \{0\}. \tag{3.88}$$

In the context of multiple polylogarithms, we may take $z_1 \ldots z_n$ as **letters** and obtain a shuffle product in correspondence with (3.80),

$$G\,[z_1, \ldots, z_i; x] \, G\,[z_{i+1}, \ldots, z_n; x] = \sum_\sigma G\,[z_{\sigma(1)}, \ldots, z_{\sigma(n)}; x], \tag{3.89}$$

where σ permutes all indices without changing the internal order of $(1, \ldots, i)$ and $(i+1, \ldots, n)$. Multiple polylogarithms, therefore, obey a **shuffle algebra**.

The shuffle product of multiple polylogarithms (3.89) makes it possible to remove so-called trailing zeros, i.e. $z_{n-j-1} \neq 0$ and $z_{n-j} = \ldots = z_n = 0$. We find for example

$$
\begin{aligned}
G\left[0; x\right] G\left[z_1; x\right] &= G\left[0, z_1; x\right] + G\left[z_1, 0; x\right], \\
\Rightarrow G\left[z_1, 0; x\right] &= -G\left[0, z_1; x\right] + G\left[0; x\right] G\left[z_1; x\right] \\
&= -G\left[0, z_1; x\right] + \ln\left[x\right] G\left[z_1; x\right].
\end{aligned}
$$

For our toy example, the general solution of the i-th order in epsilon $J^{(i)}$ can be given in terms of multiple polylogarithms,

$$
\begin{aligned}
J^{(i)} = B^{(0)} C^i \, G[\underbrace{z, \ldots, z}_{i \text{ times}}; x] + B^{(1)} C^{(i-1)} \, G[\underbrace{z, \ldots, z}_{(i-1)\text{times}}; x] \\
+ B^{(2)} C^{(i-2)} \, G[\underbrace{z, \ldots, z}_{(i-2) \text{ times}}; x] + \ldots + B^{(i-1)} C \, G\left[z; x\right] + B^{(i)}.
\end{aligned}
$$

Implying for the full solution

$$
\begin{aligned}
J(x) = B^{(0)} + \epsilon \left(B^{(0)} C \, G\left[z; x\right] + B^{(1)} \right) \\
+ \epsilon^2 \left(B^{(0)} C^2 \, G\left[z, z; x\right] + B^{(1)} C \, G\left[z; x\right] + B^{(2)} \right) \\
+ \epsilon^3 \left(B^{(0)} C^3 \, G\left[z, z, z; x\right] + B^{(1)} C^2 \, G\left[z, z; x\right] + B^{(2)} C \, G\left[z; x\right] + B^{(3)} \right) + \mathcal{O}\!\left(\epsilon^4\right).
\end{aligned}
$$

We know, that the solution to a canonical differential equation has uniform weight, more specifically uniform weight zero if its series starts with an ϵ^0-term. With a rational number C, this determines the weight of all constants in the solution. We know that ϵ^j has weight $(-j)$ and $G\left[z_1, \ldots, z_j; x\right]$ weight j. It follows, that a non-zero constant $B^{(j)}$ must have weight j as well to ensure uniform weight. Boundary constants are determined by boundary conditions. A boundary condition could, for example, be found at $x = 0$, where J amounts to

$$
J(0) = a^{(0)} + \epsilon a^{(1)} + \epsilon^2 a^{(2)} + \epsilon^3 a^{(3)} + \ldots.
$$

The definition of the ϵ-form (3.72) places the requirement on its non-zero boundary constants to be of uniform weight. Hence, each $a^{(j)}$ has to be either a transcendental number of weight j or zero. Every $B^{(j)}$ has to be equal to $a^{(j)}$, yielding correct weight properties.

We demonstrated that multiple polylogarithms are a class of functions sufficient to express the solution of a differential equation in ϵ-form possessing an alphabet free of non-rational functions. We gave a definition in terms of iterated integrals (3.87). Multiple polylogarithms have also a sum representation, for more information we refer to [57] chapter 8.

3.6 On the solution strategy for the system of differential equations

In section 3.5, we introduced the method of differential equations as a solution strategy for a set of master integrals. The ϵ-form of differential equations (3.72) is thereby an especially desirable form, as discussed in the last two subsections. Its solution may be written as Taylor series in ϵ. Each series coefficient consists of iterated integrals, or more specifically multiple polylogarithms (see section 3.5.2). Furthermore, the j-th series coefficient has weight j yielding a solution of uniform weight zero. Hence, we search for integrals of uniform weight while searching for a canonical basis.

At the beginning of section 3.5.1 we started with an arbitrary basis of master integrals $\vec{I} = (I_1, \ldots, I_{N_{MI}})^T$ and its system of differential equations with respect to kinematic variables $x_1, \ldots, x_{N_v}$. Afterwards, we performed a transformation to obtain a canonical basis $\vec{J} = (J_1, \ldots, J_{N_{MI}})^T$. As mentioned in section 3.5.1, it may happen that a basis transformation U causes a linear dependence in ϵ, but leads to square roots in arguments of some dlog-forms ω_i. To solve this issue, a variable transformation rationalising all square roots can be applied. A summary of the complete procedure is sketched in box 1.

Box 1: Canonical master integrals as solution strategy within the framework of differential equations

A pre-canonical basis of master integrals $\vec{I} = (I_1, \ldots, I_{N_{MI}})^T$, depending on kinematic variables $(x_1, \ldots, x_{N_v})$ may be solved within the framework of differential equations:

Pre-canonical system of differential equations:
$$d\vec{I} = A\left(\epsilon, x_1, \ldots, x_{N_v}\right)\vec{I}, \qquad A = \sum_{i}^{N_v} A_{x_i} dx_i$$

$$\Downarrow$$

Basis transformation:
$$\vec{I} = U\left(\epsilon, x_1, \ldots, x_{N_v}\right)\vec{J} \qquad \rightarrow \text{factor out } \epsilon$$

$$\Downarrow$$

Variable transformation:
$$\left(x_1, \ldots, x_{N_v}\right) \rightarrow \left(x_1', \ldots, x_{N_v}'\right) \qquad \rightarrow \text{rationalise roots}$$

$$\Downarrow$$

Canonical system of differential equations:
$$d\vec{J} = \epsilon\tilde{A}\left(x_1', \ldots, x_{N_v}'\right)\vec{J}, \qquad \tilde{A} = \sum_i C_i \omega_i$$

$$\Downarrow$$

Solve order by order in $\epsilon \quad \rightarrow \quad$ expressible in $G\left[z_1, \ldots, z_n; x'\right]$ (see (3.87))

- -

Here, A_{x_i} and C_i are $N_{MI} \times N_{MI}$-dimensional matrices. A_{x_i} may depend on kinematic variables and $\epsilon = \frac{4-D}{2}$, whereas C_i purely consists of rational numbers. ω_i are dlog-forms containing rational functions of the kinematic variables.

Clearly, the main task within the method of differential equations is the search for a canonical basis $\vec{J}$, i.e. the search for an appropriate transformation U. And, if necessary the search for a variable transformation. Unfortunately, no general method for finding U is known. Deterministic algorithms exist [68–70, 72–74], however they cannot handle complex problems like the one considered in this thesis. In this thesis we use a heuristic method, which will be discussed in section 5.4.4. In this section we introduce a main tool regarding this method as well as an algorithm determining variable transformations.

Before we actually try to find a canonical basis, we may simplify our problem, utilising the structure of matrices within the system of differential equations,

$$
d\begin{pmatrix}\vec{I}^{sec_1}\\\vec{I}^{sec_2}\\\vec{I}^{sec_3}\\\dots\end{pmatrix} = \begin{pmatrix}A^{(1)} & 0 & 0 & \dots\\A^{(1\times2)} & A^{(2)} & 0 & \\A^{(1\times3)} & A^{(2\times3)} & A^{(3)} & \\\dots & & &\end{pmatrix}\begin{pmatrix}\vec{I}^{sec_1}\\\vec{I}^{sec_2}\\\vec{I}^{sec_3}\\\dots\end{pmatrix}, \tag{3.90}
$$

$$
A^{(j)} = \sum_i^{N_v} A^{(j)}_{x_i} dx_i, \quad \frac{\partial}{\partial x_i}\vec{I}^{sec_j} = A^{(j)}_{x_i}\vec{I}^{sec_j},
$$

$\vec{I}^{sec_j}$ denotes the set of master integrals belonging to sector j. $A^{(j)}_{x_i}$, $A^{(l\times j)}_{x_i}$ denote matrices with dimensions determined by the length of $\vec{I}^{sec_j}$ or the length of $\vec{I}^{sec_l}$ and $\vec{I}^{sec_j}$ respectively.

Figure 3.5: Block decomposition: Illustrative sketch of workflow regarding a system with three sectors containing 2, 2 and 1 master integral, respectively.

We observe, that A_{x_i} are lower block-triangular matrices. This results from the fact, that master integrals are ordered starting with those belonging to the simplest sector, as described in section 3.5 on page 44. Sectors manifest themselves as blocks on the diagonal, sub-sectors contributions appear to their left. Hence, we may divide the complete differential equation into equations for each sector,

$$
\frac{\partial}{\partial x}\vec{I}^{sec_j} = A^{(j)}\vec{I}^{sec_j} + \sum_{l<j} A^{(l\times j)}\vec{I}^{sec_l},
$$

and treat each block in (3.90) individually.

We may transform the complete matrix by transforming its blocks moving from its top to its bottom and from right to left as illustrated in fig.3.5. Thereby, we must not change blocks we already transformed, but we may change blocks we did not investigate yet. Details on this procedure will be given in section 5.4.2.

An important tool for the study of diagonal blocks is introduced in the following subsection, namely maximal cuts of Feynman integrals. Afterwards, in section 3.6.2, we discuss a rationalisation algorithm most helpful in constructing appropriate variable transformations.

3.6.1 Maximal Cuts

Previously, we stressed the fact that matrices of a system of differential equations are lower block triangular and we may find appropriate transformations for each block individually. In this section we discuss an operation that projects a differential equation onto its homogeneous part, allowing the dedicated study of diagonal blocks [75]. This operation refers to taking the maximal cut of a Feynman integral in Baikov representation.

We recall the Baikov representation of Feynman integrals

$$I_{\nu_1,\ldots,\nu_n} = K \int_{\mathcal{C}} d^n z \, \mathcal{B}(z)^{\frac{D-l-e-1}{2}} \prod_{j=1}^{n} z_j^{-\nu_j}, \tag{3.91}$$

where z_j are Baikov variables, i.e. essentially the propagators of the regarded integral, the $\nu_i \in \mathbb{Z}$ their exponents and $\mathcal{B}(z)$ denotes the Baikov polynomial (3.43). (l is the number of loops, e the number of independent external momenta and D the dimension.) The prefactor K and the integration domain C can be read off from (3.44) and (3.45), but are of no importance here. We only need to remember that C was rather complicated.

In the following, we first discuss the cut of a single edge i with a propagator raised to power one, $\nu_i = 1$. In order to cut a propagator z_i with $\nu_i = 1$ of I, we may view the integral as

$$I_{\nu_1,\ldots,\nu_i=1,\ldots,\nu_n} \sim \int_{\mathcal{C}} \frac{f(z)}{z_i} dz_i,$$

where $f(z) \sim \mathcal{B}(z)^{\frac{D-l-e-1}{2}} \prod_{j\neq i} z_j^{-\nu_j}$. To cut z_i we replace the integration contour by a small anti-clockwise circle around $z_i = 0$, which amounts to taking the residue at $z_i = 0$,

$$I_{\nu_1,\ldots,\nu_i=1,\ldots,\nu_n} \to \mathrm{Cut}|_i \left(I_{\nu_1,\ldots,\nu_i=1,\ldots,\nu_n} \right),$$

$$\int_{\mathcal{C}} \frac{f(z)}{z_i} dz_i \to \oint_{z_i=0} \frac{f(z)}{z_i} dz_i = 2\pi i \, \mathrm{res} \left(\frac{f(z)}{z_i}, z_i = 0 \right) = 2\pi i \int f(z)\delta(z_i)dz_i. \tag{3.92}$$

We deduce, that in practice, we may perform a **cut** of a propagator raised to power one through a substitution in the integrand

$$\frac{1}{z_i} \to 2\pi i \, \delta\left(z_i\right),$$

$$\text{Cut}|_i \left(I_{\nu_1,\dots,\nu_i=1,\dots,\nu_n} \right) = 2\pi i \, K \int_{\mathcal{C}} d^n z \, \delta\left(z_i \right) \mathcal{B}(z)^{\frac{D-l-e-1}{2}} \prod_{\substack{j=1 \\ j \neq i}}^{n} z_j^{-\nu_j}. \tag{3.93}$$

The integration of a delta function is carried out straightforwardly and corresponds to a simplification of the Baikov polynomial

$$\mathcal{B}(z) \to \mathcal{B}(z)|_{z_i=0}.$$

Now, we discuss the case $\nu_i \neq 1$, i.e. the cut of a propagator raised to powers greater or smaller than one. If $\nu_i > 1$, we may expand the integral in a Laurent series around $z_i = 0$ and find its residue as the coefficient of the $\frac{1}{z_i}$-term. If $\nu_i \leq 0$, the integral has no residue in $z_i = 0$ and the cut of z_i gives zero,

$$\text{Cut}|_i \left(I_{\dots,\nu_{i-1},0,\nu_{i+1},\dots} \right) = 0.$$

On the one hand, cutting an edge of an integral simplifies the integration over its propagators drastically. On the other hand, important properties of the original integral like integration by parts relations are preserved: For a set of master integrals fulfilling

$$d\vec{I} = A\vec{I},$$

we may take cuts of $\vec{I}$ without invalidating the differential equation [75],

$$d\text{Cut}\left(\vec{I} \right) = A \, \text{Cut}\left(\vec{I} \right).$$

This is especially useful if we cut an integral not only once, but wherever possible. The **maximal cut** is defined by the simultaneous cut of all propagators z_i with positive exponents $\nu_i > 0$. We remember how we may divide differential equations of a sector $\vec{I}^{sec_j}$ into a homogeneous part and sub-sector contributions,

$$\frac{\partial}{\partial x} \vec{I}^{sec_j} = A^{(j)} \vec{I}^{sec_j} + \sum_{l<j} A^{(l \times j)} \vec{I}^{sec_l}. \tag{3.94}$$

A sector is defined by a certain set of propagators $\{z_j\}$ with positive indices $\{\nu_j > 0\}$. Any sub-sector consists of a subset of these, hence every integral from sub-sectors in (3.94) misses at least one of the propagators from $\{z_j\}$. Cutting this missing propagator forces the sub-sector integral to vanish. Applying the maximal cut onto (3.94), i.e. cutting all $\{z_j\}$, therefore, results into

$$\frac{\partial}{\partial x} \text{MaxCut}\left(\vec{I}^{sec_j} \right) = A^{(j)} \text{MaxCut}\left(\vec{I}^{sec_j} \right) + 0.$$

The sub-sector contributions vanish, we are left with a simpler differential equation. We see, the maximal cut is a solution to the homogeneous part of (3.94).

Furthermore, it is important to note, that uniform weight properties are preserved under the maximal cut. Solutions to canonical differential equations are integrals of uniform weight, hence, their maximal cuts also have uniform weight. To gain information about weight properties of an integral, we therefore might study the simpler maximally cut

integral first. As we will explain in details in section 5.4.4 (see especially box 2), we may modify the integration contour and the integrand of a maximally cut integral, such that the leading term of its ϵ-expansion is a constant of weight zero. After modifying the integrand of the original integral accordingly, we have an ansatz for a canonical integral.

We see, maximal cuts allow the dedicated study of diagonal blocks and are an essential tool in the search for integrals of uniform weight. However, we not only have to deal with basis transformations, but also with variable transformations, hence, we will look at them in the next subsection.

3.6.2 Rationalisation algorithm

We aim at solving a differential equation and the corresponding set of master integrals in terms of multiple polylogarithms. Finding a canonical differential equation is thereby the most convenient way to achieve this goal. A canonical differential equation is linear in ϵ and expressible through dlog-forms containing only rational functions. In section 3.5.1, we mentioned how we might only find a non-rational transformation U for a set of pre-canonical master integrals $\vec{I}$ to cause a linear dependence in ϵ,

$$\vec{I} = U\vec{J} \;\Rightarrow\; d\vec{J} = \epsilon A\left(x_1, \ldots, x_{N_v}\right)\vec{J}.$$

If the resulting matrix A can not be turned into a rational matrix, it is not expressible in terms of dlog-forms which contain only rational functions. As a result, the master integrals $\vec{J}$ are not easily expressible in terms of multiple polylogarithms. However, A might be turned into a rational matrix through an appropriate variable transformation. The variable transformation has to lead to a square under each square root, rationalising all square roots. Note, that such a rationalisation is not always possible [76]. Note further, that examples of Feynman integrals with singularities involving unrationalisable roots which are still expressible in terms of multiple polylogarithms exist [77].

In the following we will sketch an algorithmic approach to the problem of rationalisation, which was introduced in [78], in a manner understandable without knowledge about its theoretical background from algebraic geometry. For further information and detailed definitions we refer to [78, 79] and to [57] section 7.2.

We consider a square root

$$r_1 = \sqrt{\frac{q_1}{q_2}},$$

which depends on the ratio of two polynomials $q_1(x_1, \ldots, x_{N_v})$, $q_2(x_1, \ldots, x_{N_v})$, where $x_1, \ldots, x_{N_v}$ is the set of kinematic variables. We seek a transformation

$$r_1 \to \phi_r(x'_0, \ldots, x'_{N_v}),$$
$$x_i \to \phi_{x_i}(x'_0, \ldots, x'_{N_v}),$$

such that ϕ_r is rational in $x'_1, \ldots, x'_n$. We may search for an appropriate variable transformation in the following way:

1. Define $f(r, x_1, \ldots, x_{N_v}) \equiv q_2 \cdot r^2 - q_1$ and identify the degree d of f.

2. Find a point $p = (a_0, \ldots, a_{N_v})$ of multiplicity $m = d - 1$, i.e. determine p such that all partial derivatives of f of order $< m$ vanish at p, but ensure that at least one none-vanishing m-th partial derivative exists.

3. Set $g(r, x_1, \ldots, x_{N_v}) \equiv f(r + a_0, x_1 + a_1, \ldots, x_{N_v} + a_{N_v})$ and collect terms with common degree: $g(r, x_1, \ldots, x_{N_v}) = g_d(r, x_1, \ldots, x_{N_v}) + g_{d-1}(r, x_1, \ldots, x_{N_v})$. Here, g_j denotes a homogeneous polynomial of degree j.

4. Now, the desired transformations are found to be

$$r_1 \to \phi_r(x_0', \ldots, x_{N_v}') = -x_0' \frac{g_{d-1}(x_0', \ldots, x_{N_v}')}{g_d(x_0', \ldots, x_{N_v}')} + a_0,$$

$$x_i \to \phi_{x_i}(x_0', \ldots, x_{N_v}') = -x_i' \frac{g_{d-1}(x_0', \ldots, x_{N_v}')}{g_d(x_0', \ldots, x_{N_v}')} + a_i, \tag{3.95}$$

whereby a single x_i', typically x_0', is set to one.

This algorithm only holds if p is not infinity. However, it may be extended to include points at infinity (see [57] section 7.2.).

We illustrate the algorithm described above, while deriving a rationalisation for

$$r_1 = \sqrt{-v(4 - v)}.$$

1. The defining function $f = r^2 + v(4 - v)$ has degree 2.

2. Hence, we determine a point p with multiplicity one. $p = (r = 0, v = 0)$ fulfills the requirements, since $f(p) = 0$ and $\frac{\partial f}{\partial v}(p) = 4 \neq 0$.

3. We set $f(r + 0, v + 0) = \underbrace{r^2 - v^2}_{=g_2} + \underbrace{4v}_{=g_1}$.

4. With $x_0' = 1$, $x_1' = x'$, we find the transformations

$$\phi_r(1, x') = -\frac{g_1(1, x')}{g_2(1, x')} + 0 = -\frac{4x'}{1 - x'^2},$$

$$\phi_{x_1}(1, x') = -x' \frac{g_1(1, x')}{g_2(1, x')} + 0 = -\frac{4x'^2}{1 - x'^2}.$$

We constructed an appropriate variable transformation,

$$v = -\frac{4x'^2}{1 - x'^2}$$

$$\Rightarrow r_1 = -\frac{4x'}{1 - x'^2}.$$

Alternatively, we may work with the transformation that we obtain after including the substitution

$$x' = \frac{1 - x}{1 + x},$$

and choosing the opposite sign of the square root,

$$\Rightarrow \ v = \frac{-(1-x)^2}{x},$$

$$\Rightarrow \ r_1 = \frac{1-x^2}{x}.$$

(3.96)

Another, more involved application of the algorithmic approach will be demonstrated in section 5.5.1, see (5.79), (5.80). There, we rationalise multiple square roots simultaneously. If multiple square roots occur, we may consecutively apply the rationalisation algorithm to each root. Afterwards we finally arrive at a canonical differential equation,

$$\frac{\partial}{\partial x_i}\vec{J} = \epsilon A_{x_i}(x_1,\ldots)\vec{J} \ \overset{x_i \to x_i'}{\longrightarrow} \ \frac{\partial}{\partial x_i'}\vec{J} = \epsilon \sum_j^{N_v} \frac{\partial x_j}{\partial x_i'} A_{x_j}(x_1',\ldots)\vec{J},$$

$$d\vec{J} = A(x_1,\ldots)\vec{J} \ \overset{x_i \to x_i'}{\longrightarrow} \ d\vec{J} = \epsilon \tilde{A}(x_1',\ldots)\vec{J},$$

where the resulting matrix-valued one-form is given by

$$\tilde{A}(x_1',\ldots) = \sum_i^{N_v} \left(\sum_j^{N_v} \frac{\partial x_j}{\partial x_i'} A_{x_j}(x_1',\ldots) \right) dx_i'.$$

FOUR

THE STRATEGY

In this chapter we provide a concise summary of the strategy employed in this thesis as well as an overview of its structure. In correspondence, this chapter serves as a road map to sections and topics. This thesis is divided into two main parts:

1) The calculation of all three-loop master integrals with internal top- and W-propagators relevant to the Higgs boson self-energy at $\mathcal{O}(\alpha^2\alpha_s)$.

2) The discussion of the mixed QCD-electroweak correction involving charged weak bosons to the Higgs boson decay rate into a bottom quark pair $\Gamma\left(H \to b\bar{b}\right)$.

The former are essential building blocks of the latter, as the optical theorem links self-energy diagrams to decay rates. They will be discussed in chapter 5. Afterwards, in chapter 6 we consider the correction to the decay rate. Here, we display the workflow of both side by side, thereby we also mention corresponding sections of theoretical background. The procedures sketched in this chapter are kept general, they may be utilised to compute any set of master integrals which can be brought to canonical form, as well as any correction to a decay rate.

We take the results from 1) to express all integrals appearing in 2). Consequently, we first have to agree on a set of topologies and top sectors sufficient to express all occurring diagrams. Afterwards, we may separate the workflow. The steps on the way to determine the correction to $\Gamma\left(H \to b\bar{b}\right)$ will be listed down below in the left column, whereas the calculation of master integrals is sketched in the right column.

- Determine all contributing Feynman diagrams → application in section 6.3.

  - Chose an appropriate auxiliary topology → application in section 5.2.

The decay rate:

$\Gamma\left(H \to b\bar{b}\right)$ with internal charged bosons at $\mathcal{O}(\alpha\alpha_s)$ → chapter 6

- Calculate all Feynman diagrams:

  - Express Feynman diagrams in terms of Feynman rules.

  → Feynman rules in section 2.2.1

  → application in sections 6.4.1, 6.4.2

  - Transform all emerging integrals to scalar integrals.

  → theory in section 3.1

  - Reduce all scalar integrals to pre-canonical master integrals,

  $$I_i = \sum_j^{N_{MI}} c_{i,j} I_j.$$

  → theory in section 3.4

  - Express pre-canonical master integrals in terms of canonical master integrals,

  $$\vec{I} = U\vec{J} \Rightarrow I_i = \sum_j^{N_{MI}} u_{i,j} J_j.$$

- Sum over all Feynman diagrams,

$$\Sigma_H^{(\alpha^2\alpha_s)_W} = \sum_{\text{diagrams}} \sum_j^{N_{MI}} f_j J_j.$$

→ application in section 6.4

The master integrals:

Higgs self-energy with internal top- and W-propagators at $\mathcal{O}(\alpha^2\alpha_s)$ → chapter 5

- Find a set of pre-canonical master integrals,

$$\vec{I} = (I_1, \ldots, I_{N_{MI}})^T.$$

→ theory in section 3.4

→ application in section 5.3

- Determine their system of differential equations,

$$d\vec{I} = A\big(\epsilon, \underbrace{x_1, \ldots, x_{N_v}}_{\text{kinematic var.}}\big)\vec{I}.$$

→ theory in begin of section 3.5

→ application in section 5.3.1

- Transform to a canonical system of differential equations:

  - Basis transformations,

  → application in section 5.4

  - Variable transformations,

  → application in section 5.5.1

  $$d\vec{J} = \epsilon\tilde{A}\left(x'_1, \ldots, x'_{N_v}\right)\vec{J}.$$

→ theory in sections 3.5.1 & 3.6

  - Canonical basis $\vec{J}$ is given by iterated integrals.

  → theory in sections 3.5.1 & 3.5.2

  → application in section 5.5, especially section 5.5.4

- Renormalisation:
    - Calculate all necessary diagrams with counterterm insertions.
    - Add them to sum

$\rightarrow$ theory in section 2.3

$\rightarrow$ application in section 6.5

- Apply the optical theorem to obtain the decay rate

$$\Gamma(H \to b\bar{b}) = \frac{1}{m_H} \mathrm{Im}\left(\mathcal{A}\left(H \to H\right)\right)$$

$\rightarrow$ theory in section 2.1.1

$\rightarrow$ discussion in section 6.2

After the construction of a (rough) strategy, we are able to proceed with the main parts of this thesis in the following chapters. We start with its major work, the derivation of master integrals as outlined above on the right. Afterwards, we discuss the decay rate as phenomenological application. In the sections highlighted above, we provide detailed information on intermediate steps as well as explanatory examples.

THREE-LOOP MASTER INTEGRALS FOR THE HIGGS BOSON SELF-ENERGY INVOLVING TOP QUARKS AND W-BOSONS

After setting up the framework of this thesis, we start with its main part: the calculation of three-loop master integrals for the Higgs boson self-energy. Master integrals are basis integrals sufficient to express one or multiple families of Feynman integrals under consideration. We already sketched the strategy we are going to apply in the preceding chapter and gave required knowledge about Feynman integrals in chapter 3. The results discussed here were published in [1]. In [1] the emphasise is on presentation of results, whereas the emphasis of this chapter is on insights into (practical) calculations.

We start this chapter with an introduction. Afterwards, in section 5.2 we show all essential top sector diagrams and find appropriate topologies. Any regarded self-energy diagram gives rise to Feynman integrals depending on the propagators of these topologies (the emergence of Feynman integrals and their expression in terms of propagators was explained in section 3.1). The respective Feynman integrals may be expressed in terms of basis integrals with the help of the Laporta algorithm (discussed in section 3.4). As sketched in chapter 4, the next step is, therefore, the generation of pre-canonical master integrals. This step will be described in section 5.3. In order to solve those, we relate them to another so-called canonical basis. A canonical basis accompanies a system of differential equations in ϵ-form, which may be solved straightforwardly order by order in the dimensional regularisation parameter (see section 3.5.1 for the definition and advantages of differential equations in ϵ-form). This solution strategy is placed within the framework of differential equations of Feynman integrals (see section 3.5). We initiate it in section 5.3.1, as we build differential equations of the pre-canonical master integrals with respect to their kinematic variables. Afterwards, we are prepared to start with the main work. In section 5.4, we discuss basis transformations leading to ϵ-factorised differential equations. We indicated in section 3.6 that we transform differential equations sector by sector starting with the lowest sector (sectors and "simplicity" in the context of sectors were discussed in section 3.4.1). We provide insights into this strategy in section 5.4.2. The homogeneous part of a sector's differential equation is solved by the construction of ansätze for integrals of uniform transcendental weight (see section 3.5.1 and section 3.5.2 for weight properties of integrals). The maximal cut introduced

in section 3.6.1 plays a crucial role. In section 5.4.4, we demonstrate its application as we find integrals of uniform weight for example sectors. A good introductory example into the topic of basis transformations, integrals with certain weight properties and the utilisation of the maximal cut is given in section 5.4.3. There we encounter again the tadpole and the bubble integral (see section 3.2). The transformed basis integrals of uniform weight zero are presented in section 5.5. After the inclusion of variable transformations in section 5.5.1, the canonical master integrals give rise to differential equations in ϵ-form. These are expressible through differential one-forms containing only simple poles, which are presented in section 5.5.2 (see section 3.5.1 for the necessity of variable transformations and section 3.6.2 for their determination). Boundary values of the integrals, i.e. values of the integrals at a specific kinematic point, are calculated in section 5.5.3. They enable the presentation of results in terms of multiple polylogarithms in section 5.5.4 (multiple polylogarithms and their arising out of differential equations in ϵ-form were discussed in section 3.5.2). We close this chapter with a conclusion and summary in section 5.6.

5.1 Introduction

The Higgs boson self-energy plays a key role in the context of Higgs precision physics. The optical theorem, for example, links its imaginary part directly to the Higgs decay rate (see chapter 6). Here, we, therefore, address contributions to the Higgs boson self-energy and determine sufficient canonical master integrals. We already discussed a one-loop contribution in an exemplary manner in section 3.2 (see fig.3.1). Higher loop contributions are naturally more complicated. Complications arise from the increase of integration variables as well as from the increase of kinematic invariants. In the context of self-energy diagrams, the increase of kinematic invariants corresponds to an increase of massive propagators. We address three-loop contributions containing two different kinds of internal masses. To be more precise, we analytically calculate all master integrals sufficient to express three-loop Higgs self-energy diagrams containing internal top and W-boson propagators. These are of order $\mathcal{O}(\alpha^2\alpha_s)$ and depend on the squared external momentum $s = p^2$ and the heavy particle masses m_W, m_t, since we neglect the bottom quark mass. We work in $D = 4 - 2\epsilon$ dimensions obeying dimensional regularisation.

We would like to mention, that the results presented here do not include all master integrals of the Higgs boson self-energy at $\mathcal{O}(\alpha^2\alpha_s)$. We are missing contributions with internal Z-boson or photon propagators. However, these involve less internal masses and are therefore less intricate. Additionally, a main set of master integrals corresponding to contributions with internal Z-boson propagators are a special case of the here discussed master integrals as they are obtained in the limit $m_t \to m_b$. We calculate a more complicated contribution to the Higgs boson self-energy at $\mathcal{O}(\alpha^2\alpha_s)$

The emergence of square roots forces us to divide the self-energy diagrams into different sets, which may be classified a priori according to proportionality to the product of Yukawa couplings $y_b y_t$. In the end, we are dealing with three systems of master integrals. The solution of each set proceeds similarly, hence, we describe our methods in a general manner. In correspondence we keep notations general. Especially in section 5.3

and section 5.4, we write $\vec{I}/\vec{J}$ for pre-canonical/canonical master integrals of any system interchangeably and may not distinguish between (matrices of) differential equations belonging to different sets. If we provide examples, we point out the respective system. We find a basis of uniform weight for each of the sets and obtain canonical differential equations. Our results are, therefore, expressible in terms of multiple polylogarithms.

5.2   The topologies

This section together with the subsequent section lays the foundation of this chapter. Here, topologies sufficient to express all occurring self-energy diagrams will be found. We set up five three-loop topologies depending on one external momentum and two different kinds of masses. In combination with their top sectors these topologies define which master integrals need to be computed. In the subsequent section, we specify this point as we specify notations regarding integrals and find a pre-canonical set of master integrals. Then, we determine differential equations for this set of master integrals.

Before we display the self-energy diagrams, we would like to make a comment about the bottom quark mass. The mass of the bottom quark is in the order of magnitude of 4 GeV. This is negligibly small compared to the boson masses $m_W \approx 80$ GeV, $m_H \approx 125$ GeV and the top quark mass $m_t \approx 173$ GeV. Hence, we only keep the dependence on the heavy particle masses m_W, m_t and neglect the bottom quark mass. In addition to the masses, all diagrams depend on the squared external momentum $s = p^2$, where the main application corresponds to $s = m_H^2$.
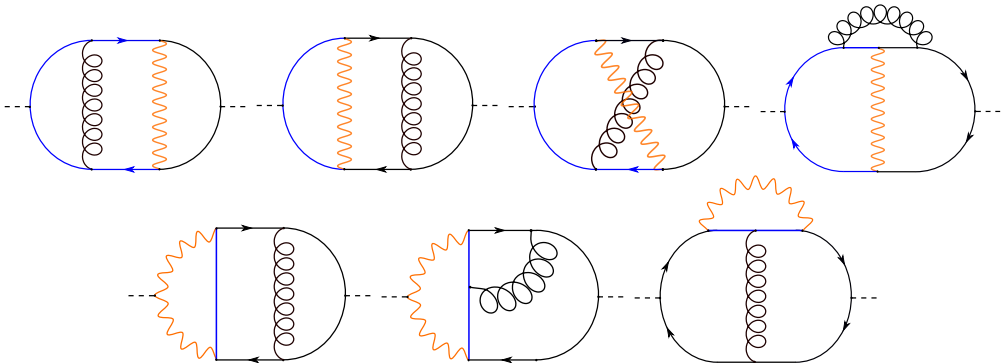
Figure 5.1: Examples of three-loop Higgs self-energy diagrams at $\mathcal{O}(\alpha^2 \alpha_s)$. Blue lines represent top quarks with mass m_t, wavy orange lines represent W-bosons (or charged Goldstone bosons) with mass m_W, curly lines represent gluons, straight black lines represent bottom quarks.

We talk about three-loop Higgs boson self-energy diagrams at $\mathcal{O}(\alpha^2 \alpha_s)$, not only involving a gluon, which contributes the factor α_s but also W-bosons or charged Goldstone bosons, which convert top quarks to bottom quarks and vice versa. The top sector diagrams are shown in fig.5.1. Sub-sector diagrams, i.e. diagrams obtained from pinching edges, are not shown here (they will be given in chapter 6).

We immediately notice two main points regarding fig.5.1. Firstly, the diagrams may

be divided into two sets, diagrams proportional to the product of Yukawa couplings $y_b y_t$ given by the first row of fig.5.1 and the complement. Secondly, the diagrams have 8 internal edges each. To demonstrate the consequences of this point, we consider the first diagram in fig.5.1. We may name its momenta obeying momentum conservation and number its edges as illustrated in fig.5.2.
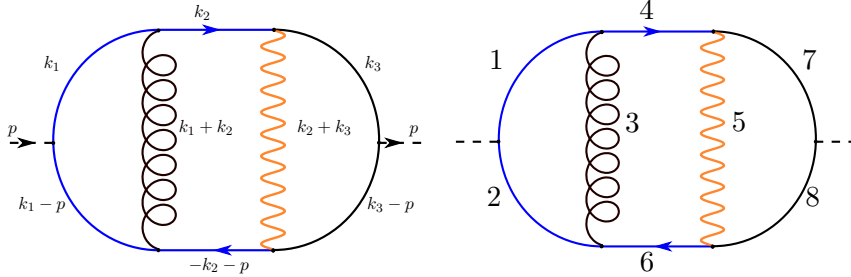
Figure 5.2: Example diagram with momenta and numbered edges. Blue lines carry mass m_t, orange lines m_W, black lines are massless.

The external momentum is called p and the three undetermined loop momenta, arising from three loops, are denoted by k_1, k_2, k_3. In correspondence, each edge gives rise to one of eight propagators. Edge 1, for example, carries momentum k_1 and mass m_t, hence, it gives rise to the propagator

$$P_1^A = -k_1^2 + m_t^2.$$

At this point, we would like to recall that within the context of Feynman integrals, we call $-q_j^2 + m_j^2$ the propagator of edge j with momentum q_j and mass m_j. Propagators are situated in the denominator of a Feynman integral, in order to place one in the numerator, they are raised to negative powers. The choice of the overall sign of propagators was motivated in chapter 3 (see especially (3.14)). We notice, no edge in fig.5.2 is accompanied by a momentum simultaneously containing k_1 and k_3. The emerging propagators suffice to express each scalar product involving k_1, k_2 or k_3 via linear combination of themselves except for $k_1 \cdot k_3$. We make similar observations for every diagram in fig.5.1. With $l = 3$ loops and $e = 1$ external momentum, we find

$$N_{scp} = \frac{l(l+1)}{2} + e \cdot l \overset{\substack{l=3 \\ e=1}}{=} 9$$

independent scalar products involving loop momenta (see (3.9)). Every diagram needs one additional propagator to be able to uniquely express every scalar product through a linear combination of propagators and to shift integrals to Baikov representation (see section 3.3.2). Appropriate auxiliary topologies with nine edges have to be found!

We may set up an auxiliary topology for the diagram in fig.5.2 as displayed in fig.5.3, now sufficient to express also $k_1 \cdot k_3$ through linear combinations of propagators, and call it topology A. The numbering of its edges coincides with the numbering in fig.5.2 and determines the numbering of propagators. Now, we may identify the diagram in fig.5.2 with a certain sector of topology A. The sector identity was defined in (3.46), it reflects the presence of edges within a diagram, since integrals with common propagators belong to the same sector. Here, edges corresponding to propagators $P_1^A - P_8^A$ are

present, yielding a sector identity of 255. Hence, sector 255 defines the top sector of topology A. Any sub-sector is represented by a smaller sector identity.

Topology A

$$P_1^A = -k_1^2 + m_t^2,$$
$$P_2^A = -(k_1 - p)^2 + m_t^2,$$
$$P_3^A = -(k_1 + k_2)^2,$$
$$P_4^A = -k_2^2 + m_t^2,$$
$$P_5^A = -(k_2 + k_3)^2 + m_W^2,$$
$$P_6^A = -(k_2 + p)^2 + m_t^2,$$
$$P_7^A = -k_3^2,$$
$$P_8^A = -(k_3 - p)^2,$$
$$P_9^A = -(k_1 - k_3)^2 + m_t^2.$$
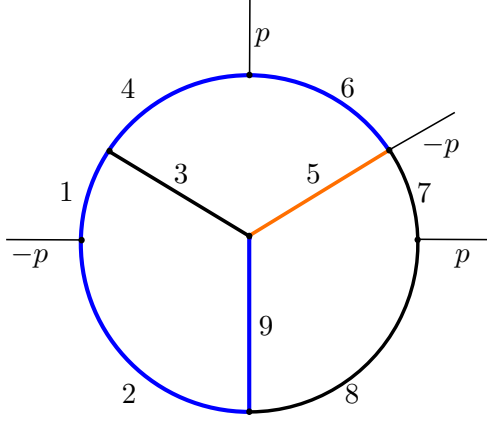
Figure 5.3: Topology A. Blue lines carry mass m_t, orange lines m_W, black lines are massless, external momenta are outgoing.
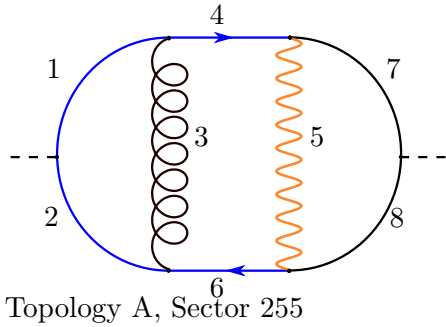
Topology A, Sector 255
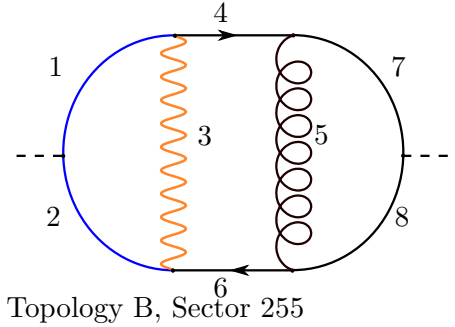
Topology B, Sector 255
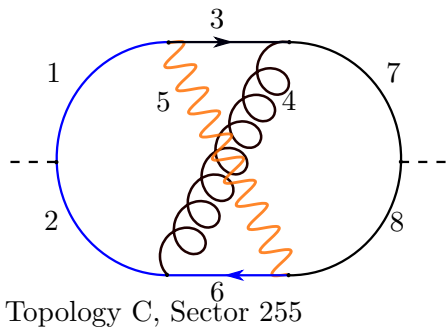
Topology C, Sector 255
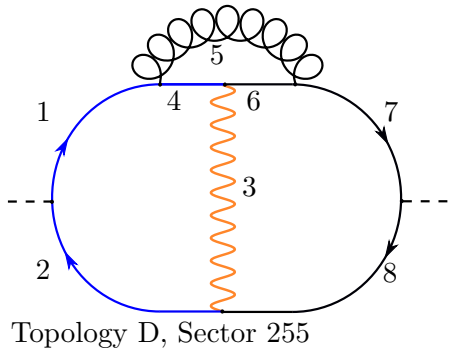
Topology D, Sector 255

Figure 5.4: Top-sector three-loop Higgs self-energy diagrams containing W- and top quarks, proportional to the product of Yukawa couplings $y_b y_t$. The colouring specifies the internal masses of propagators: Blue lines carry mass m_t, orange lines m_W, black lines are massless. External momenta are outgoing.

Topology A was constructed from the first diagram in fig.5.1. In the same manner, the

other diagrams proportional to the product of Yukawa couplings $y_b y_t$ are the starting points for the construction of topologies B,C and D. Momenta are distributed according to momentum conservation, edges are numbered as in fig.5.4 and an appropriate ninth propagator is found. The momenta of topology B match those from topology A, but less propagators of topology B are massive. Topology C corresponds to the non-planar diagram in fig.5.4. The resulting topologies are given in fig.5.5 together with topology A, for completeness. The resulting propagators will be given in table 5.1. Figure 5.4 additionally shows the resulting sector each diagram corresponds to. All topologies corresponding to diagrams proportional to the product of Yukawa couplings $y_b y_t$ have top sector 255.
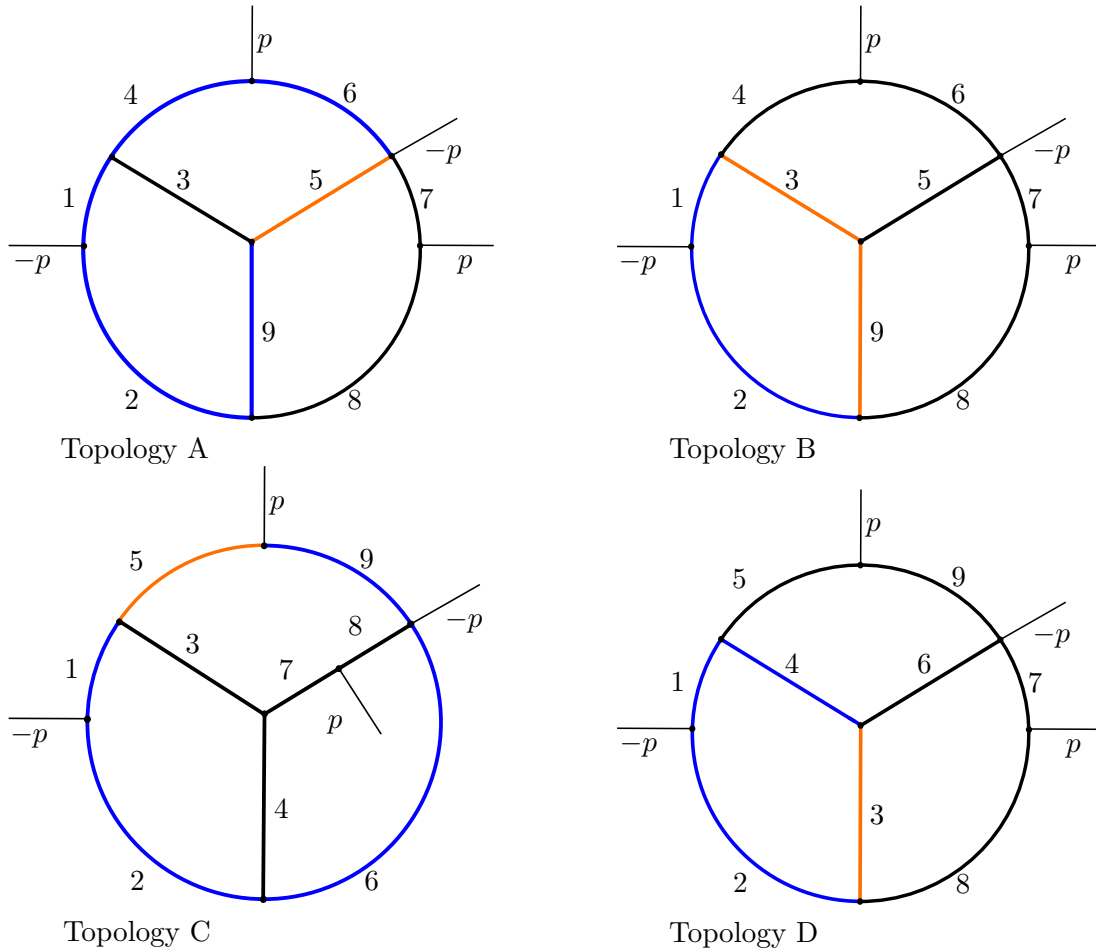
Figure 5.5: Graphs representing topologies A, B, C, D. The colouring specifies the internal masses of the propagators: Blue lines carry mass m_t, orange lines mass m_W and black lines are massless. External momenta are outgoing.

The momenta of diagrams not proportional to the product of Yukawa couplings $y_b y_t$, shown in fig.5.6, overlap such that a common set of nine propagators is easily found. The resulting topology, called topology B', resembles topology B, but its masses are exchanged $m_W \leftrightarrow m_t$. This choice is motivated as we notice that the first diagram in fig.5.6 matches the diagram corresponding to topology B, i.e. the second diagram in

fig.5.4, with exchanged masses. Resulting propagators can be read off from table 5.1. We find three different top sectors for this topology: 255, 479 and 509.

Topology B', Sector 255

Topology B', Sector 479

Topology B', Sector 509
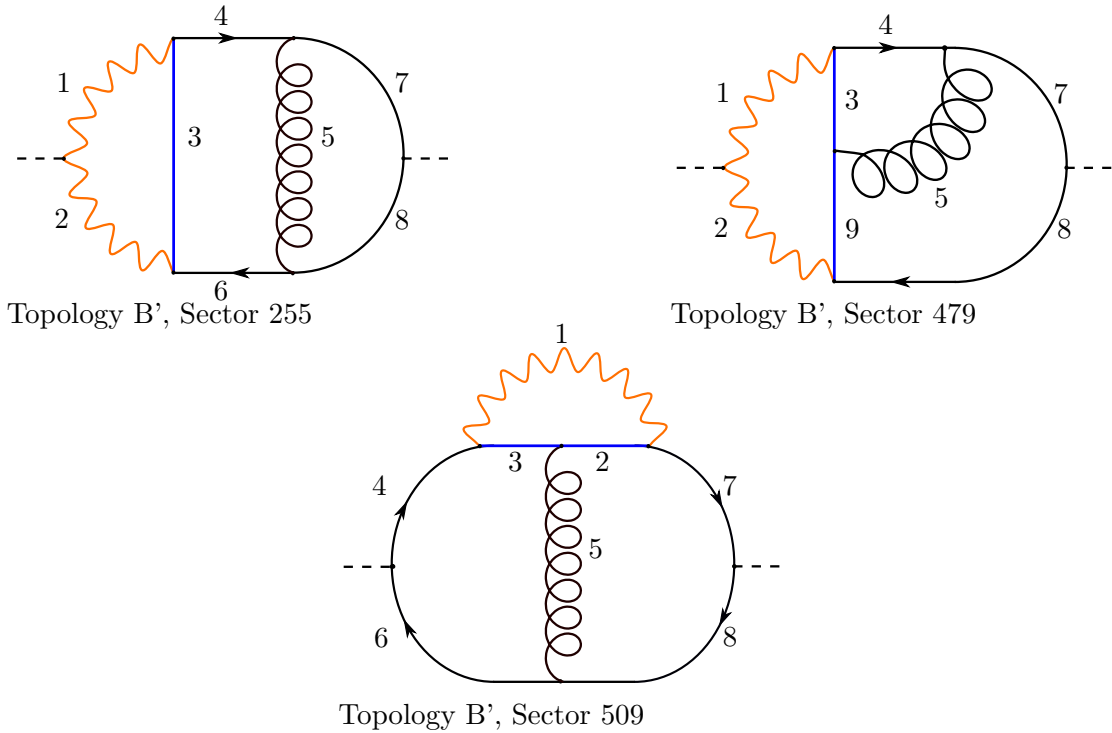
Figure 5.6: Top-sector three-loop Higgs self-energy diagrams containing W- and top quark propagators, not proportional to $y_b y_t$. Straight blue lines carry mass m_t, wavy orange lines mass m_W, curly lines represent gluons, straight black lines represent bottom quarks.
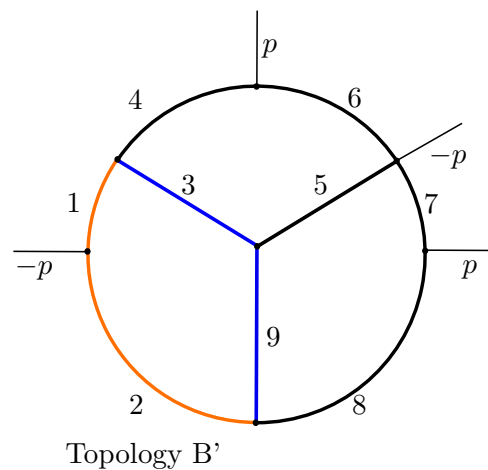
Topology B'

Figure 5.7: Graph representing the auxiliary topology B'. The colouring specifies the internal masses of the propagators: Blue lines carry mass m_t, orange lines mass m_W and black lines are massless. External momenta are outgoing.

71

Topology A:		
$P_1^A = -k_1^2 + m_t^2$	$P_2^A = -(k_1 - p)^2 + m_t^2$	$P_3^A = -(k_1 + k_2)^2$
$P_4^A = -k_2^2 + m_t^2$	$P_5^A = -(k_2 + k_3)^2 + m_W^2$	$P_6^A = -(k_2 + p)^2 + m_t^2$
$P_7^A = -k_3^2$	$P_8^A = -(k_3 - p)^2$	$P_9^A = -(k_1 - k_3)^2 + m_t^2$

Topology B:		
$P_1^B = -k_1^2 + m_t^2$	$P_2^B = -(k_1 - p)^2 + m_t^2$	$P_3^B = -(k_1 + k_2)^2 + m_W^2$
$P_4^B = -k_2^2$	$P_5^B = -(k_2 + k_3)^2$	$P_6^B = -(k_2 + p)^2$
$P_7^A = -k_3^2$	$P_8^A = -(k_3 - p)^2$	$P_9^B = -(k_1 - k_3)^2 + m_W^2$

Topology C:		
$P_1^C = -k_1^2 + m_t^2$	$P_2^C = -(k_1 - p)^2 + m_t^2$	$P_3^C = -(k_1 + k_2)^2$
$P_4^C = -(k_1 + k_2 - k_3)^2$	$P_5^C = -k_2^2 + m_W^2$	$P_6^C = -(k_2 - k_3 + p)^2 + m_t^2$
$P_7^A = -k_3^2$	$P_8^A = -(k_3 - p)^2$	$P_9^C = -(k_2 + p)^2 + m_t^2$

Topology D:		
$P_1^D = -k_1^2 + m_t^2$	$P_2^D = -(k_1 - p)^2 + m_t^2$	$P_3^D = -(k_1 - k_3)^2 + m_W^2$
$P_4^D = -(k_1 + k_2)^2 + m_t^2$	$P_5^D = -k_2^2$	$P_6^D = -(k_2 + k_3)^2$
$P_7^A = -k_3^2$	$P_8^A = -(k_3 - p)^2$	$P_9^D = -(k_2 + p)^2$

Topology B':		
$P_1^B = -k_1^2 + m_W^2$	$P_2^B = -(k_1 - p)^2 + m_W^2$	$P_3^B = -(k_1 + k_2)^2 + m_t^2$
$P_4^B = -k_2^2$	$P_5^B = -(k_2 + k_3)^2$	$P_6^B = -(k_2 + p)^2$
$P_7^A = -k_3^2$	$P_8^A = -(k_3 - p)^2$	$P_9^B = -(k_1 - k_3)^2 + m_t^2$

Table 5.1: The topologies A,B,C,D,B'. Definition of all propagators.

5.3 The pre-canonical master integrals

In the preceding section we constructed five different topologies and found their top sectors. We naturally divided them into two systems:

System 1: Topologies A, B, C and D (fig.5.5) , i.e. the topologies corresponding to all diagrams proportional to the product of Yukawa couplings $y_b y_t$ (fig.5.4). Each of them has sector 255 as top sector.

System 2: Topology B' (fig.5.7), i.e. the topology corresponding to the remaining diagrams (fig.5.6). Its top sectors are 255, 479, 509.

In correspondence with these topologies, we consider three-loop $D = (4 - 2\epsilon)$-dimensional

Feynman integrals of the following kind

$$I^X_{\nu_1\nu_2\nu_3\nu_4\nu_5\nu_6\nu_7\nu_8\nu_9} = e^{3\epsilon\gamma_E} \left(\mu^2\right)^{\nu-\frac{3D}{2}} \int \frac{d^D k_1}{i\pi^{\frac{D}{2}}} \frac{d^D k_2}{i\pi^{\frac{D}{2}}} \frac{d^D k_3}{i\pi^{\frac{D}{2}}} \prod_{j=1}^{9} \frac{1}{\left(P^X_j\right)^{\nu_j}}, \qquad (5.1)$$

where μ is an arbitrary parameter with mass dimension one and γ_E is Euler's constant. Furthermore, $\nu_j \in \mathbb{Z}$ are the exponents of propagators P^X_j, whereby

$$\nu = \sum_{j=1}^{n} \nu_j.$$

The integrals in (5.1) are given in momentum representation (see (3.29) and also (3.10) for more information on the choice of prefactors) and define the families of Feynman integrals belonging to the topologies

$$X = A, B, C, D, B',$$

defined in fig.5.5, fig.5.7 and table 5.1. The Feynman parameter representation (3.36) and the Schwinger parameter representation (3.35) were introduced in section 3.3.1. Here, they are given by

$$I^X_{\nu_1\nu_2\ldots\nu_9} = \frac{e^{\epsilon 3\gamma_E}\Gamma\left(\nu-\frac{3D}{2}\right)}{\prod\limits_{j=1}^{9}\Gamma(\nu_j)} \int_{a_j\geq 0} d^9a\, \delta\left(1-\sum_{j=1}^{9} a_j\right) \prod_{j=1}^{9} a_j^{\nu_j-1} \frac{\mathcal{U}_X(a)^{\nu-2D}}{\mathcal{F}_X(a)^{\nu-\frac{3D}{2}}}, \qquad (5.2)$$

$$I^X_{\nu_1\nu_2\ldots\nu_9} = \frac{e^{\epsilon 3\gamma_E}}{\prod\limits_{j=1}^{9}\Gamma(\nu_j)} \int_{\alpha_j\geq 0} d^9\alpha \prod_{j=1}^{9} \alpha_j^{\nu_j-1} \frac{1}{\mathcal{U}_X(\alpha)^{\frac{D}{2}}} \exp\left(-\frac{\mathcal{F}_X(\alpha)}{\mathcal{U}_X(\alpha)}\right), \qquad (5.3)$$

where $\mathcal{U}_X, \mathcal{F}_X$ are the first and second graph polynomial of topology X. They are derived from spanning trees and spanning 2-forests of the graph representing the respective topology (see (3.38)). Consequently, the first graph polynomials of topology A, topology B and topology B' are identical, since the structure of their graphs is identical. Using the abbreviation $a_{ij} = (a_i + a_j)$ the first graph polynomials evaluate to

$$\begin{aligned}
\mathcal{U}_A\,(a) =\ \mathcal{U}_B\,(a) =\ \mathcal{U}_{B'}\,(a) =\ & a_{12}\,a_3\,a_5 + a_{12}\,a_3\,a_{78} + a_{12}\,a_3\,a_9 + a_{12}\,a_{46}\,a_5 \\
& + a_{12}\,a_{46}\,a_{78} + a_{12}\,a_{46}\,a_9 + a_{12}\,a_5\,a_{78} + a_{12}\,a_5\,a_9 + a_3\,a_{46}\,a_5 + a_3\,a_{46}\,a_{78} \\
& + a_3\,a_{46}\,a_9 + a_3\,a_5\,a_{78} + a_3\,a_{78}\,a_9 + a_{46}\,a_5\,a_9 + a_{46}\,a_{78}\,a_9 + a_5\,a_{78}\,a_9, \\
\mathcal{U}_C\,(a) =\ & a_{12}\,a_3\,a_4 + a_{12}\,a_3\,a_6 + a_{12}\,a_3\,a_{78} + a_{12}\,a_4\,a_{59} + a_{12}\,a_4\,a_{78} + a_{12}\,a_{59}\,a_6 \\
& + a_{12}\,a_{59}\,a_{78} + a_{12}\,a_6\,a_{78} + a_3\,a_4\,a_{59} + a_3\,a_4\,a_6 + a_3\,a_{59}\,a_6 + a_3\,a_{59}\,a_{78} \\
& + a_3\,a_6\,a_{78} + a_4\,a_{59}\,a_6 + a_4\,a_{59}\,a_{78} + a_4\,a_6\,a_{78}, \\
\mathcal{U}_D\,(a) =\ & a_{12}\,a_3\,a_4 + a_{12}\,a_3\,a_{59} + a_{12}\,a_3\,a_6 + a_{12}\,a_4\,a_6 + a_{12}\,a_4\,a_{78} + a_{12}\,a_{59}\,a_6 \\
& + a_{12}\,a_{59}\,a_{78} + a_{12}\,a_6\,a_{78} + a_3\,a_4\,a_{59} + a_3\,a_4\,a_{78} + a_3\,a_{59}\,a_6 + a_3\,a_{59}\,a_{78} \\
& + a_3\,a_6\,a_{78} + a_4\,a_{59}\,a_6 + a_4\,a_{59}\,a_{78} + a_4\,a_6\,a_{78}. \qquad (5.4)
\end{aligned}$$

We work in $D = (4 - 2\epsilon)$-dimensions, however, we can shift the dimension of space-time with the help of the dimensional shift operator $\boldsymbol{D}^{\pm}$. The dimensional shift operator raises or lowers the dimension of a Feynman integral by 2,

$$\boldsymbol{D}^{\pm} I^X_{\nu_1 \nu_2 \nu_3 \nu_4 \nu_5 \nu_6 \nu_7 \nu_8 \nu_9} (D) = I^X_{\nu_1 \nu_2 \nu_3 \nu_4 \nu_5 \nu_6 \nu_7 \nu_8 \nu_9} (D \pm 2) . \tag{5.5}$$

During the construction of master integrals with uniform weight it is often helpful to switch to $D = (2 - 2\epsilon)$-dimensions. The tadpole (3.13), for example, has a representation of uniform weight only in $D = (2 - 2\epsilon)$-dimensions as we will explore in section 5.4.3. In order to figure out how $\boldsymbol{D}^-$ acts on an integral, we consider the Schwinger parameter representation (5.3). Its only dependence on D is through the exponent of the first graph polynomial, hence, we deduce

$$\boldsymbol{D}^- I^X_{\nu_1 \ldots \nu_9} (D) = \frac{e^{\epsilon l \gamma_E}}{\prod\limits_{j=1}^{n} \Gamma(\nu_j)} \int_{\alpha_j \geq 0} d^n \alpha \prod_{j=1}^{n} \alpha_j^{\nu_j - 1} \frac{\mathcal{U}_X(\alpha)}{\mathcal{U}_X(\alpha)^{\frac{D}{2}}} \exp\left(-\frac{\mathcal{F}_X(\alpha)}{\mathcal{U}_X(\alpha)} \right) .$$

To develop an appropriate treatment of the extra $\mathcal{U}$ in the numerator, we recall the raising operator (3.57), that acts on an integral in momentum representation like

$$\boldsymbol{j}^+ I_{\ldots, \nu_j, \ldots} = \nu_j \cdot I_{\ldots, (\nu_j + 1), \ldots} .$$

In correspondence, it acts on an integral in Schwinger parameter representation as follows,

$$\boldsymbol{j}^+ I^X_{\nu_1 \ldots \nu_9} (D) = \frac{e^{\epsilon l \gamma_E}}{\prod\limits_{j=1}^{n} \Gamma(\nu_j)} \int_{\alpha_j \geq 0} d^n \alpha \prod_{j=1}^{n} \alpha_j^{\nu_j - 1} \frac{\alpha_j}{\mathcal{U}_X(\alpha)^{\frac{D}{2}}} \exp\left(-\frac{\mathcal{F}_X(\alpha)}{\mathcal{U}_X(\alpha)} \right) .$$

The extra $\mathcal{U}_X (\alpha_1, \ldots, \alpha_9)$ in the numerator gives rise to polynomials in the Schwinger parameters (see (5.4)). Each of these parameters can be generated through the application of $\boldsymbol{j}^+$, hence, we can view $\boldsymbol{D}^-$ as [80, 81]

$$\boldsymbol{D}^- I^X_{\nu_1 \ldots \nu_9} (D) = \mathcal{U}_X \left(\boldsymbol{1}^+, \boldsymbol{2}^+, \boldsymbol{3}^+, \boldsymbol{4}^+, \boldsymbol{5}^+, \boldsymbol{6}^+, \boldsymbol{7}^+, \boldsymbol{8}^+, \boldsymbol{9}^+ \right) . \tag{5.6}$$

Any member of the integral families can be expressed through a linear combination of basis/master integrals. In the following, we determine pre-canonical master integrals for each system and afterwards we build differential equations with respect to kinematic variables. The integrals (5.1) kinematically depend on the heavy particle masses m_W and m_t as well as on the squared external momentum $s = p^2$.

We find appropriate sets of pre-canonical basis integrals through the reduction of each top sector. Integral reduction methods rely on integration by parts identities (3.52), as described in section 3.4. They may be carried out with the help of public available implementations of the Laporta algorithm, like Kira [82, 83], FIRE/LiteRed [84–87] or

`Reduze` [88, 89]. For each top sector we find the numbers of master integrals which are shown in table 5.2.

Topology	Top sector	Total number MI's
A	255	50
B	255	32
C	255	95
D	255	67
B'	255	32
B'	479	57
B'	509	43

Table 5.2: Total number of master integrals (MI's) per top sector and topology.

Pre-canonical master integral	Sector
$I^A_{100110000}$	25
$I^A_{110110000}$	27
$I^A_{011110000}$	30
$I^A_{(-1)11110000}$	30
$I^A_{101010100}$	85
$I^A_{101(-1)10100}$	85
$I^A_{011010100}$	86
$I^A_{(-1)11010100}$	86
$I^A_{011(-1)10100}$	86
$I^A_{01101(-1)100}$	86
$I^A_{100110100}$	89
$I^A_{100011100}$	113
$I^A_{10(-1)011100}$	113
$I^A_{1000111(-1)0}$	113
$I^A_{100100110}$	201
$I^A_{100010110}$	209
$I^A_{110111000}$	59
$I^A_{111010100}$	87
$I^A_{111(-1)10100}$	87
$I^A_{110110100}$	91
...	...
$I^A_{11111011(-1)}$	223
$I^A_{110111110}$	251

Table 5.3: Topology A: Possible choice of first 20 and last two pre-canonical master integrals defined as in (5.1) and the sector (3.46) they belong to.

The number of master integrals becomes a useful information only if we combine it with the sectors these master integrals belong to. The sectors and the numbers of integrals per sector encapsulate all important information about the required master integrals.

The exact formation of a pre-canonical master integral within a sector, may be chosen freely. In practice, the choice depends on ordering criteria applied by the utilised computer program. To give an example, table 5.3 shows an extract of a possible choice for the pre-canonical master integrals of topology A as well as the sectors they belong to. The full information will be given in table 5.6, table 5.7 and table 5.8.

The integrals in table 5.3 are ordered according to (3.50). First of all and most important, sectors are ordered by their number of propagators, such that the first sector is the simplest in the sense that it has the lowest number of propagators. We see, the first integral in table 5.3 has three propagators, then all integrals with four propagators line up, before sector 59 starts the line of integrals with five propagators. Integrals are ordered to ensure that reduction methods relate integrals only to simpler integrals (see section 3.4.1 for details).

Table 5.2 shows the number of master integrals if we treat each top sector individually. However, master integrals from different top sectors and different topologies may be identical or related by symmetries. Out of the 67 master integrals from topology D, for example, only one integral is not expressible through master integrals of topology A, B or C. Hence, we may exchange master integrals from one topology with those from a former topology and determine cumulative sets of master integrals. Table 5.4 displays respective numbers of the first system and table 5.5 of the second system.

Topology$_{\text{top sector}}$	independent MI's	cumulative number of MI's	
A_{255}	50	A_{255}	50
B_{255}	17	$A_{255}+B_{255}$	67
C_{255}	37	$A_{255}+B_{255}+C_{255}$	104
D_{255}	1	$A_{255}+B_{255}+C_{255}+D_{255}$	105

Table 5.4: System 1: Independent number of master integrals (MI's) per top sector and topology as well as cumulative sum.

Topology$_{\text{top sector}}$	independent MI's	cumulative number of MI's	
B'_{255}	32	B'_{255}	32
B'_{479}	29	$B'_{255} + B'_{479}$	61
B'_{509}	4	$B'_{255} + B'_{479} + B'_{509}$	65

Table 5.5: System 2: Independent number of master integrals (MI's) per top sector and topology as well as cumulative sum.

Note, the numbers in table 5.4 and table 5.5 do not take relations between integrals of different systems into account. However, topology B' resembles topology B, but has switched masses $m_W \leftrightarrow m_t$. Their integrals under top sector 255 are related.

System 1 amounts to $N_{MI}^1 = 105$ independent master integrals and system 2 to $N_{MI}^2 = 65$ master integrals. Note, that the emergence of square roots will force us to split system 2 even further, into system 2a containing top sector 255 and 479 with $N_{MI}^{2a} = 61$

integrals and system 2b containing top sector 509 with $N_{MI}^{2b} = 43$ integrals. (We will encounter square roots in section 5.4.3 and section 5.4.4 (see (5.42), (5.58)). We will deal with them in section 5.5.1.) For each system, we view the ordered sets of master integrals as vectors,

$$\vec{I}_1, \quad \vec{I}_{2a}, \quad \vec{I}_{2b}.$$

Table 5.6, table 5.7 and table 5.8 denote the ordered sectors and the numbers of integrals per sector of system 1, system 2a and system 2b, respectively. As a consequence, they completely characterise the required master integrals $\vec{I}_1, \vec{I}_{2a}, \vec{I}_{2b}$.

Topology	Sectors
A	25 , 27 , 30 , 30 , 85 , 85 , 86 , 86 , 86 , 86 , 89 , 113 , 113 , 113 , 201 , 209, 59 , 87 , 87 , 91 , 94 , 94 , 94 , 115 , 115 , 115 , 117 , 117 , 117 , 117 , 121, 203 , 206 , 206 , 211 , 213 , 119 , 119 , 123 , 215 , 215 , 215 , 222 ,222,235 , 249 , 223 , 223 , 223 , 251
B	113 , 116 , 115 , 117 , 117 , 117 , 118 , 206 , 206 , 206 , 233 , 236, 119 , 119 , 207 , 235 , 223 , 239
C	101 , 101 , 101 , 102 , 103 , 117 , 117 , 117 , 118 , 118 , 118 , 173 , 173 , 181 , 119 , 119 , 119 , 175 , 183 , 189 , 189 , 190 , 231 , 231 , 231 , 246 , 246 , 191 , 191 , 191 , 191 , 247 , 247 , 247 , 247 , 253 , 255
D	239

Table 5.6: System 1: Ordered topologies and sectors from system 1. Sector identities (3.46) define the sector. The number of equal sector identities refers to the number of master integrals required in this sector.

Sectors from Topology B'
85 , 85 , 86 , 86 , 86 , 86 , 113 , 116 , 197 , 87 , 87 , 115 , 117 , 117 , 117 , 118 , 199 , 205 , 206 , 206 , 206 , 233 , 236 , 119 , 119 , 207 , 215 , 215 , 215 , 235 , 223 , 239 ,261 , 263 , 269 , 270 , 270 , 270 , 332 , 396 , 396 , 396 , 452 , 271 , 333 , 334 , 334 , 334 , 397 , 397 , 397 , 335 , 399 , 413 , 455 , 462 , 462 , 415 , 415 , 415 , 463

Table 5.7: System 2a: Ordered sectors from system 2a. Sector identities (3.46) define the sector. The number of equal sector identities refers to the number of master integrals required in this sector.

Sectors from Topology B'
85 , 85 , 113 , 116 , 197 , 117 , 117 , 117 , 205 , 233 , 236 , 261 , 269 , 332 , 396 , 396 , 396 , 452 , 333 , 397 , 397 , 397 , 413 , 492 , 492 , 493 , 493 , 149 , 149 , 149 , 149 , 293 , 293 , 293 , 157 , 229 , 229 , 229 , 421 , 421 , 421 , 429 , 429

Table 5.8: System 2b: Ordered sectors from system 2b. Sector identities (3.46) define the sector. The number of equal sector identities refers to the number of master integrals required in this sector.

For now, we do not distinguish between the different systems $\vec{I}_1, \vec{I}_{2a}, \vec{I}_{2b}$, since the following procedure is similar for all of them. Hence we keep notations general and drop the index indicating the system. We write

$$\vec{I} = (I_1, \dots, I_{N_{MI}})^T,$$

for the master integrals of any of the systems interchangeably. If we want to emphasise their correspondence to different sectors, we divide the vector into smaller vectors

$$\vec{I} = \begin{pmatrix} \vec{I}^{sec_1} \\ \vec{I}^{sec_2} \\ \vec{I}^{sec_3} \\ \dots \end{pmatrix},$$

where the numbers $1, 2, 3, \dots$ are placeholders that may be replaced by sector identities from table 5.6, table 5.7 or table 5.8 if we talk about a certain system. To simplify notations, we do not indicate correspondences to topologies at this level, however, this should be clear from the context. At the level of specific integrals (5.1) the correspondence is completely specified.

In order to calculate $\vec{I}$, we apply the method of differential equation, described in section 3.5. We start as we set up differential equations with respect to their kinematic variables, i.e. p^2, m_W^2, m_t^2, in the following subsection.

5.3.1 Differential equations

Now, we laid the foundation for our upcoming work, because we specified the numbers, sectors and topologies of master integrals we need to compute. The 105 and 61/43 precanonical master integrals of system 1 and system 2a/b depend on $s = p^2$ and m_W^2, m_t^2. During the construction of differential equations with respect to these variables, we may treat the systems on an equal footing. We already derived differential equations with respect to squared masses for a general set of Feynman integrals in section 3.5, (3.58). Here, the result we found translates into

$$\mu^2 \frac{\partial}{\partial m_t^2} I^X_{\nu_1\nu_2\nu_3\nu_4\nu_5\nu_6\nu_7\nu_8\nu_9} = -\sum_{j \in J^X_{m_t^2}} \boldsymbol{j}^+ I^X_{\nu_1\nu_2\nu_3\nu_4\nu_5\nu_6\nu_7\nu_8\nu_9}, \tag{5.7}$$

$$\mu^2 \frac{\partial}{\partial m_W^2} I^X_{\nu_1\nu_2\nu_3\nu_4\nu_5\nu_6\nu_7\nu_8\nu_9} = -\sum_{j \in J^X_{m_W^2}} \boldsymbol{j}^+ I^X_{\nu_1\nu_2\nu_3\nu_4\nu_5\nu_6\nu_7\nu_8\nu_9}, \tag{5.8}$$

where $\boldsymbol{j}^+$ is the raising operator (3.57),

$$\boldsymbol{j}^+ I_{\dots,\nu_j,\dots} = \nu_j \cdot I_{\dots,(\nu_j+1),\dots}.$$

$J^X_{m_t^2}$ and $J^X_{m_W^2}$ are the sets of edges of topology $X = A, B, C, D, B'$ that carry mass m_t^2 and m_W^2, respectively.

$$J^A_{m_t^2} = \{1,2,4,6,9\} \qquad\qquad J^A_{m_W^2} = \{5\}$$

$$J^B_{m_t^2} = \{1,2\} \qquad\qquad J^B_{m_W^2} = \{3,9\}$$

$$J^C_{m_t^2} = \{1,2,6,9\} \qquad\qquad J^C_{m_W^2} = \{5\}$$

$$J^D_{m_t^2} = \{1,2,4\} \qquad\qquad J^D_{m_W^2} = \{3\}$$

$$J^{B'}_{m_t^2} = \{3,9\} \qquad\qquad J^{B'}_{m_W^2} = \{1,2\}$$

We show an example, a sub sector of topology B' with top sector 479, namely sector 334. Sector 334 gives rise to three master integrals,

$$\vec{I}^{sec334} = \begin{pmatrix} I^{B'}_{011100101} \\ I^{B'}_{(-1)11100101} \\ I^{B'}_{0111(-1)0101} \end{pmatrix}. \tag{5.9}$$

The integrals contain both top quark propagators $P_3^{B'}, P_9^{B'}$ up to power one, hence, differentiating them with respect to m_t^2 yields

$$\mu^2 \frac{\partial}{\partial m_t^2} I^{B'}_{011100101} = -I^{B'}_{012100101} - I^{B'}_{011100102},$$

$$\mu^2 \frac{\partial}{\partial m_t^2} I^{B'}_{(-1)11100101} = -I^{B'}_{(-1)12100101} - I^{B'}_{(-1)11100102},$$

$$\mu^2 \frac{\partial}{\partial m_t^2} I^{B'}_{0111(-1)0101} = -I^{B'}_{0121(-1)0101} - I^{B'}_{0111(-1)0102}. \tag{5.10}$$

The only W-boson propagator the first and third integral contain is $P_2^{B'}$, the second integral, however, carries $P_1^{B'}$ raised to power minus one. This minus one becomes a zero after applying $\mathbf{1}^+$, additionally the sign of the integral changes,

$$\mathbf{1}^+ I^{B'}_{(-1)11100101} = -I^{B'}_{011100101}.$$

Differentiating the integrals with respect to m_W^2, therefore, leads to

$$\mu^2 \frac{\partial}{\partial m_W^2} I^{B'}_{011100101} = -I^{B'}_{021100101},$$

$$\mu^2 \frac{\partial}{\partial m_W^2} I^{B'}_{(-1)11100101} = I^{B'}_{011100101} - I^{B'}_{(-1)21100101},$$

$$\mu^2 \frac{\partial}{\partial m_W^2} I^{B'}_{0111(-1)0101} = -I^{B'}_{0211(-1)0101}. \tag{5.11}$$

To differentiate an integral with respect to s, we will obtain a relation among differential equations with respect to different variables. In this way, the derivative with respect to s can be constructed from those with respect to masses. This relation holds independently of the specific set of kinematic variables, hence, we keep a general set $x_1, \ldots, x_{N_v+1}$,

which we abbreviate by x. It may be re-translated via $x_1 = s$, $x_2 = m_W^2$, $x_3 = m_t^2$. The relation can be constructed within momentum representation through a scaling of loop momenta $k \to \frac{k}{\lambda}$ and the subsequent application of $\lambda^2 \frac{\partial}{\partial \lambda^2}$ to the integral. A quicker derivation may be performed within Feynman parameter representation (3.36), which was introduced in section 3.3.1,

$$I = \frac{e^{\epsilon l \gamma_E} \Gamma\left(\nu - \frac{lD}{2}\right)}{\prod_{j=1}^n \Gamma(\nu_j)} \int_{a_j \geq 0} d^n a \; \delta\left(1 - \sum_{j=1}^n a_j\right) \prod_{j=1}^n a_j^{\nu_j - 1} \frac{\mathcal{U}(a)^{\nu - \frac{(l+1)D}{2}}}{\mathcal{F}(a)^{\nu - \frac{lD}{2}}}, \qquad (5.12)$$

where $\mathcal{U}, \mathcal{F}$ (3.34) are the first and second graph polynomials. $\mathcal{U}$ solely depends on Feynman parameters a_j in contrast to $\mathcal{F}$. In the end of section 3.3.1 in (3.38), we deduced that $\mathcal{F}$ depends linearly on kinematic variables. In correspondence, we may write for the second graph polynomial

$$\mathcal{F}(a, x) = \sum_{i=1}^{N_v + 1} \mathcal{F}'_{x_i} \cdot x_i,$$

where

$$\mathcal{F}'_{x_i} = \frac{\partial}{\partial x_i} \mathcal{F}(a, x).$$

In order to construct the desired relation, an integral (5.12) is differentiated with respect to every kinematic variable while multiplying with the respective variable,

$$\sum_{i=1}^{N_v + 1} x_i \frac{\partial}{\partial x_i} I =$$

$$\frac{e^{\epsilon l \gamma_E} \Gamma\left(\nu - \frac{lD}{2}\right)}{\prod_{j=1}^n \Gamma(\nu_j)} \int_{a_j \geq 0} d^n a \; \delta\left(1 - \sum_{j=1}^n a_j\right) \prod_{j=1}^n a_j^{\nu_j - 1} \sum_{i=1}^{N_v + 1} x_i \frac{\partial}{\partial x_i} \frac{\mathcal{U}(a)^{\nu - \frac{(l+1)D}{2}}}{\mathcal{F}(a)^{\nu - \frac{lD}{2}}}.$$

Evaluating the derivatives,

$$\sum_{i=1}^{N_v + 1} x_i \frac{\partial}{\partial x_i} \frac{\mathcal{U}(a)^{\nu - \frac{(l+1)D}{2}}}{\mathcal{F}(a)^{\nu - \frac{lD}{2}}} = -\left(\nu - \frac{lD}{2}\right) \sum_{i=1}^{N_v + 1} \frac{x_i \mathcal{F}'_{x_i} \mathcal{U}(a)^{\nu - \frac{(l+1)D}{2}}}{\mathcal{F}(a)^{\nu - \frac{lD}{2} + 1}}$$

$$= \left(\frac{lD}{2} - \nu\right) \frac{\mathcal{F}(a) \, \mathcal{U}(a)^{\nu - \frac{(l+1)D}{2}}}{\mathcal{F}(a)^{\nu - \frac{lD}{2} + 1}}$$

$$= \left(\frac{lD}{2} - \nu\right) \frac{\mathcal{U}(a)^{\nu - \frac{(l+1)D}{2}}}{\mathcal{F}(a)^{\nu - \frac{lD}{2}}},$$

results into the sought after relation

$$\sum_{i=1}^{N_v + 1} x_i \frac{\partial}{\partial x_i} I = \left(\frac{lD}{2} - \nu\right) I. \qquad (5.13)$$

Coming back to $x_1 = s$, $x_2 = m_W^2$, $x_3 = m_t^2$, $l = 3$ we obtain

$$\left(\nu - \frac{3D}{2} + s \frac{\partial}{\partial s} + m_W^2 \frac{\partial}{\partial m_W^2} + m_t^2 \frac{\partial}{\partial m_t^2} \right) I = 0. \tag{5.14}$$

Combining (5.7) and (5.8) with (5.14) we find the resulting derivative with respect to s,

$$\mu^2 \frac{\partial}{\partial s} I^X_{\nu_1 \nu_2 \nu_3 \nu_4 \nu_5 \nu_6 \nu_7 \nu_8 \nu_9} = \left(\frac{3D}{2} - \nu \right) \frac{\mu^2}{s} I^X_{\nu_1 \nu_2 \nu_3 \nu_4 \nu_5 \nu_6 \nu_7 \nu_8 \nu_9}$$
$$+ \frac{m_W^2}{s} \sum_{j \in J^X_{m_w^2}} \boldsymbol{j}^+ I^X_{\nu_1 \nu_2 \nu_3 \nu_4 \nu_5 \nu_6 \nu_7 \nu_8 \nu_9} + \frac{m_t^2}{s} \sum_{j \in J^X_{m_t^2}} \boldsymbol{j}^+ I^X_{\nu_1 \nu_2 \nu_3 \nu_4 \nu_5 \nu_6 \nu_7 \nu_8 \nu_9}. \tag{5.15}$$

Applying (5.15) to the first integral from our example sector 334 (5.9), we find with $\nu = 5$,

$$\mu^2 \frac{\partial}{\partial s} I^{B'}_{011100101} = \underbrace{\left(\frac{3D}{2} - 5 \right)}_{= (1 - 3\epsilon)} \frac{\mu^2}{s} I^{B'}_{011100101} + \frac{m_W^2}{s} I^{B'}_{021100101} + \frac{m_t^2}{s} \left(I^{B'}_{012100101} + I^{B'}_{011100102} \right). \tag{5.16}$$

The second and third integral from sector 334 have $\nu = 4$. Their derivatives with respect to s evaluate to

$$\mu^2 \frac{\partial}{\partial s} I^{B'}_{(-1)11100101} = \underbrace{\left(\frac{3D}{2} - 4 \right)}_{= (2 - 3\epsilon)} \frac{\mu^2}{s} I^{B'}_{(-1)11100101} + \frac{m_W^2}{s} \left(-I^{B'}_{011100101} + I^{B'}_{(-1)21100101} \right)$$
$$+ \frac{m_t^2}{s} \left(I^{B'}_{(-1)12100101} + I^{B'}_{(-1)11100102} \right),$$
$$\mu^2 \frac{\partial}{\partial s} I^{B'}_{0111(-1)0101} = (2 - 3\epsilon) \frac{\mu^2}{s} I^{B'}_{0111(-1)0101} + \frac{m_W^2}{s} I^{B'}_{0211(-1)0101}$$
$$+ \frac{m_t^2}{s} \left(I^{B'}_{0121(-1)0101} + I^{B'}_{0111(-1)0102} \right). \tag{5.17}$$

Now, we are able to differentiate the pre-canonical master integrals with respect to m_t^2, m_W^2 (5.7),(5.8) and p^2 (5.15). We recall, the factors of μ^2 in the definition of integrals (5.1) shall ensure that integrals depend on scalar, dimensionless kinematic variables (see (3.10)). We may set

$$\mu^2 = m_t^2,$$

and consequently the integrals kinematically depend on the following variables

$$v = \frac{p^2}{m_t^2}, \quad w = \frac{m_W^2}{m_t^2}. \tag{5.18}$$

Derivatives with respect to w, v can be directly read off from (5.8) and (5.15), since

$$
\frac{\partial}{\partial w} I^X_{\nu_1\nu_2\nu_3\nu_4\nu_5\nu_6\nu_7\nu_8\nu_9} = \mu^2 \frac{\partial}{\partial m_W^2} I^X_{\nu_1\nu_2\nu_3\nu_4\nu_5\nu_6\nu_7\nu_8\nu_9},
$$

$$
\frac{\partial}{\partial v} I^X_{\nu_1\nu_2\nu_3\nu_4\nu_5\nu_6\nu_7\nu_8\nu_9} = \mu^2 \frac{\partial}{\partial s} I^X_{\nu_1\nu_2\nu_3\nu_4\nu_5\nu_6\nu_7\nu_8\nu_9}.
$$

Derivatives of the integrals from sector 334, for example, are obtained from (5.11), (5.16) and (5.16),

$$
\frac{\partial}{\partial w} I^{B'}_{011100101} = -I^{B'}_{021100101},
$$

$$
\frac{\partial}{\partial w} I^{B'}_{(-1)11100101} = I^{B'}_{011100101} - I^{B'}_{(-1)21100101},
$$

$$
\frac{\partial}{\partial w} I^{B'}_{0111(-1)0101} = -I^{B'}_{0211(-1)0101}, \tag{5.19}
$$

$$
\frac{\partial}{\partial v} I^{B'}_{011100101} = \frac{1}{s}\left[(1 - 3\epsilon)I^{B'}_{011100101} + wI^{B'}_{021100101} + I^{B'}_{012100101} + I^{B'}_{011100102}\right],
$$

$$
\frac{\partial}{\partial v} I^{B'}_{(-1)11100101} = \frac{1}{s}\left[(2 - 3\epsilon)I^{B'}_{(-1)11100101} + w\left(-I^{B'}_{011100101} + I^{B'}_{(-1)21100101}\right)\right.
$$
$$
\left. + I^{B'}_{(-1)12100101} + I^{B'}_{(-1)11100102}\right],
$$

$$
\frac{\partial}{\partial v} I^{B'}_{0111(-1)0101} = \frac{1}{s}\left[(2 - 3\epsilon)I^{B'}_{0111(-1)0101} + wI^{B'}_{0211(-1)0101} + I^{B'}_{0121(-1)0101} + I^{B'}_{0111(-1)0102}\right]. \tag{5.20}
$$

By construction, some of the integrals on the right hand sides of (5.19) and (5.20) have additional dots, i.e. propagators raised to power two, compared to the basis integrals of sector 334 (5.9). Applying integration by parts reduction methods, they are again expressible through linear combinations of master integrals of sector 334 and sub-sectors. The integral with a dot on the second propagator, for example, can be re-expressed as

$$
I^{B'}_{021100101} = \frac{1}{2w\left(v^2 - 2v(w+1) + (w-1)^2\right)}\left\{I^{B'}_{011100101}\left[v^2(-2\epsilon(w - 3) + 2w - 5)\right.\right.
$$

$$
+ v\left(-2\epsilon\left(2w^2 - 7w + 3\right) + 4w^2 - 11w + 5\right) + 2(w - 1)w(\epsilon(3w - 7) - 3w + 5)\Big]
$$

$$
+ I^{B'}_{(-1)11100101}\left[-2\epsilon\left(v^2 + 2vw + v - 3w^2 - w - 2\right) + 2v^2 + 4vw + v - 6w^2 - w - 3\right]
$$

$$
- I^{B'}_{0111(-1)0101}\left[2(\epsilon - 1)\left(v^2 + v(2w - 1) - 3w^2 + w\right)\right]
$$

$$
- I^{B'}_{101000001}2(\epsilon - 1)(v + 3w - 1)
$$

$$
+ I^{B'}_{011100001}2(\epsilon - 1)\left(v^2 + v(w - 1) - 2w(3w + 1)\right) + I^{B'}_{(-1)11100001}2(\epsilon - 1)(v + 3w - 1)
$$

$$
+ I^{B'}_{01110(-1)001}4(\epsilon - 1)(v + 3w - 1)
$$

$$
+ I^{B'}_{001100101}(4\epsilon(v + 2w - 1) - 3v - 5w + 3)\Big\}. \tag{5.21}
$$

We see, here, the sub-sector contributions come from the master integral belonging to sector 261 with master integral $\vec{I}^{sec261} = \left(I^{B'}_{101000001}\right)$, from sector 270 with master

integrals

$$\vec{I}^{sec270} = \begin{pmatrix} I^{B'}_{011100001} \\ I^{B'}_{(-1)11100001} \\ I^{B'}_{01110(-1)001} \end{pmatrix},$$

and sector 332 with $\vec{I}^{sec332} = \left(I^{B'}_{001100101} \right)$. Relations like the integration by parts relation in (5.21) make it possible to construct differential equations for the integrals from sector 334,

$$\frac{\partial}{\partial v} \vec{I}^{sec334} = A^{(334)}_v \vec{I}^{sec334} + \text{sub-sector contributions},$$

$$\frac{\partial}{\partial w} \vec{I}^{sec334} = A^{(334)}_w \vec{I}^{sec334} + \text{sub-sector contributions},$$

where $A^{(334)}_v, A^{(334)}_w$ are 3×3-dimensional matrices, depending on v, w, ϵ. The matrices' components are rather long, hence, we do not display them here in full. Instead we give a short example regarding their construction. Combining the derivative of the first master integral from sector 334 with respect to w (5.19) with the relation in (5.21), we obtain the complete first row of $A^{(334)}_w$,

$$\begin{aligned} A^{(334)}_w(1) = \frac{1}{2w \left(v^2 - 2v(w+1) + (w-1)^2 \right)} &\left\{ \left[v^2(-2\epsilon(w-3) + 2w - 5) \right. \right. \\ &+ v \left(-2\epsilon \left(2w^2 - 7w + 3 \right) + 4w^2 - 11w + 5 \right) + 2(w-1)w(\epsilon(3w-7) - 3w + 5) \right], \\ &\left[-2\epsilon \left(v^2 + 2vw + v - 3w^2 - w - 2 \right) + 2v^2 + 4vw + v - 6w^2 - w - 3 \right], \\ &\left. - \left[2(\epsilon - 1) \left(v^2 + v(2w-1) - 3w^2 + w \right) \right] \right\}. \end{aligned}$$

The sub-sector contributions take the form

$$\sum_{l=\{261,270,332\}} A^{(l\times 334)}_{v/w} \vec{I}^{sec_l},$$

where $A^{(l\times 334)}_{v/w}$ are matrices of respective sizes.

Analogously, we may write for the complete vectors of master integrals $\vec{I}$ (either from system 1 or system 2a/b),

$$\frac{\partial}{\partial w} \vec{I} = \mu^2 \frac{\partial}{\partial m_W^2} \vec{I} \overset{\text{IBP}}{=} A_w \vec{I},$$

$$\frac{\partial}{\partial v} \vec{I} = \mu^2 \frac{\partial}{\partial s} \vec{I} \overset{\text{IBP}}{=} A_v \vec{I},$$

where A_w, A_v are (105×105)-dimensional $((61 \times 61)/(43 \times 43)$-dimensional) matrices in the case of system 1 (system 2a/b). They depend on v, w and the dimensional regularisation parameter.

We summarise our findings as we set up systems of differential equations

$$d\vec{I} = A\left(\epsilon, v, w\right)\vec{I},$$
$$A = A_w dw + A_v dv,$$

(5.22)

where d denotes the total derivative. The systems fulfil the integrability condition (3.64),

$$\partial_w A_v - \partial_v A_w - [A_w, A_v] = 0,$$

where $[,]$ denotes the commutator.

In correspondence with our discussion in section 3.6, the ordering of master integrals results in differential equations consisting of lower block-triangular matrices. Sectors manifest themselves as blocks on the diagonal, sub-sector contributions appear to their left. A schematic representation of the first fifteen rows and columns of the matrix corresponding to system 1 is shown in an exemplary manner in fig.5.8. The corresponding first fifteen pre-canonical master integrals from system 1 as well as their sectors can be read off from table 5.3. In correspondence, we find blocks on the diagonal of fig.5.8 with dimensions according to the numbers of integrals per sectors.
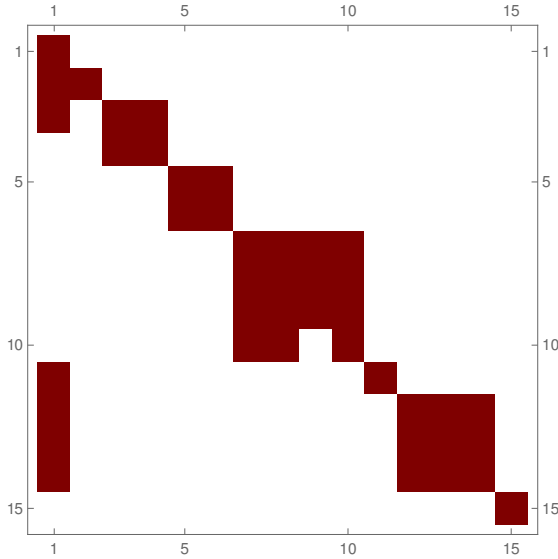
Figure 5.8: Block structure: A schematic representation of $A_{(1-15,1-15)}$, where $d\vec{I} = A\vec{I}$ belongs to system 1. White areas represent zeros, red areas are non zero.

5.4 Basis transformations

We recall from section 3.5.1 that we are seeking a system of differential equations in canonical form, i.e.

$$d\vec{J} = \epsilon\tilde{A},$$

$$\tilde{A} = \sum_i C_i \omega_i,$$

where C_i are $N_{MI} \times N_{MI}$- dimensional matrices consisting of algebraic numbers and ω_i are one-forms depending on kinematic variables, containing only simple poles. As summarised in box 1 in section 3.6, differential equations of pre-canonical master integrals $\vec{I}$ (5.22) arrive there through the application of:

1. Basis transformations: Find appropriate basis transformations $U\left(\vec{I} = U\vec{J}\right)$, which factor out ϵ.

2. Variable transformations: Find appropriate variable transformations that rationalise all occurring square roots.

This section treats the first point, basis transformations. The second point, will be discussed in section 5.5.1, however, already in this section we will encounter the need for variable transformations.

We left the previous section with two main conclusions. Firstly, we found three sets (system 1 and system 2a/b) of pre-canonical master integrals $\vec{I}$ and built their systems of differential equations (5.22),

$$d\vec{I} = (A_w dw + A_v dv)\,\vec{I},$$
$$\frac{\partial}{\partial w}\vec{I} = A_w \vec{I}, \quad \frac{\partial}{\partial v}\vec{I} = A_v \vec{I}. \tag{5.23}$$

The emerging matrices depend on the kinematic variables v, w as well as on the dimensional regularisation parameter ϵ. In this section we will employ a heuristic approach to find master integrals of uniform weight $\vec{J}$, yielding a differential equation with linear dependence on ϵ,

$$d\vec{J} = \epsilon\tilde{A}, \tag{5.24}$$

where $\tilde{A}$ is independent of ϵ. Heuristic approaches may seem to be less powerful than algorithmic approaches, since their success is not predestined. In our case, however, their success is easily verified or falsified. We simply calculate the resulting differential equation. Since existing algorithms [68–70, 72–74] cannot handle problems of this complexity, our heuristic approach yields a welcome and easy to handle method. As before, we describe our methods in a general manner if they apply to each of the three sets. In correspondence we keep our notations general.

The second conclusion of the preceding section concerns the structure of the systems of differential equations. As shown in fig.5.8, systems of differential equations consist of lower block-triangular matrices with sectors represented by blocks on the diagonal and sub-sectors contributions to their left. This is rather obvious as reduction methods are designed to relate integrals only to simpler integrals. However, it is still important for our ongoing strategy because it allows us to divide the complete differential equation into equations for each sector,

$$
\frac{\partial}{\partial v}
\begin{pmatrix}
\vec{I}^{sec_1} \\
\vec{I}^{sec_2} \\
\vec{I}^{sec_3} \\
\cdots
\end{pmatrix}
=
\begin{pmatrix}
A_v^{(1)} & 0 & 0 & \cdots \\
A_v^{(1\times2)} & A_v^{(2)} & 0 & \\
A_v^{(1\times3)} & A_v^{(2\times3)} & A_v^{(3)} & \\
\cdots & & &
\end{pmatrix}
\begin{pmatrix}
\vec{I}^{sec_1} \\
\vec{I}^{sec_2} \\
\vec{I}^{sec_3} \\
\cdots
\end{pmatrix},
$$

$$
\frac{\partial}{\partial v}\vec{I}^{sec_j} = A_v^{(j)}\vec{I}^{sec_j} + \sum_{l<j} A_v^{(l\times j)}\vec{I}^{sec_l},
$$

$$
\frac{\partial}{\partial w}
\begin{pmatrix}
\vec{I}^{sec_1} \\
\vec{I}^{sec_2} \\
\vec{I}^{sec_3} \\
\cdots
\end{pmatrix}
=
\begin{pmatrix}
A_w^{(1)} & 0 & 0 & \cdots \\
A_w^{(1\times2)} & A_w^{(2)} & 0 & \\
A_w^{(1\times3)} & A_w^{(2\times3)} & A_w^{(3)} & \\
\cdots & & &
\end{pmatrix}
\begin{pmatrix}
\vec{I}^{sec_1} \\
\vec{I}^{sec_2} \\
\vec{I}^{sec_3} \\
\cdots
\end{pmatrix},
\tag{5.25}
$$

$$
\frac{\partial}{\partial w}\vec{I}^{sec_j} = A_w^{(j)}\vec{I}^{sec_j} + \sum_{l<j} A_w^{(l\times j)}\vec{I}^{sec_l}.
$$

$\vec{I}^{sec_j}$ denotes the set of master integrals belonging to sector j. $A_{v/w}^{(j)}$, $A_{v/w}^{(l\times j)}$ denote matrices with dimensions determined by the length of $\vec{I}^{sec_j}$ or the length of $\vec{I}^{sec_l}$ and $\vec{I}^{sec_j}$ respectively. In the following, we may write $A^{(j)}$, $A^{(l\times j)}$ instead of $A_{v/w}^{(j)}$, $A_{v/w}^{(l\times j)}$ if we talk about procedures applying to both differential equations in the same way.

We benefit from the block structure of the differential equations as it enables us to treat blocks individually instead of altogether. In this thesis we employ a bottom-up approach, i.e. we, thereby, start with the first block of the differential equation. We outline this approach in section 5.4.2, after discussing two important types of transformations in the following section. A good strategy for the treatment of diagonal blocks consists of finding an ansatz for an integral of uniform weight. In section 5.4.3 we find representations of the tadpole and bubble integral as integrals of uniform weight. There, we define our first canonical master integrals and understand the necessity of the dimensional shift operator (5.5). Integrals of uniform weight can be determined through the application of maximal cuts and the analysis of their leading singularities. This will be described in section 5.4.4.

Consequently, we may specify the listing made at the beginning of this section as we divide the first point into tasks regarding diagonal or off-diagonal blocks of the differential equation:

1. Basis transformations: Find appropriate basis transformations U that factor out ϵ utilising a bottom-up approach:

   – Diagonal blocks: Leading singularity analyses of maximal cuts provides ansatz for integral of uniform weight

   – Off-diagonal blocks: Transformations on the matrix itself force terms not proportional to ϵ to vanish

2. Variable transformations: Find appropriate variable transformations that rationalise all occurring roots

5.4.1 Transformations of differential equations

On our way transforming (5.25) into an ϵ-factorised form, we will encounter two different kinds of transformations: 1) Transformations on diagonal blocks and 2) transformations serving the purpose of bringing an off-diagonal block into ϵ-form. We recapitulate the transformation behaviour of differential equations under any basis transformation U (see (3.69), (3.70)),

$$
d\vec{I} = A\vec{I}, \quad \vec{I} = U\vec{J}
$$
$$
\Rightarrow d\vec{J} = A'\vec{J},
$$
$$
A' = U \cdot A \cdot U^{-1} - U \cdot dU^{-1}. \tag{5.26}
$$

A transformation matrix of the first kind takes the form

$$
U_1 = \begin{pmatrix} & & \cdots & & \\ \cdots & \mathbb{1}^{(i-1)} & 0 & 0 & \\ & 0 & U^{(i)} & 0 & \\ & 0 & 0 & \mathbb{1}^{(i+1)} & \cdots \\ & & \cdots & & \end{pmatrix}, \tag{5.27}
$$

with

$$
U_1^{-1} = \begin{pmatrix} & & \cdots & & \\ \cdots & \mathbb{1}^{(i-1)} & 0 & 0 & \\ & 0 & \left(U^{(i)}\right)^{-1} & 0 & \\ & 0 & 0 & \mathbb{1}^{(i+1)} & \cdots \\ & & \cdots & & \end{pmatrix},
$$

where $\mathbb{1}^{(j)}$ is the identity matrix with a size determined by the length of $\vec{I}^{sec_j}$ and 0's indicate zero matrices with appropriate size. $U^{(i)}$ is a square matrix designed to transform the diagonal block $A^{(i)}$ into an ϵ-form, hence, it has the same dimensions as $A^{(i)}$. Under the application of U_1, the differential equation (5.25) becomes

$$
A'_{U_1} = U_1 \cdot A \cdot U_1^{-1} - U_1 \cdot dU_1^{-1}
$$
$$
= \begin{pmatrix} & & \cdots & & \\ \cdots & A^{(i-1)} & 0 & 0 & \\ & U^{(i)}.A^{((i-1)\times i)} & U^{(i)} \cdot A^{(i)}.\left(U^{(i)}\right)^{-1} - U^{(i)}.d\left(U^{(i)}\right)^{-1} & 0 & \\ & A^{((i-1)\times(i+1))} & A^{(i\times(i+1))}.\left(U^{(i)}\right)^{-1} & A^{(i+1)} & \cdots \\ & & \cdots & & \end{pmatrix}. \tag{5.28}
$$

In addition to $A^{(i)}$, the transformation changes the row to the left of $A^{(i)}$ and the column below $A^{(i)}$. In other words, U_1 only influences sub-sector contributions to $A^{(i)}$ and sub-sector contributions from $A^{(i)}$ to higher sector. U_1 is designed to have no influence on other diagonal blocks. We will encounter two different applications of U_1. On the one hand, U_1 corresponds to transformations on diagonal blocks. In section 5.4.4, U_1 completes the transformation of a sector (5.61), (5.62). On the other hand, a version solely depending on ϵ (5.33) may be utilised to obtain easy to handle sub-sector contributions (5.32), as demonstrated in the following section.

The second kind of transformations serve the purpose of bringing an off-diagonal block $A^{(j \times i)}$, $j < i$ into ϵ-form,

$$
U_2 = \begin{pmatrix} & & \cdots & & & \\ \cdots & \mathbb{1}^{(i-1)} & 0 & 0 & \\ & U^{(j \times i)} & \mathbb{1}^{(i)} & 0 & \\ & 0 & 0 & \mathbb{1}^{(i+1)} & \cdots \\ & & \cdots & & & \end{pmatrix}, \tag{5.29}
$$

$$
U_2^{-1} = \begin{pmatrix} & & \cdots & & & \\ \cdots & \mathbb{1}^{(i-1)} & 0 & 0 & \\ & -U^{(j \times i)} & \mathbb{1}^{(i)} & 0 & \\ & 0 & 0 & \mathbb{1}^{(i+1)} & \cdots \\ & & \cdots & & & \end{pmatrix}.
$$

Again, $\mathbb{1}^{(i)}$ is a identity matrix of the size determined by the length of sector i and 0's indicate zero matrices with appropriate size, $U^{(j \times i)}$ has the same dimension as $A^{(j \times i)}$. U_2 transforms $A^{(j \times i)} \to A_{U_2}^{(j \times i)}$ only, and leaves every other block unchanged,

$$
A_{U_2}^{(j \times i)} = \left(U^{(j \times i)} \cdot A^{(j)} - A^{(i)} \cdot U^{(j \times i)} + A^{(j \times i)} + dU^{(j \times i)} \right). \tag{5.30}
$$

We see, we may decompose the task of finding an appropriate transformation U for the complete matrix A into multiple tasks of finding transformations U_1 and U_2 for the diagonal and off-diagonal blocks in A. From the structure of the differential equation (5.25), we deduce that it is best to start looking for a transformation in the simplest sector. Additionally, the transformation behaviour under U_1 and U_2 suggests to move from top to bottom and right to left in A, while searching appropriate transformations.

5.4.2 Transforming differential equations bottom-up

In the following we introduce a technique structuring and thereby simplifying the workflow in the search for an ϵ-factorised differential equation. This technique utilises the block structure of the differential equation (5.25) as it separates the task of finding an ϵ-factorised form for the complete system into smaller tasks of finding ϵ-factorised blocks $A^{(j)}$, $A^{(l \times j)}$ (see also begin of section 3.6). From the previous sections, we deduce, that it is best to transform the basis of master integrals working bottom-up as indicated in fig.5.9. We start with the simplest sector and move from top to bottom and right to left in A. The procedure does not change along the way, however, the more sectors are involved the more intricate its practical execution becomes. In this section, we describe the first few steps in a general manner writing x as arbitrary variable. This general description serves the purpose of showing the larger picture of the applied workflow as well as demonstrating the inclusion of sub-sector contributions. In the next section we give an example, namely the first two integrals of system 1.
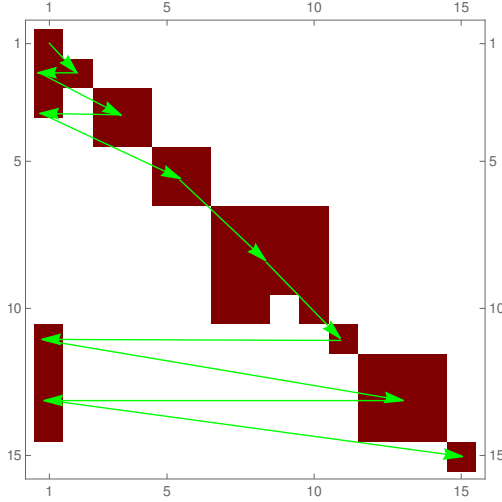
Figure 5.9: Block structure: A schematic representation of $A_{(1-15,1-15)}$, where $d\vec{I} = A\vec{I}$ belongs to system 1. White areas represent zeros, red areas are non zero. Arrows indicate the workflow during the search for basis transformations.

Differential equations regarding the lowest sector are by construction homogeneous,

$$\frac{\partial}{\partial x} \vec{I}^{sec_1} = A^{(1)} \vec{I}^{sec_1}.$$

We may solve them first by making an ansatz for a set of master integrals of uniform weight $\vec{J}^{sec_1}$,

$$\vec{J}^{sec_1} = U^{(1)} \vec{I}^{sec_1}.$$

A promising approach on finding such an ansatz deals with the integrals' maximal cut and will be explained in section 5.4.4. If the ansatz yields indeed a linear dependence on ϵ,

$$d.\vec{J}^{sec_1} = U^{(1)} \cdot A^{(1)} \cdot \left(U^{(1)}\right)^{-1} - U^{(1)}.d\left(U^{(1)}\right)^{-1}$$
$$= \epsilon \tilde{A}^{(1)}\left(x_1, \ldots, x_{N_v}\right) \vec{J}^{sec_1},$$

we move on to the next sector. Note, that the transformation $U^{(1)}$ changes the sub-sector contributions from the first sector to higher sectors $A^{(1\times j)} \to \left(A^{(1\times j)} \cdot \left(U^{(1)}\right)^{-1}\right)$, $j > 1$. To keep the following description simple, however, we redefine $\left(A^{(1\times j)} \cdot \left(U^{(1)}\right)^{-1}\right)$ to be $A^{(1\times j)}$.

The differential equations of the second lowest sector,

$$\frac{\partial}{\partial x} \vec{I}^{sec_2} = A^{(2)} \vec{I}^{sec_2} + A^{(1\times 2)} \vec{I}^{sec_1},$$

need not to be homogeneous. They may contain contributions from the first sector. This is no problem at all, since we already know the solution for the lowest sector $\vec{J}^{sec_1}$.

Hence, we may focus on solving the homogeneous parts of the differential equations

$$\frac{\partial}{\partial x} \vec{I}^{sec_2} = A^{(2)} \vec{I}^{sec_2}.$$

We make an ansatz $\vec{J'}^{sec_2}$ and verify if it yields an ϵ-factorised form on the sector

$$d\vec{J'}^{sec_2} = \epsilon \tilde{A}^{(2)}\left(x_1, \ldots, x_{N_v}\right) \vec{J'}^{sec_2}.$$

Now, the differential equation becomes

$$\frac{\partial}{\partial x} \begin{pmatrix} \vec{J}^{sec_1} \\ \vec{J'}^{sec_2} \\ \vec{I}^{sec_3} \\ \ldots \end{pmatrix} = \begin{pmatrix} \epsilon \tilde{A}^{(1)} & 0 & 0 & \ldots \\ A^{(1\times 2)} & \epsilon \tilde{A}^{(2)} & 0 & \\ A^{(1\times 3)} & A^{(2\times 3)} & A^{(3)} & \\ \ldots & & & \end{pmatrix} \begin{pmatrix} \vec{J}^{sec_1} \\ \vec{J'}^{sec_2} \\ \vec{I}^{sec_3} \\ \ldots \end{pmatrix}, \tag{5.31}$$

where matrices $\tilde{A}$ are independent of ϵ as opposed to matrices A. In the next step, we include the sub-sector contribution of the second sector, i.e. we transform $A^{(1\times 2)}$. Thereby, we must not change $\tilde{A}^{(1)}$ and $\tilde{A}^{(2)}$. We first look at the appearance of ϵ in $A^{(1\times 2)}$. In the end, we seek an ϵ-form,

$$A^{(1\times 2)} \rightarrow \epsilon \tilde{A}^{(1\times 2)}.$$

If $A^{(1\times 2)}$ is not already in ϵ-form, a helpful intermediate step is a matrix containing a part proportional to ϵ^0 and a part proportional to ϵ^1,

$$A^{(1\times 2)} \rightarrow A_0^{(1\times 2)} + \epsilon A_1^{(1\times 2)} \rightarrow \epsilon \tilde{A}^{(1\times 2)}.$$

Determining master integrals according to the properties of their maximal cut (see upcoming section) usually leads to a uniform appearance of ϵ in $A^{(1\times 2)}$. Often, sub-sector contributions already take the intermediate simple form

$$A^{(1\times 2)} = A_0^{(1\times 2)} + \epsilon A_1^{(1\times 2)}. \tag{5.32}$$

Otherwise, they are at least given by

$$A^{(1\times 2)} = g\left(\epsilon\right) \left[A_0^{(1\times 2)} + \epsilon A_1^{(1\times 2)} \right],$$

where $g\left(\epsilon\right)$ is a polynomial in ϵ. This polynomial vanishes if we substitute

$$\vec{J'}^{sec_2} \rightarrow \frac{1}{g\left(\epsilon\right)} \vec{J'}^{sec_2}.$$

The corresponding transformation matrix has the structure of U_1 (5.27) and depends solely on ϵ,

$$\begin{pmatrix} \mathbb{1}^{(1)} & 0 & 0 \\ 0 & \frac{1}{g(\epsilon)}\mathbb{1}^{(2)} & 0 \\ 0 & 0 & \mathbb{1}^{(3)} \\ \ldots & & \end{pmatrix}, \tag{5.33}$$

where $\mathbb{1}^{(i)}$ is an identity matrix of size determined by the length of sector i, and 0's indicate zero matrices with appropriate size. From (5.28) we find, that the matrix of the differential equation (5.31) becomes

$$A' = \begin{pmatrix} \epsilon\tilde{A}^{(1)} & 0 & 0 \\ \frac{1}{g(\epsilon)}g\left(\epsilon\right)\left[A_0^{(1\times2)} + \epsilon A_1^{(1\times2)}\right] & \epsilon\tilde{A}^{(2)} & 0 \\ A^{(1\times3)} & g\left(\epsilon\right)A^{(2\times3)} & A^{(3)} \\ & \cdots & \end{pmatrix}. \tag{5.34}$$

After converting the sub-sector contribution to (5.32), we need to find a transformation

$$A_0^{(1\times2)} + \epsilon A_1^{(1\times2)} \to \epsilon\tilde{A}^{(1\times2)}.$$

We, therefore, utilise a transformation matrix of the second kind (5.29),

$$\begin{pmatrix} \mathbb{1}^{(1)} & 0 & 0 \\ U^{(1\times2)} & \mathbb{1}^{(2)} & 0 \\ 0 & 0 & \mathbb{1}^{(3)} \\ \cdots & & \end{pmatrix}.$$

Again, $\mathbb{1}^{(i)}$ is an identity matrix of size determined by the length of sector i and 0's indicate zero matrices with appropriate size, $U^{(1\times2)}$ has the same dimension as $A^{(1\times2)}$. We know that this transformation solely affects $A^{(1\times2)}$. The resulting matrix is given by

$$A'' =$$

$$\begin{pmatrix} \epsilon\tilde{A}^{(1)} & 0 & \cdots \\ \epsilon\left(U^{(1\times2)} \cdot \tilde{A}^{(1)} - \tilde{A}^{(2)} \cdot U^{(1\times2)} + A_1^{(1\times2)}\right) + A_0^{(1\times2)} + dU^{(1\times2)} & \epsilon\tilde{A}^{(2)} & \\ \cdots & & \end{pmatrix}.$$

Hence, a possible transformation $U^{(1\times2)}$ corresponds to the solution of the differential equation

$$\epsilon\left(U^{(1\times2)} \cdot \tilde{A}^{(1)} - \tilde{A}^{(2)} \cdot U^{(1\times2)}\right) + dU^{(1\times2)} = -A_0^{(1\times2)}.$$

In practice, the ansatz

$$U^{(1\times2)} = -\int A_0^{(1\times2)}dx,$$

often suffices.

After completing the second sector, we move on to the third sector. We first solve the homogeneous part of its differential equation by making an ansatz. Then we check for contributions of the second sector to the third sector. We may fix them in the same way we fixed the contribution from the lowest sector to the second, we first derive a simple dependence on ϵ and then remove left over parts. Before we are ready to inspect the fourth sector, we transform possible contributions from the first sector to the third. We proceed in the same way and transform the complete matrix finishing with the most complicated sector, as indicated in fig.5.9.

5.4.3 Tadpole and bubble integral as integrals of uniform weight zero

This section links the preceding section to the next section. Besides proceeding as outlined in section 5.4.2, we give an introductory example to the method described in section 5.4.4. This section provides first practical insights, for example, into the necessity and advantages of introducing a dimensional shift operator or the structure of "good" master integrals, i.e. master integrals of uniform weight zero. We will encounter the massive tadpole and massive bubble integral known from section 3.2 again, while considering the first two pre-canonical master integrals of system 1 (see table 5.3),

$$\text{sector 25: } I^A_{100110000},$$
$$\text{sector 27: } I^A_{110110000}.$$

These integrals correspond to one sector each, to sector 25 and 27 of topology A. Their graphs are drawn in fig.5.10 and fig.5.11. We can see in fig.5.9 that the first integral contributes to the second. Their differential equations amount to

$$\frac{\partial}{\partial v} I^A_{100110000} = 0,$$
$$\frac{\partial}{\partial w} I^A_{100110000} = \frac{d-2}{2w} I^A_{100110000}, \tag{5.35}$$

$$\frac{\partial}{\partial v} I^A_{110110000} = \frac{4+(d-4)v}{2(v-4)v} I^A_{110110000} + \frac{d-2}{(v-4)v} I^A_{100110000},$$
$$\frac{\partial}{\partial w} I^A_{110110000} = \frac{d-2}{2w} I^A_{110110000}. \tag{5.36}$$
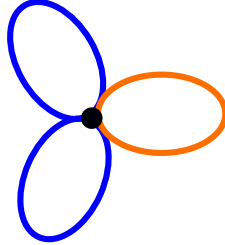
Figure 5.10: Graph of sector 25 of topology A. The graph consists of three tadpoles. Blue lines denote propagators with mass m_t^2, orange lines denote propagators with m_W^2.

We start as we try to find an ansatz for the first integral. Solutions to differential equations in ϵ-form are of uniform weight zero. Hence, an optimal ansatz has as well uniform weight zero (see section 3.5.1 and section 3.5.2 on details regarding weight properties). We recall that rational numbers have weight zero, zeta values ζ_n weight n and ϵ weight minus one. Fig.5.10 shows that the first integral consists of three tadpoles, two with mass m_t and one with mass m_W. We may concentrate on the former first. The tadpole was derived in (3.21) for a general mass,

$$T_\nu \left(D, \frac{m^2}{\mu^2} \right) = e^{\epsilon \gamma_E} \left(\frac{m^2}{\mu^2} \right)^{\frac{D}{2}-\nu} \frac{\Gamma(\nu - \frac{D}{2})}{\Gamma(\nu)}. \tag{5.37}$$

For

$$\mu^2 = m_t^2,$$

we found in $D = (4 - 2\epsilon)$-dimensions

$$T_1 (4 - 2\epsilon) = e^{\epsilon\gamma_E} \Gamma(\epsilon - 1)$$
$$= -\frac{1}{\epsilon} - 1 - \left(1 - \frac{1}{2}\zeta_2\right)\epsilon + \left(\frac{1}{3}\zeta_3 - \frac{1}{2}\zeta_2 - 1\right)\epsilon^2 + \mathcal{O}(\epsilon^3).$$

This series is not of uniform weight, even if we multiply it with ϵ,

$$\epsilon T_1 (4 - 2\epsilon) = \underbrace{-1}_{\text{weight: } 0} - \underbrace{\epsilon}_{-1} - \underbrace{\epsilon^2}_{-2} + \frac{1}{2}\underbrace{\zeta_2\epsilon^2}_{0} + \frac{1}{3}\underbrace{\zeta_3\epsilon^3}_{0} - \frac{1}{2}\underbrace{\zeta_2\epsilon^3}_{-1} - \underbrace{\epsilon^3}_{-3} + \mathcal{O}(\epsilon^4).$$

However, in $D = (2 - 2\epsilon)$-dimensions, we deduce from (5.37)

$$\epsilon T_1 (2 - 2\epsilon) = e^{\epsilon\gamma_E} \epsilon \Gamma(\epsilon) = e^{\epsilon\gamma_E} \Gamma(1 + \epsilon)$$
$$= 1 + \frac{1}{2}\underbrace{\zeta_2\epsilon^2}_{2-2=0} - \frac{1}{3}\underbrace{\zeta_3\epsilon^3}_{3-3} + \frac{9}{16}\underbrace{\zeta_4\epsilon^4}_{4-4} - \left(\frac{1}{5}\underbrace{\zeta_5}_{5} + \frac{1}{6}\underbrace{\zeta_2\zeta_3}_{2+3}\right)\underbrace{\epsilon^5}_{-5} + \mathcal{O}(\epsilon^6), \quad (5.38)$$

and find that every term in the series has weight zero. A similar candidate arises for a tadpole depending on another mass, like m_W^2,

$$\epsilon T_1 (2 - 2\epsilon, w) = e^{\epsilon\gamma_E} (w)^{-\epsilon} \epsilon \Gamma(\epsilon) = e^{\epsilon\gamma_E} e^{-\epsilon\ln(w)} \Gamma(1 + \epsilon)$$
$$= 1 - \ln(w)\epsilon + \frac{1}{2}\left(\ln(w)^2 + \zeta_2\right)\epsilon^2$$
$$- \left(\frac{1}{2}\zeta_2\ln(w) + \frac{1}{6}\ln(w)^3 + \frac{1}{3}\zeta_3\right)\epsilon^3 + \mathcal{O}(\epsilon^4). \quad (5.39)$$

We draw an important conclusion: Tadpole integrals in $(2 - 2\epsilon)$-dimensions multiplied with ϵ have uniform weight zero. In order to express the first master integral through them, we need to shift its dimension from $(4 - 2\epsilon)$ to $(2 - 2\epsilon)$. For this purpose, we introduced the dimensional shift operator $\boldsymbol{D}^-$ (5.5) earlier. Hence, we construct our first canonical integral J_1 as the product of three tadpoles in $(2 - 2\epsilon)$ dimensions each multiplied with ϵ, (5.38) and (5.39),

$$J_1 = \epsilon^3 \boldsymbol{D}^- I_{100110000}^A.$$

We relate it back to the first master integral in $(4 - 2\epsilon)$-dimensions,

$$J_1 = \epsilon^3 \boldsymbol{D}^- I_{100110000}^A$$
$$\overset{(5.6)}{=} \epsilon^3 I_{200220000}^A$$
$$\overset{\text{IBP}}{=} \underbrace{\frac{\left((4 - 2\epsilon)^3 - 6(4 - 2\epsilon)^2 + 12(4 - 2\epsilon) - 8\right)\epsilon^3}{8w}}_{=U^{(1)}} I_{100110000}^A,$$

and construct the differential equation of J_1 with (5.26) from (5.35),

$$A' = U^{(1)} A \left(U^{(1)} \right)^{(-1)} - U^{(1)} d \left(U^{(1)} \right)^{(-1)} \implies \begin{cases} \frac{\partial}{\partial v} J_1 = 0, \\ \frac{\partial}{\partial w} J_1 = \frac{-\epsilon}{w} I^A_{100110000}. \end{cases} \tag{5.40}$$
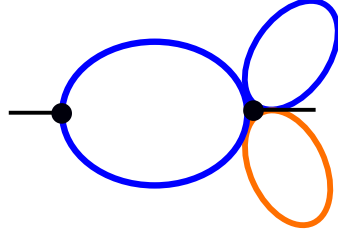
Figure 5.11: Graph of sector 27 of topology A. The graph consists of two tadpoles and a bubble. Blue lines denote propagators with mass m_t^2, orange lines denote propagators with m_W^2.

The second master integral $I^A_{110110000}$ consists of two tadpoles with masses m_t and m_W and a bubble with mass m_t as shown in fig.5.11. We already learned how to convert tadpoles into integrals of uniform weight zero. The remaining bubble integral will serve as introductory example to the method we use in this thesis to convert diagonal blocks. We start with the conversion of the bubble integral from momentum representation (5.1)

$$\text{—} \bigcirc \text{—} \;=\; I_{11}(D) \;=\; e^{\epsilon \gamma_E} \left(\mu^2 \right)^{2 - \frac{3D}{2}} \int \frac{d^D k_1}{i \pi^{\frac{D}{2}}} \frac{1}{\left(-k_1^2 + m_t^2 \right) \left(-(k_1 - p)^2 + m_t^2 \right)},$$

to Baikov representation (3.44)

$$I_{11}(D) = \frac{e^{\epsilon \gamma_E} \left(\mu^2 \right)^{2 - \frac{D}{2}} \det G \left(p \right)^{\frac{2 - D}{2}}}{-2 \pi^{\frac{1}{2}} \Gamma \left(\frac{D-1}{2} \right)} \int_{\mathcal{C}} dz_1 dz_2 \, \frac{\mathcal{B}(z_1, z_2)^{\frac{D-3}{2}}}{z_1 z_2},$$

where the Baikov polynomial $\mathcal{B}(z_1, z_2)$ is given by the Gram determinant $\det G \left(k_1, p \right)$ (3.41) expressed in terms of the Baikov variables

$$z_1 = \left(-k_1^2 + m_t^2 \right), \quad z_2 = \left(-(k_1 - p)^2 + m_t^2 \right).$$

The integration domain is not important here, it can be read off from (3.45). We calculate the Baikov polynomial and find

$$I_{11}(D) = \frac{-2^{(2-D)} e^{\epsilon \gamma_E} \left(m_t^2 \right)^{2 - \frac{D}{2}} \left(-p^2 \right)^{\frac{2-D}{2}}}{\pi^{\frac{1}{2}} \Gamma \left(\frac{D-1}{2} \right)} \int_{\mathcal{C}} dz_1 dz_2$$

$$\frac{\left(s \left(4 m_t^2 - s \right) - 2 z_1 \left(s - z_2 \right) - 2 s z_2 - z_1^2 - z_2^2 \right)^{\frac{D-3}{2}}}{z_1 z_2}.$$

We aim at investigating the leading term of the Laurent expansion around $\epsilon = 0$ of the maximal cut. Hence, we set $D = 2$ during our investigation instead of setting $D = (2 - 2\epsilon)$. (Tadpoles also contributing to the second master integral must be taken in $(2 - 2\epsilon)$ dimensions, therefore, we are not considering $D = 4$. Apart from that, bubble integrals in four dimensions do not fulfil the desired properties, i.e. they are not of uniform weight.)

$$I_{11}(2) = \int_{\mathcal{C}} dz_1 dz_2 \frac{-e^{\epsilon \gamma_E} m_t^2}{\pi z_1 z_2 \sqrt{s\left(4m_t^2 - s\right) - 2z_1\left(s - z_2\right) - 2sz_2 - z_1^2 - z_2^2}}.$$

We apply the maximal cut (see section 3.6.1) through the exchange

$$\frac{1}{z_1 z_2} \rightarrow (2\pi i)^2 \, \delta\left(z_1\right) \delta\left(z_2\right),$$

and obtain

$$\mathrm{MaxCut}\left(I_{11}(2)\right) = \frac{4\pi m_t^2}{\sqrt{s\left(4m_t^2 - s\right)}}. \tag{5.41}$$

We recall, that solutions to canonical differential equations are integrals of uniform weight, hence, their maximal cuts should also be of uniform weight. The result we found, however is not a constant of weight zero. If we consider

$$\frac{\sqrt{s\left(4m_t^2 - s\right)}}{m_t^2} I_{11}(2),$$

we obtain a constant of weight one after applying the maximal cut

$$\mathrm{MaxCut}\left(\frac{\sqrt{s\left(4m_t^2 - s\right)}}{m_t^2} I_{11}(2)\right) = 4\pi.$$

Additional multiplication with ϵ, finally yields a constant of weight zero

$$\mathrm{MaxCut}\left(\epsilon \frac{\sqrt{s\left(4m_t^2 - s\right)}}{m_t^2} I_{11}(2)\right) = 4\epsilon\pi. \tag{5.42}$$

In conclusion, we determine our second master integral as the product of two tadpoles in $D = (2 - 2\epsilon)$-dimensions multiplied with ϵ ((5.38),(5.39)) and an accordingly modified bubble in $D = (2 - 2\epsilon)$-dimensions (5.42),

$$J_2 = \epsilon^3 r_1 \boldsymbol{D}^- I_{110110000}^A, \tag{5.43}$$

where we defined

$$r_1 = \sqrt{-v\left(4 - v\right)}.$$

The resulting differential equations are linear in ϵ, where the kinematic variables are defined as in (5.18),

$$
\begin{aligned}
J_2 &= \epsilon^3 r_1 \left(I^A_{120220000} + I^A_{210220000} \right) \\
&= -\frac{(\epsilon-1)^2((1-\epsilon)I^A_{100110000} + (1-2\epsilon)I^A_{110110000})}{(v-4)w} \\
&\stackrel{(5.36)}{\Rightarrow}
\begin{cases}
\frac{\partial}{\partial w} J_2 = \frac{-\epsilon}{w} I^A_{110110000}, \\
\frac{\partial}{\partial v} J_2 = \frac{2\epsilon}{r_1} I^A_{100110000} + \frac{\epsilon}{4-v} I^A_{110110000}
\end{cases}.
\end{aligned}
\tag{5.44}
$$

We see, not only the contribution of sector 27 itself is now linear in ϵ, but also the sub-sector contribution from sector 25. Constructing master integrals of uniform weight, sub-sector contributions are often already linear in ϵ or at least close to that form as in (5.32). Furthermore, we would like to point out the occurrence of a square root: r_1. The transformation $I^A_{110110000} \to J_2$ we found is not rational, consequently, the differential equation of J_2 is not rational. Appropriate variable transformations are required. We acquire those in section 5.5.1 after transforming the complete basis of master integrals into a basis with uniform weight zero (section 5.5). The investigations on the massive bubble tell us in addition something about the massless bubble. From (5.42) we conclude that a massless bubble in $D = (2-2\epsilon)$-dimensions must be multiplied with the factor (ϵv) to become uniform in weight. In the upcoming section, we generalise the way we treated the bubble integral utilising the maximal cut.

5.4.4 Maximal cuts and constant leading singularities

Diagonal blocks in differential equations of master integrals reflect their division into sectors (5.25). In conclusion, section 5.4.2 described a way of transforming a differential equation bottom-up, sector by sector, into an equation linear in ϵ,

$$
\vec{J}^{sec_i} = U^{(i)} \vec{I}^{sec_i}
$$
$$
\Rightarrow d\vec{J}^{sec_i} = \epsilon \tilde{A}^{(i)} \vec{J}^{sec_i}.
$$

However, section 5.4.2 raised the question: How are appropriate transformations $U^{(i)}$ of diagonal blocks found? To phrase this question differently: How are ansätze for "good" master integrals of a sector $\vec{J}^{sec_i}$ obtained? This question will be answered here. We elaborate the method already applied in the former section with regards to the bubble integral. The method is a heuristic approach in the search for "good" master integrals relying on two main facts:

1. Solutions to canonical differential equations are integrals of uniform weight (section 3.5.1, 3.5.2).

→ "Good" master integrals are, therefore, master integrals of uniform weight.

2. Weight properties of integrals are preserved under the application of cuts. The maximal cut of an integral of uniform weight remains to be of uniform weight (section 3.6.1).

→ To gain information about weight properties of an integral, we may study the simpler maximally cut integral, first.

Although the success of a heuristic approaches is not predestined, it is easily verified or falsified through the calculation of the resulting differential equation. In combination with direct transformations (discussed in section 5.4.1) the heuristic approach sufficed to transform all three systems of master integrals (system 1, system 2a/b, see section 5.3) into differential equations linear in ϵ. It utilises maximal cuts of Feynman integrals in Baikov representation [66, 90]. The Baikov representation was defined in section 3.3.2 and maximal cuts were discussed in section 3.6.1. Box 2 provides a concise summary of the approach.

Box 2: Leading singularity analyses

Momentum representation:
$$I \sim \int d^D k_1 d^D k_2 d^D k_3 \prod_{j=1}^{9} \left(P_j^X \right)^{-\nu_j}$$

Baikov rep.: democratic (3.44)
$$I \sim \int d^9 z \mathcal{B}(z)^{\frac{D-l-e-1}{2}} \prod_{j=1}^{9} z_j^{-\nu_j}$$
$$\mathcal{B}(z) = \det G\left(k_1, k_2, k_3, p\right)$$

Baikov rep.: loop by loop (3.42)
$$d^D k \sim \det G\,(\text{mom. ext. to loop})^{\frac{-D+e+1}{2}} \cdot$$
$$\det G\,(k, \text{mom. ext. to loop})^{\frac{D-e-2}{2}} d^z$$

Maximal Cut: cut all propagators with $\nu_j > 0$
$$\frac{1}{z_j} \to 2\pi i \delta(z_j) \Rightarrow \text{MaxCut}\,(I_i) = \int_{\mathcal{C}_{\text{MaxCut}}} \varphi_i$$
$$\downarrow$$
Search $\mathcal{C}_i$ & modify φ_i such that the **leading term of the Laurent expansion** ($\epsilon = 0$) of $\int_{\mathcal{C}_i} \varphi_i'$ is a **constant of weight zero**; π: weight 1, ζ_n: weight n, ϵ: weight -1

An introductory example was already given in the end of section 5.4.3. There, we multiplied the two-dimensional bubble integral with a prefactor depending on kinematic variables as demanded by its maximal cut. We modified the maximal cut to obtain a constant of weight zero. Here, we describe this approach in more detail with the help of more involved examples. Our fist example demonstrates how maximal cuts may leave us behind with integrations requiring modifications not only on the integrand level but also regarding the integration contour. Afterwards, we give a short definition of constant leading singularities. Then, our second example demonstrates an alternative way of constructing the Baikov representation.

We start with the 104$^{\text{th}}$ master integral of system 1, i.e. the last master integral of topology C,

$$\text{sector } 255: \ I_{111111110}^C = e^{3\epsilon\gamma_E} \left(\mu^2\right)^{8-\frac{3D}{2}} \int \frac{d^D k_1}{i\pi^{\frac{D}{2}}} \frac{d^D k_2}{i\pi^{\frac{D}{2}}} \frac{d^D k_3}{i\pi^{\frac{D}{2}}} \prod_{j=1}^{8} \frac{1}{\left(P_j^C\right)}.$$

The definitions of propagators P_j^C can be read off from fig.5.5, table 5.1. First, we convert the integral to Baikov representation. We may work directly in $D = 4$ dimensions, since we are only interested in the leading term of its maximal cut. We obtain the

Baikov representation democratically, i.e. via the application of equation (3.44). We replace each propagator P_j^C in the numerator of $I_{111111110}^C$ with a Baikov variable z_j, additionally we compute the Baikov polynomial and adjust prefactors to find

$$I_{111111110}^C (D = 4) = \frac{\mu^4 \det G\, (p)^{-1}}{\pi^3 \det(C) \prod_{i=1}^{3} \Gamma\left(\frac{4-i}{2}\right)} \int_{\mathcal{C}} d^9z\, \mathcal{B}(z)^{\left(-\frac{1}{2}\right)} \prod_{j=1}^{8} z_j^{-1}$$

$$= \int_{\mathcal{C}} d^9z\, \frac{-\mu^4}{\left(8\pi^4 s z_1 z_2 z_3 z_4 z_5 z_6 z_7 z_8\right) \mathcal{B}(z)^{\left(\frac{1}{2}\right)}}, \tag{5.45}$$

where $\mathcal{B}(z)^{\left(\frac{1}{2}\right)}$ is a square root depending on all kinematic variables and all Baikov variables $z_1 - z_9$. The maximal cut of the integral refers to the cut (3.93) of all edges belonging to the integral. Hence, the parts within the Baikov polynomial proportional to $z_1 - z_8$ are not important, since we cut these Baikov variables in the next step,

$$\frac{1}{z_1 z_2 z_3 z_4 z_5 z_6 z_7 z_8} \to (2\pi i)^8 \sum_{i=1}^{8} \delta\left(z_i\right). \tag{5.46}$$

The parts within $\mathcal{B}(z)^{\left(\frac{1}{2}\right)}$ solely proportional to z_9 yield squared terms cancelling the root and we are left with

$$\overset{(5.46)}{\Rightarrow} \text{MaxCut}\left(I_{111111110}^C (D = 4)\right) = \int_{\mathcal{C}_{\text{MaxCut}}} dz_9\, \frac{32\pi^4 \mu^4}{s z_9 \left(m_t^2 - m_W^2 - s - z_9\right)}.$$

Sometimes the maximal cut leaves no integration variable behind as in the introductory example (5.41). In other cases, we replace integration contours of the maximal cut $\mathcal{C}_{\text{MaxCut}}$ with simpler contours, usually around poles. Here, we choose an anticlockwise circle around $z_9 = 0$ (alternatively around $z_9 = m_t^2 - m_W^2 - s$). We know that

$$\oint_{z=z_0} \frac{f(z)}{z - z_0} dz = 2\pi i\, \text{res}\left(\frac{f(z)}{z - z_0}, z = z_0\right) = 2\pi i f(z_0). \tag{5.47}$$

Hence, we deduce

$$\oint_{z_9=0} dz_9\, \frac{32\pi^4 \mu^4}{s z_9 \left(m_t^2 - m_W^2 - s - z_9\right)} = \frac{64 i \pi^5 \mu^4}{s \left(m_t^2 - m_W^2 - s\right)} = \frac{64 i \pi^5}{v \left(1 - w - v\right)},$$

with

$$\mu^2 = m_t^2, \quad v = \frac{p^2}{m_t^2}, \quad w = \frac{m_W^2}{m_t^2}.$$

We aim at constructing a constant of weight zero, thereby, we may also modify the integrand of the maximal cut. We multiply with a prefactor cancelling appearances of kinematic variables,

$$v\left(1 - w - v\right) \oint_{z_9=0} dz_9\, \frac{32\pi^4 \mu^4}{s z_9 \left(m_t^2 - m_W^2 - s - z_9\right)} = \underbrace{64 i \pi^5}_{\text{constant of weight 5}}.$$

Since weights are summed if factors are multiplied π^5 has weight five and we multiply with ϵ^5 in order to balance the weight,

$$\epsilon^5 v \left(1 - w - v\right) \oint_{z_9 = 0} dz_9 \, \frac{32\pi^4 \mu^4}{s z_9 \left(m_t^2 - m_W^2 - s - z_9\right)} = \underbrace{64 i \epsilon^5 \pi^5}_{\text{constant of weight 0}} .$$

Accordingly, we modify

$$I_{111111110}^C \rightarrow J_{104} = \epsilon^5 v \left(1 - w - v\right) I_{111111110}^C. \tag{5.48}$$

and obtain a candidate for a master integral of uniform weight.

We verify that (5.48) yields a linear dependence on ϵ in the corresponding diagonal block of the differential equation. However, its sub-sector contributions are proportional to $\frac{\epsilon}{(1-2\epsilon)}$ requiring an additional factor of $(1 - 2\epsilon)$, i.e. a transformation matrix of the first kind (5.27) (see also (5.33),(5.34) with $A_0^{(1 \times 2)} = 0$),

$$J_{104} = \epsilon^5 \left(1 - 2\epsilon\right) v \left(1 - w - v\right) I_{111111110}^C. \tag{5.49}$$

Before we move on to the next example, we summarise the above described procedure in a more formal way. We looked at the leading term of the maximal cut

$$\text{MaxCut} \left(I \left(\epsilon = 0\right)\right) = \int_{\mathcal{C}_{\text{MaxCut}}} \varphi,$$

and modified its integration contour,

$$\mathcal{C}_{\text{MaxCut}} \rightarrow \mathcal{C}',$$

and integrand,

$$\varphi \rightarrow \varphi',$$

to obtain a constant of weight zero,

$$\int_{\mathcal{C}'} \varphi' = \text{constant of weight zero}.$$

In accordance, we say

$$\int_{\mathcal{C}_{\text{MaxCut}}} \varphi'$$

has constant leading singularities [91, 92].

In order to modify the integration contour and the integrand of a maximally cut integral efficiently, we not only rely on (5.47), we may also consider an integration along a closed, anticlockwise contour around a slit $[a, b]$,

$$\oint_{[a,b]} \frac{dz}{\sqrt{(z - a)(z - b)}} = 2\pi i. \tag{5.50}$$

Furthermore, the package `DlogBasis` [93] can be a helpful tool for the calculations of leading singularities.

Our next example is more involved. We look at a sector containing three master integrals. Furthermore, we are going to derive the Baikov representation loop-by-loop.

$$\vec{I}^{sec334} = \begin{pmatrix} I^{B'}_{011100101} \\ I^{B'}_{(-1)11100101} \\ I^{B'}_{0111(-1)0101} \end{pmatrix}. \quad (5.51)$$
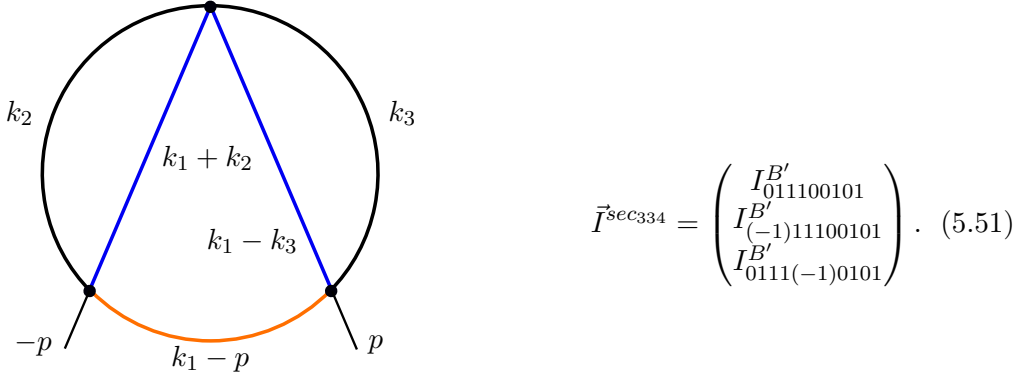
Figure 5.12: Graph of sector 334 from topology B'.
Blue lines denote propagators with mass m_t^2, orange lines denote propagators with m_W^2.

We look at sector 334 from topology B' containing three master integrals given in (5.51). The master integrals appear on $46^{\text{th}}, 47^{\text{th}}$ and 48th place in the vector of pre-canonical master integrals of system 2a. Later on, we will call the vector of canonical master integrals of system 2a $\vec{K}$. Here, we search for canonical master integrals of sector 334. In order to be consistent, we call them K_{46}, K_{47}, K_{48}. We work with the first integral in (5.51), because it completely specifies the sector,

$$I^{B'}_{011100101} = e^{\epsilon 3\gamma_E} \left(\mu^2\right)^{5-\frac{3D}{2}} \int \frac{d^D k_1}{i\pi^{D/2}} \frac{d^D k_2}{i\pi^{D/2}} \frac{d^D k_3}{i\pi^{D/2}}$$
$$\frac{1}{\left(-(k_1-p)^2+m_W^2\right)\left(-(k_1+k_2)^2+m_t^2\right)\left(-k_2^2\right)\left(-k_3^2\right)\left(-(k_1-k_3)^2+m_t^2\right)}.$$
$$(5.52)$$

The exact composition of the second and third integral in (5.51), like placement of propagators in the numerator, is not important and depends on the chosen integration by parts reduction program. As before, we start with the derivation of the Baikov representation. We number Baikov variables in the same way we number edges,

$$\begin{array}{lll} z_1 = -k_1^2 + m_W^2, & z_2 = -(k_1-p)^2 + m_W^2, & z_3 = -(k_1+k_2)^2 + m_t^2, \\ z_4 = -k_2^2, & z_5 = -(k_2+k_3)^2, & z_6 = -(k_2+p)^2, \\ z_7 = -k_3^2 & z_8 = -(k_3-p)^2, & z_9 = -(k_1-k_3)^2 + m_t^2. \end{array}$$

Building the Baikov representation democratically, i.e. via (3.44), all nine Baikov variables would be integration variables. Out of those only five belong to sector 334, namely

z_2, z_3, z_4, z_7, z_9. Taking the maximal cut of an integral from sector 334, corresponds to cutting those propagators. As consequence, the democratic Baikov representation would result into four integration variables. We know, however, that an alternative way of constructing the Baikov representation exists. The integration measures $\frac{d^D k_j}{i\pi^{\frac{D}{2}}}$ can be replaced loop by loop with (3.42). In this way the Baikov representation consists of as many integration variables as scalar products involving loop momenta appear in the integral. Due to this simplification, we usually build the Baikov representation loop-by-loop, with the exception of top sectors as in our previous example or, more general, sectors with a sufficient amount of edges. (In our previous example, the loop-by-loop approach would not have simplified the Baikov representation, moreover it would have been more difficult to construct.) From fig.5.12, we deduce that building the Baikov representation loop by loop results into six integration variables $z_1, z_2, z_3, z_4, z_7, z_9$ since six scalar products involving loop momenta occur, namely $k_1^2, k_2^2, k_3^2, k_1 \cdot k_2, k_1 \cdot k_3, k_1 \cdot p$.

We recall the Baikov measure

$$\frac{d^D k}{i\pi^{\frac{D}{2}}} = \frac{\det G \,(\text{momenta external to loop})^{\frac{-D+e+1}{2}}}{\pi^{\frac{e}{2}} (\det C) \Gamma\left(\frac{D-e}{2}\right)} \, \det G \,(k, \text{momenta external to loop})^{\frac{D-e-2}{2}} \, d^{N_v} z,$$

where $\det G$ denotes the Gram determinant (3.41), e is the number of momenta external to the loop, N_v is the number of scalar products involving loop momenta, which is here $e+1$. Changing from integration over scalar products involving the loop momentum to integration over Baikov variables z yields the Jacobian $\det C$.

We may start obtaining the Baikov representation for (5.52) loop by loop with the left loop in fig.5.12. Viewing this loop individually, it is a bubble with loop momentum k_2 and external momentum k_1. One external momentum results in two scalar products involving the loop momentum, namely k_2^2 and $k_2 \cdot k_1$. These scalar products are part of z_3, z_4. Hence, we convert from an integration over k_2 to an integration over z_3, z_4,

$$\frac{d^D k_2}{i\pi^{\frac{D}{2}}} = \frac{\det G \,(k_1)^{\frac{-D+2}{2}}}{\pi^{\frac{1}{2}} (\det C_2) \Gamma\left(\frac{D-1}{2}\right)} \, \det G \,(k_2, k_1)^{\frac{D-3}{2}} \, dz_3 dz_4,$$

$$\det C_2 = \det\left(\begin{pmatrix} \frac{\partial z_3}{\partial\left(-k_2^2\right)} & \frac{\partial z_3}{\partial\left(-k_2 \cdot k_3\right)} \\ \frac{\partial z_4}{\partial\left(-k_2^2\right)} & \frac{\partial z_4}{\partial\left(-k_2 \cdot k_3\right)} \end{pmatrix}\right) = \det\left(\begin{pmatrix} 1 & 2 \\ 1 & 0 \end{pmatrix}\right) = -2.$$

We conclude, working in $D = 2$ dimensions one Gram determinant vanishes and we obtain

$$\frac{d^D k_2}{i\pi^{\frac{D}{2}}} = \frac{1}{\pi^{\frac{1}{2}} (\det C_2) \Gamma\left(\frac{1}{2}\right)} \, \det G \,(k_2, k_1)^{\left(-\frac{1}{2}\right)} \, dz_3 dz_4.$$

We express the remaining Gram determinant,

$$\det G \,(k_2, k_1) = \det\left(\begin{pmatrix} -k_2^2 & -k_2 \cdot k_1 \\ -k_1 \cdot k_2 & -k_1^2 \end{pmatrix}\right)$$

$$= \det\left(\begin{pmatrix} z_4 & \frac{1}{2}\left(-m_t^2 + m_W^2 - z_1 + z_3 - z_4\right) \\ \frac{1}{2}\left(-m_t^2 + m_W^2 - z_1 + z_3 - z_4\right) & z_1 - m_W^2 \end{pmatrix}\right)$$

$$= \frac{1}{4} \left(-m_t^4 + 2z_3 \left(m_t^2 - m_W^2 + z_4 \right) + 2z_1 \left(-m_t^2 + m_W^2 + z_3 + z_4 \right) \right.$$
$$\left. + 2m_t^2 m_W^2 - 2m_t^2 z_4 - m_W^4 - 2m_W^2 z_4 - z_1^2 - z_3^2 - z_4^2 \right),$$

in terms of Baikov variables z_1, z_3, z_4 and find

$$\frac{d^D k_2}{i\pi^{\frac{D}{2}}} = \frac{1}{\pi^{\frac{1}{2}} (\det C_2) \Gamma\left(\frac{1}{2}\right)} \det G\left(k_2, k_1\right)^{\left(-\frac{1}{2}\right)} dz_3 dz_4$$

$$= -\frac{dz_3 dz_4}{\pi} \left[-m_t^4 + 2z_3 \left(m_t^2 - m_W^2 + z_4 \right) + 2z_1 \left(-m_t^2 + m_W^2 + z_3 + z_4 \right) + 2m_t^2 m_W^2 \right.$$

$$\left. - 2m_t^2 z_4 - m_W^4 - 2m_W^2 z_4 - z_1^2 - z_3^2 - z_4^2 \right]^{\left(-\frac{1}{2}\right)}. \tag{5.53}$$

Next, we approach the right loop in fig.5.12 with loop momentum k_3 and external momentum k_1. The arising scalar products $k_3^2, k_3 \cdot k_1$ correspond to the Baikov variables z_7, z_9. We obtain

$$\frac{d^{(D=2)} k_3}{i\pi^{\frac{D}{2}}} = \frac{1}{\pi^{\frac{1}{2}} (\det C_3) \Gamma\left(\frac{1}{2}\right)} \det G\left(k_3, k_1\right)^{\left(-\frac{1}{2}\right)} dz_7 dz_9 =$$

$$\frac{-dz_7 dz_9}{\pi \sqrt{2z_1 \left(-m_t^2 + m_W^2 + z_7 + z_9 \right) - \left(-m_t^2 + m_W^2 + z_9 \right)^2 - 2z_7 \left(m_t^2 + m_W^2 - z_9 \right) - z_1^2 - z_7^2}}. \tag{5.54}$$

The remaining loop carries loop momentum k_1 and external momentum p. The last measure evaluates to

$$\frac{d^{(D=2)} k_1}{i\pi^{\frac{D}{2}}} = \frac{1}{\pi^{\frac{1}{2}} (\det C_1) \Gamma\left(\frac{1}{2}\right)} \det G\left(k_1, p\right)^{\left(-\frac{1}{2}\right)} dz_1 dz_2$$

$$= -\frac{dz_1 dz_2}{\pi \sqrt{s \left(4m_W^2 - s \right) - 2z_1 \left(s - z_2 \right) - 2s z_2 - z_1^2 - z_2^2}}. \tag{5.55}$$

To obtain the final representation of $I^{B'}_{011100101} (D = 2)$, we plug (5.53),(5.54) and (5.55) into (5.52) and replace propagators with respective Baikov variables,

$$I^{B'}_{011100101} (D = 2) = -m_t^4 \int dz_1 dz_2 dz_3 dz_4 dz_7 dz_9 \left[\pi^3 z_2 z_3 z_4 z_7 z_9 \left\{ \left(-m_t^4 \right. \right. \right.$$

$$+ 2z_3 \left(m_t^2 - m_W^2 + z_4 \right) + 2z_1 \left(-m_t^2 + m_W^2 + z_3 + z_4 \right) + 2m_t^2 m_W^2$$

$$- 2m_t^2 z_4 - m_W^4 - 2m_W^2 z_4 - z_1^2 - z_3^2 - z_4^2 \right) \left(2z_1 \left(-m_t^2 + m_W^2 + z_7 + z_9 \right) \right.$$

$$\left. - \left(-m_t^2 + m_W^2 + z_9 \right)^2 - 2z_7 \left(m_t^2 + m_W^2 - z_9 \right) - z_1^2 - z_7^2 \right) \right\}^{\left(-\frac{1}{2}\right)}$$

$$\left. \sqrt{s \left(4m_W^2 - s \right) - 2z_1 \left(s - z_2 \right) - 2s z_2 - z_1^2 - z_2^2} \right]^{(-1)}.$$

Now, we are able to maximally cut the integral via the replacement

$$\frac{1}{z_2 z_3 z_4 z_7 z_9} \rightarrow (2\pi i)^5 \; \delta\left(z_2\right) \delta\left(z_3\right) \delta\left(z_4\right) \delta\left(z_7\right) \delta\left(z_9\right),$$

$$\text{MaxCut} I_{011100101}^{B'}(2) = \int_{\mathcal{C}_{\text{MaxCut}}} dz_1 \frac{32 i \pi^2 m_t^4}{\left(m_t^2 - m_W^2 + z_1\right)^2 \sqrt{s\left(4m_W^2 - s\right) - 2sz_1 - z_1^2}}$$

$$= \int_{\mathcal{C}_{\text{MaxCut}}} \varphi_{334}. \tag{5.56}$$

We are left with one integration over z_1. We name the resulting integrand φ_{334}. Before we continue, we recall that the dimensional shift operator (5.6) $\boldsymbol{D}^- I(D) = I(D-2)$, makes it possible to relate results obtained in $D = (2 - 2\epsilon)$ space-time dimensions back to $D = (4 - 2\epsilon)$ dimensions.

φ_{334} is integrated straightforwardly after transforming it to a simpler form, like (5.47) or (5.50). We immediately recognise, that a multiplication with $\left(m_t^2 - m_W^2 + z_1\right)^2$ results in an integrand similar to (5.50), which may be integrated along a counterclockwise circle around the slit $[(-2m_W\sqrt{s} - s), (2m_W\sqrt{s} - s)] \equiv [a_{334}, b_{334}]$,

$$\oint_{[a_{334}, b_{334}]} \left(m_t^2 - m_W^2 + z_1\right)^2 \varphi_{334} = \oint_{[a_{334}, b_{334}]} dz_1 \frac{32 i \pi^2 m_t^4}{\sqrt{s\left(4m_W^2 - s\right) - 2sz_1 - z_1^2}}$$

$$= \oint_{[a_{334}, b_{334}]} dz_1 \frac{32 \pi^2 m_t^4}{\sqrt{\left(z_1 - (-2m_W\sqrt{s} - s)\right)\left(z_1 - (2m_W\sqrt{s} - s)\right)}} = 64\pi^3 i.$$

The result is proportional to π^3 and therefore of weight three. A multiplication with ϵ^3 results into a constant of weight zero,

$$\epsilon^3 \oint_{[(-2m_W\sqrt{s} - s), (2m_W\sqrt{s} - s)]} \left(m_t^2 - m_W^2 + z_1\right)^2 \varphi_{334} = 64\epsilon^3 \pi^3 i.$$

To obtain the first ansatz for an integral of uniform weight K_{46} we multiply the original integrand of $I_{011100101}^{B'}(D = 2 - 2\epsilon) = \boldsymbol{D}^- I_{011100101}^{B'}$ with the prefactor that led to a constant of weight zero,

$$\epsilon^3 \left(m_t^2 - m_W^2 + z_1\right)^2 = \epsilon^3 \left((m_t^2 - m_W^2)^2 + 2z_1(m_t^2 - m_W^2) + z_1^2\right),$$

whereby a multiplication with z_1 corresponds to an additional Baikov variable z_1 in the numerator,

$$\int dz_1 dz_2 dz_3 dz_4 dz_7 dz_9 \frac{1}{z_2 z_3 z_4 z_7 z_9} \xrightarrow{\cdot z_1} \int dz_1 dz_2 dz_3 dz_4 dz_7 dz_9 \frac{z_1}{z_2 z_3 z_4 z_7 z_9},$$

raising ν_1 by minus one. Accordingly, a multiplication with z_1^2 raises ν_1 by minus two. We find

$$K_{46} = \epsilon^3 \left((1-w)^2 \boldsymbol{D}^- I_{011100101}^{B'} + 2(1-w)\boldsymbol{D}^- I_{(-1)11100101}^{B'} + \boldsymbol{D}^- I_{(-2)11100101}^{B'}\right), \tag{5.57}$$

We find an ansatz for the second integral in the same way. We recognise, that a multiplication of φ_{334} with $\left(m_t^2 - m_W^2 + z_1\right)$ results into an integrand similar to (5.47), which may be integrated along a counterclockwise circle around the pole $z_1 = -m_t^2 + m_W^2$,

$$
\oint_{z_1 = -m_t^2 + m_W^2} \left(m_t^2 - m_W^2 + z_1\right) \varphi_{334}
$$

$$
= \oint_{z_1 = -m_t^2 + m_W^2} dz_1 \frac{32 i \pi^2 m_t^4}{\left(m_t^2 - m_W^2 + z_1\right) \sqrt{s \left(4 m_W^2 - s\right) - 2 s z_1 - z_1^2}}
$$

$$
= \left. \frac{64 i^2 \pi^2 m_t^4}{\sqrt{s \left(4 m_W^2 - s\right) - 2 s z_1 - z_1^2}} \right|_{z_1 = -m_t^2 + m_W^2} = \frac{64 i \pi^3}{r_2}, \tag{5.58}
$$

with

$$
r_2 = \sqrt{\lambda\left(v, w, 1\right)},
$$

where λ is the Källen function defined by

$$
\lambda\left(x, y, z\right) = x^2 + y^2 + z^2 - 2xy - 2xz - 2yz.
$$

We deduce that an additional multiplication with $\epsilon^3 r_2$,

$$
\varphi_{334} \to \epsilon^3 r_2 \left(m_t^2 - m_W^2 + z_1\right) \varphi_{334},
$$

leads to a maximal cut with constant leading singularities. Accordingly we multiply the integrand of $\boldsymbol{D}^- I_{011100101}^{B'}$ with $\epsilon^3 r_2 \left(1 - w + z_1\right)$ and find

$$
K_{47} = \epsilon^3 r_2 \left(\left(1 - w\right) \boldsymbol{D}^- I_{011100101}^{B'} + \boldsymbol{D}^- I_{(-1)11100101}^{B'}\right). \tag{5.59}
$$

We noticed that we encountered a second square root r_2 in addition to the square root we found in the previous section r_1.

We found two integrals of uniform weight (5.57), (5.59) as intermediate result. We derived them as we analysed the leading singularity of the maximal cut (5.56). To verify these ansätze, we may calculate their differential equation, thereby, we make a guess for the third integral based on the dimensions and dependence on ϵ of the first two integrals,

$$
\vec{I}^{(334)} = \begin{pmatrix} I_{011100101}^{B'} \\ I_{(-1)11100101}^{B'} \\ I_{0111(-1)0101}^{B'} \end{pmatrix} \to \vec{I'}^{(334)} = \begin{pmatrix} K_{46} \\ K_{47} \\ \epsilon^3 \boldsymbol{D}^- I_{0111(-1)0101}^{B'} \end{pmatrix}.
$$

We already calculated the differential equations of $\vec{I}^{(334)}$ in (5.19) and (5.20). The transformed system of differential equation is found as usual (5.26), where the transformation matrix is obtained with the help of integration by parts reductions. We notice that the resulting system of differential equations

$$d\vec{I}'^{(334)} = \left(A_v^{(334)} dv + A_w^{(334)} dw \right) \vec{I}'^{(334)},$$

$$A_v^{(334)} = \begin{pmatrix} -\frac{\epsilon\left(7v^2-4vw-4v-3w^2+6w-3\right)}{v(v^2-2vw-2v+w^2-2w+1)} & \frac{2\epsilon(-v+w-1)}{r_2 v} & \frac{2\epsilon(w-v)(3v+w-1)}{r_2 v} \\ -\frac{2\epsilon(-v+w-1)}{r_2 v} & -\frac{\epsilon}{v} & -\frac{2\epsilon(w-v)}{v} \\ \frac{\epsilon(3v+w-1)}{r_2 v(v-w)} & -\frac{\epsilon}{v(w-v)} & \frac{1}{w-v} - \frac{2\epsilon}{w-v} \end{pmatrix},$$

$$A_w^{(334)} = \begin{pmatrix} \frac{2\epsilon\left(v^2+3vw-2v-4w^2+3w+1\right)}{w(v^2-2vw-2v+w^2-2w+1)} & \frac{2\epsilon(v-w-1)}{r_2 w} & \frac{2\epsilon(v-w)(v+3w-1)}{r_2 w} \\ -\frac{2\epsilon(v-w-1)}{r_2 w} & -\frac{2\epsilon}{w} & -\frac{2\epsilon(v-w)}{w} \\ -\frac{\epsilon(v+3w-1)}{r_2 w(v-w)} & -\frac{\epsilon}{w(v-w)} & \frac{1}{v-w} - \frac{\epsilon(v+w)}{w(v-w)} \end{pmatrix},$$

is almost linear in ϵ. The lower right corners contain additional parts proportional to ϵ^0. We may solve this issue for a general variable x as placeholder for v, w, writing symbolically

$$\frac{\partial}{\partial x} \vec{I}'^{(334)} = A_x^{(334)} \vec{I}'^{(334)} = \begin{pmatrix} \epsilon a_{11}^x & \epsilon a_{12}^x & \epsilon a_{13}^x \\ \epsilon a_{21}^x & \epsilon a_{22}^x & \epsilon a_{23}^x \\ \epsilon a_{31}^x & \epsilon a_{32}^x & \epsilon \left(a_{33}^x\right)^{(1)} + \left(a_{33}^x\right)^{(0)} \end{pmatrix} \vec{I}'^{(334)}. \qquad (5.60)$$

The part $\left(a_{33}^x\right)^{(0)}$ may be removed through a transformation matrix of the first kind (5.27) with

$$U^{(334)} = \begin{pmatrix} 1 & 0 & 0 \\ 0 & 1 & 0 \\ 0 & 0 & u(x) \end{pmatrix}, \qquad (5.61)$$

which acts on the differential equation (5.60) like

$$U^{(334)}.A_x^{(334)}.\left(U^{(334)}\right)^{(-1)} - U^{(334)}.d\left(U^{(334)}\right)^{(-1)}$$

$$= \begin{pmatrix} \epsilon a_{11}^x & \epsilon a_{12}^x & \epsilon \frac{a_{13}^x}{u} \\ \epsilon a_{21}^x & \epsilon a_{22}^x & \epsilon \frac{a_{23}^x}{u} \\ \epsilon u a_{31}^x & \epsilon u a_{32}^x & \epsilon \left(a_{33}^x\right)^{(1)} + \left(a_{33}^x\right)^{(0)} + \frac{\partial u}{u \partial x} \end{pmatrix}.$$

In conclusion, the part $\left(a_{33}^x\right)^{(0)}$ vanishes if $u(x)$ is a solution to

$$\left(a_{33}^x\right)^{(0)} u(x) + \frac{\partial u(x)}{\partial x} \overset{!}{=} 0. \qquad (5.62)$$

This differential equation is solved by

$$u(x) = \exp\left(-\int \left(a_{33}^x\right)^{(0)} dx \right). \qquad (5.63)$$

Returning to v, w the requirement (5.62) yields

$$\frac{1}{w-v} u(v) + \frac{\partial u(v)}{\partial v} = 0,$$

$$\Rightarrow u(v) = \exp\left(-\int \frac{1}{w-v}dv\right) = w - v,$$

$$\frac{1}{v-w}u(w) + \frac{\partial u(w)}{\partial w} = 0,$$

$$\Rightarrow u(w) = \exp\left(-\int \frac{1}{v-w}dw\right) = w - v.$$

We insert $u(v,w) = (w-v)$ into U (5.61) and obtain the following integrals and differential equations,

$$d\begin{pmatrix} K_{46} \\ K_{47} \\ \epsilon^3 \, (w-v)\, \boldsymbol{D}^- I^{B'}_{0111(-1)0101} \end{pmatrix} = \left(\tilde{A}^{(334)}_v dv + \tilde{A}^{(334)}_w dw\right)\begin{pmatrix} K_{46} \\ K_{47} \\ \epsilon^3 \, (w-v)\, \boldsymbol{D}^- I^{B'}_{0111(-1)0101} \end{pmatrix},$$

$$\tilde{A}^{(334)}_v = \begin{pmatrix} -\frac{\epsilon\left(7v^2-4vw-4v-3w^2+6w-3\right)}{v(v^2-2vw-2v+w^2-2w+1)} & -\frac{2\epsilon(v-w+1)}{vr_2} & \frac{2\epsilon(3v+w-1)}{vr_2} \\ \frac{2\epsilon(v-w+1)}{vr_2} & -\frac{\epsilon}{v} & -\frac{2\epsilon}{v} \\ -\frac{\epsilon(3v+w-1)}{vr_2} & -\frac{\epsilon}{v} & \frac{2\epsilon}{v-w} \end{pmatrix},$$

$$\tilde{A}^{(334)}_w = \begin{pmatrix} -\frac{2\epsilon\left(-v^2-3vw+2v+4w^2-3w-1\right)}{w(v^2-2vw-2v+w^2-2w+1)} & \frac{2\epsilon(v-w-1)}{wr_2} & -\frac{2\epsilon(v+3w-1)}{wr_2} \\ -\frac{2\epsilon(v-w-1)}{wr_2} & -\frac{2\epsilon}{w} & \frac{2\epsilon}{w} \\ \frac{\epsilon(v+3w-1)}{wr_2} & \frac{\epsilon}{w} & -\frac{\epsilon(v+w)}{w(v-w)} \end{pmatrix}.$$

The diagonal block corresponding to sector 334 is linear in ϵ! Considering the complete matrix of system 2a, we find that the third integral misses a sub-sector contribution. The parts not proportional to ϵ are removed with a transformation matrix of the second kind (5.29). We find

$$K_{46} = \epsilon^3\left((1-w)^2\,\boldsymbol{D}^- I^{B'}_{011100101} + 2(1-w)\boldsymbol{D}^- I^{B'}_{(-1)11100101} + \boldsymbol{D}^- I^{B'}_{(-2)11100101}\right),$$

$$K_{47} = \epsilon^3 r_2\left((1-w)\boldsymbol{D}^- I^{B'}_{011100101} + \boldsymbol{D}^- I^{B'}_{(-1)11100101}\right),$$

$$K_{48} = \epsilon^3\,(w-v)\left(\boldsymbol{D}^- I^{B'}_{0111(-1)0101} - 2\boldsymbol{D}^- I^{B'}_{001100011}\right).$$

In this section we explored a method providing ansätze for integrals of uniform weight. We demonstrated its application by means of two example sectors. We studied the weight properties of the leading term of a maximal cut with the aim of obtaining constant leading singularities. The maximal cut projects the differential equation of the corresponding integral onto its homogeneous part, hence, this method is best suited for the study of diagonal blocks. Furthermore, the leading term of the maximal cut is drastically simpler then the original integral, which makes the study of weight properties accessible in the first place. We may generalise this method for a sector with N master integrals, whose maximal cut leaves integration's behind. We select N independent integration domains

$$\mathcal{C}_{\text{MaxCut}} \to \mathcal{C}_1, \ldots, \mathcal{C}_N.$$

These are usually around poles in order to be as simple as possible (see (5.47) and (5.50)). In addition, we modify the integrand

$$\varphi \to \varphi_1, \ldots, \varphi_N,$$

to obtain a constants of weight zero. Applying the same modifications to the original integral provides the sought-after ansätze. In this section, we, furthermore, encountered another square root (5.58) and utilised a transformation matrix (5.61) to fix our results. In the next section we return to the larger picture and give a complete list of all integrals of uniform weight.

5.5   Master integrals

In the preceding sections, we illustrated different techniques applied in the search for appropriate master integrals, i.e. master integrals leading to differential equations linear in the dimensional regularisation parameter ϵ. We obtained three systems of pre-canonical master integrals in section 5.3. We transformed the resulting differential equations of all systems bottom-up (section 5.4.2). We constructed ansätze for master integrals of uniform weight in order to transform sectors, i.e. blocks on the diagonal of differential equations. Thereby, we also worked in $(2 - 2\epsilon)$ dimensions, since the dimensional shift operator (5.6) is able to transfer results back to $(4 - 2\epsilon)$ dimensions. One way to find such an ansatz is through relations to (simpler) integrals, which are already known. In section 5.4.3, for example, we found expressions of uniform weight for the tadpole and bubble integral and were therefore able to construct ansätze for the first two integrals of system 1. If the integrals become more complex the leading singularity analyses (Box 2) is a helpful tool. We explained this approach in the previous section. Instead of the integral itself we may study the weight properties of the leading term of the simpler maximally cut integral. To obtain the maximal cut, we first convert the integral to Baikov representation democratically or loop by loop. We modify the maximal cut to obtain a constant of weight zero. If the maximal cut does not remove all integrations, we change not only the integrand but also the integration domain. The chosen integration domains are usually around poles. The modifications applied to the integrand of the maximal cut are applied to the original integrand in order to obtain the desired ansatz. Transformation matrices of the first kind (5.33) may fix resulting ansätze (see for example (5.61), (5.62)). After obtaining differential equations linear in ϵ on the sector, we consider its sub-sector contributions. Sub-sector contributions appear on the left of diagonal blocks. They are brought to a form linear in ϵ with the help of transformations on the matrix (section 5.4). Non-linear contributions of single sub-sectors are removed by transformation matrices of the second kind (5.29). Sometimes, we need to put a prefactor depending on ϵ in front of the considered integral itself. This transformation matrix of the first kind (5.33), solely depending on ϵ, either removes unwanted sub-sector contributions completely or transforms them to a simple form (5.32). This simple form is again fixed by transformation matrices of the second kind (5.29).

We are dealing with a huge amount of master integrals as opposed to the few examples we gave. In practice, we automatised main parts of the procedures as we implemented

them within `Mathematica`. In this section, we give all resulting master integrals of uniform weight.

We have seen how square roots may arise in the construction of integrals of uniform weight. In section 5.4.3 we encountered r_1 in (5.42) and in section 5.4.4 r_2 in (5.58). Furthermore, we find the square roots r_3, r_4,

$$
\begin{aligned}
r_1 &= \sqrt{-v\,(4-v)}, \\
r_2 &= \sqrt{\lambda\,(v,w,1)}, \\
r_3 &= \sqrt{-v\,(4w-v)}, \\
r_4 &= \sqrt{-v\,(-4-v)},
\end{aligned}
\tag{5.64}
$$

where λ is the Källen function defined by

$$
\lambda\,(x,y,z) = x^2 + y^2 + z^2 - 2xy - 2xz - 2yz.
\tag{5.65}
$$

As we are seeking canonical differential equations (3.72) (see section 3.5.1), which are expressible in terms of dlog forms containing rational functions, these must be rationalised (see section 3.6.2). We are not able to rationalise all square roots simultaneously. Hence, we divide the master integrals into three systems, each containing a subset of square roots which can be rationalised. These rationalisations will be given in section 5.5.1. Accordingly we find three systems of differential equations linear in ϵ, all fulfilling the integrability condition (3.64).

System 1 consists of topologies A, B, C and D (fig.5.5, table 5.6) with sectors 255 as top sectors. We call the corresponding master integrals of uniform weight $\vec{J}$ and present them in (5.69). They fulfil the system of differential equations

$$
\begin{aligned}
d\vec{J} &= \epsilon \tilde{A}\,(v,w)\,\vec{J}, \\
\tilde{A}\,(v,w) &= \tilde{A}_v dv + \tilde{A}_w dw,
\end{aligned}
\tag{5.66}
$$

where $\tilde{A}_v, \tilde{A}_w$ are 105×105-dimensional matrices depending on v, w and thereby also on the following square roots

$$
(r_1, r_2)\,.
$$

System 2a contains topology B' (fig.5.7, table 5.7) with top sectors 255 and 479. Here, we call the master integrals of uniform weight, given in (5.70), $\vec{K}$. Their system of differential equations evaluates to

$$
\begin{aligned}
d\vec{K} &= \epsilon \tilde{B}\,(v,w)\,\vec{K}, \\
\tilde{B}\,(v,w) &= \tilde{B}_v dv + \tilde{B}_w dw,
\end{aligned}
\tag{5.67}
$$

where B_v, B_w are 61×61-dimensional matrices depending on v, w and thereby also on the following square roots

$$
(r_1, r_2, r_3)\,.
$$

System 2b contains topology B' (fig.5.7, table 5.8) with top sector 509. We call the last set of master integrals of uniform weight $\vec{L}$ (5.71). Their system of differential equations amounts to

$$d\vec{L} = \epsilon \tilde{C}(v, w) \, \vec{L},$$
$$\tilde{C}(v, w) = \tilde{C}_v dv + \tilde{C}_w dw, \tag{5.68}$$

where C_v, C_w are 43×43-dimensional matrices depending on v, w and thereby also on

$$(r_1, r_2, r_4) \, .$$

Defining three systems is in some sense redundant, as several integrals of different systems are related to each other. Topology B' resembles topology B, but masses are exchanged $m_W \leftrightarrow m_t$. Hence, its master integrals under top sector 255 correspond to those of topology B. Furthermore, system 2a and system 2b share common sub-sectors. As already shown in table 5.5, only four integrals from system 2b, namely $L_{40} - L_{43}$, are no part of system 2a.

The master integrals are completely defined by their alphabet and corresponding co-efficient matrix, which will be discussed in section 5.5.2, as well as their boundary values. We take $(v, w) = (0, 1)$ as boundary point, since most master integrals vanish there. The remaining boundary values will be given in section 5.5.3

The master integrals of uniform weight for system 1, $\vec{J}$, are presented in the following. Furthermore, a summary is given in appendix B.1.

$$J_1 = \epsilon^3 \, \boldsymbol{D}^- I^A_{100110000},$$
$$J_2 = \epsilon^3 \, r_1 \, \boldsymbol{D}^- I^A_{110110000},$$
$$J_3 = \epsilon^3 \, r_1 \, \boldsymbol{D}^- I^A_{011110000},$$
$$J_4 = \epsilon^3 \, \boldsymbol{D}^- I^A_{(-1)11110000},$$
$$J_5 = \epsilon^3 \, (1 - w) \, \boldsymbol{D}^- I^A_{101010100},$$
$$J_6 = \epsilon^3 \, \boldsymbol{D}^- I^A_{101(-1)10100},$$
$$J_7 = \epsilon^3 \, r_2 \, \boldsymbol{D}^- I^A_{011010100},$$
$$J_8 = \epsilon^3 \, \left[\boldsymbol{D}^- I^A_{011(-1)10100} - (1 - w) \, \boldsymbol{D}^- I^A_{011010100} \right],$$
$$J_9 = \epsilon^3 \, \boldsymbol{D}^- I^A_{01101(-1)100},$$
$$J_{10} = \epsilon^3 \, \left[\boldsymbol{D}^- I^A_{0110101(-1)0} + v \, \boldsymbol{D}^- I^A_{011010100} \right],$$
$$J_{11} = \epsilon^3 \, (1 - w) \, \boldsymbol{D}^- I^A_{100110100},$$
$$J_{12} = \epsilon^3 \, r_2 \, \boldsymbol{D}^- I^A_{100011100},$$
$$J_{13} = \epsilon^3 \, \left[\boldsymbol{D}^- I^A_{100(-1)11100} - (1 - w) \, \boldsymbol{D}^- I^A_{100011100} \right],$$
$$J_{14} = \epsilon^3 \, \left[\boldsymbol{D}^- I^A_{1000111(-1)0} + v \, \boldsymbol{D}^- I^A_{100011100} \right],$$

$J_{15} = \epsilon^3 \, v \, \boldsymbol{D}^- I^A_{100100110},$

$J_{16} = \epsilon^3 \, v \, \boldsymbol{D}^- I^A_{100010110},$

$J_{17} = \epsilon^3 \, v \, (4-v) \, \boldsymbol{D}^- I^A_{110111000},$

$J_{18} = \epsilon^3 \, r_1 \left[\boldsymbol{D}^- I^A_{111(-1)10100} - (1-w) \, \boldsymbol{D}^- I^A_{111010100} \right],$

$J_{19} = \epsilon^3 \, r_1 \left[\boldsymbol{D}^- I^A_{111(-1)10100} - \boldsymbol{D}^- I^A_{011010100} \right],$

$J_{20} = \epsilon^3 \, (1-w) \, r_1 \, \boldsymbol{D}^- I^A_{110110100},$

$J_{21} = \epsilon^3 \, r_1 \left[(1-w) \, \boldsymbol{D}^- I^A_{011110100} - \boldsymbol{D}^- I^A_{011010100} \right],$

$J_{22} = \epsilon^3 \, (1-w) \left[\boldsymbol{D}^- I^A_{(-1)11110100} - \boldsymbol{D}^- I^A_{011010100} \right],$

$J_{23} = \epsilon^3 \, (1-w) \, \boldsymbol{D}^- I^A_{01111(-1)100},$

$J_{24} = \epsilon^3 \, r_1 r_2 \, \boldsymbol{D}^- I^A_{110011100},$

$J_{25} = \epsilon^3 \, r_1 \left[\boldsymbol{D}^- I^A_{110(-1)11100} - (1-w) \, \boldsymbol{D}^- I^A_{110011100} \right],$

$J_{26} = \epsilon^3 \, r_1 \left[\boldsymbol{D}^- I^A_{1100111(-1)0} + v \, \boldsymbol{D}^- I^A_{110011100} \right],$

$J_{27} = \epsilon^3 \, r_2 \, \boldsymbol{D}^- I^A_{101(-1)11100},$

$J_{28} = \epsilon^3 \, r_1 \left[\boldsymbol{D}^- I^A_{101(-1)11100} - (1-w) \, \boldsymbol{D}^- I^A_{101011100} \right],$

$J_{29} = \epsilon^3 \left[\boldsymbol{D}^- I^A_{101(-2)11100} - (1-w) \, \boldsymbol{D}^- I^A_{101(-1)11100} \right],$

$J_{30} = \epsilon^3 \, (1-v) \left[\boldsymbol{D}^- I^A_{101(-1)11100} + \boldsymbol{D}^- I^A_{10101110(-1)} - (1-w) \, \boldsymbol{D}^- I^A_{101011100} \right],$

$J_{31} = \epsilon^3 \, r_1 \left[(1-w) \, \boldsymbol{D}^- I^A_{100111100} - \boldsymbol{D}^- I^A_{100011100} \right],$

$J_{32} = \epsilon^3 \, v r_1 \, \boldsymbol{D}^- I^A_{110100110},$

$J_{33} = \epsilon^3 \, v r_1 \, \boldsymbol{D}^- I^A_{011100110},$

$J_{34} = \epsilon^3 \, v \, \boldsymbol{D}^- I^A_{(-1)11100110},$

$J_{35} = \epsilon^3 \, v r_1 \, \boldsymbol{D}^- I^A_{110010110},$

$J_{36} = \epsilon^3 \, (1-w) \left[v \, \boldsymbol{D}^- I^A_{101010110} + \boldsymbol{D}^- I^A_{011010100} \right],$

$J_{37} = \epsilon^4 \, (1-2\epsilon) \, v \, I^A_{111021100},$

$J_{38} = \epsilon^4 \, (1-2\epsilon) \, v \, I^A_{111011200},$

$J_{39} = \epsilon^3 \, v \, (4-v) \left[(1-w) \, \boldsymbol{D}^- I^A_{110111100} - \boldsymbol{D}^- I^A_{110011100} \right],$

$J_{40} = \epsilon^3 v r_1 \left[\boldsymbol{D}^- I^A_{11101011(-1)} - (1-w) \, \boldsymbol{D}^- I^A_{111010110} \right],$

$J_{41} = \epsilon^4 \, (1-2\epsilon) \, v \, I^A_{112010110},$

$J_{42} = \epsilon^4 \, (1-2\epsilon) \, v \, I^A_{111020110},$

$J_{43} = \epsilon^4 \, (1-2\epsilon) \, v \, I^A_{021110110},$

$J_{44} = \epsilon^4 \, (1-2\epsilon) \, v \, I^A_{012110110},$

$J_{45} = \epsilon^3 \, v^2 \, (4-v) \, \boldsymbol{D}^- I^A_{110101110},$

$J_{46} = \epsilon^4 \, (1-\epsilon) \, (1-2\epsilon) \, v \, I^A_{100111110},$

$$J_{47} = \epsilon^5 \left(1 - 2\epsilon\right) \, v \, I^A_{111110110},$$

$$J_{48} = \epsilon^4 \left(1 - 2\epsilon\right) \, v \left(1 - w\right) \, I^A_{111120110},$$

$$J_{49} = \epsilon^4 \left(1 - 2\epsilon\right) \, v \left[I^A_{211110110} + \frac{1}{2} \left(2 - v + r_1\right) \, I^A_{121110110} \right],$$

$$J_{50} = \epsilon^4 \left(1 - 2\epsilon\right) \, v r_1 \, I^A_{210111110},$$

$$J_{51} = \epsilon^3 \, v \, \boldsymbol{D}^- I^B_{100011100},$$

$$J_{52} = \epsilon^3 \, v \, \boldsymbol{D}^- I^B_{001011100},$$

$$J_{53} = \epsilon^3 \, v r_1 \, \boldsymbol{D}^- I^B_{110011100},$$

$$J_{54} = \epsilon^3 \, r_2 \, \boldsymbol{D}^- I^B_{101(-1)11100},$$

$$J_{55} = \epsilon^3 \, \left(1 - w\right) \left[\boldsymbol{D}^- I^B_{101(-1)11100} + v \, \boldsymbol{D}^- I^B_{101011100} \right],$$

$$J_{56} = \epsilon^3 \left[\boldsymbol{D}^- I^B_{101(-2)11100} + v \, \boldsymbol{D}^- I^B_{101(-1)11100} \right],$$

$$J_{57} = \epsilon^3 \, v r_2 \, \boldsymbol{D}^- I^B_{011100110},$$

$$J_{58} = \epsilon^3 \, v \left[\boldsymbol{D}^- I^B_{(-1)11100110} - \left(1 - w\right) \, \boldsymbol{D}^- I^B_{011100110} \right],$$

$$J_{59} = \epsilon^3 \, v \, \boldsymbol{D}^- I^B_{0111(-1)0110},$$

$$J_{60} = \epsilon^3 \, v^2 \, \boldsymbol{D}^- I^B_{100101110},$$

$$J_{61} = \epsilon^3 \, v^2 \, \boldsymbol{D}^- I^B_{001101110},$$

$$J_{62} = \epsilon^4 \left(1 - 2\epsilon\right) \, v \, I^B_{111021100},$$

$$J_{63} = \epsilon^3 \, r_1 \left\{ \left(1 - w\right) \, \boldsymbol{D}^- I^B_{111(-1)11100} - \boldsymbol{D}^- I^B_{101(-1)11100} \right\},$$

$$J_{64} = \epsilon^3 \, v r_1 \left\{ \left(1 - w\right) \, \boldsymbol{D}^- I^B_{111100110} - \boldsymbol{D}^- I^B_{011100110} \right\},$$

$$J_{65} = \epsilon^3 \, v^2 r_1 \, \boldsymbol{D}^- I^B_{110101110},$$

$$J_{66} = \epsilon^5 \left(1 - 2\epsilon\right) \, v \, I^B_{111110110},$$

$$J_{67} = \epsilon^4 \left(1 - 2\epsilon\right)^2 \, v \, I^B_{111101110},$$

$$J_{68} = \epsilon^3 \, r_1 \, \boldsymbol{D}^- I^C_{101001100},$$

$$J_{69} = \epsilon^3 \, \boldsymbol{D}^- I^C_{1(-1)1001100},$$

$$J_{70} = \epsilon^3 \, \boldsymbol{D}^- I^C_{10100110(-1)},$$

$$J_{71} = \epsilon^2 \left(1 + 4\epsilon\right) \, \boldsymbol{D}^- I^C_{011001100},$$

$$J_{72} = \epsilon^3 r_1 \, \boldsymbol{D}^- I^C_{11100110(-1)},$$

$$J_{73} = \epsilon^3 \, r_2 \left[\left(1 - w\right) \, \boldsymbol{D}^- I^C_{101011100} + \boldsymbol{D}^- I^C_{101001100} \right],$$

$$J_{74} = \epsilon^3 \, \left(1 - w\right) \, \boldsymbol{D}^- I^C_{10101110(-1)},$$

$$J_{75} = \epsilon^3 \, \left(1 - w\right) \left[\boldsymbol{D}^- I^C_{1010111(-1)0} + v \, \boldsymbol{D}^- I^C_{101011100} \right],$$

$$J_{76} = \epsilon^3 \, r_2 \, \boldsymbol{D}^- I^C_{01101110(-1)},$$

$$J_{77} = \epsilon^3 \, \boldsymbol{D}^- I^C_{01101110(-2)},$$

$$J_{78} = \epsilon^3 \, \left(w - v\right) \left\{ \boldsymbol{D}^- I^C_{011(-1)11100} - 2 \, \boldsymbol{D}^- I^A_{100011100} \right\},$$

$$J_{79} = \epsilon^3 \, r_1 \left\{ 2 \, \boldsymbol{D}^- I^C_{1(-1)1101010} + v \, \boldsymbol{D}^- I^C_{101101010} - \boldsymbol{D}^- I^C_{011001100} - 2 \, \boldsymbol{D}^- I^C_{101100010} \right\},$$

$$J_{80} = \epsilon^3 \, v \left[2 \left(1 - 3\epsilon \right) \left(I^C_{202101010} - \epsilon \, I^C_{102101010} \right) + \epsilon \left(1 - 2\epsilon \right) I^C_{101201010} \right],$$

$$J_{81} = \epsilon^3 \left(1 - w \right) \left[\left(1 - w \right) \, \boldsymbol{D}^- I^C_{101011010} + \boldsymbol{D}^- I^C_{011001100} \right],$$

$$J_{82} = \epsilon^3 \, r_1 \left\{ \left(1 - w \right) \, \boldsymbol{D}^- I^C_{11101110(-1)} - \boldsymbol{D}^- I^C_{01101110(-1)} \right\},$$

$$J_{83} = \epsilon^4 \left(1 - 2\epsilon \right) v \, I^C_{111011200},$$

$$J_{84} = \epsilon^4 \left(1 - 2\epsilon \right) v \, I^C_{111012100},$$

$$J_{85} = \epsilon^4 \left(1 - 2\epsilon \right) v \, I^C_{112101010},$$

$$J_{86} = \epsilon^3 \left(1 - w \right) r_1 \left[\left(1 - w \right) \, \boldsymbol{D}^- I^C_{111011010} - \boldsymbol{D}^- I^C_{101011100} + \boldsymbol{D}^- I^C_{111001100} \right],$$

$$J_{87} = \epsilon^4 \left(1 - 2\epsilon \right) \left[I^C_{101111010} - \frac{1}{2} \left(1 - w \right) I^C_{201111010} - \frac{3}{2} I^C_{101211(-1)10} + \frac{1}{4} v \, I^C_{101201010} \right.$$
$$\left. - \frac{1}{2} I^C_{201101010} + \frac{1}{2} I^C_{200111010} + \frac{3}{2} I^C_{100211010} \right] + \frac{\epsilon^3}{2} \left(1 - 3\epsilon \right) v \left[I^C_{202101010} - \epsilon \, I^C_{102101010} \right],$$

$$J_{88} = \epsilon^4 \left(1 - 2\epsilon \right) v \, I^C_{101211010},$$

$$J_{89} = \epsilon^4 \left(1 - 2\epsilon \right) v \, I^C_{012111010},$$

$$J_{90} = \epsilon^4 \left(1 - 2\epsilon \right) v \, I^C_{112001110},$$

$$J_{91} = \epsilon^4 \left(1 - 2\epsilon \right) v \, I^C_{111002110},$$

$$J_{92} = \epsilon^2 \, r_1 \left[\left(1 - 2\epsilon \right)^2 v \, I^C_{211001210} - \epsilon \left(1 - 2\epsilon \right) I^C_{111002110} - I^C_{202002100} - v \, I^A_{210200210} \right],$$

$$J_{93} = \epsilon^4 \left(1 - 2\epsilon \right) v \, I^C_{021011110},$$

$$J_{94} = \epsilon^4 \left(1 - 2\epsilon \right) v \, I^C_{012011110},$$

$$J_{95} = \epsilon^5 \left(1 - 2\epsilon \right) v \, I^C_{111111010},$$

$$J_{96} = \epsilon^4 \left(1 - 2\epsilon \right) vw \, I^C_{111121010},$$

$$J_{97} = \epsilon^4 \left(1 - 2\epsilon \right) v \left(1 - w \right) I^C_{111111020},$$

$$J_{98} = \epsilon^4 \left(1 - 2\epsilon \right) r_1 \left(I^C_{211111010} + I^C_{121111010} + I^C_{111112010} + w \, I^C_{111121010} - 4\epsilon \, I^C_{111111010} \right),$$

$$J_{99} = \epsilon^5 \left(1 - 2\epsilon \right) v \, I^C_{111011110},$$

$$J_{100} = \epsilon^4 \left(1 - 2\epsilon \right) v \left(1 - w \right) I^C_{111012110},$$

$$J_{101} = \epsilon^4 \left(1 - 2\epsilon \right) v \left(1 - w \right) I^C_{112011110},$$

$$J_{102} = \epsilon^4 \left(1 - 2\epsilon \right) vr_1 \, I^C_{121011110},$$

$$J_{103} = \epsilon^5 \left(1 - 2\epsilon \right) v \, I^C_{101111110},$$

$$J_{104} = \epsilon^5 \left(1 - 2\epsilon \right) v \left(1 - v - w \right) I^C_{111111110},$$

$$J_{105} = \epsilon^4 \left(1 - 2\epsilon \right) vw \, I^D_{111201110}. \tag{5.69}$$

The master integrals for system 2a are

$$K_1 = \epsilon^3 \left(1 - w \right) \boldsymbol{D}^- I^{B'}_{101010100},$$

$$K_2 = \epsilon^3 \, \boldsymbol{D}^- I^{B'}_{101(-1)10100},$$

$$K_3 = \epsilon^3 \, r_2 \, \boldsymbol{D}^- I^{B'}_{011010100},$$

$$K_4 = \epsilon^3 \left[\boldsymbol{D}^- I^{B'}_{(-1)11010100} + (1-w) \, \boldsymbol{D}^- I^{B'}_{011010100} \right],$$

$$K_5 = \epsilon^3 \left[\boldsymbol{D}^- I^{B'}_{01101(-1)100} + v \, \boldsymbol{D}^- I^{B'}_{011010100} \right],$$

$$K_6 = \epsilon^3 \left[\boldsymbol{D}^- I^{B'}_{0110101(-1)0} + v \, \boldsymbol{D}^- I^{B'}_{011010100} \right],$$

$$K_7 = \epsilon^3 \, v \, \boldsymbol{D}^- I^{B'}_{100011100},$$

$$K_8 = \epsilon^3 \, v \, \boldsymbol{D}^- I^{B'}_{001011100},$$

$$K_9 = \epsilon^3 \, v \, \boldsymbol{D}^- I^{B'}_{101000110},$$

$$K_{10} = \epsilon^3 \, r_3 \left[\boldsymbol{D}^- I^{B'}_{011010100} + \boldsymbol{D}^- I^{B'}_{111(-1)10100} + (1-w) \, \boldsymbol{D}^- I^{B'}_{111010100} \right],$$

$$K_{11} = \epsilon^3 \, r_3 \, \boldsymbol{D}^- I^{B'}_{111(-1)10100},$$

$$K_{12} = \epsilon^3 \, v \, r_3 \, \boldsymbol{D}^- I^{B'}_{110011100},$$

$$K_{13} = \epsilon^3 \, r_2 \, \boldsymbol{D}^- I^{B'}_{101(-1)11100},$$

$$K_{14} = \epsilon^3 \, (1-w) \left[\boldsymbol{D}^- I^{B'}_{101(-1)11100} + v \, \boldsymbol{D}^- I^{B'}_{101011100} \right],$$

$$K_{15} = \epsilon^3 \left[\boldsymbol{D}^- I^{B'}_{101(-2)11100} + v \, \boldsymbol{D}^- I^{B'}_{101(-1)11100} \right],$$

$$K_{16} = \epsilon^3 \, (1-w) \left[v \, \boldsymbol{D}^- I^{B'}_{011011100} + \boldsymbol{D}^- I^{B'}_{011010100} \right],$$

$$K_{17} = \epsilon^3 \, v \, r_3 \, \boldsymbol{D}^- I^{B'}_{111000110},$$

$$K_{18} = \epsilon^3 \, v \, (1-w) \, \boldsymbol{D}^- I^{B'}_{101100110},$$

$$K_{19} = \epsilon^3 \, v \, r_2 \, \boldsymbol{D}^- I^{B'}_{011100110},$$

$$K_{20} = \epsilon^3 \, v \left[\boldsymbol{D}^- I^{B'}_{(-1)11100110} + (1-w) \, \boldsymbol{D}^- I^{B'}_{011100110} \right],$$

$$K_{21} = \epsilon^3 \, v \, \boldsymbol{D}^- I^{B'}_{0111(-1)0110},$$

$$K_{22} = \epsilon^3 \, v^2 \, \boldsymbol{D}^- I^{B'}_{100101110},$$

$$K_{23} = \epsilon^3 \, v^2 \, \boldsymbol{D}^- I^{B'}_{001101110},$$

$$K_{24} = \epsilon^4 \, (1-2\epsilon) \, v \, I^{B'}_{111021100},$$

$$K_{25} = \epsilon^3 \, r_3 \left[(1-w) \, \boldsymbol{D}^- I^{B'}_{111(-1)11100} + \boldsymbol{D}^- I^{B'}_{101(-1)11100} \right],$$

$$K_{26} = \epsilon^3 \, v \, r_3 \left[(1-w) \, \boldsymbol{D}^- I^{B'}_{111100110} + \boldsymbol{D}^- I^{B'}_{011100110} \right],$$

$$K_{27} = \epsilon^3 \, v \, r_3 \, \boldsymbol{D}^- I^{B'}_{11101011(-1)},$$

$$K_{28} = \epsilon^4 \, (1-2\epsilon) \, v \, I^{B'}_{112010110},$$

$$K_{29} = \epsilon^4 \, (1-2\epsilon) \, v \, I^{B'}_{111020110},$$

$$K_{30} = \epsilon^3 \, v^2 \, r_3 \, \boldsymbol{D}^- I^{B'}_{110101110},$$

$$K_{31} = \epsilon^5 \, (1-2\epsilon) \, v \, I^{B'}_{111110110},$$

$$K_{32} = \epsilon^4 \, (1-2\epsilon)^2 \, v \, I^{B'}_{111101110},$$

$$K_{33} = \epsilon^3 \, \boldsymbol{D}^- I^{B'}_{101000001},$$

$$K_{34} = \epsilon^3 \, r_3 \, \boldsymbol{D}^- I^{B'}_{111000001},$$

$K_{35} = \epsilon^3 \ (1-w) \ \boldsymbol{D}^- I^{B'}_{101100001},$

$K_{36} = \epsilon^3 \ r_2 \ \boldsymbol{D}^- I^{B'}_{011100001},$

$K_{37} = \epsilon^3 \left[\boldsymbol{D}^- I^{B'}_{(-1)11100001} + (1-w) \ \boldsymbol{D}^- I^{B'}_{011100001} \right],$

$K_{38} = \epsilon^3 \left[\boldsymbol{D}^- I^{B'}_{01110(-1)001} + v \ \boldsymbol{D}^- I^{B'}_{011100001} \right],$

$K_{39} = \epsilon^2 \ (1+4\epsilon) \ \boldsymbol{D}^- I^{B'}_{001100101},$

$K_{40} = \epsilon^3 \ r_1 \ \boldsymbol{D}^- I^{B'}_{001100011},$

$K_{41} = \epsilon^3 \left[\boldsymbol{D}^- I^{B'}_{(-1)01100011} + (1-w) \ \boldsymbol{D}^- I^{B'}_{001100011} \right],$

$K_{42} = \epsilon^3 \left[\boldsymbol{D}^- I^{B'}_{0011(-1)0011} + v \ \boldsymbol{D}^- I^{B'}_{001100011} \right],$

$K_{43} = \epsilon^3 \ v \ \boldsymbol{D}^- I^{B'}_{001000111},$

$K_{44} = \epsilon^3 \ r_3 \left[(1-w) \ \boldsymbol{D}^- I^{B'}_{111100001} + \boldsymbol{D}^- I^{B'}_{011100001} \right],$

$K_{45} = \epsilon^3 \ (1-w) \left[(1-w) \ \boldsymbol{D}^- I^{B'}_{101100101} + \boldsymbol{D}^- I^{B'}_{001100101} \right],$

$K_{46} = \epsilon^3 \ r_2 \left[\boldsymbol{D}^- I^{B'}_{(-1)11100101} + (1-w) \ \boldsymbol{D}^- I^{B'}_{011100101} \right],$

$K_{47} = \epsilon^3 \left[\boldsymbol{D}^- I^{B'}_{(-2)11100101} + 2\,(1-w) \ \boldsymbol{D}^- I^{B'}_{(-1)11100101} + (1-w)^2 \ \boldsymbol{D}^- I^{B'}_{011100101} \right],$

$K_{48} = \epsilon^3 \ (w-v) \left[\boldsymbol{D}^- I^{B'}_{0111(-1)0101} - 2\,\boldsymbol{D}^- I^{B'}_{011000101} \right],$

$K_{49} = \epsilon^3 \ r_2 \left[(1-w) \ \boldsymbol{D}^- I^{B'}_{101100011} + \boldsymbol{D}^- I^{B'}_{001100011} \right],$

$K_{50} = \epsilon^3 \ (1-w) \left[\boldsymbol{D}^- I^{B'}_{1(-1)1100011} + (1-w) \ \boldsymbol{D}^- I^{B'}_{101100011} \right],$

$K_{51} = \epsilon^3 \ (1-w) \left[\boldsymbol{D}^- I^{B'}_{101100(-1)11} + v \ \boldsymbol{D}^- I^{B'}_{101100011} \right],$

$K_{52} = \epsilon^3 \ r_3 \left[(1-w)^2 \ \boldsymbol{D}^- I^{B'}_{111100101} + 2\,(1-w) \ \boldsymbol{D}^- I^{B'}_{011100101} + \boldsymbol{D}^- I^{B'}_{(-1)11100101} \right],$

$K_{53} = \epsilon^3 \ r_3 \left[(1-w)^2 \ \boldsymbol{D}^- I^{B'}_{111100011} + (1-w) \left(\boldsymbol{D}^- I^{B'}_{011100011} + \boldsymbol{D}^- I^{B'}_{101100011} \right) + \boldsymbol{D}^- I^{B'}_{001100011} \right],$

$K_{54} = \epsilon^4 \ (1-2\epsilon) \ v \ I^{B'}_{101110021},$

$K_{55} = \epsilon^4 \ (1-2\epsilon) \ v \ I^{B'}_{112000111},$

$K_{56} = \epsilon^4 \ (1-2\epsilon) \ v \ I^{B'}_{012100111},$

$K_{57} = \epsilon^4 \ (1-2\epsilon) \ v \ I^{B'}_{011200111},$

$K_{58} = \epsilon^5 \ (1-2\epsilon) \ v \ I^{B'}_{111110011},$

$K_{59} = \epsilon^4 \ (1-2\epsilon) \ v \ I^{B'}_{112110011},$

$K_{60} = \epsilon^4 \ (1-2\epsilon) \ r_3 \left[w \ I^{B'}_{211110011} + I^{B'}_{112110011} - 2\epsilon \ I^{B'}_{111110011} \right],$

$K_{61} = \epsilon^4 \ (1-2\epsilon) \ vw \ I^{B'}_{112100111}. \tag{5.70}$

The master integrals for system 2b amount to

$L_1 = K_1 \ = \ \epsilon^3 \ (1-w) \ \boldsymbol{D}^- I^{B'}_{101010100},$

$L_2 = K_2 \ = \ \epsilon^3 \ \boldsymbol{D}^- I^{B'}_{101(-1)10100},$

$$L_3 = K_3 \ = \ \epsilon^3 \, r_2 \, \boldsymbol{D}^- I^{B'}_{011010100},$$

$$L_4 = K_4 \ = \ \epsilon^3 \left[\boldsymbol{D}^- I^{B'}_{(-1)11010100} + (1-w) \, \boldsymbol{D}^- I^{B'}_{011010100} \right],$$

$$L_5 = K_5 \ = \ \epsilon^3 \left[\boldsymbol{D}^- I^{B'}_{01101(-1)100} + v \, \boldsymbol{D}^- I^{B'}_{011010100} \right],$$

$$L_6 = K_6 \ = \ \epsilon^3 \left[\boldsymbol{D}^- I^{B'}_{0110101(-1)0} + v \, \boldsymbol{D}^- I^{B'}_{011010100} \right],$$

$$L_7 = K_7 \ = \ \epsilon^3 \, v \, \boldsymbol{D}^- I^{B'}_{100011100},$$

$$L_8 = K_8 \ = \ \epsilon^3 \, v \, \boldsymbol{D}^- I^{B'}_{001011100},$$

$$L_9 = K_9 \ = \ \epsilon^3 \, v \, \boldsymbol{D}^- I^{B'}_{101000110},$$

$$L_{10} = K_{13} \ = \ \epsilon^3 \, r_2 \, \boldsymbol{D}^- I^{B'}_{101(-1)11100},$$

$$L_{11} = K_{14} \ = \ \epsilon^3 \, (1-w) \left[\boldsymbol{D}^- I^{B'}_{101(-1)11100} + v \, \boldsymbol{D}^- I^{B'}_{101011100} \right],$$

$$L_{12} = K_{15} \ = \ \epsilon^3 \left[\boldsymbol{D}^- I^{B'}_{101(-2)11100} + v \, \boldsymbol{D}^- I^{B'}_{101(-1)11100} \right],$$

$$L_{13} = K_{16} \ = \ \epsilon^3 \, (1-w) \left[v \, \boldsymbol{D}^- I^{B'}_{011011100} + \boldsymbol{D}^- I^{B'}_{011010100} \right],$$

$$L_{14} = K_{18} \ = \ \epsilon^3 \, v \, (1-w) \, \boldsymbol{D}^- I^{B'}_{101100110},$$

$$L_{15} = K_{19} \ = \ \epsilon^3 \, v \, r_2 \, \boldsymbol{D}^- I^{B'}_{011100110},$$

$$L_{16} = K_{20} \ = \ \epsilon^3 \, v \left[\boldsymbol{D}^- I^{B'}_{(-1)11100110} + (1-w) \, \boldsymbol{D}^- I^{B'}_{011100110} \right],$$

$$L_{17} = K_{21} \ = \ \epsilon^3 \, v \, \boldsymbol{D}^- I^{B'}_{0111(-1)0110},$$

$$L_{18} = K_{22} \ = \ \epsilon^3 \, v^2 \, \boldsymbol{D}^- I^{B'}_{100101110},$$

$$L_{19} = K_{23} \ = \ \epsilon^3 \, v^2 \, \boldsymbol{D}^- I^{B'}_{001101110},$$

$$L_{20} = K_{33} \ = \ \epsilon^3 \, \boldsymbol{D}^- I^{B'}_{101000001},$$

$$L_{21} = K_{35} \ = \ \epsilon^3 \, (1-w) \, \boldsymbol{D}^- I^{B'}_{101100001},$$

$$L_{22} = K_{36} \ = \ \epsilon^3 \, r_2 \, \boldsymbol{D}^- I^{B'}_{011100001},$$

$$L_{23} = K_{37} \ = \ \epsilon^3 \left[\boldsymbol{D}^- I^{B'}_{(-1)11100001} + (1-w) \, \boldsymbol{D}^- I^{B'}_{011100001} \right],$$

$$L_{24} = K_{38} \ = \ \epsilon^3 \left[\boldsymbol{D}^- I^{B'}_{01110(-1)001} + v \, \boldsymbol{D}^- I^{B'}_{011100001} \right],$$

$$L_{25} = K_{39} \ = \ \epsilon^2 \, (1+4\epsilon) \, \boldsymbol{D}^- I^{B'}_{001100101},$$

$$L_{26} = K_{40} \ = \ \epsilon^3 \, r_1 \, \boldsymbol{D}^- I^{B'}_{001100011},$$

$$L_{27} = K_{41} \ = \ \epsilon^3 \left[\boldsymbol{D}^- I^{B'}_{(-1)01100011} + (1-w) \, \boldsymbol{D}^- I^{B'}_{001100011} \right],$$

$$L_{28} = K_{42} \ = \ \epsilon^3 \left[\boldsymbol{D}^- I^{B'}_{0011(-1)0011} + v \, \boldsymbol{D}^- I^{B'}_{001100011} \right],$$

$$L_{29} = K_{43} \ = \ \epsilon^3 \, v \, \boldsymbol{D}^- I^{B'}_{001000111},$$

$$L_{30} = K_{45} \ = \ \epsilon^3 \, (1-w) \left[(1-w) \, \boldsymbol{D}^- I^{B'}_{101100101} + \boldsymbol{D}^- I^{B'}_{001100101} \right],$$

$$L_{31} = K_{46} \ = \ \epsilon^3 \, r_2 \left[\boldsymbol{D}^- I^{B'}_{(-1)11100101} + (1-w) \, \boldsymbol{D}^- I^{B'}_{011100101} \right],$$

$$L_{32} = K_{47} \ = \ \epsilon^3 \left[\boldsymbol{D}^- I^{B'}_{(-2)11100101} + 2(1-w) \, \boldsymbol{D}^- I^{B'}_{(-1)11100101} + (1-w)^2 \, \boldsymbol{D}^- I^{B'}_{011100101} \right],$$

$$L_{33} = K_{48} = \epsilon^3 \ (w - v) \left[\boldsymbol{D}^- I^{B'}_{0111(-1)0101} - 2 \ \boldsymbol{D}^- I^{B'}_{011000101} \right],$$

$$L_{34} = K_{49} = \epsilon^3 \ r_2 \left[(1 - w) \ \boldsymbol{D}^- I^{B'}_{101100011} + \boldsymbol{D}^- I^{B'}_{001100011} \right],$$

$$L_{35} = K_{50} = \epsilon^3 \ (1 - w) \left[\boldsymbol{D}^- I^{B'}_{1(-1)1100011} + (1 - w) \ \boldsymbol{D}^- I^{B'}_{101100011} \right],$$

$$L_{36} = K_{51} = \epsilon^3 \ (1 - w) \left[\boldsymbol{D}^- I^{B'}_{101100(-1)11} + v \ \boldsymbol{D}^- I^{B'}_{101100011} \right],$$

$$L_{37} = K_{54} = \epsilon^4 \ (1 - 2\epsilon) \ v \ I^{B'}_{101110021},$$

$$L_{38} = K_{56} = \epsilon^4 \ (1 - 2\epsilon) \ v \ I^{B'}_{012100111},$$

$$L_{39} = K_{57} = \epsilon^4 \ (1 - 2\epsilon) \ v \ I^{B'}_{011200111},$$

$$L_{40} = \epsilon^3 \ r_4 \left[v \ \boldsymbol{D}^- I^{B'}_{0011(-1)1111} + 2 \ \boldsymbol{D}^- I^{B'}_{001100011} \right],$$

$$L_{41} = \epsilon^4 \ (1 - 2\epsilon) \ v \ I^{B'}_{002101111},$$

$$L_{42} = \epsilon^5 \ (1 - 2\epsilon) \ v \ I^{B'}_{101101111},$$

$$L_{43} = \epsilon^4 \ (1 - 2\epsilon) \ v \ (1 - w) \ I^{B'}_{102101111}. \tag{5.71}$$

5.5.1 Variable transformations

Multiple polylogarithms (section 3.5.2) are a well understood class of functions, hence, we want to be able to express our results in terms of them. The most efficient strategy is thereby generating a differential equation in ϵ-form free of square roots. We recall, that the master integrals given in the previous section depend on the following kinematic variables,

$$v = \frac{p^2}{m_t^2}, \quad w = \frac{m_W^2}{m_t^2}. \tag{5.72}$$

Unfortunately, this dependence is not free of square roots, we encounter

$$r_1 = \sqrt{-v \, (4 - v)},$$
$$r_2 = \sqrt{\lambda \, (v, w, 1)},$$
$$r_3 = \sqrt{-v \, (4w - v)},$$
$$r_4 = \sqrt{-v \, (-4 - v)}, \tag{5.73}$$

where λ is the Källen function defined by (5.65).

As stressed in the previous section, we are not able to rationalise all four square roots simultaneously. However, we are able to rationalise the sets of square-roots as demanded by each system,

$$\text{System 1 (5.66): } (r_1, r_2),$$
$$\text{System 2a (5.67): } (r_1, r_2, r_3),$$
$$\text{System 2b (5.68): } (r_1, r_2, r_4).$$

We start with the simultaneous rationalisation of r_1 and r_2. In section 3.6.2 we already derived a possible rationalisation for r_1 (3.96): The variable shift $v \to x$, where x is

defined by

$$v = \frac{-(1-x)^2}{x},$$

$$\Rightarrow x = \frac{1}{2}\left(2 - v - r_1\right), \tag{5.74}$$

leads to

$$r_1 = \sqrt{-v\left(4 - v\right)} \quad \overset{v=\frac{-(1-x)^2}{x}}{\Rightarrow} \quad r_1 = \frac{1 - x^2}{x}. \tag{5.75}$$

A variable shift $w \to y$ rationalising r_2 in addition was introduced in [94] based on the method of [78, 79], where

$$w = \frac{(1 - y + 2xy)\left(x - 2y + xy\right)}{x\left(1 - y^2\right)}, \tag{5.76}$$

$$\Rightarrow y = \frac{r_2 - r_1}{1 - w + 2v}, \tag{5.77}$$

$$\Rightarrow r_2 = \frac{(1 - x)\left[(1 - y)^2 + x\left(1 + y\right)^2\right]}{x\left(1 - y^2\right)}.$$

the variable transformation to x and y suffices to rationalise the square roots of all 105 master integrals $\vec{J}$ of the first system. We have to determine boundary values of the integrals to be able to solve their differential equations. As boundary point, we choose $(v, w) = (0, 1)$, corresponding in (x, y)-space to the line at $x = 1$. In conclusion, we can integrate the differential equation solely in x keeping a constant y. The integration paths of multiple polylogarithms (3.85) are defined to start at 0. This leads us to an additional change of variables $x \to x'$, where

$$x' = 1 - x. \tag{5.78}$$

This way, the boundary point corresponds to $x' = 0$ and integrations start at 0.

The algorithmic approach of [78] was sketched in section 3.6.2. We may use it as well to find a rationalisation for r_3 in addition to r_1, r_2, i.e. appropriate variables for system 2a. Of course we want to keep the rationalisations of r_1, r_2, hence, we insert x and y into r_3 and deal with the outcome,

$$r_3 = \sqrt{\frac{(1-x)^2}{x^2(1-y^2)}\left(x^2\left(7y^2 + 8y + 1\right) + x\left(2 - 18y^2\right) + 7y^2 - 8y + 1\right)}$$

$$= \frac{1 - x}{x}\sqrt{\frac{\left(x^2\left(7y^2 + 8y + 1\right) + x\left(2 - 18y^2\right) + 7y^2 - 8y + 1\right)}{(1 - y^2)}}.$$

We conclude we need to rationalise

$$\sqrt{\frac{\left(x^2\left(7y^2 + 8y + 1\right) + x\left(2 - 18y^2\right) + 7y^2 - 8y + 1\right)}{(1 - y^2)}} \equiv \sqrt{\frac{q_1}{q_2}}.$$

We follow the steps outlined in section 3.6.2 and start with the following definition,

$$f(r, x) = q_2 \cdot r^2 - q_1$$
$$= (1 - y^2)r^2 - \left(x^2 \left(7y^2 + 8y + 1\right) + x \left(2 - 18y^2\right) + 7y^2 - 8y + 1\right). \quad (5.79)$$

Setting $y = $ constant, we imply that we search for a variable transformation in x. The function f is of degree $d = 2$. Hence, we need to determine a point $p = (a_0, a_1)$ of multiplicity $2 - 1 = 1$. f must vanish at this point, but at least one partial derivative must stay non-zero. The polynomial q_1 simplifies drastically after inserting $x = 1$,

$$f(r, x = 1) = (1 - y^2)r^2 - 4(1 - y^2).$$

A possible candidate for p becomes immediately apparent,

$$f(r = 2, x = 1) = (1 - y^2)4 - 4(1 - y^2) = 0,$$
$$\frac{\partial f}{\partial x}(r = 2, x = 1) = 4\left(y^2 - 4y - 1\right) \neq 0$$
$$\Rightarrow p = (2, 1).$$

The next step demands us to collect the terms of common degree within $f(r + a_0, x + a_1)$, to find two polynomials $g_d(r, x), g_{d-1}(r, x)$,

$$f(r + 2, x + 1) = (r + 2)^2 \left(1 - y^2\right) - (x + 1)\left(2 - 18y^2\right)$$
$$- (x + 1)^2 \left(7y^2 + 8y + 1\right) - 7y^2 + 8y - 1$$
$$= \underbrace{r^2 \left(1 - y^2\right) + x^2 \left(-7y^2 - 8y - 1\right)}_{= g_2(r,x)} \underbrace{-4r \left(y^2 - 1\right) + x \left(4y^2 - 16y - 4\right)}_{= g_1(r,x)}.$$

Now, the resulting variable transformation $x \to \hat{x}$ is found as stated in (3.95),

$$x = -\hat{x}\frac{g_1(1, \hat{x})}{g_2(1, \hat{x})} + a_1$$
$$= -\frac{\hat{x}\left(-\hat{x}\left(-4y^2 + 16y + 4\right) - 4\left(y^2 - 1\right)\right)}{-\hat{x}\left(7\hat{x}y^2 + 8\hat{x}y + \hat{x}\right) - y^2 + 1} + 1$$
$$= \frac{(y - 1)\left(\hat{x}^2(11y + 3) - 4\hat{x}(y + 1) + y + 1\right)}{(y + 1)\left(\hat{x}^2(7y + 1) + y - 1\right)}$$
$$\Leftrightarrow \hat{x} = \frac{\left(1 - y^2\right)}{(1 - x)}\frac{(2(1 - x) - xr_3)}{(3 + x + 8y - 11y^2 + 8xy + 7xy^2)}. \quad (5.80)$$

The variables $\hat{x}, y$ rationalise r_1, r_2 and r_3 simultaneously,

$$r_1 = \frac{8\hat{x}\left(\hat{x}\left(y^2 - 4y - 1\right) - y^2 + 1\right)\left(\hat{x}^2\left(9y^2 - 1\right) - 2\hat{x}\left(y^2 - 1\right) + y^2 - 1\right)}{(1 - y^2)\left(\hat{x}^2(7y + 1) + y - 1\right)\left(\hat{x}^2(11y + 3) - 4\hat{x}(y + 1) + y + 1\right)},$$
$$r_2 = \frac{8\hat{x}\left(\hat{x}\left(y^2 - 4y - 1\right) - y^2 + 1\right)\left(\hat{x}^2\left(9y^2 + 4y + 1\right) - 2\hat{x}(y + 1)^2 + y^2 + 1\right)}{(1 - y^2)\left(-\left(\hat{x}^2(7y + 1)\right) - y + 1\right)\left(\hat{x}^2(11y + 3) - 4\hat{x}(y + 1) + y + 1\right)},$$
$$r_3 = \frac{8\hat{x}\left[1 - y^2 - \left(1 + 4y - y^2\right)\hat{x}\right]\left[1 - y^2 - 2\left(1 + 4y - y^2\right)\hat{x} + (1 + y)(1 + 7y)\hat{x}^2\right]}{(1 - y^2)\left[1 - y - (1 + 7y)\hat{x}^2\right]\left[(1 + y)(1 - 4\hat{x}) + (3 + 11y)\hat{x}^2\right]}.$$

Fortunately, the boundary point $x = 1$ corresponds to $\hat{x} = 0$.

The remaining set of square roots is (r_1, r_2, r_4). To rationalise simultaneously r_1 and r_4, we take the variable $\tilde{x}$, where

$$
x = \tilde{x}\frac{(1 - \tilde{x})}{(1 + \tilde{x})},
$$

$$
\tilde{x} = \frac{1}{2}\left(1 - x - \sqrt{x^2 - 6x + 1}\right), \tag{5.81}
$$

which already appeared in [95]. The roots evaluate to

$$
r_1 = \frac{\left(-\tilde{x}^2 + 2\tilde{x} + 1\right)\left(\tilde{x}^2 + 1\right)}{\tilde{x}\left(1 - \tilde{x}^2\right)},
$$

$$
r_2 = \frac{\left(\tilde{x}^2 + 1\right)\left(\tilde{x}^2\left(-y^2\right) - 2\tilde{x}^2 y - \tilde{x}^2 + 2\tilde{x}y^2 + 2\tilde{x} + y^2 - 2y + 1\right)}{\tilde{x}\left(1 - \tilde{x}^2\right)\left(1 - y^2\right)},
$$

$$
r_4 = \frac{\left(1 + \tilde{x}^2\right)\left(1 - 2\tilde{x} - \tilde{x}^2\right)}{\tilde{x}\left(1 - \tilde{x}^2\right)}.
$$

The value $x = 1 + i\delta$, where δ is infinitesimal small positive number, corresponds to $\tilde{x} = i$. Setting

$$
\tilde{x}' = i - \tilde{x}, \tag{5.82}
$$

the value $x = 1 + i\delta$ corresponds to $\tilde{x}' = 0$.

In summary, we found appropriate variable transformations for all three systems,

$$
\begin{aligned}
&\text{System 1 (5.66): } (x\ (5.74), y\ (5.77))\,, \\
&\text{System 2a (5.67): } (\hat{x}\ (5.80), y\ (5.77))\,, \\
&\text{System 2b (5.68): } (\tilde{x}\ (5.81), y\ (5.77))\,.
\end{aligned}
$$

Now we are able to express the differential equations in terms of dlog-forms containing only rational square roots.

5.5.2 Differential one-forms

The differential equations of all three systems (5.66), (5.67), (5.68) are linear in ϵ. They can be written in terms of dlog-forms ω_i (see section 3.5.1). In the former section, we found variable transformations for all systems. Hence, the dlog-forms contain rational arguments. The definition of three systems solely served this purpose. Systems still share subsets of integrals and, consequently, also dlog-forms. In this section we, therefore, present a complete list of all sufficient dlog-forms as functions of v, w (5.72). Note, however, that behind the scenes calculations may be carried out in terms of $x, \hat{x}, \tilde{x}, y$ (5.74),(5.80),(5.81),(5.77).

We start with a small example demonstrating dependencies on dlog-forms. In section

5.4.3, we determined the differential equation of J_1 (5.40) and J_2 (5.44). We see, that the first entries of $\tilde{A}$ (5.66) can be written as

$$\epsilon \tilde{A}_{(1,1)} = -\frac{\epsilon}{w} dw = -\epsilon \, d\log\left(w\right),$$

$$\epsilon \tilde{A}_{(2,1)} = \frac{2\epsilon}{r_1} dv = \epsilon \, \frac{2x}{1-x^2} \frac{\partial v}{\partial x} dx = \epsilon \, \frac{2x}{1-x^2} \left(-\frac{1-x^2}{x^2}\right) dx = \epsilon \, \frac{-2}{x} dx$$

$$= -\epsilon \, d\log\left(x^2\right) = -\epsilon \, d\log\left(\frac{2-v-r_1}{2-v+r_1}\right),$$

$$\epsilon \tilde{A}_{(2,2)} = \frac{\epsilon}{4-v} dv - \frac{\epsilon}{w} dw = -\epsilon \, d\log\left(w\right) - \epsilon \, d\log\left(4-v\right). \tag{5.83}$$

In practice, dlog-forms ω_k and coefficient matrices can be found, for example, with the help of `FiniteFlow` [96, 97]. An (oversized) set of possible dlog-forms is determined by the arguments of logarithmic functions emerging through naive integration of $\tilde{A}$ with respect to either v or w. A subsequent linear fit fixes a sufficient set of ω's and coefficient matrices. The first system (5.66) amounts to

$$\tilde{A} = \sum_{k=1}^{19} M_k \omega_k$$

$$= \begin{pmatrix} -\omega_1 & 0 & 0 & 0 & 0 & 0 & \cdots \\ -\omega_{13} & -\omega_1 - \omega_5 & 0 & 0 & 0 & 0 \\ \omega_{13} & 0 & -\omega_1 - \omega_3 - 3\omega_5 & -3\omega_{13} & 0 & 0 \\ 0 & 0 & \frac{\omega_{13}}{2} & \omega_3 - \omega_1 & 0 & 0 \\ 0 & 0 & 0 & 0 & 2\left(\omega_1 - 2\omega_2\right) & -3\omega_1 \\ 0 & 0 & 0 & 0 & 2\left(\omega_1 - \omega_2\right) & -3\omega_1 \\ & & & & & & \\ \cdots & & & & & \end{pmatrix},$$

$$\tag{5.84}$$

where coefficient matrices M_k are 105×105-dimensional, with rational numbers as entries. The complete matrix $\epsilon \sum_{k=1}^{19} M_k \omega_k$ is attached to the arXiv version of [1] under the name A. The 19 sufficient differential one-forms ω_k are given by

$$\omega_1 = d\log\left(w\right),$$
$$\omega_2 = d\log\left(1-w\right),$$
$$\omega_3 = d\log\left(-v\right),$$
$$\omega_4 = d\log\left(1-v\right),$$
$$\omega_5 = d\log\left(4-v\right),$$
$$\omega_6 = d\log\left(w-v\right),$$
$$\omega_7 = d\log\left(1-w-v\right),$$
$$\omega_8 = d\log\left(1-w+v\right),$$
$$\omega_9 = d\log\left(w^2 + v\left(1-w\right)\right),$$
$$\omega_{10} = d\log\left(\left(1-w\right)^2 + vw\right),$$

$$\omega_{11} = d\log\left((1-w)^2 + v(2-w)\right),$$

$$\omega_{12} = d\log\left(\lambda(v,w,1)\right),$$

$$\omega_{13} = d\log\left(\frac{2-v-r_1}{2-v+r_1}\right),$$

$$\omega_{14} = d\log\left(\frac{2w + v(1-w) - (1-w)r_1}{2w + v(1-w) + (1-w)r_1}\right),$$

$$\omega_{15} = d\log\left(\frac{2(1-w) + vw - wr_1}{2(1-w) + vw + wr_1}\right),$$

$$\omega_{16} = d\log\left(\frac{wv^2 + (1-2w-w^2)v + 2(1-w)^2 - (1-w^2+vw)r_1}{wv^2 + (1-2w-w^2)v + 2(1-w)^2 + (1-w^2+vw)r_1}\right),$$

$$\omega_{17} = d\log\left(\frac{1+w-v-r_2}{1+w-v+r_2}\right),$$

$$\omega_{18} = d\log\left(\frac{(1-w)^2 - v(1+w) - (1-w)r_2}{(1-w)^2 - v(1+w) + (1-w)r_2}\right),$$

$$\omega_{19} = d\log\left(\frac{-v(3-v+w) - r_1 r_2}{-v(3-v+w) + r_1 r_2}\right). \tag{5.85}$$

The variable transformation to x, y (5.74),(5.77) yields rational functions within all dlog-forms

$$\omega_i = d\log(f_i),$$

where f_i are compositions of polynomials

$$
\begin{aligned}
&f_1 = -p_1^{-1}p_5^{-1}p_6^{-1}p_8 p_9, &&f_2 = 2p_1^{-1}p_2 p_4 p_5^{-1}p_6^{-1}p_7, &&f_3 = p_1^{-1}p_2^2, \\
&f_4 = p_1^{-1}p_{17}, &&f_5 = p_1^{-1}p_3^2, &&f_6 = -p_1^{-1}p_5^{-1}p_6^{-1}p_{18}, \\
&f_7 = p_1^{-1}p_2 p_5^{-1}p_6^{-1}p_{16}, &&f_8 = p_1^{-1}p_2 p_5^{-1}p_6^{-1}p_{12}, &&f_9 = p_1^{-2}p_5^{-2}p_6^{-2}p_{19}p_{20}, \\
&f_{10} = p_1^{-2}p_2^2 p_5^{-2}p_6^{-2}p_{14}p_{15}, &&f_{11} = p_1^{-2}p_2^2 p_5^{-2}p_6^{-2}p_{10}p_{13}, &&f_{12} = p_1^{-2}p_2^2 p_5^{-2}p_6^{-2}p_{11}^2, \\
&f_{13} = p_1^2, &&f_{14} = p_1^{-2}p_{19}p_{20}^{-1}, &&f_{15} = p_1^{-2}p_{14}^{-1}p_{15}, \\
&f_{16} = p_1^{-2}p_{10}^{-1}p_{13}p_{14}^{-1}p_{15}, &&f_{17} = -p_1 p_5^{-1}p_6 p_8 p_9^{-1}, &&f_{18} = -p_1^{-1}p_5^3 p_6^{-3}p_8 p_9^{-1}, \\
&f_{19} = -4p_1 p_4^2 p_7^{-2}. &&&& \tag{5.86}
\end{aligned}
$$

The set of polynomials rational in x and y is given by

$$
\begin{aligned}
p_1 &= x, \\
p_2 &= x - 1, \\
p_3 &= x + 1, \\
p_4 &= y, \\
p_5 &= y - 1, \\
p_6 &= y + 1, \\
p_7 &= xy + x - y + 1, \\
p_8 &= xy + x - 2y,
\end{aligned}
$$

$$p_9 = 2xy - y + 1,$$
$$p_{10} = xy^2 + 2xy - 2y^2 + x + 2y,$$
$$p_{11} = xy^2 + 2xy + y^2 + x - 2y + 1,$$
$$p_{12} = xy^2 + 2xy - y^2 + x + 2y - 1,$$
$$p_{13} = 2xy^2 + 2xy - y^2 + 2y - 1,$$
$$p_{14} = 2xy^2 + 2xy - 3y^2 + 2y + 1,$$
$$p_{15} = 3xy^2 + 2xy - 2y^2 - x + 2y,$$
$$p_{16} = 3xy^2 + 2xy - 3y^2 - x + 2y + 1,$$
$$p_{17} = x^2 - x + 1,$$
$$p_{18} = x^2y^2 + 2x^2y - 3xy^2 + x^2 + y^2 - x - 2y + 1,$$
$$p_{19} = x^2y^2 + 2x^2y - 4xy^2 + x^2 + 2y^2 - 2y,$$
$$p_{20} = 2x^2y^2 + 2x^2y - 4xy^2 + y^2 - 2y + 1. \tag{5.87}$$

The polynomials linear in x, p_1-p_{16}, appeared already in the two-loop mixed QCD-electroweak corrections to $H \to b\bar{b}$ through a $Ht\bar{t}$-coupling [94]. Four polynomials, p_{17}-p_{20}, are quadratic in x.

System 2a (5.67) and system 2b (5.68) require additional differential one-forms (5.90), however not all dlog-forms of (5.85) occur. The lists of sufficient dlog-forms are

$$K : \{\omega_1, \omega_2, \omega_3, \omega_5, \omega_6, \omega_8, \omega_{12}, \omega_{13}, \omega_{17}, \omega_{18}, \omega_{19}, \omega_{20}, \omega_{21}, \omega_{22}, \omega_{23}, \omega_{24}\},$$
$$L : \{\omega_1, \omega_2, \omega_3, \omega_5, \omega_6, \omega_8, \omega_{12}, \omega_{13}, \omega_{17}, \omega_{18}, \omega_{19}, \omega_{25}, \omega_{26}, \omega_{27}, \omega_{28}\}.$$

In correspondence, the differential equations amount to

$$\tilde{B} = \sum_{k=1}^{28} M'_k \omega_k, \tag{5.88}$$

$$\tilde{C} = \sum_{k=1}^{28} M''_k \omega_k, \tag{5.89}$$

where M'_k are rational 61×61-matrices and M''_k rational 43×43-matrices. The complete matrices $\epsilon \sum_{k=1}^{19} M'_k \omega_k$ and $\epsilon \sum_{k=1}^{19} M''_k \omega_k$ are attached to the arXiv version of [1] under the name B and C. The additional differential one-forms are given by

$$\omega_{20} = d\log\left(4w - v\right),$$
$$\omega_{21} = d\log\left((1 - w)^2 + v\right),$$
$$\omega_{22} = d\log\left(\frac{2w - v - r_3}{2w - v + r_3}\right),$$
$$\omega_{23} = d\log\left(\frac{2w(1 - w) - v - r_3}{2w(1 - w) - v + r_3}\right),$$
$$\omega_{24} = d\log\left(\frac{-v(1 - v + 3w) - r_2 r_3}{-v(1 - v + 3w) + r_2 r_3}\right),$$

$$\omega_{25} = d\log\left(4 + v\right),$$

$$\omega_{26} = d\log\left((1 - w)^2 - vw\right),$$

$$\omega_{27} = d\log\left(\frac{2 + v - r_4}{2 + v + r_4}\right),$$

$$\omega_{28} = d\log\left(\frac{-v\left(1 + w\right) - \left(1 - w\right)r_4}{-v\left(1 + w\right) + \left(1 - w\right)r_4}\right). \tag{5.90}$$

Under the variable change of system 2a to $\hat{x}, y$ (5.80),(5.77) the differential one-forms become

$$d\ln\left(\hat{p}_1(\hat{x}, y)\right), \ldots, d\ln\left(\hat{p}_{20}(\hat{x}, y)\right).$$

We note that the dlog-form $\omega_6 = d\ln(w - v)$ leads to a quartic polynomial in $\hat{x}$,

$$\begin{aligned}
\hat{p}_{20} = {}& 1 - 4\,\hat{x} - 2\,y^2 - 16\,y\hat{x} + 18\,\hat{x}^2 + 8\,y^2\hat{x} + 48\,\hat{x}^2 y - 28\,\hat{x}^3 + y^4 + 16\,y^3\hat{x} + 44\,\hat{x}^2 y^2 \\
& - 144\,\hat{x}^3 y + 13\,\hat{x}^4 - 4\,y^4\hat{x} - 48\,\hat{x}^2 y^3 - 104\,y^2\hat{x}^3 + 112\,\hat{x}^4 y + 2\,y^4\hat{x}^2 + 16\,y^3\hat{x}^3 \\
& + 246\,\hat{x}^4 y^2 + 4\,y^4\hat{x}^3 + 16\,y^3\hat{x}^4 + 61\,y^4\hat{x}^4.
\end{aligned}$$

The remaining polynomials are at most quadratic in $\hat{x}$. $\hat{p}_{20}$ yields roots of a quartic polynomial within the arguments of multiple polylogarithms if the differential equation is integrated along $\hat{x}$ for generic and constant y.

Accordingly, the variable change of system 2b to $\tilde{x}, y$ (5.81),(5.77) leads to

$$d\ln\left(\tilde{p}_1\right), \ldots, d\ln\left(\tilde{p}_{17}\right).$$

Again the dlog-form $\omega_6 = d\ln(w - v)$ leads to a quartic polynomial,

$$\begin{aligned}
\tilde{p}_{17} = {}& 1 - 2\,y + \tilde{x} + y^2 - 4\,y\tilde{x} + 2\,\tilde{x}^2 - y^2\tilde{x} - \tilde{x}^3 + 2\,y^2\tilde{x}^2 - 4\,\tilde{x}^3 y + \tilde{x}^4 + \tilde{x}^3 y^2 \\
& + 2\,\tilde{x}^4 y + \tilde{x}^4 y^2.
\end{aligned}$$

$\tilde{p}_1$-$\tilde{p}_{16}$ are at most quadratic in $\tilde{x}$. Furthermore, all polynomials are quadratic in y.

The set of all sufficient dlog-forms and coefficient matrices specifies in combination with boundary values the resulting integrals. Appropriate boundary values will be determined in the next section.

5.5.3 Boundary values

Each master integral is a Laurent series in the dimensional regularisation parameter. In sections 3.5.1 and 3.5.2 we sketched the iterative construction of solutions to master integrals in orders of ϵ. All constants emerging in the solution of master integrals are thereby set with the help of boundary values. A boundary value corresponds to the value of an integral at the boundary point. As already mentioned, we take

$$s = 0,\ m_W^2 = m_t^2$$

$$\Leftrightarrow v = 0, \quad w = 1,$$

as boundary point. Integrals without singularities at $v = 0$ vanish at the boundary point if their prefactor evaluates to zero. J_2 or J_5 (5.69), for example, vanish, since r_1 and $(1 - w)$ become zero at $v = 0, w = 1$. This explains our choice for the boundary point, most master integrals vanish. In this section we find the remaining non-trivial boundary values. In (x, y)-space, the boundary point translates to the line $x = 1$, as discussed in section 5.5.1.

We start with a dedicated integral reduction at $s = 0$, $m_W^2 = m_t^2$ reducing the number of integrals we have to compute. To give an example, we look at the following integrals

$$J_6 = \epsilon^3 \, \boldsymbol{D}^- I^A_{101(-1)10100},$$

$$J_8 = \epsilon^3 \left[\boldsymbol{D}^- I^A_{011(-1)10100} - (1 - w) \, \boldsymbol{D}^- I^A_{011010100} \right] \overset{w=1}{=} \epsilon^3 \, \boldsymbol{D}^- I^A_{011(-1)10100},$$

$$J_9 = \epsilon^3 \, \boldsymbol{D}^- I^A_{01101(-1)100},$$

$$J_{29} = \epsilon^3 \left[\boldsymbol{D}^- I^A_{101(-2)11100} - (1 - w) \, \boldsymbol{D}^- I^A_{101(-1)11100} \right] \overset{w=1}{=} \epsilon^3 \, \boldsymbol{D}^- I^A_{101(-2)11100}.$$

From the definitions of the propagators (table 5.1), we deduce that these integrals must evaluate to the same integral at $s = 0$, $m_W^2 = m_t^2$. The integral reduction reveals indeed

$$J_6|_{x=1} = J_8|_{x=1} = J_9|_{x=1} = J_{29}|_{x=1} = \epsilon^3 \frac{2 - 15\epsilon + 40\epsilon^2 - 45\epsilon^3 + 18\epsilon^4}{2 - 8\epsilon} I^A_{101010100}.$$

Furthermore, we may derive relations from the coefficient matrices accompanying

$$\omega_2 = d\log(1 - w) = \frac{-dw}{(1 - w)},$$

for example for system 2a (5.88),

$$d\vec{K} = \left(M'_2 \omega_2 \right) \vec{K} + \left(\sum_{\substack{k=1 \\ k \neq 2}}^{28} M'_k \omega_k \right) \vec{K},$$

the master integrals should have no logarithmic singularity at $w = 1$. From this condition, we deduce

$$M'_2 . \vec{K} = \begin{pmatrix} -4K_1 \\ 0 \\ \dots \\ 0 \\ 4K_{11} - 4K_{10} \\ 0 \\ 0 \\ 0 \\ 2K_1 - 2K_{14} \\ 0 \\ 6K_4 + 6K_6 + 2K_7 - 2K_8 - 2K_{16} \\ 0 \\ -2K_{18} \\ \dots \end{pmatrix} \overset{!}{=} \vec{0}.$$

We find an even stronger statement considering the behaviour of complete systems of differential equations at $x = 1$. Master integrals $\vec{J}$ must be constant at the boundary point,

$$\vec{J}\Big|_{x=1} = \text{constant}$$

$$\Rightarrow d\left(\vec{J}\Big|_{x=1}\right) = \vec{0},$$

implying that $\vec{J}$ is in the kernel of $\tilde{A}$ at $x = 1$,

$$\overset{d\vec{J}=\tilde{A}\vec{J}}{\Rightarrow} \tilde{A}\left(\vec{J}\Big|_{x=1}\right) = \vec{0}. \tag{5.91}$$

We derive additional relations thereof and confirm the disappearance of certain integrals.

Finally, a few integrals have to be computed explicitly, J_1 for example. In section 5.4.3, we determined

$$J_1 = \epsilon^3 \, \boldsymbol{D}^- I^A_{100110000} = \epsilon^3 T_1 \left(2 - 2\epsilon\right)^2 T_1 \left(2 - 2\epsilon, w\right)$$

to be the product of three tadpoles and, therefore, constant. Consequently, the first boundary value is given by the product of two tadpoles with mass m_t^2 (5.38) and one tadpole with mass m_W^2 (5.39),

$$\epsilon T_1 \left(2 - 2\epsilon\right) = e^{\epsilon \gamma_E} \Gamma(1 + \epsilon),$$
$$\epsilon T_1 \left(2 - 2\epsilon, w\right) = e^{\epsilon \gamma_E} w^{-\epsilon} \Gamma(1 + \epsilon),$$
$$\Rightarrow J_1 = C_1 w^{-\epsilon},$$
$$C_1 = e^{3\gamma_E \epsilon} \left(\Gamma(1 + \epsilon)\right)^3. \tag{5.92}$$

The next non-vanishing boundary value corresponds to

$$J_{15} = \epsilon^3 \, v \, \boldsymbol{D}^- I^A_{100100110},$$

which consists of two massive tadpoles and a massless bubble. A general formula for the massless bubble was derived in (3.39). In $D = (2 - 2\epsilon)$ dimensions, it translates to

$$B_{11}(2 - 2\epsilon; p^2, 0, 0) = (-v)^{-1-\epsilon} \frac{e^{\epsilon \gamma_E} \Gamma\left(1 + \epsilon\right) \Gamma\left(-\epsilon\right) \Gamma\left(-\epsilon\right)}{\Gamma\left(-2\epsilon\right)}. \tag{5.93}$$

In the end of section 5.4.3 (see (5.42)), we determined that a massless bubble integral in two dimensions requires a prefactor (ϵv) to be of uniform weight,

$$\epsilon \, v \, B_{11}(2 - 2\epsilon; p^2, 0, 0) = -(-v)^{-\epsilon} \frac{-2e^{\epsilon \gamma_E} \Gamma\left(1 + \epsilon\right) \left(\epsilon^2 \Gamma\left(-\epsilon\right)^2\right)}{-2\epsilon \Gamma\left(-2\epsilon\right)}$$

$$= (-v)^{-\epsilon} \frac{2e^{\epsilon \gamma_E} \Gamma\left(1 + \epsilon\right) \left(\Gamma\left(1 - \epsilon\right)\right)^2}{\Gamma\left(1 - 2\epsilon\right)},$$

implying for J_{15},

$$J_{15} = \epsilon^3 \, v \, \boldsymbol{D}^- I^A_{100100110} = \epsilon^2 \, T_1 \, (2 - 2\epsilon)^2 \, \epsilon \, v \, B_{11}(2 - 2\epsilon; p^2, 0, 0),$$
$$\Rightarrow J_{15} = (-v)^{-\epsilon} \, C_{15},$$
$$C_{15} = 2e^{3\epsilon\gamma_E} \frac{\Gamma(1 + \epsilon)^3 \Gamma(1 - \epsilon)^2}{\Gamma(1 - 2\epsilon)}. \tag{5.94}$$

J_{15} has a logarithmic singularity at $v = 0$. The same holds for J_{51} and J_{60}.

The list of non-zero boundary values from system 1 is

$$J_1 = C_1 w^{-\epsilon}, \, J_{15} = C_{15} \, (-v)^{-\epsilon}, \, J_{51} = C_{51} \, (-v)^{-2\epsilon} \, w^{-\epsilon},$$
$$J_{60} = C_{60} \, (-v)^{-2\epsilon}, \, J_{71} = C_{71}, \tag{5.95}$$

with

$$C_1 = e^{3\gamma_E\epsilon} \left(\Gamma(1 + \epsilon)\right)^3,$$
$$C_{15} = 2e^{3\gamma_E\epsilon} \frac{\left(\Gamma(1 + \epsilon)\right)^3 \left(\Gamma(1 - \epsilon)\right)^2}{\Gamma(1 - 2\epsilon)},$$
$$C_{51} = -3e^{3\gamma_E\epsilon} \frac{\Gamma(1 + \epsilon) \left(\Gamma(1 - \epsilon)\right)^3 \Gamma(1 + 2\epsilon)}{\Gamma(1 - 3\epsilon)},$$
$$C_{60} = 4e^{3\gamma_E\epsilon} \frac{\left(\Gamma(1 + \epsilon)\right)^3 \left(\Gamma(1 - \epsilon)\right)^4}{\Gamma(1 - 2\epsilon)^2},$$
$$C_{71} = e^{3\gamma_E\epsilon} \frac{\Gamma(1 - \epsilon) \Gamma(1 + \epsilon) \Gamma(1 + 2\epsilon)^2 \Gamma(1 + 3\epsilon)}{\Gamma(1 + 4\epsilon)}. \tag{5.96}$$

The remaining non-zero boundary values are given by

$$
\begin{aligned}
J_{14}|_{x=1} &= J_1|_{x=1}, \\
J_{16}|_{x=1} &= J_{59}|_{x=1} = J_{15}|_{x=1}, \\
J_{52}|_{x=1} &= J_{51}|_{x=1}, \\
J_{61}|_{x=1} &= J_{60}|_{x=1}, \\
J_6|_{x=1} &= J_8|_{x=1} = J_9|_{x=1} = J_{29}|_{x=1} = J_{70}|_{x=1} = J_{77}|_{x=1} = \frac{1}{3} J_{71}|_{x=1}, \\
J_{56}|_{x=1} &= -\frac{2}{3} J_{71}|_{x=1}, \\
J_{30}|_{x=1} &= -\frac{1}{2} J_1|_{x=1} + \frac{1}{2} J_{71}|_{x=1}, \\
J_{78}|_{x=1} &= \frac{1}{2} J_1|_{x=1} - \frac{1}{2} J_{71}|_{x=1}, \\
J_{87}|_{x=1} &= -\frac{1}{4} J_1|_{x=1} + \frac{1}{4} J_{71}|_{x=1}.
\end{aligned}
$$

The boundary values of system 2a and system 2b are related to those from system 1 as follows,

$$K_{33}|_{x=1} = K_{38}|_{x=1} = J_1|_{x=1},$$

$$
\begin{aligned}
K_9|_{x=1} &= K_{21}|_{x=1} = K_{43}|_{x=1} = J_{15}|_{x=1}, \\
K_7|_{x=1} &= K_8|_{x=1} = J_{51}|_{x=1}, \\
K_{22}|_{x=1} &= K_{23}|_{x=1} = J_{60}|_{x=1}, \\
K_{39}|_{x=1} &= J_{71}|_{x=1}, \\
K_{41}|_{x=1} &= K_{47}|_{x=1} = \frac{1}{3} J_{71}|_{x=1}, \\
K_2|_{x=1} &= K_5|_{x=1} = K_{15}|_{x=1} = K_{42}|_{x=1} = -\frac{2}{3} J_{71}|_{x=1}, \\
K_{48}|_{x=1} &= \frac{1}{2} J_1|_{x=1} - \frac{1}{2} J_{71}|_{x=1}, \\
L_{20}|_{x=1} &= L_{24}|_{x=1} = J_1|_{x=1}, \\
L_9|_{x=1} &= L_{17}|_{x=1} = L_{29}|_{x=1} = J_{15}|_{x=1}, \\
L_7|_{x=1} &= L_8|_{x=1} = J_{51}|_{x=1}, \\
L_{18}|_{x=1} &= L_{19}|_{x=1} = J_{60}|_{x=1}, \\
L_{25}|_{x=1} &= J_{71}|_{x=1}, \\
L_{27}|_{x=1} &= L_{32}|_{x=1} = \frac{1}{3} J_{71}|_{x=1}, \\
L_2|_{x=1} &= L_5|_{x=1} = L_{12}|_{x=1} = L_{28}|_{x=1} = \frac{-2}{3} J_{71}|_{x=1}, \\
L_{33}|_{x=1} &= \frac{1}{2} J_1|_{x=1} - \frac{1}{2} J_{71}|_{x=1}.
\end{aligned}
$$

We found boundary values for all master integrals. The boundary values along with the dlog-forms defined in (5.85), (5.90) and corresponding coefficient matrices (5.84), (5.88), (5.89) comprise all information about the three systems.

5.5.4 Results

We transformed the pre-canonical bases of master integrals obtained in section 5.3 to a canonical basis given in section 5.5 via methods discussed in section 5.4. In section 5.5.1 we rationalised all square roots. Hence, we were able to express the systems of differential equations through dlog-forms containing rational functions (5.85), (5.90) in section 5.5.2. In the preceding section we finalised our work with the calculation of boundary values of the master integrals at $v = 0$, $w = 1$ (5.96). All ingredients needed to express results in terms of multiple polylogarithms are available. Hence, they are presented in this section.

A differential equation in ϵ-form is solved order by order in the dimensional regularisation parameter, as described in section 3.5.1. Hence, each order in ϵ arises from its lower order, as derived in (3.77),

$$
\begin{aligned}
d\vec{J}^{(0)} &= 0, \\
d\vec{J}^{(q+1)} &= \sum_i C_i \omega_i \, \vec{J}^{(q)}.
\end{aligned}
\tag{5.97}
$$

In section 3.5.2, we explained how solutions in terms of multiple polylogarithms are constructed. Here, we give another example. We consider again

$$J_1 = \epsilon^3 \, \boldsymbol{D}^- I^A_{100110000}.$$

We expressed the differential equation of J_1 through a dlog-form in (5.83),

$$dJ_1 = -\frac{\epsilon}{w} dw J_1 = -\epsilon \, d\log(w) \, J_1 = -\epsilon \, \omega_1 J_1, \tag{5.98}$$

and determined its boundary value in (5.92),

$$J_1 = w^{-\epsilon} e^{3\gamma_E \epsilon} \left(\Gamma(1+\epsilon)\right)^3 = 1 - \epsilon \log(w) + \epsilon^2 \frac{1}{4} \left(\pi^2 + 2\log(w)^2\right) + \mathcal{O}\!\left(\epsilon^3\right),$$

$$\Rightarrow J_1|_{w=1} = 1 + \epsilon^2 \frac{1}{4}\pi^2 + \mathcal{O}\!\left(\epsilon^3\right). \tag{5.99}$$

From (5.97) and (5.98) follows

$$dJ_1^{(0)} = 0, \tag{5.100}$$

$$dJ_1^{(q+1)} = -\omega_1 \, J_1^{(q)}. \tag{5.101}$$

The boundary value of J_1 at order ϵ^0 is 1 (5.99), yielding immediately

$$\stackrel{(5.99),(5.100)}{\Rightarrow} J_1^{(0)} = 1.$$

The differential equation of the first order in ϵ becomes

$$dJ_1^{(1)} = -d\log(w), \tag{5.102}$$

in (v, w)-space. The appearing square roots (5.73) force us to move to (x, y)-space. The boundary point in (x, y)-space corresponds to the line at $x = 1$. In conclusion, we can integrate the differential equation solely in x in (x, y)-space. We recall from section 3.5.2, that the integration paths of multiple polylogarithms (3.85) are defined to start at 0. As we want to obtain multiple polylogarithms we need to shift the lower integration boundary from 1 to 0. This leads us to an additional change of variables $x \to x'$, where

$$x = 1 - x'. \tag{5.103}$$

The boundary point corresponds to $x' = 0$. Equation (5.102) transforms as follows,

$$dJ_1^{(1)} = -d\log(w)$$

$$= -\frac{\partial w}{\partial x}\frac{\partial x}{\partial x'}\frac{1}{w}dx',$$

where w is given by (5.76) and x by (5.103). After performing partial fraction decomposition, we obtain

$$dJ_1^{(1)} = - \left(\frac{2y}{2x'y - y - 1} + \frac{y+1}{x'(y+1)+y-1} - \frac{1}{x'-1} \right) dx'$$

$$= - \left(\frac{1}{x' - \frac{1+y}{2y}} + \frac{1}{x' - \frac{1-y}{1+y}} - \frac{1}{x'-1} \right) dx',$$

and $J_1^{(1)}$ evaluates to

$$J_1^{(1)} = - \left(\int_0^{x'} \frac{dx_1}{x_1 - \frac{1+y}{2y}} + \int_0^{x'} \frac{dx_1}{x_1 - \frac{1-y}{1+y}} - \int_0^{x'} \frac{dx_1}{x_1 - 1} \right) \tag{5.104}$$

$$= - \left(G\left[\frac{1+y}{2y}; x'\right] + G\left[\frac{1-y}{1+y}; x'\right] - G\left[1; x'\right] \right) + B_1^{(1)},$$

where multiple polylogarithms G are defined in (3.87). Multiple polylogarithms vanish at $x' = 0$. Furthermore, the boundary value of J_1 (5.99) has no ϵ^1-term, hence,

$$B_1^{(1)} = 0.$$

The next order in ϵ follows,

$$\stackrel{(5.101),(5.104)}{\Longrightarrow} J_1^{(2)} = \left(\int_0^{x'} \frac{dx_1}{x_1 - \frac{1+y}{2y}} \left(\int_0^{x_1} \frac{dx_2}{x_2 - \frac{1+y}{2y}} + \int_0^{x_1} \frac{dx_2}{x_2 - \frac{1-y}{1+y}} - \int_0^{x_1} \frac{dx_2}{x_2 - 1} \right) \right)$$

$$+ \left(\int_0^{x'} \frac{dx_1}{x_1 - \frac{1-y}{1+y}} \left(\int_0^{x_1} \frac{dx_2}{x_2 - \frac{1+y}{2y}} + \int_0^{x_1} \frac{dx_2}{x_2 - \frac{1-y}{1+y}} - \int_0^{x_1} \frac{dx_2}{x_2 - 1} \right) \right)$$

$$+ \left(- \int_0^{x'} \frac{dx_1}{x_1 - 1} \left(\int_0^{x_1} \frac{dx_2}{x_2 - \frac{1+y}{2y}} + \int_0^{x_1} \frac{dx_2}{x_2 - \frac{1-y}{1+y}} - \int_0^{x_1} \frac{dx_2}{x_2 - 1} \right) \right).$$

The resulting multiple polylogarithms vanish again on the boundary point. The integration constant is $\frac{1}{4}\pi^2$ as demanded by (5.99). We derive

$$J_1 = 1 + \epsilon \left(-G\left[\frac{y+1}{2y}; x'\right] - G\left[\frac{1-y}{y+1}; x'\right] + G[1; x'] \right)$$

$$+ \epsilon^2 \left(G\left[\frac{y+1}{2y}, \frac{y+1}{2y}; x'\right] + G\left[\frac{y+1}{2y}, \frac{1-y}{y+1}; x'\right] - G\left[\frac{y+1}{2y}, 1; x'\right] \right.$$

$$+ G\left[\frac{1-y}{y+1}, \frac{y+1}{2y}; x'\right] + G\left[\frac{1-y}{y+1}, \frac{1-y}{y+1}; x'\right] - G\left[\frac{1-y}{y+1}, 1; x'\right]$$

$$\left. -G\left[1, \frac{y+1}{2y}; x'\right] - G\left[1, \frac{1-y}{y+1}; x'\right] + G[1, 1; x'] + \frac{1}{4}\pi^2 \right) + O\left(\epsilon^3\right). \tag{5.105}$$

We verify that J_1 is of uniform weight zero. In practice, we may utilise the `Mathematica` package `PolyLogTools` [98] to deal with emerging multiple polylogarithms.

All multiple polylogarithms arising in the solutions of master integrals $\vec{J}$ depend on letters $l'_1, \ldots, l'^k$ and may be written like

$$G\left[l'_1, \ldots, l'_k; x'\right].$$

J_1, for example, evaluates to

$$
\begin{aligned}
J_1 = {} & 1 + \epsilon \left(-G \left[x'_9; x' \right] - G \left[x'_8; x' \right] + G[1; x'] \right) \\
& + \epsilon^2 \Big(G \left[x'_9, x'_9; x' \right] + G \left[x'_9, x'_8; x' \right] - G \left[x'_9, 1; x' \right] \\
& + G \left[x'_8, x'_9; x' \right] + G \left[x'_8, x'_8; x' \right] - G \left[x'_8, 1; x' \right] \\
& - G \left[1, x'_9; x' \right] - G \left[1, x'_8; x' \right] + G[1, 1; x'] + \frac{1}{4}\pi^2 \Big) + O \left(\epsilon^3 \right).
\end{aligned}
$$

The 21 sufficient letters form the following alphabet,

$$
\begin{aligned}
\mathcal{A} = \big\{ & 0, 1, 2, x'_7, x'_8, x'_9, x'_{10}, x'_{11}, x'_{12}, x'_{13}, x'_{14}, x'_{15}, x'_{16}, \\
& x'_{17,a}, x'_{17,b}, x'_{18,a}, x'_{18,b}, x'_{19,a}, x'_{19,b}, x'_{20,a}, x'_{20,b} \big\},
\end{aligned}
\tag{5.106}
$$

with

$$
x'_7 = \frac{2}{1+y}, \qquad\qquad x'_8 = \frac{1-y}{1+y}, \qquad\qquad x'_9 = \frac{1+y}{2y},
$$

$$
x'_{10} = \frac{1 + 4y - y^2}{(1+y)^2}, \qquad x'_{11} = \frac{2\left(1 + y^2\right)}{(1+y)^2}, \qquad x'_{12} = \frac{4y}{(1+y)^2},
$$

$$
x'_{13} = -\frac{1 - 4y - y^2}{2y(1+y)}, \qquad x'_{14} = \frac{1 + 4y - y^2}{2y(1+y)}, \qquad x'_{15} = \frac{1 - 4y - y^2}{(1+y)(1-3y)},
$$

$$
x'_{16} = -\frac{4y}{(1+y)(1-3y)},
\tag{5.107}
$$

and

$$
x'_{17,a} = e^{\frac{\pi i}{3}}, \qquad x'_{17,b} = e^{-\frac{\pi i}{3}},
$$

$$
x'_{18,a} = \frac{1 + 4y - y^2 + i\sqrt{\left(3 + y^2\right)\left(1 - 5y^2\right)}}{2(1+y)^2},
$$

$$
x'_{18,b} = \frac{1 + 4y - y^2 - i\sqrt{\left(3 + y^2\right)\left(1 - 5y^2\right)}}{2(1+y)^2},
$$

$$
x'_{19,a} = \frac{1 + 2y - y^2 + \sqrt{2y\left(1 + y - y^2 + y^3\right)}}{(1+y)^2},
$$

$$
x'_{19,b} = \frac{1 + 2y - y^2 - \sqrt{2y\left(1 + y - y^2 + y^3\right)}}{(1+y)^2},
$$

$$
x'_{20,a} = \frac{2y + i\sqrt{2y\left(1 - y - y^2 - y^3\right)}}{2y(1+y)},
$$

$$
x'_{20,b} = \frac{2y - i\sqrt{2y\left(1 - y - y^2 - y^3\right)}}{2y(1+y)}.
\tag{5.108}
$$

The rational arguments of all sufficient dlog-forms are compositions of polynomials, as described in section 5.5.2. Each letter corresponds to a root of such a polynomial. The just defined letters of system 1, hence, correspond to roots of p_1-p_{20} (5.87) in x' with x replaced by $1 - x'$. The letters for the other systems are obtained as roots of respective

polynomials in $\hat{x}$ and $\tilde{x}'$.

For all master integrals,

$$J_k = \sum_{j=0}^{\infty} \epsilon^j J_k^{(j)},$$

we confirm, that the ϵ^j-term $J_k^{(j)}$ is of uniform weight j. To provide another example, we display

$$
\begin{aligned}
J_{67} = 2\,\big[&G\left[0, x'_8, x'_9; x'\right] + G\left[0, x'_9, x'_8; x'\right] - G\left[x'_{15}, x'_8, 0; x'\right] - G\left[x'_{14}, x'_9, 0; x'\right] \\
&- G\left[x'_{14}, x'_8, 0; x'\right] - G\left[x'_{15}, x'_9, 0; x'\right] + G\left[x'_{14}, x'_8, x'_9; x'\right] + G\left[x'_{14}, x'_9, x'_8; x'\right] \\
&+ G\left[x'_{15}, x'_8, x'_9; x'\right] + G\left[x'_{15}, x'_9, x'_8; x'\right] - G\left[1, x'_9, x'_8; x'\right] + G\left[x'_{15}, x'_9, 1; x'\right] \\
&- G\left[x'_7, x'_9, 1; x'\right] + G\left[x'_7, 1, x'_9; x'\right] - G\left[0, x'_8, 1; x'\right] - G\left[1, x'_9, 1; x'\right] \\
&- G\left[0, 1, x'_8; x'\right] - 2\,G\left[x'_7, 1, 0; x'\right] + G\left[1, 0, 1; x'\right] - G\left[x'_{14}, x'_8, 1; x'\right] \\
&+ 2\,G\left[x'_{15}, 1, 0; x'\right] + 2\,G\left[x'_7, x'_8, 0; x'\right] + 2\,G\left[x'_7, x'_9, 0; x'\right] - G\left[x'_{15}, x'_7, 1; x'\right] \\
&- G\left[x'_7, x'_9, x'_8; x'\right] - G\left[x'_{15}, 1, x'_9; x'\right] - G\left[x'_7, x'_8, x'_9; x'\right] - G\left[x'_{14}, x'_7, x'_9; x'\right] \\
&- G\left[x'_{15}, x'_7, x'_8; x'\right] - G\left[1, x'_8, x'_9; x'\right] + 2\,G\left[x'_{14}, x'_7, 1; x'\right] + G\left[1, x'_7, 1; x'\right] \\
&+ G\left[1, x'_7, x'_8; x'\right]\big]\,\epsilon^3 + \mathcal{O}\!\left(\epsilon^4\right).
\end{aligned}
$$

Results can be validated through numerical checks. We may evaluate the master integrals expressed through multiple polylogarithms at a specific kinematic point with the help of `GiNaC` [99, 100]. We make a counter-check if we evaluate the master integrals in (5.69),(5.70),(5.71) at the same kinematic point applying the `Mathematica` package `AMFlow` [101–103] or the program `sector_decomposition` [104, 105]. In appendix B.2 (table B.4 and table B.5) we present numerical results of system 1 as reference value at the kinematic point $p^2 = m_H^2 = 125.2\text{GeV}$.

5.6 Summary and conclusion

We analytically calculated all master integrals relevant for the three-loop Higgs boson self-energy diagrams with internal W- and top-propagators (fig.5.1), keeping the full dependence on m_W^2, m_t^2, p^2. We created five topologies, summarised in table 5.1 and illustrated in fig.5.5 and fig.5.7, sufficient to express all occurring diagrams. We divided the diagrams into those proportional to the product of Yukawa couplings $y_b y_t$ (fig.5.4) and the complement (fig.5.6). The appearance of square roots (see for example (5.42), (5.58)) forced us to divide even further into three systems and to transform the original kinematic variables, which were given by

$$v = \frac{p^2}{m_t^2}, \quad w = \frac{m_W^2}{m_t^2}.$$

The three systems, their corresponding topologies and top sectors as well as emerging square roots rationalised by subsequently introduced kinematic variables are summarised in table 5.9.

	System 1 (5.66)	System 2a (5.67)	System 2b (5.68)
defined in	fig.5.5, table 5.6	fig.5.7, table 5.7	fig.5.7, table 5.8
Topology$_\text{Top Sector}$	$A_{255}, B_{255}, C_{255}, D_{255}$	B'_{255}, B'_{479}	B'_{509}
Canonical Master integrals	$\vec{J}$ (5.69)	$\vec{K}$ (5.70)	$\vec{L}$ (5.71)
Cumulative Number	105	61	43
Differential equations	$d\vec{J} = \epsilon \sum\limits_{k=1}^{19} M_k \omega_k \vec{J}$	$d\vec{K} = \epsilon \sum\limits_{k=1}^{28} M'_k \omega_k \vec{K}$	$d\vec{L} = \epsilon \sum\limits_{k=1}^{28} M''_k \omega_k \vec{L}$
Square roots	r_1, r_2	r_1, r_2, r_3	r_1, r_2, r_4
Final variables	$(x'$ (5.78), y (5.77)$)$	$(\hat{x}$ (5.80), y (5.77)$)$	$(\tilde{x}'$ (5.82), y (5.77)$)$

Table 5.9: Summary of the three systems of master integrals for the three-loop Higgs boson self-energy with internal W- and top-propagators. Coefficient matrices M_k, M'_k, M''_k are rational and independent of ϵ, dlog forms ω_k are defined in (5.85) and (5.90), and square roots in (5.64).

In section 5.3.1, we obtained differential equations for all pre-canonical master integrals. Each system was transformed through appropriate basis transformations (see section 5.4), with the aim of factoring out the dimensional regularisation parameter. We studied diagonal blocks within differential equations with the help of the maximal cut. We altered maximally cut integrals to have constant leading singularities to find ansätze for integrals of uniform transcendental weight (section 5.4.4). Integrals of uniform transcendental weight depending on variables rationalising occurring square roots (section 5.5.1) lead to canonical differential equations. After calculating boundary values (section 5.5.3), the resulting canonical master integrals are expressible in terms of multiple polylogarithms to any order in the dimensional regularisation parameter (section 5.5.4).

The resulting integrals are essential building blocks within precision Higgs physics. A possible application is the determination of the mixed QCD-electroweak correction to the Higgs decay rate into a bottom quark pair. We discuss the decay rate $\Gamma\left(H \to b\bar{b}\right)$ in the following chapter.

MIXED QCD-ELECTROWEAK CORRECTION TO THE HIGGS BOSON DECAY RATE INTO A BOTTOM QUARK PAIR

In this chapter we consider a phenomenological application of the three-loop master integrals derived in the preceding chapter: The mixed QCD-electroweak correction to the Higgs boson decay rate into a bottom quark pair. Required theoretical knowledge was reviewed in chapter 2 and the strategy sketched in chapter 4. The calculations described here are still work in progress, hence, no final result is presented. Nevertheless, this chapter presents diversified aspects of analytical calculations of scattering amplitudes within the Standard Model. After an introduction, we discuss the decay rate $\Gamma\left(H \to b\bar{b}\right)$ and how to calculate it via the optical theorem in section 6.2. We derive all contributing Feynman diagrams in section 6.3. In section 6.4, we encounter colour factors from QCD and handle γ_5, which arises within electroweak interactions, while discussing the scattering amplitude. We apply Feynman rules and give some exemplary calculations in sections 6.4.1 and 6.4.2. Section 6.5 treats occurring divergences. We close this chapter with an outlook in section 6.6.

6.1 Introduction

The Higgs boson is an essential cornerstone of the Standard Model of particle physics (see section 2.2). Studies of its decays are crucial in order to determine its properties and, therefore, probe the Standard Model. From a theoretical point of view, the study of decays $H \to f\bar{f}$ corresponds to the study of partial decay widths $\Gamma(H \to f\bar{f})$ which we introduced in section 2.1 (see (2.8)). However, those are not directly observable. From an experimental point of view, branching ratios $BR(H \to f\bar{f})$ are called for. Both are related as a branching ratio gives the fraction of the total decay width $\Gamma_{H,\text{total}}$ corresponding to the considered partial decay width,

$$\Gamma\left(H \to f\bar{f}\right) = \Gamma_{H,\text{total}} \cdot BR\left(H \to f\bar{f}\right).$$

With a mass of $m_H = 125$ GeV the Higgs boson decays predominantly into a bottom quark pair, the heaviest possible final state with $m_b = 4$ GeV. The vast contribution of

this decay to the Higgs boson's total decay width exceeds 50%! Its branching ratio is [106]

$$BR\left(H \to b\bar{b}\right) = 58\%.$$

Since the Higgs boson's total decay width is in the order of $4 \cdot 10^{-3}\text{GeV}$ [107], its partial decay width into a bottom quark pair is roughly $2 \cdot 10^{-3}\text{GeV}$. The Higgs boson's second most frequent decay is the decay into off-shell W-bosons with a branching ratio of 21%. The huge difference between both top branching ratios emphasises the importance of $H \to b\bar{b}$. Large background makes the observation of $H \to b\bar{b}$ rather complicated. It was only accomplished in 2018 at the LHC [108, 109], six years after the Higgs boson discovery. However, future colliders like FCC-ee [110] will enable groundbreaking experimental work. Furthermore, due to its major contribution to the Higgs boson's total decay width, $\Gamma(H \to b\bar{b})$ significantly influences each Higgs boson branching ratio. A precise theoretical prediction of its value is therefore indispensable.

The Higgs boson decay rate into a bottom quark pair can be written as a perturbative expansion,

$$\Gamma\left(H \to b\bar{b}\right) = \Gamma^{(0)}(1 + \Delta^{(\alpha_s)} + \Delta^{(\alpha)} + \Delta^{(\alpha\alpha_s)} + ...),$$

where $\Gamma^{(0)}$ denotes the Born decay rate (6.2), $\Delta^{(\alpha_s)}$ denotes QCD-corrections, $\Delta^{(\alpha)}$ denotes electroweak-corrections and $\Delta^{(\alpha\alpha_s)}$ denotes mixed QCD-electroweak corrections. QCD corrections are known up to $\mathcal{O}\left(\alpha_s^3\right)$ [111]. The next to leading order QCD correction amount to roughly 20% and the two-loop QCD corrections to 3.8%. In comparison, the one-loop electroweak correction is only about $(-1)\%$ [45]. The dominant term of the two-loop electroweak correction corresponds approximately to 0.047% relative to the Born decay rate [112]. As a consequence, the mixed QCD-electroweak corrections are of particular interest. In [45] those were computed via Padé approximations. Techniques to compute Feynman integrals have evolved. Hence, the mixed QCD-electroweak corrections should be approached again.

We consider the NNLO QCD-electroweak corrections involving W-bosons or charged Goldstone bosons. In addition to the masses of the Higgs boson $m_H = 125.25 \pm 0.17$ GeV and the bottom quarks $m_b = 4.18^{+0.03}_{-02}$ GeV, the W-boson mass $m_W = 80.377 \pm 0.012$ GeV and top quark masses $m_t = 172.69 \pm 0.3$ GeV enter [107]. Considering the relative size of m_b, we only keep its leading term m_b^2, otherwise we work in massless bottom quark approximation. We work in dimensional regularisation as explained in section 2.3. Hence, momenta are taken in $D = (4 - 2\epsilon)$ dimensions. We choose Feynman gauge in the electroweak sector, i.e. $\xi_W = 1$, to avoid appearances of ξ_W in the denominator of W-/Goldstone boson propagators (see section 2.2 on R_ξ-gauge and Feynman rules). We maintain the general gauge parameter ξ_g of the gluon propagator. The final result should be independent of the chosen gauge and therefore also of ξ_g. Keeping ξ_g, we obtain a consistency check. We use the optical theorem discussed in section 2.1.1 and encounter therefore two-point three-loop Feynman diagrams. In the following section, we clarify this point after discussing the Higgs boson decay rate into a bottom quark pair more closely.
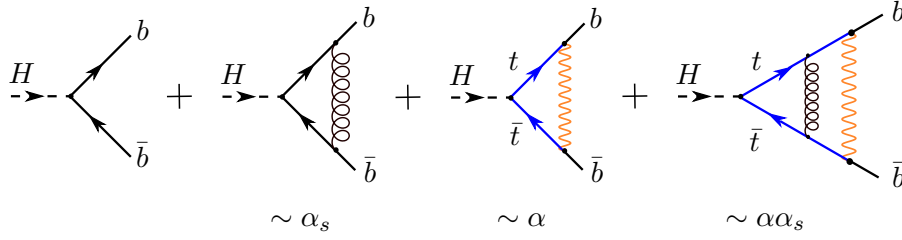
6.2 The decay rate

Figure 6.1: Structure of the perturbative expansion $H \to b\bar{b}$. Dashed lines denote Higgs bosons, curled lines gluons, orange lines W-bosons, straight black lines bottom quarks and blue lines top-quarks.

The perturbative expansion of the Higgs boson decay rate into a bottom quark pair, illustrated in fig.6.1, can be written as

$$\Gamma\left(H \to b\bar{b}\right) = \Gamma^{(0)}(1 + \Delta^{(\alpha_s)} + \Delta^{(\alpha)} + \Delta^{(\alpha\alpha_s)} + ...), \tag{6.1}$$

where $\Gamma^{(0)}$ denotes the Born decay rate, $\Delta^{(\alpha_s)}$ denotes α_s-corrections, $\Delta^{(\alpha)}$ denotes α-corrections and $\Delta^{(\alpha\alpha_s)}$ denotes mixed QCD-electroweak corrections, i.e. $\alpha\alpha_s$-corrections.

The Born decay rate is

$$\Gamma^{(0)} = \frac{N_C \alpha m_b^2 m_H \beta^3}{8 \sin\left(\Theta_W\right)^2 m_W^2},$$

with N_C being the number of colours, Θ_W the weak mixing angle and

$$\beta = \sqrt{1 - 4\frac{m_b^2}{m_H^2}} \approx 1 - 2\frac{m_b^2}{m_H^2} - \mathcal{O}\left(\left(\frac{m_b^2}{m_H^2}\right)^2\right)$$

the velocity of b-quarks, which we set to one as we only keep the leading power of m_b^2. We may express the resulting Born decay rate,

$$\Gamma^{(0)} = \frac{N_C \alpha m_b^2 m_H}{8 \sin\left(\Theta_W\right) m_W^2},$$

in terms of Fermi's constant

$$\Gamma_{G_F}^{(0)} = \frac{N_C G_F m_b^2 m_H}{4\sqrt{2}\pi}, \tag{6.2}$$

$$\frac{G_F}{\sqrt{2}} = \frac{\pi\alpha}{2/; \sin\left(\Theta_W\right)^2 m_W^2 \left(1 - \Delta r\right)}, \tag{6.3}$$

where Δr gives radiative corrections to the muon decay beyond QED corrections within the effective four-fermion theory [113].

The first order QCD and electroweak corrections to (6.1) are

$$\Delta^{(\alpha_s)} = \frac{C_F \alpha_s}{\pi}\left(\frac{17}{4} - \frac{3}{2}\ln\left(\frac{m_H^2}{\mu^2}\right)\right),$$

$$\Delta^{(\alpha)} = \frac{Q_b^2 \alpha}{\pi}\left(\frac{17}{4} - \frac{3}{2}\ln\left(\frac{m_H^2}{\mu^2}\right)\right),$$

whereby the latter can be derived from the former through a substitution $C_F \alpha_s \to Q_b^2 \alpha$.

Here, we address mixed QCD-electroweak corrections $\Delta^{(\alpha\alpha_s)}$ to the decay rate. We decompose them into mixed QED-QCD contributions $\Delta_\gamma^{(\alpha\alpha_s)}$, contributions involving Z-bosons or neutral Goldstone bosons $\Delta_Z^{(\alpha\alpha_s)}$ and contributions involving W-bosons or charged Goldstone bosons $\Delta_W^{(\alpha\alpha_s)}$,

$$\Delta^{(\alpha\alpha_s)} = \Delta_\gamma^{(\alpha\alpha_s)} + \Delta_Z^{(\alpha\alpha_s)} + \Delta_W^{(\alpha\alpha_s)}. \tag{6.4}$$

The mixed QED-QCD contributions were analytically calculated in [114],

$$\Delta_\gamma^{(\alpha\alpha_s)} = \frac{C_F \alpha_s}{\pi}\frac{Q_b^2 \alpha}{\pi}\left(\frac{691}{32} - \frac{9}{2}\zeta_2 - \frac{9}{2}\zeta_3 - \frac{105}{8}\ln\left(\frac{m_H^2}{\mu^2}\right) + \frac{9}{4}\ln\left(\frac{m_H^2}{\mu^2}\right)^2\right).$$

The remaining mixed QCD-electroweak contributions are so far only computed with the help of Padé approximations [45],

$$\Delta_Z^{(\alpha\alpha_s)} \approx -0.002, \quad \Delta_W^{(\alpha\alpha_s)} \approx -0.0009.$$

In this thesis, we consider the - due to more internal masses - more complicated contribution, the mixed QCD-electroweak correction involving W-bosons or charged Goldstone bosons $\Delta_W^{(\alpha\alpha_s)}$.

We defined decay rates in (2.8) as phase space integrations over squared scattering amplitudes. In this context, the scattering amplitude corresponds to diagrams like the ones in fig.6.1. Instead of calculating the decay rate via (2.8), we avoid phase space integration and emerging infrared divergences through the application of the optical theorem (see section 2.1.1). It relates the imaginary part of a two-point function to a total decay rate,

$$\text{Im}(M(A \to A)) = m_A \sum_X \Gamma(A \to X) = m_A \Gamma_{A,\text{total}}. \tag{6.5}$$

In order to derive a partial decay width for a specified final state, the matching term on the left hand side of (6.5) is selected. In the case of $H \to b\bar{b}$, we take the imaginary part of on-shell Higgs boson two-point functions ending in an $Hb\bar{b}$-vertex,

$$\Gamma\left(H \to b\bar{b}\right) = \frac{1}{m_H}\text{Im}\left(\Sigma_H(p^2 = m_H^2 + i\epsilon)\right). \tag{6.6}$$

The optical theorem holds for any order in perturbation theory. Since we want to calculate $\alpha\alpha_s$-corrections on the left hand side of (6.6), we have to consider $\alpha^2\alpha_s$-corrections on the right hand side. Consequently, we do not deal with three-point two-loop diagrams like the last one in fig.6.1, but with two-point three-loop diagrams. As indicated in fig.6.2, the three-loop diagrams are obtained from the two-loop diagrams if we close them on their right.
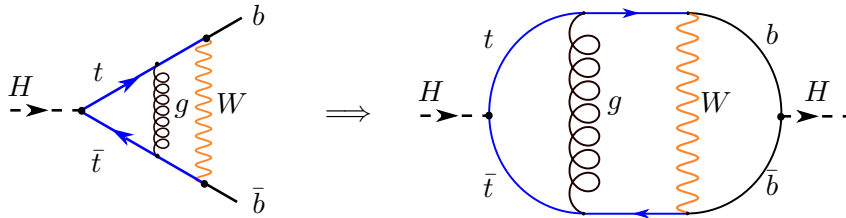

Figure 6.2: Sketch of the application of the optical theorem. Feynman diagrams are closed. Dashed lines denote Higgs bosons, curled lines gluons, orange lines W-bosons, straight black lines bottom quarks and blue lines top-quarks.

In the following section, we present all relevant Feynman diagrams before we discuss their evaluation in section 6.4.

6.3 Contributing Feynman diagrams

The first step for the determination of the mixed QCD-electroweak correction $\Delta_W^{(\alpha\alpha_s)}$ to the decay rate $\Gamma\left(H \to b\bar{b}\right)$ (6.1) via the optical theorem (6.6) is the generation of all contributing Feynman diagrams. This is achieved with the help of QGRAF [115] and FeynArts [116]. We summarise all diagrams in table 6.1 and table 6.2. As already sketched in the previous section (see fig.6.2), we consider three-loop Higgs boson self-energy diagrams at $\mathcal{O}\left(\alpha^2\alpha_s\right)$ ending in an $Hb\bar{b}$ vertex. An internal W or charged Goldstone boson, accompanied by a factor $\alpha = \frac{g^2}{4\pi}$, converts top (antitop) quarks into bottom (antibottom) quarks. An internal gluon yields a factor $\alpha_s = \frac{g_s^2}{4\pi}$.

The diagrams are not new within this thesis. In chapter 5, we derived master integrals of uniform weight sufficient to express them. In section 5.2, we already discussed all top-sector diagrams and explained the need for auxiliary topologies with nine propagators: The three-loop diagrams give rise to nine scalar products involving loop momenta, but only to eight propagators. Since we want to turn all Feynman integrals into scalar integrals, we need to be able to express all of these scalar products in terms of propagators. The auxiliary topologies introduce an appropriate ninth propagator. Furthermore, only keeping the leading term in the bottom quark mass m_b^2, we can work with massless bottom quark propagators: Each required Feynman diagram ends in an $Hb\bar{b}$ vertex. The corresponding Feynman rule provides a factor of m_b (see section 2.2.1). Considering the prefactor m_b times a bottom quark propagator, setting $\mathcal{O}(m_b^3)$ to zero corresponds to

taking a massless propagator,

$$m_b \frac{1}{q^2 - m_b^2} = m_b \left(\frac{1}{q^2} + \frac{m_b^2}{q^4} + \mathcal{O}(m_b^4)\right) = m_b \frac{1}{q^2} + \underbrace{\mathcal{O}(m_b^3)}_{\to 0}.$$

In conclusion, we work with the topologies derived in section 5.2, illustrated in fig.5.5, fig.5.7 and summarised in table 5.1. Consequently, we already assign each diagram to a topology and a sector as we list them in table 6.1 and table 6.2. Furthermore, we divide the diagrams by their coupling, i.e. by the vertices attached to the external Higgs boson. This division corresponds exactly to the three systems, we introduced in chapter 5 and summarised in table 5.9.

Multiple diagrams arise in one sector. Gluon loops can be attached to different edges without changing the set of required propagators and, therefore, without changing the sector the diagram belongs to. In addition, rotated diagrams may enter as well. Furthermore, the diagrams come in pairs. Each diagram enters once containing a W-boson and once containing a charged Goldstone boson instead.

In the second column of table 6.1 and table 6.2, we display one representative diagram per sector and topology, whereby topologies and sectors are specified in the third and fourth column. Instead of presenting each diagram of one sector graphically, they are indicated as the last column in table 6.1, and table 6.2 gives the number of diagrams per sector. The factor of two, thereby, indicates the diagrams containing Goldstone bosons instead of W-bosons. Column two and column five have to be considered simultaneously to gain full information on required diagrams.

In the following section, we discuss the Feynman diagrams more closely by expressing them in terms of Feynman rules.

Higgs-vertices	Diagrams	Topology	Sector	Number of diagrams
$Ht\bar{t} \to Hb\bar{b}$ $\Rightarrow$ System 1		A	255	$2 \cdot 2$
		B	255	$2 \cdot 2$
		C	255	$2 \cdot 4$
		D	255	$2 \cdot 4$
			223	$2 \cdot 4$
			247	$2 \cdot 4$
$HW^+W^- \to Hb\bar{b}$ $\Rightarrow$ System 2a		B'	255	$2 \cdot 2$
			479	$2 \cdot 4$
			475	$2 \cdot 4$
			471	$2 \cdot 2$

Table 6.1: List of all diagrams, Part 1. See description of table 6.2.

Higgs-vertices	Diagrams	Topology	Sector	Number of diagrams
$Hb\bar{b} \to Hb\bar{b}$ $\Rightarrow$ System 2b		B'	509	$2 \cdot 2$
			505	$2 \cdot 4$
			497	$2 \cdot 4$
			473	$2 \cdot 4$
			469	$2 \cdot 2$
			381	$2 \cdot 4$
			221	$2 \cdot 2$

Table 6.2: List of all diagrams, Part 2. Systems are summarised in table 5.9. Dashed lines denote Higgs bosons, curled lines gluons, orange lines W-bosons/charged Goldstone bosons, straight black lines bottom quarks and blue lines top-quarks. Topologies are defined in table 5.1. Sector identities in (3.46). The last column corresponds to the number of diagrams emerging within the respective sector, accounting for the exchange of W-bosons with Goldstone bosons and the possibility to reposition the edge of a gluon.

6.4 The scattering amplitude

In the subsequent section (table 6.1 and table 6.2) we presented all Feynman diagrams required for the two-point three-loop scattering amplitude corresponding to $H \to b\bar{b} \to H$ containing an internal W-boson or charged Goldstone boson and an internal gluon. We denote the scattering amplitude by

$$\Sigma_H^{(\alpha^2 \alpha_s)_W}.$$

In this section, we calculate the scattering amplitude by expressing the diagrams via Feynman rules, listed in section 2.2.1. Its imaginary part is related to the mixed QCD-electroweak correction $\Delta_W^{(\alpha\alpha_s)}$ to the decay rate $\Gamma\left(H \to b\bar{b}\right)$ (6.1) via the optical theorem (6.6),

$$\Gamma\left(H \to b\bar{b}\right) = \frac{1}{m_H}\text{Im}\left(\Sigma_H(p^2 = m_H^2 + i\epsilon)\right),$$

$$\Rightarrow \Delta_W^{(\alpha\alpha_s)} = \frac{1}{m_H}\text{Im}\left(\Sigma_H^{(\alpha^2\alpha_s)_W}(p^2 = m_H^2 + i\epsilon)\right). \tag{6.7}$$

We start this section with a brief discussion about the application of Feynman rules. Next, we consider some common properties of all diagrams, namely their colour factor and the appearance of the fifth Dirac matrix γ_5. After transforming all emerging integrals to scalar integrals, we are able to express the results in terms of the master integrals from chapter 5.

Each diagram in table 6.1 and table 6.2 is translated into a mathematical expression via Feynman rules from section 2.2.1. At first we label the momenta of all edges with respect to momentum conservation. We thereby name the momenta in correspondence with the topologies from table 5.1. The diagrams consist of closed quark loops, which contributes a factor (-1). We take the trace of the quark loop and insert a Feynman propagator for each edge and a vertex rule for each vertex. The trace is multiplied by the occurring boson propagators. Furthermore, we need to integrate over all three undetermined loop momenta k_1, k_2, k_3. Explicit calculations of individual, representative diagrams will be given in section 6.4.1 and section 6.4.2. We receive expressions of the following structure

$$\int \frac{d^D k_1}{(2\pi)^D} \frac{d^D k_2}{(2\pi)^D} \frac{d^D k_3}{(2\pi)^D} \prod_{j=1}^{9} \frac{\mathcal{N}(k_1, k_2, k_2, m_W, m_t, m_H)}{P_j^X}, \quad X \in \{A, B, C, D, B'\}, \tag{6.8}$$

where X represents the respective topology and $\mathcal{N}$ inherits the trace of the closed quark loop as well as the boson propagators. The scattering amplitude is given by the sum over all diagrams.
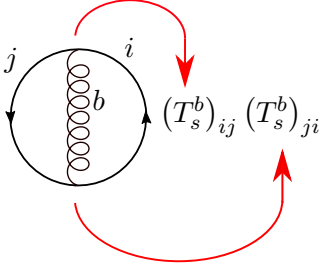
141

Figure 6.3: Sketch illustrating the colour flow. A gluon (curled line) is connected to a quark loop.

The vertex rule representing a gluon coupling to quarks contains $\left(T_s^b\right)$, with $b \in \{1,...,8\}$, which leads to the appearance of a colour factor (see section 2.2 for information on T_s^b, the generators of $SU(3)_c$. Colour factors handle colour degrees of freedom of Feynman diagrams within QCD. All diagrams in table 6.1 and table 6.2 contain the same arrangement of one gluon connected to a quark loop as illustrated in fig.6.3.

Hence, each diagram yields the same colour factor. The gluon changes the quark's colour from j to i and i to j, where $j, i \in \{red, green, blue\}$, manifested by the emergence of $\left(T_s^b\right)_{ij}$ and $\left(T_s^b\right)_{ji}$, $b \in \{1,...,8\}$. The resulting colour factor is $N_C C_F = 4$. $N_C = 3$ represents the number of colours and $C_F = \frac{4}{3}$,

$$\left(T_s^b\right)_{ij}\left(T_s^b\right)_{ji} = \left(T_s^b T_s^b\right)_{ii} = Tr\left[T_s^b T_s^b\right] = \frac{1}{2}\delta^{bb} = 4. \tag{6.9}$$

Vertices of W- or Goldstone bosons with quarks introduce the fifth gamma matrix (see (3.4) for Dirac algebra). In four dimensions γ_5 is defined by

$$\gamma_5 = \frac{i}{4!}\epsilon_{\mu\nu\alpha\beta}\gamma^\mu\gamma^\nu\gamma^\alpha\gamma^\beta, \tag{6.10}$$

and fulfils the following properties

$$\gamma_5^2 = 1, \tag{6.11}$$
$$\{\gamma_5, \gamma^\mu\} = 0, \tag{6.12}$$
$$Tr[\gamma_\mu\gamma_\nu\gamma_\sigma\gamma_\tau\gamma_5] = i4\epsilon_{\mu\nu\sigma\tau}. \tag{6.13}$$

We require a D-dimensional fifth Dirac matrix, since we work in dimensional regularisation. Unfortunately, we cannot transport all properties of the four-dimensional γ_5 to D dimensions. Contradictions arise if we consider D times a trace containing an even number of Dirac matrices and γ_5 and contract the outcome with an epsilon tensor. The calculation, demonstrated in appendix C.1, makes use of (6.12) and of the cyclicity of the trace. It leads to

$$(D-4)\epsilon^{\mu\nu\sigma\rho}Tr\left[\gamma_\mu\gamma_\nu\gamma_\sigma\gamma_\rho\gamma_5\right] = 0, \tag{6.14}$$

implying for $D \neq 4$ that $Tr\left[\gamma_\mu\gamma_\nu\gamma_\sigma\gamma_\rho\gamma_5\right] = 0$ in contrast to the property in (6.13) in four dimensions. We see, one property violates the other. Consequently, we have to chose an appropriate scheme defining the fifth Dirac matrix in D dimensions. One possibility is the scheme by t'Hooft and Veltman [52], where γ_5 is defined as in four dimensions, i.e via (6.10). This scheme preserves the trace identity (6.13). However, it violates the anticommuting property (6.12), since $\{\gamma_5, \gamma^\mu\} = 0$ for $\mu = 0, 1, 2, 3$, but $[\gamma_5, \gamma^\mu] = 0$

otherwise. Another possibility is the so-called "naive dimensional regularisation scheme" (NDR) originally introduced in [117]. Within NDR γ_5 is defined by (6.11) and (6.12),

$$\gamma_5^2 = 1, \tag{6.15}$$

$$\{\gamma_5, \gamma^\mu\} = 0, \tag{6.16}$$

where the anticommuting property (6.16) holds for all μ, independent of the dimension. The "naive" choice of the fifth gamma matrix is not mathematically well-defined. However, if we encounter even numbers of γ_5 within a trace it is appropriate, since we may eliminate γ_5 completely via (6.15) and (6.16) before evaluating the trace. The schemes do not differ in the physical case $D \to 4$.

If we evaluate the diagrams in table 6.1 and table 6.2 within t'Hooft and Veltman scheme, for example with the help of `FeynCalc` [118], we notice that only traces containing even numbers of γ_5 survive: Evaluation within t'Hooft and Veltman scheme leads to terms proportional to γ_5 of the following structure

$$\left(\Sigma_H^{(\alpha^2 \alpha_s)_W} \right)_{\sim \gamma_5} = i g^4 g_s^2 \int \frac{d^D k_1}{(2\pi)^D} \int \frac{d^D k_2}{(2\pi)^D} \int \frac{d^D k_3}{(2\pi)^D} \, \epsilon^{k_1 k_2 k_3 p} \, f_s,$$

where $\epsilon^{k_1 k_2 k_3 p}$ denotes the epsilon tensor contracted with all three loop momenta k_1, k_2, k_3 and the external momentum p. f_s denotes a scalar function depending on propagators and D. Following the Passarino-Veltman reduction technique (see section 3.1), an integral over three momenta carrying three indices must evaluate to a tensor structure carrying the respective three indices. In our case, the tensor structure must consist of the only external momentum p and the metric tensor,

$$\int d^D k_1 \int d^D k_2 \int d^D k_3 \, k_1^\alpha k_2^\beta k_3^\gamma \, f(k_1, k_2, k_3)$$

$$= C_1 p^\alpha p^\beta p^\gamma + C_{2,a} p^\alpha g^{\beta\gamma} + C_{2,b} p^\beta g^{\alpha\gamma} + C_{2,c} p^\gamma g^{\alpha\beta}, \quad (6.17)$$

with f being an arbitrary scalar function and $C_1, C_{2,a}, C_{2,b}, C_{2,c}$ constant. This implies for the terms of the scattering amplitude solely containing one γ_5,

$$\left(\Sigma_H^{(\alpha^2 \alpha_s)_W} \right)_{\sim \gamma_5} = i g^4 g_s^2 \, \epsilon_{\alpha\beta\gamma\delta} p^\delta \int d^D k_1 \int d^D k_2 \int d^D k_3 \, k_1^\alpha k_2^\beta k_3^\gamma \, f_s$$

$$\overset{(6.17)}{=} \underbrace{\epsilon_{\alpha\beta\gamma\delta}}_{\text{antisymmetric}} \left(C_1 \underbrace{p^\alpha p^\beta p^\gamma p^\delta}_{\text{symmetric}} + C_{2,a} \underbrace{p^\alpha g^{\beta\gamma} p^\delta}_{\text{symmetric}} + C_{2,b} \underbrace{p^\beta g^{\alpha\gamma} p^\delta}_{\text{symmetric}} + C_{2,c} \underbrace{p^\gamma g^{\alpha\beta} p^\delta}_{\text{symmetric}} \right)$$

$$= C_1 \cdot 0 + C_{2,a} \cdot 0 + C_{2,b} \cdot 0 + C_{2,c} \cdot 0 = 0. \tag{6.18}$$

The terms proportional to the fifth Dirac matrix vanish. As a consequence, we may use NDR. In (6.27) and (6.29), we demonstrate how (6.15) and (6.16) are utilised to eliminate γ_5 completely.

After dealing with γ_5, we are able to continue the calculation of the expressions of diagrams (6.8). We evaluate the traces representing closed quark loops and contract

the result with the boson propagators. For this purpose, we utilise `FORM` [119]. Scalar products involving loop momenta arise in the numerators. Those are replaced by linear combinations of propagators of the corresponding topology. We present the combinations of propagators for topology A,B,C,D in table 6.3 and for topology B' in table 6.4.

Topology A	Topology B
$k_1^2 = m_t^2 - P_1^A$	$k_1^2 = -P_1^B + m_t^2$
$k_2^2 = m_t^2 - P_4^A$	$k_2^2 = -P_4^B$
$k_3^2 = -P_7^A$	$k_3^2 = -P_7^B$
$p.k_1 = \dfrac{1}{2}\left[-P_1^A + P_2^A + s\right]$	$p.k_1 = \dfrac{1}{2}\left[-P_1^B + P_2^B + s\right]$
$p.k_2 = \dfrac{1}{2}\left[P_4^A - P_6^A - s\right]$	$p.k_2 = \dfrac{1}{2}\left[P_4^B - P_6^B - s\right]$
$p.k_3 = \dfrac{1}{2}\left[-P_7^A + P_8^A + s\right]$	$p.k_3 = \dfrac{1}{2}\left[-P_7^B + P_8^B + s\right]$
$k_1.k_2 = \dfrac{1}{2}\left[P_1^A - P_3^A + P_4^A - 2m_t^2\right]$	$k_1.k_2 = \dfrac{1}{2}\left[P_1^B - P_3^B + P_4^B - m_t^2 + m_W^2\right]$
$k_1.k_3 = \dfrac{1}{2}\left[-P_1^A - P_7^A + P_9^A\right]$	$k_1.k_3 = \dfrac{1}{2}\left[-P_1^B - P_7^B + P_9^B + m_t^2 - m_W^2\right]$
$k_2.k_3 = \dfrac{1}{2}\left[P_4^A - P_5^A + P_7^A - m_t^2 + m_W^2\right]$	$k_2.k_3 = \dfrac{1}{2}\left[P_4^B - P_5^B + P_7^B\right]$

Topology B	Topology C
$k_1^2 = -P_1^C + m_t^2$	$k_1^2 = -P_1^D + m_t^2$
$k_2^2 = -P_5^C + m_W^2$	$k_2^2 = -P_5^D$
$k_3^2 = -P_7^A$	$k_3^2 = -P_7^A$
$p.k_1 = \dfrac{1}{2}\left[-P_1^C + P_2^C + s\right]$	$p.k_1 = \dfrac{1}{2}\left[-P_1^D + P_2^D + s\right]$
$p.k_2 = \dfrac{1}{2}\left[P_5^C - P_9^C - s - m_W^2 + m_t^2\right]$	$p.k_2 = \dfrac{1}{2}\left[P_5^D - P_9^D - s\right]$
$p.k_3 = \dfrac{1}{2}\left[-P_7^C + P_8^C + s\right]$	$p.k_3 = \dfrac{1}{2}\left[-P_7^D + P_8^D + s\right]$
$k_1.k_2 = \dfrac{1}{2}\left[P_1^C - P_3^C + P_5^C - m_W^2 - m_t^2\right]$	$k_1.k_2 = \dfrac{1}{2}\left[P_1^D - P_4^D + P_5^D\right]$
$k_1.k_3 = \dfrac{1}{2}\left[-P_3^C + P_4^C - P_6^C - P_7^C \right.$ $\left. + P_8^C + P_9^C + s\right]$	$k_1.k_3 = \dfrac{1}{2}\left[-P_1^D + P_3^D - P_7^D + m_t^2 - m_W^2\right]$
$k_2.k_3 = \dfrac{1}{2}\left[P_6^C - P_8^C - P_9^C - s\right]$	$k_2.k_3 = \dfrac{1}{2}\left[P_5^D - P_6^D + P_7^D\right]$

Table 6.3: Scalar products involving loop momenta in terms of linear combinations of propagators, Part 1. Propagators were defined in table 5.1.

Topology B'
$k_1^2 = -P_1^{B'} - m_W^2$
$k_2^2 = -P_4^{B'}$
$k_3^2 = -P_7^{B'}$
$p.k_1 = \dfrac{1}{2}\left[-P_1^{B'} + P_2^{B'} + s\right]$
$p.k_2 = \dfrac{1}{2}\left[P_4^{B'} - P_6^{B'} - s\right]$
$p.k_3 = \dfrac{1}{2}\left[-P_7^{B'} + P_8^{B'} + s\right]$
$k_1.k_2 = \dfrac{1}{2}\left[P_1^{B'} - P_3^{B'} + P_4^{B'} + m_t^2 - m_W^2\right]$
$k_1.k_3 = \dfrac{1}{2}\left[-P_1^{B'} - P_7^{B'} + P_9^{B'} - m_t^2 + m_W^2\right]$
$k_2.k_3 = \dfrac{1}{2}\left[P_4^{B'} - P_5^{B'} + P_7^{B'}\right]$

Table 6.4: Scalar products involving loop momenta in terms of linear combinations of propagators, Part 2. Propagators were defined in table 5.1.

After replacing all scalar products involving loop momenta as given in table 6.3 and table 6.4, the diagrams consist of sums of scalar integrals (see section 3.1 for information about scalar integrals).

$$\Sigma_H^{(\alpha^2\alpha_s)_W}(p) = \sum_{Diagrams} \int \frac{d^D k_1}{(2\pi)^D}\frac{d^D k_2}{(2\pi)^D}\frac{d^D k_3}{(2\pi)^D} \; \prod_{j=1}^{9} \frac{\mathcal{N}(k_1, k_2, k_2, m_W, m_t, m_H)}{P_j^X}$$

$$\Big\downarrow \text{ Evaluation \& Replacement of scalar products}$$

$$\Sigma_H^{(\alpha^2\alpha_s)_W}(p) = N_C C_F g^4 g_s^2 \sum_i c_i^X \hat{I}_i^X = N_C C_F \left(\alpha 4\pi\right)^2 \left(\alpha_s 4\pi\right) \sum_i c_i^X \hat{I}_i^X, \qquad (6.19)$$

with rational prefactors c_i^X and $X \in \{A, B, C, D, B'\}$. The scalar integrals in (6.19) are defined by

$$\hat{I}_{\nu_1\nu_2\nu_3\nu_4\nu_5\nu_6\nu_7\nu_8\nu_9}^X = \int \frac{d^D k_1}{(2\pi)^D}\int \frac{d^D k_2}{(2\pi)^D}\int \frac{d^D k_3}{(2\pi)^D} \; \prod_{j=1}^{9} \frac{1}{\left(P_j^X\right)^{\nu_j^X}}, \quad \nu_j^X \in \mathbb{Z}. \qquad (6.20)$$

The sum in (6.19) contains a vast amount of integrals. The first two diagrams in table 6.1, i.e. the diagrams evaluated within topology A and B, each give rise to a sum over 104 integrals. The third diagram in table 6.1, which corresponds to topology C, even exceeds this number as it gathers 198 different scalar integrals. Fortunately, as explained in section 3.4 and discussed in section 5.3, there is no need to deal with all of

145

these integrals. We reduce them to a basis set of integrals. For this purpose, we utilise an integration by parts reduction program like `Kira` [82, 83]. The pre-canonical master integrals coincide with those characterised in table 5.6, table 5.7 and table 5.8, since we work within the same topologies and top-sectors as in the previous chapter. We have $\vec{I}_1$ for system 1, i.e. the diagrams starting with a $Ht\bar{t}$-vertex, $\vec{I}_{2a}$ for system 2a, i.e. the diagrams starting with a HW^+W^- vertex and $\vec{I}_{2b}$ for system 2b, i.e. the diagrams starting with a $Hb\bar{b}$ vertex. The numbers of master integrals are $N^1_{MI} = 105$ for system 1, $N^{2a}_{MI} = 61$ for system 2a and $N^{2b}_{MI} = 43$ for system 2b. During the reduction we set

$$\mu^2 = m_t^2,$$

hence, the integrals kinematically depend on the following variables

$$v = \frac{p^2}{m_t^2}, \quad w = \frac{m_W^2}{m_t^2}, \tag{6.21}$$

and are given by

$$\hat{I}_i = \sum_j^{N^s_{MI}} \tilde{c}^s_{i,j} I^s_j, \quad s = 1, 2a, 2b, \tag{6.22}$$

where I^s_j denotes a pre-canonical master integral of system s and $\tilde{c}^s_{i,j}$ rational prefactors depending on v, w and the dimension $D = (4 - 2\epsilon)$. This implies for the scattering amplitude

$$\Sigma^{(\alpha^2 \alpha_s)_W}_H (p) = N_C C_F g^4 g_s^2 \sum_i c^X_i \hat{I}^X_i$$

$$\Big\downarrow \text{ IBP reduction (6.22)}$$

$$\Sigma^{(\alpha^2 \alpha_s)_W}_H (p) = N_C C_F g^4 g_s^2 \sum_{systems} \sum_j^{N^s_{MI}} \hat{c}^s_j I^s_j, \tag{6.23}$$

where

$$\hat{c}^s_j = \sum_i \tilde{c}^s_{i,j} c_i.$$

We spend the last chapter finding canonical master integrals expressible in terms of multiple polylogarithms (see section 5.5.4). In section 5.4, we found basis transformations U. We presented the resulting integrals in section 5.5. The canonical master integrals from system 1, $\vec{J}$, were given in (5.69), those from system 2a, $\vec{K}$, in (5.70) and those from system 2b, $\vec{L}$, in (5.71). Inverting the transformation matrices U, we are able to express each pre-canonical master integrals in terms of an integral of uniform weight,

$$\vec{J} \overset{(5.69)}{=} U_1 \vec{I}_1 \quad \Rightarrow \quad \vec{I}_1 = U^{(-1)} \vec{J},$$

$$\vec{K} \overset{(5.70)}{=} U_{2a} \vec{I}_{2a} \Rightarrow \quad \vec{I}_{2a} = U^{(-1)}_{2a} \vec{K},$$

$$\vec{L} \overset{(5.71)}{=} U_{2b}\vec{I}_{2b} \;\Rightarrow\; \vec{I}_{2b} = U_{2b}^{(-1)}\vec{L}. \tag{6.24}$$

In practice, we sum up all diagrams only now to obtain the scattering amplitude, which then evaluates to

$$\Sigma_H^{(\alpha^2\alpha_s)_W}(p) = N_C C_F g^4 g_s^2 \sum_{systems} \sum_{j}^{N_{MI}^s} \hat{c}_j^s I_j^s$$

$$\Big\downarrow \text{ transforming master integrals (6.24)}$$

$$\Sigma_H^{(\alpha^2\alpha_s)_W}(p) = N_C C_F g^4 g_s^2 \left(\sum_{j}^{N_{MI}^1} f_j^1 J_j + \sum_{j}^{N_{MI}^{2a}} f_j^{2a} K_j + \sum_{j}^{N_{MI}^{2b}} f_j^{2b} L_j \right), \tag{6.25}$$

where the rational factors f_j^s are obtained from $\hat{c}_j^s$ and (6.24).

The resulting scattering amplitude (6.25) is a sum over the master integrals we already evaluated in section 5.5.4. However, the master integrals still contain divergences manifested through poles in the dimensional regularisation parameter (see section 2.3 on divergences in Feynman integrals). We discuss renormalisation, a method eliminating divergences, in section 6.5. Beforehand, we give some insights into calculations of diagrams in the following subsections. In table 6.1 and table 6.2, we divided the diagrams according to the system they belong to. The calculation of diagrams belonging to the same system yield the same structure and prefactor, hence, we only show a selection of diagrams to illustrate the procedure. First, we discuss diagrams starting with an $Ht\bar{t}$-vertex in section 6.4.1, i.e. diagrams proportional to the product of Yukawa couplings $y_b y_t$. Afterwards, we consider diagrams containing an HW^+W^- vertex and diagrams containing two $Hb\bar{b}$-vertices in section 6.4.2.

6.4.1 Diagrams proportional to the product of Yukawa couplings $y_b y_t$
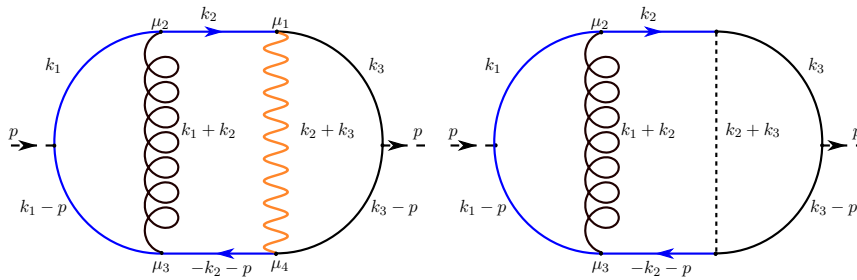
Figure 6.4: The diagrams corresponding to topology A sector 255. Dashed lines denote Higgs bosons, curled lines gluons, orange lines W-bosons, dotted lines charged Goldstone bosons, straight black lines bottom quarks and blue lines top-quarks.

Here, we provide a detailed example application of Feynman rules. Note, that the calculations presented in this subsection were already part of my master thesis. We consider the first diagram in table 6.1. Like each required diagram, this diagram enters once

containing a W-boson and once containing a charged Goldstone boson. Furthermore, rotated versions have to be taken into account. However, those amount to the same expression in terms of Feynman rules and are, therefore, accounted for by a factor 2. We already discussed in section 5.2 (see fig.5.2) how to label its momenta according to momentum conservation at each vertex, with p being the external momentum. Consequently, we obtain the two diagrams in fig.6.4. The left diagram (W-boson) corresponds to $\Sigma_W^A(p)$ and the right diagram (Goldstone boson) to $\Sigma_{GB}^A(p)$.

We express the diagrams in terms of Feynman rules from section 2.2.1. We move along the closed quark loop against its momentum flow and translate each edge into a Feynman propagator and each vertex via a vertex rule. Furthermore, we multiply a gluon and a W-boson or Goldstone boson propagator. Within the gluon propagator, we keep the general gauge parameter ξ_g. For the W-/Goldstone boson, we choose Feynman gauge $\xi_W = 1$. The CKM-matrix is taken to be the identity matrix $|V_{tb}|^2 = 1$ (see section 2.2 on R_ξ-gauge and the CKM-matrix).

$$
\begin{aligned}
\Sigma_W^A(p) = &\int \frac{d^D k_1}{(2\pi)^D} \int \frac{d^D k_2}{(2\pi)^D} \int \frac{d^D k_3}{(2\pi)^D} \, |V_{tb}|^2 (-1) \, Tr\Bigg[\left(-i\frac{g}{2}\frac{m_b}{m_W}\right) i\frac{\slashed{k}_3 + m_b}{k_3^2 - m_b^2} \\
&\left(i\frac{g}{\sqrt{2}}\gamma^{\mu_1}\frac{1-\gamma_5}{2}\right) i\frac{-\slashed{k}_2 + m_t}{k_2^2 - m_t^2} \left(ig_s\gamma^{\mu_2}\frac{\lambda_a}{2}\right) i\frac{\slashed{k}_1 + m_t}{k_1^2 - m_t^2} \left(-i\frac{g}{2}\frac{m_t}{m_W}\right) \\
&i\frac{\slashed{k}_1 - \slashed{p} + m_t}{(k_1 - p)^2 - m_t^2} \left(ig_s\gamma^{\mu_3}\frac{\lambda_a}{2}\right) i\frac{-(\slashed{k}_2 + \slashed{p}) + m_t}{(k_2 + p)^2 - m_t^2} \left(i\frac{g}{\sqrt{2}}\gamma^{\mu_4}\frac{1-\gamma_5}{2}\right) \\
&i\frac{\slashed{k}_3 - \slashed{p} + m_b}{(k_3 - p)^2 - m_b^2}\Bigg] \frac{i}{(k_1 + k_2)^2}\left(-g_{\mu_2\mu_3} + (1-\xi_g)\frac{(k_1 + k_2)_{\mu_2}(k_1 + k_2)_{\mu_3}}{(k_1 + k_2)^2}\right) \\
&\left(\frac{-ig_{\mu_1\mu_4}}{(k_2 + k_3)^2 - m_W^2}\right) \\
= &N_C C_F \frac{g^4 g_s^2}{32} \frac{m_t m_b}{m_W^2} \int \frac{d^D k_1}{(2\pi)^D} \int \frac{d^D k_2}{(2\pi)^D} \int \frac{d^D k_3}{(2\pi)^D} \left[\prod_{i=1}^{8} P_i^A\right]^{-1} \\
&\left(-g_{\mu_2\mu_3} + (1-\xi_g)\frac{(k_1 + k_2)_{\mu_2}(k_1 + k_2)_{\mu_3}}{P_3^A}\right)(-g_{\mu_1\mu_4})\,\mathcal{T}_W^A, \quad\quad (6.26)
\end{aligned}
$$

where the propagators P_i^A were defined in table 5.1. The trace of the closed quark loop of the left diagram in fig.6.4 is

$$
\begin{aligned}
\mathcal{T}_W^A = \; & Tr\Big[(\slashed{k}_3 + m_b)\gamma^{\mu_1}(1-\gamma_5)(-\slashed{k}_2 + m_t)\gamma^{\mu_2}(\slashed{k}_1 + m_t)(\slashed{k}_1 - \slashed{p} + m_t) \\
& \gamma^{\mu_3}(-\slashed{k}_2 - \slashed{p} + m_t)\gamma^{\mu_4}(1-\gamma_5)(\slashed{k}_3 - \slashed{p} + m_b)\Big]. \quad\quad (6.27)
\end{aligned}
$$

The right diagram in fig.6.4 amounts to

$$\Sigma^A_{GB}(p) = \int \frac{d^D k_1}{(2\pi)^D} \int \frac{d^D k_2}{(2\pi)^D} \int \frac{d^D k_3}{(2\pi)^D} |V_{tb}|^2 (-1) \left(\frac{i}{(k_2 + k_3)^2 - m_W^2} \right)$$

$$Tr \Bigg[\left(-i \frac{g}{2} \frac{m_b}{m_W} \right) i \frac{\slashed{k}_3 + m_b}{k_3^2 - m_b^2} i \frac{g}{2\sqrt{2}} \left[(1 - \gamma_5) \frac{m_b}{m_W} - (1 + \gamma_5) \frac{m_t}{m_W} \right] i \frac{-\slashed{k}_2 + m_t}{k_2^2 - m_t^2}$$

$$\left(i g_s \gamma^{\mu_2} \frac{\lambda_a}{2} \right) i \frac{\slashed{k}_1 + m_t}{k_1^2 - m_t^2} \left(-i \frac{g}{2} \frac{m_t}{m_W} \right) i \frac{\slashed{k}_1 - \slashed{p} + m_t}{(k_1 - p)^2 - m_t^2} \left(i g_s \gamma^{\mu_3} \frac{\lambda_a}{2} \right)$$

$$i \frac{-(\slashed{k}_2 + \slashed{p}) + m_t}{(k_2 + p)^2 - m_t^2} \frac{g}{2\sqrt{2}} \left[(1 + \gamma_5) \frac{m_b}{m_W} - (1 - \gamma_5) \frac{m_t}{m_W} \right] i \frac{\slashed{k}_3 - \slashed{p} + m_b}{(k_3 - p)^2 - m_b^2} \Bigg]$$

$$\frac{i}{(k_1 + k_2)^2} \left(-g_{\mu_2 \mu_3} + (1 - \xi_g) \frac{(k_1 + k_2)_{\mu_2} (k_1 + k_2)_{\mu_3}}{(k_1 + k_2)^2} \right)$$

$$= N_C C_F \frac{g^4 g_s^2}{32} \frac{m_t m_b}{m_W^2} \int \frac{d^D k_1}{(2\pi)^D} \int \frac{d^D k_2}{(2\pi)^D} \int \frac{d^D k_3}{(2\pi)^D} \left[\prod_{i=1}^8 P_i^A \right]^{-1}$$

$$\left(-g_{\mu_2 \mu_3} + (1 - \xi_g) \frac{(k_1 + k_2)_{\mu_2} (k_1 + k_2)_{\mu_3}}{P_3^A} \right) \mathcal{T}^A_{GB}, \tag{6.28}$$

where the propagators P_i^C were defined in table 5.1. The trace of the closed quark loop of the right diagram in fig.6.4 is

$$\mathcal{T}^A_{GB} = Tr \Bigg[(\slashed{k}_3 + m_b) \left[(1 - \gamma_5) \frac{m_b}{m_W} - (1 + \gamma_5) \frac{m_t}{m_W} \right] (-\slashed{k}_2 + m_t) \gamma^{\mu_2} (\slashed{k}_1 + m_t)$$

$$(\slashed{k}_1 - \slashed{p} + m_t) \gamma^{\mu_3} (-\slashed{k}_2 - \slashed{p} + m_t) \left[(1 + \gamma_5) \frac{m_b}{m_W} - (1 - \gamma_5) \frac{m_t}{m_W} \right] (\slashed{k}_3 - \slashed{p} + m_b) \Bigg]. \tag{6.29}$$

We evaluated in (6.18), that terms within the traces (6.27), (6.29) solely containing one γ_5 vanish. We may eliminate the fifth Dirac matrix completely in (6.30) and (6.31) through the application of the properties (6.15) and (6.16),

$$\mathcal{T}^A_W = Tr \Bigg[(\slashed{k}_3 + m_b) \gamma^{\mu_1} \Big((-\slashed{k}_2 + m_t) \gamma^{\mu_2} (\slashed{k}_1 + m_t)(\slashed{k}_1 - \slashed{p} + m_t) \gamma^{\mu_3} (-\slashed{k}_2 - \slashed{p} + m_t) \gamma^{\mu_4}$$

$$+ \underbrace{\gamma_5 (-\slashed{k}_2 + m_t) \gamma^{\mu_2} (\slashed{k}_1 + m_t)(\slashed{k}_1 - \slashed{p} + m_t) \gamma^{\mu_3} (-\slashed{k}_2 - \slashed{p} + m_t) \gamma^{\mu_4} \gamma_5} \Big) (\slashed{k}_3 - \slashed{p} + m_b) \Bigg],$$

$$= (\slashed{k}_2 + m_t) \gamma_5 \gamma^{\mu_2} (\slashed{k}_1 + m_t)(\slashed{k}_1 - \slashed{p} + m_t) \gamma^{\mu_3} \gamma_5 (-\slashed{k}_2 - \slashed{p} - m_t) \gamma^{\mu_4}$$

$$= (\slashed{k}_2 + m_t) \gamma^{\mu_2} (\slashed{k}_1 - m_t) \underbrace{\gamma_5 \gamma_5}_{=1} (\slashed{k}_1 - \slashed{p} - m_t) \gamma^{\mu_3} (-\slashed{k}_2 - \slashed{p} - m_t) \gamma^{\mu_4}$$

$$\tag{6.30}$$

$$\mathcal{T}^A_{GB} = Tr \Bigg[(\slashed{k}_3 + m_b) \big\{ M_- (-\slashed{k}_2 + m_t) \gamma^{\mu_2} (\slashed{k}_1 + m_t)(\slashed{k}_1 - \slashed{p} + m_t) \gamma^{\mu_3} (-\slashed{k}_2 - \slashed{p} + m_t)$$

$$- M_+ \underbrace{\gamma_5 (-\slashed{k}_2 + m_t) \gamma^{\mu_2} (\slashed{k}_1 + m_t)(\slashed{k}_1 - \slashed{p} + m_t) \gamma^{\mu_3} (-\slashed{k}_2 - \slashed{p} + m_t) \gamma_5} \big\} (\slashed{k}_3 - \slashed{p} + m_b) \Bigg],$$

$$= (\slashed{k}_2 + m_t) \gamma^{\mu_2} (\slashed{k}_1 - m_t) \underbrace{\gamma_5 \gamma_5}_{=1} (\slashed{k}_1 - \slashed{p} - m_t) \gamma^{\mu_3} (\slashed{k}_2 + \slashed{p} + m_t)$$

$$\tag{6.31}$$

149

with

$$M_- \equiv \frac{(m_b - m_t)^2}{m_W^2}, \quad M_+ \equiv \frac{(m_t + m_b)^2}{m_W^2}. \tag{6.32}$$

Every other diagram from table 6.1 starting with an $Ht\bar{t}$ vertex reveals a similar structure after expressing it through Feynman rules. They are summarised in table 6.5&6.6.
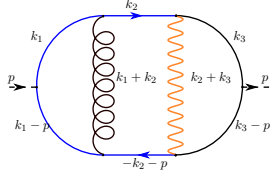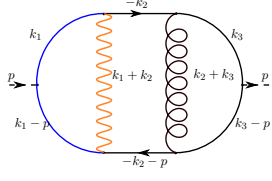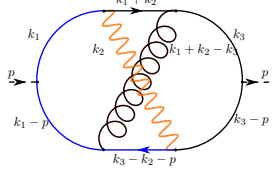
Diagrams	Expressions via Feynman rules
A_{255}	$\Sigma^A(p) = N_C C_F \frac{g^4 g_s^2}{32} \frac{m_t m_b}{m_W^2} \int \frac{d^D k_1}{(2\pi)^D} \int \frac{d^D k_2}{(2\pi)^D} \int \frac{d^D k_3}{(2\pi)^D} \left[\prod_{i=1}^8 P_i^A\right]^{-1}$ $\left(-g_{\mu_2\mu_3} + (1-\xi_g)\frac{(k_1+k_2)_{\mu_2}(k_1+k_2)_{\mu_3}}{P_3^A}\right)\left(-g_{\mu_1\mu_4}\mathcal{T}_W^A + \mathcal{T}_{GB}^A\right),$ $\mathcal{T}_W^A = Tr\left[(\slashed{k}_3+m_b)\gamma^{\mu_1}\left((-\slashed{k}_2+m_t)\gamma^{\mu_2}(\slashed{k}_1+m_t)(\slashed{k}_1-\slashed{p}+m_t)\gamma^{\mu_3}(-\slashed{k}_2-\slashed{p}+m_t)\gamma^{\mu_4}\right.\right.$ $\left.\left.+(\slashed{k}_2+m_t)\gamma^{\mu_2}(\slashed{k}_1-m_t)\underbrace{\gamma_5\gamma_5}_{=1}(\slashed{k}_1-\slashed{p}-m_t)\gamma^{\mu_3}(-\slashed{k}_2-\slashed{p}-m_t)\gamma^{\mu_4}\right)(\slashed{k}_3-\slashed{p}+m_b)\right],$ $\mathcal{T}_{GB}^A = Tr\left[(\slashed{k}_3+m_b)\left\{M_-(-\slashed{k}_2+m_t)\gamma^{\mu_2}(\slashed{k}_1+m_t)(\slashed{k}_1-\slashed{p}+m_t)\gamma^{\mu_3}(-\slashed{k}_2-\slashed{p}+m_t)\right.\right.$ $\left.\left.-M_+(\slashed{k}_2+m_t)\gamma^{\mu_2}(\slashed{k}_1-m_t)\underbrace{\gamma_5\gamma_5}_{=1}(\slashed{k}_1-\slashed{p}-m_t)\gamma^{\mu_3}(\slashed{k}_2+\slashed{p}+m_t)\right\}(\slashed{k}_3-\slashed{p}+m_b)\right].$
B_{255}	$\Sigma^B(p) = N_C C_F \frac{g^4 g_s^2}{32} \frac{m_t m_b}{m_W^2} \int \frac{d^D k_1}{(2\pi)^D} \int \frac{d^D k_2}{(2\pi)^D} \int \frac{d^D k_3}{(2\pi)^D} \left[\prod_{i=1}^8 P_i^B\right]^{-1}$ $\left(-g_{\mu_1\mu_4} + (1-\xi_g)\frac{(k_2+k_3)_{\mu_1}(k_2+k_3)_{\mu_4}}{P_5^B}\right)\left(-g_{\mu_2\mu_3}\mathcal{T}_W^B + \mathcal{T}_{GB}^B\right),$ $\mathcal{T}_W^B = Tr\left[(\slashed{k}_3+m_b)\gamma^{\mu_1}(-\slashed{k}_2+m_b)\gamma^{\mu_2}\left\{(\slashed{k}_1+m_t)(\slashed{k}_1-\slashed{p}+m_t)\right.\right.$ $\left.\left.+(-\slashed{k}_1+m_t)\underbrace{\gamma_5\gamma_5}_{=1}(\slashed{k}_1-\slashed{p}-m_t)\right\}\gamma^{\mu_3}(-(\slashed{k}_2+\slashed{p})+m_b)\gamma^{\mu_4}(\slashed{k}_3-\slashed{p}+m_b)\right],$ $\mathcal{T}_{GB}^B = Tr\left[(\slashed{k}_3+m_b)\gamma^{\mu_1}(-\slashed{k}_2+m_b)\left\{M_-(\slashed{k}_1+m_t)(\slashed{k}_1-\slashed{p}+m_t)\right.\right.$ $\left.\left.-M_+(-\slashed{k}_1+m_t)\underbrace{\gamma_5\gamma_5}_{=1}(-\slashed{k}_1+\slashed{p}+m_t)\right\}(-\slashed{k}_2-\slashed{p}+m_b)\gamma^{\mu_4}(\slashed{k}_3-\slashed{p}+m_b)\right]$
C_{255}	$\Sigma^C(p) = N_C C_F \frac{g^4 g_s^2}{32} \frac{m_t m_b}{m_W^2} \int \frac{d^D k_1}{(2\pi)^D} \int \frac{d^D k_2}{(2\pi)^D} \int \frac{d^D k_3}{(2\pi)^D} \left[\prod_{i=1}^8 P_i^C\right]^{-1}$ $\left(-g_{\mu_2\mu_4}\mathcal{T}_W^C + \mathcal{T}_{GB}^C\right)\left(-g_{\mu_1\mu_3} + (1-\xi_g)\frac{(k_1+k_2-k_3)_{\mu_1}(k_1+k_2-k_3)_{\mu_3}}{P_4^C}\right),$ $\mathcal{T}_W^C = Tr\left[(\slashed{k}_3+m_b)\gamma^{\mu_1}(\slashed{k}_1+\slashed{k}_2+m_b)\gamma^{\mu_2}\left\{(\slashed{k}_1+m_t)(\slashed{k}_1-\slashed{p}+m_t)\gamma^{\mu_3}(\slashed{k}_3-\slashed{k}_2-\slashed{p}+m_t)\right.\right.$ $\left.\left.+(-\slashed{k}_1+m_t)\underbrace{\gamma_5\gamma_5}_{=1}(\slashed{k}_1-\slashed{p}-m_t)\gamma^{\mu_3}(\slashed{k}_3-\slashed{k}_2-\slashed{p}-m_t)\right\}\gamma^{\mu_4}(\slashed{k}_3-\slashed{p}+m_b)\right],$ $\mathcal{T}_{GB}^C = Tr\left[(\slashed{k}_3+m_b)\gamma^{\mu_1}(\slashed{k}_1+\slashed{k}_2+m_b)\left\{M_-(\slashed{k}_1+m_t)(\slashed{k}_1-\slashed{p}+m_t)\gamma^{\mu_3}(\slashed{k}_3-\slashed{k}_2-\slashed{p}+m_t)\right.\right.$ $\left.\left.-M_+(-\slashed{k}_1+m_t)(\slashed{k}_1-\slashed{p}-m_t)\gamma^{\mu_3}\underbrace{\gamma_5\gamma_5}_{=1}(-\slashed{k}_3+\slashed{k}_2+\slashed{p}+m_t)\right\}(\slashed{k}_3-\slashed{p}+m_b)\right].$

Table 6.5: Diagrams proportional to the product of Yukawa couplings $y_b y_t$ expressed via Feynman rules from section 2.2.1; Part 1. Dashed lines denote Higgs bosons, curled lines gluons, orange lines W-bosons/charged Goldstone bosons, straight black lines bottom quarks and blue lines top-quarks. Propagators P_i^X are defined in table 5.1, M_+, M_- in (6.32).
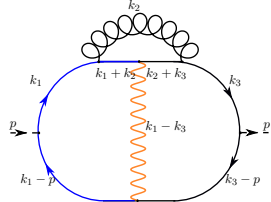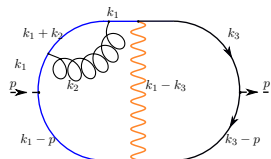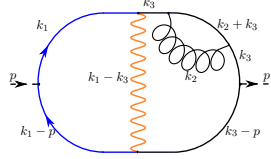
Diagrams	Expressions via Feynman rules
D_{255}	$\Sigma_{225}^D(p) = N_C C_F \frac{g^4 g_s^2}{32} \frac{m_t m_b}{m_W^2} \int \frac{d^D k_1}{(2\pi)^D} \int \frac{d^D k_2}{(2\pi)^D} \int \frac{d^D k_3}{(2\pi)^D} \left[\prod_{i=1}^8 P_i^D\right]^{-1}$ $\left(-g_{\mu_1\mu_3} + (1-\xi_g)\frac{(k_2)_{\mu_1}(k_2)_{\mu_3}}{P_5^D}\right)\left(-g_{\mu_2\mu_4}\mathcal{T}_W^D + \mathcal{T}_{GB}^D\right),$ $\mathcal{T}_W^D = Tr\Big[(\slashed{k}_3+m_b)\gamma^{\mu_1}(\slashed{k}_2+\slashed{k}_3+m_b)\gamma^{\mu_2}\big\{(\slashed{k}_1+\slashed{k}_2+m_t)\gamma^{\mu_3}(\slashed{k}_1+m_t)(\slashed{k}_1-\slashed{p}+m_t)\gamma^{\mu_4}$ $+(-\slashed{k}_1-\slashed{k}_2+m_t)\underbrace{\gamma_5\gamma_5}_{=1}\gamma^{\mu_3}(\slashed{k}_1-m_t)(\slashed{k}_1-\slashed{p}-m_t)\gamma^{\mu_4}\big\}(\slashed{k}_3-\slashed{p}+m_b)\Big],$ $\mathcal{T}_{GB}^D = Tr\Big[(\slashed{k}_3+m_b)\gamma^{\mu_1}(\slashed{k}_2+\slashed{k}_3+m_b)\big\{M_-(\slashed{k}_1+\slashed{k}_2+m_t)\gamma^{\mu_3}(\slashed{k}_1+m_t)(\slashed{k}_1-\slashed{p}+m_t)$ $-M_+(-\slashed{k}_1-\slashed{k}_2+m_t)\underbrace{\gamma_5\gamma_5}_{=1}\gamma^{\mu_3}(\slashed{k}_1-m_t)(-\slashed{k}_1+\slashed{p}+m_t)\big\}(\slashed{k}_3-\slashed{p}+m_b)\Big].$
D_{223}	$\Sigma_{223}^D(p) = N_C C_F \frac{g^4 g_s^2}{32} \frac{m_t m_b}{m_W^2} \int \frac{d^D k_1}{(2\pi)^D} \int \frac{d^D k_2}{(2\pi)^D} \int \frac{d^D k_3}{(2\pi)^D}$ $\left(-g_{\mu_2\mu_3} + (1-\xi_g)\frac{(k_2)_{\mu_2}(k_2)_{\mu_3}}{P_5^D}\right)\left(\frac{-g_{\mu_1\mu_4}\mathcal{T}_W^E + \mathcal{T}_{GB}^E}{(P_1^D)^2 P_2^D P_3^D P_4^D P_5^D P_7^D P_8^D}\right),$ $\mathcal{T}_W^E = Tr\Big[(\slashed{k}_3+m_b)\gamma^{\mu_1}\big\{(\slashed{k}_1+m_t)\gamma^{\mu_2}(\slashed{k}_1+\slashed{k}_2+m_t)\gamma^{\mu_3}(\slashed{k}_1+m_t)(\slashed{k}_1-\slashed{p}+m_t)$ $+(-\slashed{k}_1+m_t)\underbrace{\gamma_5\gamma_5}_{=1}\gamma^{\mu_2}(\slashed{k}_1+\slashed{k}_2-m_t)\gamma^{\mu_3}(\slashed{k}_1-m_t)(\slashed{k}_1-\slashed{p}-m_t)\big\}\gamma^{\mu_4}(\slashed{k}_3-\slashed{p}+m_b)\Big],$ $\mathcal{T}_{GB}^E = Tr\Big[(\slashed{k}_3+m_b)\big\{M_-(\slashed{k}_1+m_t)\gamma^{\mu_2}(\slashed{k}_1+\slashed{k}_2+m_t)\gamma^{\mu_3}(\slashed{k}_1+m_t)(\slashed{k}_1-\slashed{p}+m_t)$ $-M_+(-\slashed{k}_1+m_t)\underbrace{\gamma_5\gamma_5}_{=1}\gamma^{\mu_2}(\slashed{k}_1+\slashed{k}_2-m_t)\gamma^{\mu_3}(\slashed{k}_1-m_t)(-\slashed{k}_1+\slashed{p}+m_t)\big\}(\slashed{k}_3-\slashed{p}+m_b)\Big]$
D_{247}	$\Sigma_{247}^D(p) = N_C C_F \frac{g^4 g_s^2}{32} \frac{m_t m_b}{m_W^2} \int \frac{d^D k_1}{(2\pi)^D} \int \frac{d^D k_2}{(2\pi)^D} \int \frac{d^D k_3}{(2\pi)^D}$ $\left(-g_{\mu_1\mu_2} + (1-\xi_g)\frac{(k_2)_{\mu_1}(k_2)_{\mu_2}}{P_5^D}\right)\left(\frac{-g_{\mu_3\mu_4}\mathcal{T}_W^F + \mathcal{T}_{GB}^F}{P_1^D P_2^D P_3^D P_5^D P_6^D (P_7^D)^2 P_8^D}\right),$ $\mathcal{T}_W^F = Tr\Big[(\slashed{k}_3+m_b)\gamma^{\mu_1}(\slashed{k}_2+\slashed{k}_3+m_b)\gamma^{\mu_2}(\slashed{k}_3+m_b)\gamma^{\mu_3}\big\{(\slashed{k}_1+m_t)(\slashed{k}_1-\slashed{p}+m_t)$ $+(-\slashed{k}_1+m_t)\underbrace{\gamma_5\gamma_5}_{=1}(\slashed{k}_1-\slashed{p}-m_t)\big\}\gamma^{\mu_4}(\slashed{k}_3-\slashed{p}+m_b)\Big],$ $\mathcal{T}_{GB}^F = Tr\Big[(\slashed{k}_3+m_b)\gamma^{\mu_1}(\slashed{k}_2+\slashed{k}_3+m_b)\gamma^{\mu_2}(\slashed{k}_3+m_b)\big\{M_-(\slashed{k}_1+m_t)(\slashed{k}_1-\slashed{p}+m_t)$ $-M_+(-\slashed{k}_1+m_t)\underbrace{\gamma_5\gamma_5}_{=1}(-\slashed{k}_1+\slashed{p}+m_t)\big\}(\slashed{k}_3-\slashed{p}+m_b)\Big].$

Table 6.6: Diagrams proportional to the product of Yukawa couplings $y_b y_t$ expressed via Feynman rules from section 2.2.1; Part 2. Dashed lines denote Higgs bosons, curled lines gluons, orange lines W-bosons/charged Goldstone bosons, straight black lines bottom quarks and blue lines top-quarks. Propagators P_i^D are defined in table 5.1, M_+, M_- in (6.32).

The diagrams starting with an $Ht\bar{t}$ vertex involving a W-boson yield the same prefactor as those involving a charged Goldstone boson. The former contain W-boson propagators and therefore an additional metric tensor as opposed to the latter containing scalar Goldstone boson propagators.

6.4.2 Diagrams not proportional to the product of Yukawa couplings $y_b y_t$

The diagrams containing either an HW^+W^- or an $H\Phi^+\Phi^-$ vertex differ in there prefactor and structure. We provide one explanatory example, the seventh diagram in table 6.1. We start with the version of the diagram containing two W-boson propagators, displayed in fig.6.5.
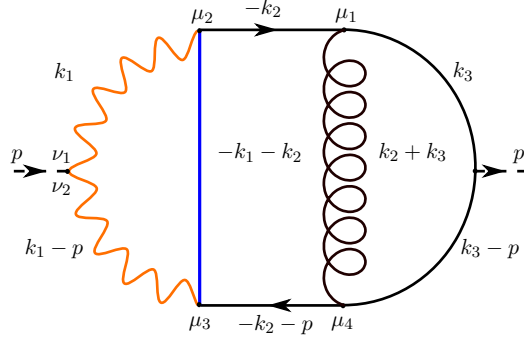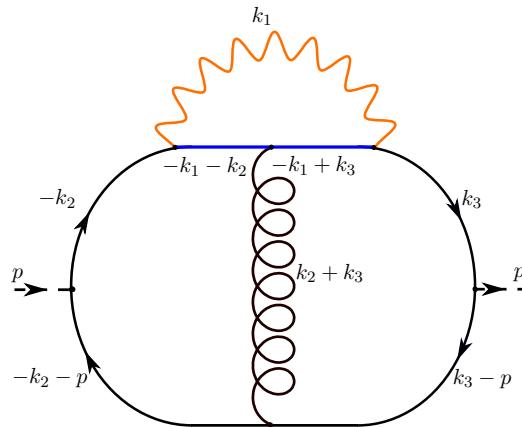

Figure 6.5: The diagram corresponding to topology B' sector 255 with W-boson. Dashed lines denote Higgs bosons, curled lines gluons, orange lines W-bosons, straight black lines bottom quarks and blue lines top-quarks.

We express fig.6.5 in terms of Feynman rules (section 2.2.1) and simplify the outcome,

$$\Sigma_W^{B',255}(p) = -N_C C_F \frac{g^4 g_s^2 m_b}{16} \int \frac{d^D k_1}{(2\pi)^D} \int \frac{d^D k_2}{(2\pi)^D} \int \frac{d^D k_3}{(2\pi)^D} \left[\prod_{i=1}^{8} P_i^{B'}\right]^{-1} \mathcal{T}_W^{B'}$$
$$\left(-g_{\mu_1\mu_4} + (1-\xi_g)\frac{(k_2+k_3)_{\mu_1}(k_2+k_3)_{\mu_4}}{P_5^{B'}}\right)\underbrace{(-g_{\mu_2\nu_1})(g^{\nu_1\nu_2})(-g_{\nu_2\mu_3})}_{=g_{\mu_2\mu_3}},$$

where the propagators of topology B', $P_i^{B'}$, were defined in table 5.1. The trace of the closed quark loop is

$$\mathcal{T}_W^{B',255} = Tr\Big[(\slashed{k}_3 + m_b)\gamma^{\mu_1}(-\slashed{k}_2 + m_b)\gamma^{\mu_2}(1-\gamma_5)(-\slashed{k}_1 - \slashed{k}_2 + m_t)\gamma^{\mu_3}(1-\gamma_5)$$
$$(-\left(\slashed{k}_2+\slashed{p}\right) + m_b)\gamma^{\mu_4}(\slashed{k}_3 - \slashed{p} + m_b)\Big]$$
$$= Tr\Big[(\slashed{k}_3 + m_b)\gamma^{\mu_1}(-\slashed{k}_2 + m_b)\gamma^{\mu_2}\big\{(-\slashed{k}_1 - \slashed{k}_2 + m_t)$$
$$+ \underbrace{\gamma_5\gamma_5}_{=1}(-\slashed{k}_1 - \slashed{k}_2 - m_t)\big\}\gamma^{\mu_3}(-\left(\slashed{k}_2+\slashed{p}\right) + m_b)\gamma^{\mu_4}(\slashed{k}_3 - \slashed{p} + m_b)\Big].$$

The version of fig.6.5 containing two charged Goldstone bosons instead of W-bosons evaluates to

$$\Sigma_{GB}^{B',255}(p) = - \, N_C C_F \frac{g^4 g_s^2}{32} \frac{m_b m_h^2}{m_W^2} \int \frac{d^D k_1}{(2\pi)^D} \int \frac{d^D k_2}{(2\pi)^D} \int \frac{d^D k_3}{(2\pi)^D} \left[\prod_{i=1}^{8} P_i^{B'} \right]^{-1} \mathcal{T}_{GB}^{B'}$$

$$\left(-g_{\mu_1\mu_4} + (1-\xi_g) \frac{(k_2+k_3)_{\mu_1}(k_2+k_3)_{\mu_4}}{P_5^{B'}} \right), \tag{6.33}$$

where the trace is

$$\mathcal{T}_{GB}^{B',255} = Tr\Big[(\slashed{k}_3 + m_b)\gamma^{\mu_1}(-\slashed{k}_2 + m_b)\big\{ M_-((-\slashed{k}_1 - \slashed{k}_2 + m_t) $$
$$- M_+ \underbrace{\gamma_5\gamma_5}_{=1}(\slashed{k}_1 + \slashed{k}_2 + m_t)\big\}(-\slashed{k}_2 - \slashed{p} + m_b)\gamma^{\mu_4}(\slashed{k}_3 - \slashed{p} + m_b)\Big],$$

with M_+, M_- defined in (6.32).

We unite (6.33) and (6.33) to demonstrate the general structure of all pairs of diagrams containing a HW^+W^- and $H\Phi^+\Phi^-$ vertex, respectively.

$$\Sigma_{255}^{B'} = \Sigma_W^{B',255}(p) + \Sigma_{GB}^{B',255}(p) = N_C C_F \frac{g^4 g_s^2 m_b}{16} \int \frac{d^D k_1}{(2\pi)^D} \int \frac{d^D k_2}{(2\pi)^D} \int \frac{d^D k_3}{(2\pi)^D} \left[\prod_{i=1}^{8} P_i^{B'} \right]^{-1}$$

$$\left(-g_{\mu_1\mu_4} + (1-\xi_g) \frac{(k_2+k_3)_{\mu_1}(k_2+k_3)_{\mu_4}}{P_5^{B'}} \right) \left(-g_{\mu_2\mu_3} \mathcal{T}_W^{B',255} - \frac{m_h^2}{2m_W^2} \mathcal{T}_{GB}^{B',255} \right), \tag{6.34}$$

The diagrams proportional to the product of Yukawa coupling $y_b y_b$, i.e. the diagrams involving two $Hb\bar{b}$ vertices, contain the smallest prefactor, due to the ratio $\frac{m_b^2}{m_W^2}$. Here, we provide one explanatory example as well, namely the first diagram in table 6.2. The diagram with W-boson is illustrated in fig.6.6.

Figure 6.6: The diagram corresponding to topology B' sector 509 with W-boson. Dashed lines denote Higgs bosons, curled lines gluons, orange lines W-bosons, straight black lines bottom quarks and blue lines top-quarks.

Together with the corresponding diagram containing a Goldstone boson, fig.6.6 expressed via Feynman rules (section 2.2.1) and simplified afterwards becomes

$$
\begin{aligned}
\Sigma_{509}^{B'}(p) =& N_C C_F \frac{g^4 g_s^2}{32} \frac{m_b^2}{m_W^2} \int \frac{d^D k_1}{(2\pi)^D} \int \frac{d^D k_2}{(2\pi)^D} \int \frac{d^D k_3}{(2\pi)^D} \prod_{\substack{i=1\\i\neq 2}}^{9} \left(P_i^{B'}\right)^{-1} \\
& \left(-g_{\mu_2\mu_4} + (1-\xi_g)\frac{(k_2+k_3)_{\mu_2}(k_2+k_3)_{\mu_4}}{P_5^{B'}}\right)\left(-g_{\mu_1\mu_3}\mathcal{T}_W^{B',509} + \mathcal{T}_{GB}^{B',509}\right),
\end{aligned}
$$

$$(6.35)$$

where the respective traces are

$$
\begin{aligned}
\mathcal{T}_W^{B',509} =& Tr\Big[(\slashed{k}_3 + m_b)\gamma^{\mu_1}(1-\gamma_5)(-\slashed{k}_1+\slashed{k}_3+m_t)\gamma^{\mu_2}(-\slashed{k}_1-\slashed{k}_2+m_t) \\
& \gamma^{\mu_3}(1-\gamma_5)(-\slashed{k}_2+m_b)(-\slashed{k}_2-\slashed{p}+m_b)\gamma^{\mu_4}(\slashed{k}_3-\slashed{p}+m_b)\Big] \\
=& Tr\Big[(\slashed{k}_3 + m_b)\gamma^{\mu_1}\big\{(-\slashed{k}_1+\slashed{k}_3+m_t)\gamma^{\mu_2}(-\slashed{k}_1-\slashed{k}_2+m_t) + (-\slashed{k}_1+\slashed{k}_3-m_t)\gamma^{\mu_2} \\
& \underbrace{\gamma_5\gamma_5}_{=1}(-\slashed{k}_1-\slashed{k}_2-m_t)\big\}\gamma^{\mu_3}(-\slashed{k}_2+m_b)(-\slashed{k}_2-\slashed{p}+m_b)\gamma^{\mu_4}(\slashed{k}_3-\slashed{p}+m_b)\Big],
\end{aligned}
$$

$$
\begin{aligned}
\mathcal{T}_{GB}^{B',509} =& \\
& Tr\Big[(\slashed{k}_3 + m_b)\left((1+\gamma_5)\frac{m_t}{m_W} - (1-\gamma_5)\frac{m_b}{m_W}\right)(-\slashed{k}_1+\slashed{k}_3+m_t)\gamma^{\mu_2}(-\slashed{k}_1-\slashed{k}_2+m_t) \\
& \left((1-\gamma_5)\frac{m_t}{m_W} - (1+\gamma_5)\frac{m_b}{m_W}\right)(-\slashed{k}_2+m_b)(-\slashed{k}_2-\slashed{p}+m_b)\gamma^{\mu_4}(\slashed{k}_3-\slashed{p}+m_b)\Big] \\
=& Tr\Big[(\slashed{k}_3 + m_b)\big\{M_-(-\slashed{k}_1+\slashed{k}_3+m_t)\gamma^{\mu_2}(-\slashed{k}_1-\slashed{k}_2+m_t) - M_+(-\slashed{k}_1+\slashed{k}_3-m_t)\gamma^{\mu_2} \\
& \underbrace{\gamma_5\gamma_5}_{=1}(\slashed{k}_1+\slashed{k}_2+m_t)\big\}(-\slashed{k}_2+m_b)(-\slashed{k}_2-\slashed{p}+m_b)\gamma^{\mu_4}(\slashed{k}_3-\slashed{p}+m_b)\Big].
\end{aligned}
$$

In this section, we explained the steps accompanying the evaluation of the scattering amplitude $\Sigma_H^{(\alpha^2\alpha_s)_W}$ related to the mixed QCD-electroweak corrections to the decay rate $H \to b\bar{b}$ via the optical theorem (6.7), see especially (6.19), (6.23) and (6.25). We discussed the emerging colour factor (6.9) and the fifth Dirac matrix in NDR (6.15), (6.16). The resulting scattering amplitude (6.25) depends on the master integrals, we derived in the subsequent chapter (5.69), (5.70), (5.71). As already mentioned they contain ultraviolet divergences. Hence, we consider renormalisation in the next section.

6.5 Renormalisation

In section 6.2, we decided to calculate the mixed QCD-electroweak corrections involving W-/charged Goldstone bosons $\Delta_W^{(\alpha\alpha_s)}$ to $\Gamma\left(H \to b\bar{b}\right)$ with the help of the optical theorem (6.7). Consequently, we started calculating a three-loop two-point scattering amplitude in section 6.4. The scattering amplitude corresponds to a sum over the master integrals

derived in the subsequent chapter (5.69), (5.70), (5.71),

$$\Sigma_H^{(\alpha^2\alpha_s)_W}(p) = N_C C_F g^4 g_s^2 \left(\sum_j^{N_{MI}^1} f_j^1 J_j + \sum_j^{N_{MI}^{2a}} f_j^{2a} K_j + \sum_j^{N_{MI}^{2b}} f_j^{2b} L_j \right),$$

with rational factors f_j^s. Feynman diagrams may give rise to integrals containing divergences, as elaborated in section 2.3. Sine we work in dimensional regularisation with $D = (4 - 2\epsilon)$, these manifest themselves as poles in the dimensional regularisation parameter $\frac{1}{\epsilon}$. We may remove the ultraviolet divergent parts emerging out of the diagrams in table 6.1 and table 6.2 if we consider appropriate counter term diagrams. Evaluating them we obtain the same poles in ϵ, but with inverse sign. Appropriate counter term diagrams are found if loops of the original diagrams are pinched and counter term insertions are placed instead. They may also be generated with QGRAF [115] or FeynArts [116]. In this section, we discuss the counter term diagrams corresponding to the diagrams proportional to the product of Yukawa couplings $y_b y_t$ (table 6.5, table 6.6) in order to illustrate the concept of renormalisation.

We consider the diagram corresponding to topology A sector 255 (see section 6.4.1, fig.6.4) as example and display the diagrams cancelling its UV-divergent parts in fig.6.7. These diagrams are obtained as we close one or both loops and insert a counterterm instead, denoted by a cross. The former exchange particle demands the proportionality of the inserted counterterm. Closing the right loop of the original diagram containing a W-/charged Goldstone, we construct the diagram in the middle of fig.6.7, with a counterterm insertion proportional to $\alpha = \frac{g^2}{4\pi}$. We construct the diagram in the right of fig.6.7 if we close the left loop of the original diagram containing a gluon and place a counterterm insertion proportional to $\alpha_s = \frac{g_s^2}{4\pi}$ instead. Pinching both loops simultaneously, we obtain the first diagram in fig.6.7.
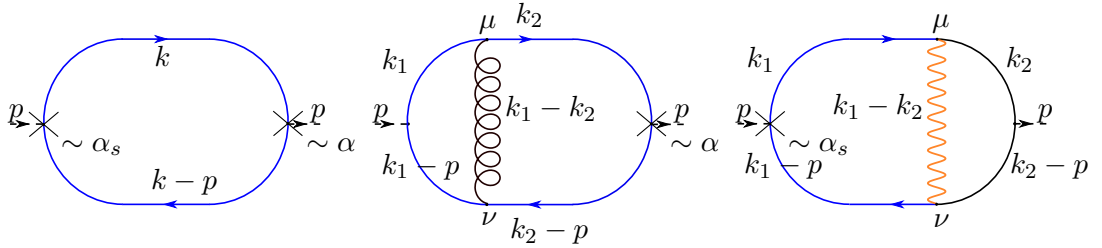
Figure 6.7: The counterterm diagrams cancelling the UV-divergent parts of the diagrams corresponding to topology A sector 255 displayed in fig.6.4. Dashed lines denote Higgs bosons, curled lines gluons, orange lines W-bosons, straight black lines bottom quarks and blue lines top-quarks. Counterterm insertions are denoted by a cross.

We calculate the diagrams in fig.6.7 in the same way we calculated the original Feynman diagrams. We label momenta according to momentum conservation and apply Feynman rules. The Feynman rules for counterterm insertions are listed in the appendix C.2. They depend on renormalisation constants, defined by the chosen renormalisation scheme. We have to take the renormalisation constant at the correct order of coupling constants (see (C.7), (C.2), (C.2)). In correspondence, the one-loop diagram of fig.6.7 evaluates to

$$\Sigma_{CT}^{A,1}(p, m_t^2)$$

$$= \int \frac{d^D k}{(2\pi)^D} N_C Tr\left[-i\frac{\alpha}{4\pi} Z_{Hqq}^{\alpha,1} \frac{gm_t}{2m_W} i\frac{\slashed{k}+m_t}{k^2-m_t^2}\left(-i\frac{\alpha_s}{4\pi} Z_{Hqq}^{\alpha_s,1}\frac{gm_t}{2m_W}\right) i\frac{\slashed{k}-\slashed{p}+m_t}{(k-p)^2-m_t^2}\right]$$

$$= \int \frac{d^D k}{(2\pi)^D} N_C \frac{\alpha^2 \alpha_s}{4^2\pi}\frac{m_t^2}{m_W^2} Z_{Hqq}^{\alpha,1} Z_{Hqq}^{1,\alpha_s} \underbrace{\frac{Tr\left[(\slashed{k}+m_t)(\slashed{k}-\slashed{p}+m_t)\right]}{\left(k^2-m_t^2\right)\left((k-p)^2-m_t^2\right)}}_{\frac{4(k.(k-p)+m_t^2)}{(k^2-m_t^2)((k-p)^2-m_t^2)}}$$

$$=\left(\frac{2}{k^2-m_t^2}+\frac{2}{(k-p)^2-m_t^2}+\frac{8m_t^2-2p^2}{(k^2-m_t^2)((k-p)^2-m_t^2)}\right)$$

$$= ie^{-\epsilon\gamma_E} N_C \frac{\alpha^2 \alpha_s}{4^{D/2+2}\pi^{D/2+1}}\frac{m_t^2}{m_W^2} Z_{Hqq}^{\alpha,1} Z_{Hqq}^{\alpha_s,1}$$

$$\left(-2\left(\mu^2\right)^{\frac{D}{2}-1} T_1(D, m_t^2) + 2\left(4m_t^2 - p^2\right)\left(\mu^2\right)^{\frac{D}{2}-2} B_{11}(p^2, m_t^2, m_t^2)\right),$$

with the tadpole T_ν (3.13) and the bubble integral $B_{\nu_1\nu_2}$ (3.24) as defined in section 3.2.

The diagram in the middle of fig.6.7 with a counterterm insertion proportional to α becomes

$$\Sigma_{CT}^{A,2,gluon}(p, m_t^2) = \int \frac{d^D k_1}{(2\pi)^D}\int \frac{d^D k_2}{(2\pi)^D} i\alpha^2 \alpha_s \pi N_C C_F \frac{m_t^2}{m_W^2}$$

$$Z_{Hqq}^{\alpha,1}\left[-g_{\mu\nu} + (1-\xi_q)\frac{(k_1-k_2)_\mu(k_1-k_2)_\nu}{(k_1-k_2)^2}\right]$$

$$\frac{Tr\left[(\slashed{k}_2+m_t)\gamma^\mu(\slashed{k}_1+m_t)(\slashed{k}_1-\slashed{p}+m_t)\gamma^\nu(\slashed{k}_2-\slashed{p}+m_t)\right]}{(k_2^2-m_t^2)(k_1^2-m_t^2)\left((k_1-p)^2-m_t^2\right)\left((k_2-p)^2-m_t^2\right)(k_1-k_2)^2}.$$

The resulting Feynman integrals correspond to topology $CT1$ with propagators P^{CT1},

$$P_1^{CT1} = k_1^2 - m_t^2,$$
$$P_2^{CT1} = k_2^2 - m_t^2,$$
$$P_3^{CT1} = (k_1-p)^2 - m_t^2,$$
$$P_4^{CT1} = (k_2-p)^2 - m_t^2,$$
$$P_5^{CT1} = (k_1-k_2)^2. \tag{6.36}$$

We have to consider the diagram in the right of fig.6.7 with a counterterm insertion proportional to α_s twice, once containing a W-boson $\Sigma_{CT}^{A,2,W}$ and once containing a charged Goldstone boson $\Sigma_{CT}^{A,2,GB}$. We find

$$\Sigma_{CT}^{A,2,W}(p) = \int \frac{d^D k_1}{(2\pi)^D}\int \frac{d^D k_2}{(2\pi)^D} N_C \frac{i\alpha_s\alpha^2\pi}{8}\frac{m_b m_t}{m_W^2} Z_{Hqq}^{\alpha_s,1}\left[-g_{\mu\nu}\right]$$

$$\frac{Tr\left[(\slashed{k}_2+m_b)\gamma^\mu(1-\gamma_5)(\slashed{k}_1+m_t)(\slashed{k}_1-\slashed{p}+m_t)\gamma^\nu(1-\gamma_5)(\slashed{k}_2-\slashed{p}+m_b)\right]}{(k_2^2-m_b^2)(k_1^2-m_t^2)\left((k_1-p)^2-m_t^2\right)\left((k_2-p)^2-m_b^2\right)\left((k_1-k_2)^2-m_W^2\right)},$$

where the trace may be split into

$$Tr\Big[(\not{k}_2 + m_b)\gamma^\mu\Big((\not{k}_1 + m_t)(\not{k}_1 - \not{p} + m_t)\gamma^\nu - \{\gamma_5, (\not{k}_1 + m_t)(\not{k}_1 - \not{p} + m_t)\gamma^\nu\}$$
$$+ \underbrace{\gamma_5(\not{k}_1 + m_t)(\not{k}_1 - \not{p} + m_t)\gamma^\nu\gamma_5}_{=(-\not{k}_1 + m_t)(\not{k}_1 - \not{p} - m_t)\gamma^\nu}\Big)(\not{k}_2 - \not{p} + m_b)\Big]. \tag{6.37}$$

Furthermore,

$$\Sigma_{CT}^{A,2,GB}(p) = \int \frac{d^D k_1}{(2\pi)^D} \int \frac{d^D k_2}{(2\pi)^D} N_C \frac{i\alpha_s\alpha}{8} \frac{g^2 m_b m_t}{4m_W^2} Z_{Hqq}^{\alpha_s,1} \, Tr\Big[(\not{k}_2 + m_b)\Big(\frac{m_t - m_b}{m_W}$$
$$+ \gamma_5 \frac{m_t + m_b}{m_W}\Big)(\not{k}_1 + m_t)(\not{k}_1 - \not{p} + m_t)\Big(\frac{m_t - m_b}{m_W} - \gamma_5 \frac{m_t + m_b}{m_W}\Big)(\not{k}_2 - \not{p} + m_b)\Big]$$
$$\Big[(k_2^2 - m_b^2)(k_1^2 - m_t^2)\big((k_1 - p)^2 - m_t^2\big)\big((k_2 - p)^2 - m_b^2\big)\big((k_1 - k_2)^2 - m_W^2\big)\Big]^{-1},$$

where the trace is

$$Tr\Big[(\not{k}_2 + m_b)\Big(\frac{(m_t - m_b)^2}{m_W^2}(\not{k}_1 + m_t)(\not{k}_1 - \not{p} + m_t) + \frac{m_t^2 + m_b^2}{m_W^2}\Big[\gamma_5, (\not{k}_1 + m_t)(\not{k}_1 - \not{p} + m_t)\Big]$$
$$- \frac{(m_t + m_b)^2}{m_W^2} \underbrace{\gamma_5(\not{k}_1 + m_t)(\not{k}_1 - \not{p} + m_t)\gamma_5}_{=(-\not{k}_1 + m_t)(-\not{k}_1 + \not{p} + m_t)}\Big)(\not{k}_2 - \not{p} + m_b)\Big]. \tag{6.38}$$

The emerging Feynman integrals correspond to topology $CT2$ with propagators P^{CT2},

$$P_1^{CT2} = k_1^2 - m_t^2,$$
$$P_2^{CT2} = k_2^2,$$
$$P_3^{CT2} = (k_1 - p)^2 - m_t^2,$$
$$P_4^{CT2} = (k_2 - p)^2,$$
$$P_5^{CT2} = (k_1 - k_2)^2 - m_W^2. \tag{6.39}$$

We summarise all diagrams with counterterm insertion sufficient to remove the UV-divergent parts of the diagrams proportional to the product of Yukawa couplings $y_b y_t$ (table 6.5, table 6.6) in table 6.7 and table 6.8. We thereby require a third topology,

$$P_1^{CT3} = k_1^2 - m_t^2,$$
$$P_2^{CT3} = k_2^2,$$
$$P_3^{CT3} = (k_1 - k_2)^2 - m_t^2,$$
$$P_4^{CT3} = (k_1 - p)^2 - m_t^2,$$
$$P_5^{CT3} = (k_2 - p)^2. \tag{6.40}$$
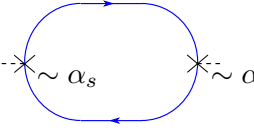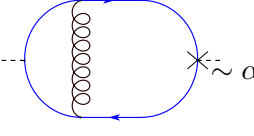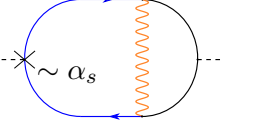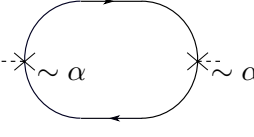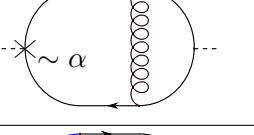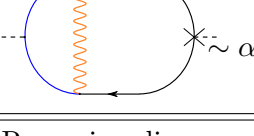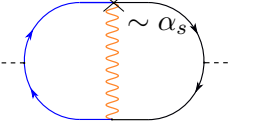
Diagrams	**Expressions via Feynman rules**	**Topology**
Removing divergences from A_{255}, fig.6.4		
	$\Sigma_{CT}^{A,1}(p,m_t^2)=ie^{-\epsilon\gamma_E}N_C\frac{\alpha^2\alpha_s}{4^{D/2+2}\pi^{D/2+1}}\frac{m_t^2}{m_W^2}Z_{Hqq}^{\alpha,1}Z_{Hqq}^{\alpha_s,1}$ $\left(-2(\mu^2)^{\frac{D}{2}-1}T_1(D,m_t^2)+2(4m_t^2-p^2)(\mu^2)^{\frac{D}{2}-2}B_{11}(p^2,m_t^2,m_t^2)\right)$	
	$\Sigma_{CT}^{A,2,gluon}(p,m_t^2)=\int\frac{d^Dk_1}{(2\pi)^D}\int\frac{d^Dk_2}{(2\pi)^D}$ $i\alpha\alpha_sN_CC_F\frac{g^2m_t^2}{4m_W^2}Z_{Hqq}^{\alpha,1}\left[-g_{\mu\nu}+(1-\xi_g)\frac{(k_1-k_2)_\mu(k_1-k_2)_\nu}{(k_1-k_2)^2}\right]$ $\frac{Tr[(k\!\!/_2+m_t)\gamma^\mu(k\!\!/_1+m_t)(k\!\!/_1-p\!\!/+m_t)\gamma^\nu(k\!\!/_2-p\!\!/+m_t)]}{(k_2^2-m_t^2)(k_1^2-m_t^2)((k_1-p)^2-m_t^2)((k_2-p)^2-m_t^2)(k_1-k_2)^2}$	(6.36)
	$\Sigma_{CT}^{A,2,W}(p)=\int\frac{d^Dk_1}{(2\pi)^D}\int\frac{d^Dk_2}{(2\pi)^D}N_C\frac{i\alpha_s\alpha^2\pi}{8}\frac{m_bm_t}{m_W^2}Z_{Hqq}^{\alpha_s,1}[-g_{\mu\nu}]$ $\frac{Tr[(k\!\!/_2+m_b)\gamma^\mu(1-\gamma_5)(k\!\!/_1+m_t)(k\!\!/_1-p\!\!/+m_t)\gamma^\nu(1-\gamma_5)(k\!\!/_2-p\!\!/+m_b)]}{(k_2^2-m_b^2)(k_1^2-m_t^2)((k_1-p)^2-m_t^2)((k_2-p)^2-m_b^2)((k_1-k_2)^2-m_W^2)},$ $\Sigma_{CT}^{A,2,GB}(p)=\int\frac{d^Dk_1}{(2\pi)^D}\int\frac{d^Dk_2}{(2\pi)^D}N_C\frac{i\alpha_s\alpha}{8}\frac{g^2m_bm_t}{4m_W^2}Z_{Hqq}^{\alpha_s,1}$ $Tr\left[(k\!\!/_2+m_b)\left(\frac{m_t-m_b}{m_W}+\gamma_5\frac{m_t+m_b}{m_W}\right)(k\!\!/_1+m_t)\right.$ $\left.(k\!\!/_1-p\!\!/+m_t)\left(\frac{m_t-m_b}{m_W}-\gamma_5\frac{m_t+m_b}{m_W}\right)(k\!\!/_2-p\!\!/+m_b)\right]$ $\left[(k_2^2-m_b^2)(k_1^2-m_t^2)((k_1-p)^2-m_t^2)((k_2-p)^2-m_b^2)((k_1-k_2)^2-m_W^2)\right]^{-1}$	(6.39)
Removing divergences from B_{255}		
	$\Sigma_{CT}^{B,1}=\Sigma_{CT}^{A,1}(p,m_b^2)$	
	$\Sigma_{CT}^{B,2,gluon}=\Sigma_{CT}^{A,2,gluon}(p,m_b^2)$	(6.36)
	$\Sigma_{CT}^{B,2,W+GB}=\Sigma_{CT}^{A,2,W+GB}(p)$	(6.39)
Removing divergences from D_{255}		
	$\Sigma_{CT}^{D}(p)=\frac{Z_{Wqq}^{\alpha_s,1}}{Z_{Hqq}^{\alpha_s,1}}\Sigma_{CT}^{A,2,W+GB}(p)$	(6.39)

Table 6.7: Diagrams removing the UV-divergent parts of the three-loop diagrams proportional to the product of Yukawa couplings y_by_t, which are denoted by topology$_{\text{sector}}$ (table 6.5, table 6.6); Part 1. See description of table 6.8.
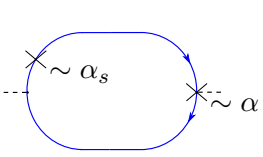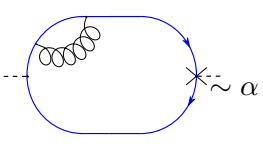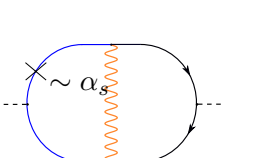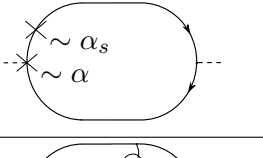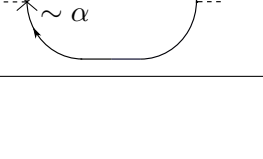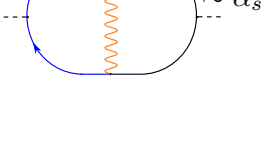
Diagrams	Expressions via Feynman rules	Topology
Removing divergences from D_{223}		
	$\Sigma_{CT}^{E,1}(p,m_t^2)=\int \frac{d^D k}{(2\pi)^D}\frac{N_C\alpha^2\alpha_s}{4^2\pi}$ $\frac{m_t^2}{m_W^2}Z_{Hqq}^{\alpha,1}\frac{Tr\left[\left(Z_2^1\slashed{k}-(Z_2^1+Z_m^1)m_t\right)(\slashed{k}-\slashed{p}+m_t)\right]}{(k-p)^2-m_t^2}$ $=e^{-\epsilon\gamma_E}\left(\mu^2\right)^{\frac{D}{2}-1}\frac{N_C\alpha^2\alpha_s}{4^{D/2+4}\pi^{D/2+3}}\frac{m_t^2}{m_W^2}$ $Z_{Hqq}^{\alpha,1}\left[(3Z_2^1-Z_m^1)m_t^2 T_1(4-2\epsilon,m_t^2)\right]$	
	$\Sigma_{CT}^{E,2,gluon}(p,m_t^2)=\int \frac{d^D k_1}{(2\pi)^D}\int \frac{d^D k_2}{(2\pi)^D}i\alpha\alpha_s N_C C_F\frac{g^2 m_t^2}{4m_W^2}$ $Z_{Hqq}^{\alpha,1}\left[-g_{\mu\nu}+(1-\xi_g)\frac{k_{2\mu}k_{2\nu}}{k_2^2}\right]$ $\frac{Tr\left[(\slashed{k}_1+m_t)\gamma^\mu(\slashed{k}_1-\slashed{k}_2+m_t)\gamma^\nu(\slashed{k}_1+m_t)(\slashed{k}_1-\slashed{p}+m_t)\right]}{(k_1^2-m_t^2)^2((k_1-p)^2-m_t^2)((k_1-k_2)^2-m_t^2)k_2^2}$	(6.40)
	$\Sigma_{CT}^{E,2,W}(p)=\int \frac{d^D k_1}{(2\pi)^D}\int \frac{d^D k_2}{(2\pi)^D}N_C\frac{i\alpha_s\alpha^2\pi}{8}\frac{m_b m_t}{m_W^2}[-g_{\mu\nu}]$ $\frac{Tr\left[(\slashed{k}_2+m_b)\gamma^\mu(1-\gamma_5)\left[Z_2^1\slashed{k}_1-(Z_2^1+Z_m^1)m_t\right](\slashed{k}_1-\slashed{p}+m_t)\gamma^\nu(1-\gamma_5)(\slashed{k}_2-\slashed{p}+m_b)\right]}{(k_2^2-m_b^2)((k_1-p)^2-m_t^2)((k_2-p)^2-m_b^2)((k_1-k_2)^2-m_W^2)}$, $\Sigma_{CT}^{E,2,GB}(p)=\int \frac{d^D k_1}{(2\pi)^D}\int \frac{d^D k_2}{(2\pi)^D}N_C\frac{i\alpha_s\alpha^2\pi}{8}\frac{m_b m_t}{m_W^2}$ $Tr\left[(\slashed{k}_2+m_b)\left(\frac{m_t-m_b}{m_W}\gamma_5\frac{m_t+m_b}{m_W}\right)\left[Z_2^1\slashed{k}_1-(Z_2^1+Z_m^1)m_t\right]\right.$ $\left.(\slashed{k}_1-\slashed{p}+m_t)\left(\frac{m_t-m_b}{m_W}-\gamma_5\frac{m_t+m_b}{m_W}\right)(\slashed{k}_2-\slashed{p}+m_b)\right]$ $\left[(k_2^2-m_b^2)((k_1-p)^2-m_t^2)((k_2-p)^2-m_b^2)((k_1-k_2)^2-m_W^2)\right]^{-1}$	(6.39)
Removing divergences from D_{247}		
	$\Sigma_{CT}^{F,1}=\Sigma_{CT}^{E,1}(p,m_b^2)$	
	$\Sigma_{CT}^{F,2,gluon}=\Sigma_{CT}^{E,2,gluon}(p,m_b^2)$	(6.40)
	$\Sigma_{CT}^{F,2,W}(p)=\int \frac{d^D k_1}{(2\pi)^D}\int \frac{d^D k_2}{(2\pi)^D}N_C\frac{i\alpha_s\alpha^2\pi}{8}\frac{m_b m_t}{m_W^2}[-g_{\mu\nu}]$ $\frac{Tr\left[\left(Z_2^1\slashed{k}_2-(Z_2^1+Z_m^1)m_b\right)\gamma^\mu(1-\gamma_5)(\slashed{k}_1+m_t)(\slashed{k}_1-\slashed{p}+m_t)\gamma^\nu(1-\gamma_5)(\slashed{k}_2-\slashed{p}+m_b)\right]}{(k_1^2-m_t^2)((k_1-p)^2-m_t^2)((k_2-p)^2-m_b^2)((k_1-k_2)^2-m_W^2)}$, $\Sigma_{CT}^{F,2,GB}(p)=\int \frac{d^D k_1}{(2\pi)^D}\int \frac{d^D k_2}{(2\pi)^D}N_C\frac{i\alpha_s\alpha^2\pi}{8}\frac{m_b m_t}{m_W^2}$ $Tr\left[\left(Z_2^1\slashed{k}_2-(Z_2^1+Z_m^1)m_b\right)\left(\frac{m_t-m_b}{m_W}+\gamma_5\frac{m_t+m_b}{m_W}\right)(\slashed{k}_1+m_t)\right.$ $\left.(\slashed{k}_1-\slashed{p}+m_t)\left(\frac{m_t-m_b}{m_W}-\gamma_5\frac{m_t+m_b}{m_W}\right)(\slashed{k}_2-\slashed{p}+m_b)\right]$ $\left[(k_1^2-m_t^2)((k_1-p)^2-m_t^2)((k_2-p)^2-m_b^2)((k_1-k_2)^2-m_W^2)\right]^{-1}$	(6.39)

Table 6.8: Diagrams removing the UV-divergent parts of the three-loop diagrams proportional to the product of Yukawa couplings $y_b y_t$, which are denoted by topology$_{sector}$ (table 6.5, table 6.6); Part 2. Crosses denote counterterm insertions, dashed lines denote Higgs bosons, curled lines gluons, orange lines W-/charged Goldstone bosons, straight black lines bottom quarks and blue lines top-quarks.

159

6.6   Outlook

The partial decay width of the Higgs boson's predominant decay mode,

$$\Gamma\left(H \to b\bar{b}\right) = \Gamma^{(0)}(1 + \Delta^{(\alpha_s)} + \Delta^{(\alpha)} + \Delta^{(\alpha\alpha_s)} + ...),$$

significantly influences the Higgs boson's total decay width and, therefore, its branching ratios. A precise theoretical prediction is indispensable. We address mixed QCD-electroweak corrections involving W-bosons or charged Goldstone bosons, a rather complicated contribution. As discussed in section 6.2, we utilise the optical theorem,

$$\Gamma\left(H \to b\bar{b}\right) = \frac{1}{m_H}\text{Im}\left(\Sigma_H(p^2 = m_H^2 + i\epsilon)\right),$$

$$\Rightarrow \Delta_W^{(\alpha\alpha_s)} = \frac{1}{m_H}\text{Im}\left(\Sigma_H^{(\alpha^2\alpha_s)_W}(p^2 = m_H^2 + i\epsilon)\right), \tag{6.41}$$

relating the decay rate to the imaginary part of a two-point function. In section 6.3 (table 6.1 and table 6.2), we derived all Feynman diagrams entering the right hand side of (6.41). The diagrams are expressible through the topologies discussed in section 5.2. Hence, it is possible to determine the scattering amplitude $\Sigma_H^{(\alpha^2\alpha_s)_W}$ (see section 6.4) as sum over the master integrals of uniform weight derived in chapter 5 ($\vec{J}$ (5.69), $\vec{K}$ (5.70), $\vec{L}$ (5.71)),

$$\Sigma_H^{(\alpha^2\alpha_s)_W}(p) = N_C C_F g^4 g_s^2 \left(\sum_j^{N_{MI}^1} f_j^1 J_j + \sum_j^{N_{MI}^{2a}} f_j^{2a} K_j + \sum_j^{N_{MI}^{2b}} f_j^{2b} L_j\right),$$

with rational factors f_j.

Beforehand, we have to calculate the scattering amplitude via Feynman rules. In section 6.4.1 and section 6.4.2, we demonstrated the application of Feynman rules. We automatise the calculation utilising `QGRAF` [115] and `FORM` [119]. `QGRAF` generates all required Feynman diagrams. Within `FORM`, we evaluate traces and replace scalar products to obtain scalar integrals. Furthermore, we embed relations among integrals obtained from an integration by parts reduction program like `Kira` [82, 83] or `FIRE/LiteRed` [84–87]. Afterwards, we relate those to the master integrals of uniform weight. Furthermore, we have to finish the work started in section 6.5. We have to add all counterterm diagrams to the scattering amplitude to remove poles in the dimensional regularisation parameter, which emerge out of the master integrals of uniform weight.

A similar procedure enables the analytic calculation of mixed QCD-electroweak corrections involving Z-bosons or neutral Goldstone bosons to $\Gamma\left(H \to b\bar{b}\right)$. Most of the required diagrams resemble those in table 6.1 and table 6.2, but contain a neutral weak boson and consequently only bottom quarks. Here, we may translate our results straightforwardly if we set $m_t \to m_b$. As mixed QCD-QED corrections are already calculated [114], the calculation of corrections involving gluons and Z-bosons/neutral Goldstone bosons would complete the mixed QCD-electroweak corrections to $\Gamma\left(H \to b\bar{b}\right)$.

CONCLUSION AND OUTLOOK

In this thesis, I considered three-loop Feynman integrals containing two different kinds of masses within the framework of differential equations as well as a phenomenological application of them. Feynman integrals arise in the evaluation of higher orders in perturbation theory. Hence, Feynman integrals are indispensable for precision calculations. In order to probe the successful but limited theory of the Standard Model, the determination of Feynman integrals corresponding to its properties is essential. Here, a special emphasise should be put on the Higgs boson, which gives masses to fermions as well as to W- and Z-bosons. However, the number of loops and the number of kinematic variables complicates the analytic evaluation of Feynman integrals rapidly. Beyond one-loop advanced solution methods are crucial. Within the framework of differential equations for Feynman integrals, a distinguished solution strategy involves the ϵ-form or canonical form of differential equations (3.72). After reducing Feynman integrals to a set of basis or master integrals, the ϵ-form enables a straightforward solution of their differential equations order by order in the dimensional regularisation parameter ϵ. Here, the main task is the search for two kinds of transformations resulting in the ϵ-form: basis transformations factoring out ϵ, and if required variable transformations, which eliminate square roots within differential equations (see box 1).

We analytically evaluated a previously unknown building block of Higgs precision physics: All master integrals relevant to the three-loop Higgs boson self-energy at $\mathcal{O}\left(\alpha^2\alpha_s\right)$ involving internal W-boson and top-quark propagators. We kept the full dependence on the heavy particle masses m_W, m_t and the external momentum p^2. The presence of W- and top-propagators complicates the calculations. Hence, the considered Feynman integrals are a complex contribution to this order in perturbation theory.

In chapter 5, we studied the Feynman integrals contributing to the three-loop Higgs boson self-energy with internal W-boson, gluon, top-quark and bottom-quark propagators, working in the massless bottom quark approximation. We aimed to obtain the analytic results by first transforming differential equations to an ϵ-form. We divided the Feynman diagrams and their associated integrals (5.1) into three systems. The first system corresponds to diagrams proportional to the product of Yukawa couplings $y_b y_t$. System 2a consists of diagrams containing an HW^+W^- vertex. Diagrams of system 2b

are proportional to the product of Yukawa couplings $y_b y_b$. We summarised the characteristics of each system in table 5.9. After creating all top sector diagrams (fig.5.1), we constructed appropriate topologies (fig.5.5, fig. 5.7 and table 5.1). We generated three bases of pre-canonical master integrals (system 1: table 5.6, system 2a: table 5.7, system 2b: table 5.8). After setting $\mu^2 = m_t^2$, we derived their differential equations with respect to

$$v = \frac{p^2}{m_t^2}, \quad w = \frac{m_W^2}{m_t^2}.$$

We have seen in this thesis that it is beneficial to arrange differential equations sector by sector. The resulting matrices are lower block-triangular, where sectors appear as blocks on the diagonal, and sub-sector contributions are to their left. The task ahead consists of finding transformations which bring all these blocks and thereby the whole system of differential equations into a canonical form. We discussed, that it is advantageous to transform the differential equations bottom-up, starting with the lowest sector (fig.5.9). We thereby applied two kinds of transformation matrices. U_1 (5.27) transforms diagonal blocks, leaving diagonal blocks of lower sectors unchanged. Furthermore a version of U_1 solely depending on ϵ (5.33) may be utilised to simplify the dependence of sub-sector contributions on ϵ (5.32). Afterwards U_2 (5.29), which only acts on the intended off-diagonal block, serves the purpose of bringing the sub-sector contributions into ϵ-form. To find appropriate transformations for the diagonal blocks of matrices, i.e. the homogeneous part of a sector's differential equation, we constructed ansätze for integrals of uniform transcendental weight. We have seen how to efficiently make use of the maximal cut in this context: We start as we shift the considered integral to Baikov representation either democratically (3.44) if the majority of propagators is present in the considered integral as in (5.45) or loop-by-loop (3.42) to end up with fewer integration variables (5.53),(5.54),(5.55). All Baikov variables situated in the denominator and raised to positive powers are cut (3.93). We discussed how to modify the integration contour (5.47), (5.50) and integrand of the leading term of the resulting maximally cut integral in order to obtain a constant of weight zero,

$$\text{MaxCut}\left(I\left(\epsilon = 0\right)\right) = \int_{\mathcal{C}_{\text{MaxCut}}} \varphi \quad \rightarrow \quad \int_{\mathcal{C}'} \varphi' = \text{constant of weight zero.}$$

Modifying the integrand of the original integral accordingly, we gained the sought-after ansatz (see for example (5.48)). This approach is summarised in Box 2. If the regarded sector contains multiple integrals, it is important to choose independent integration contours.

For each system, we found a basis of master integrals of uniform weight. The basis integrals are listed in (5.69), (5.70) and (5.71). We divided the master integrals into three systems to simplify dependencies on square roots and to be able to rationalise all square roots within one system simultaneously. We found appropriate variable transformations for all three systems (5.74), (5.77), (5.80), (5.81). Afterwards, each system of differential equations could be written in terms of differential one-forms containing only simple poles, i.e. dlog-forms (3.74). All sufficient dlog-forms contain only rational functions depending on kinematic variables. They are listed in (5.85), (5.90). As

boundary point, we chose $v = 0$, $w = 1$, as most integrals vanish at this point. We obtained relations between different boundary values with the help of integral reductions at the boundary point as well as from the fact that the integrals must be constant on the boundary point (5.91). We explicitly calculated remaining boundary values (5.92), (5.94). Our efforts culminate as we are able to express all master integrals via multiple polylogarithms to all orders in the dimensional regularisation parameter ϵ (section 5.5.4).

The Higgs boson self-energy is a key ingredient of Higgs precision physics. It enters the Higgs mass definition via renormalisation. Furthermore, it is linked to the Higgs boson decay rate via the optical theorem (2.8), (6.41). In chapter 6, we consequently considered the predominant decay mode of the Higgs boson, the decay into a bottom quark pair. The decay rate,

$$\Gamma\left(H \to b\bar{b}\right) = \Gamma^{(0)}(1 + \Delta^{(\alpha)} + \Delta^{(\alpha_s)} + \Delta^{(\alpha\alpha_s)} + ...),$$

consists of the Born decay rate $\Gamma^{(0)}$ (6.2) enhanced by electroweak-corrections $\Delta^{(\alpha)}$, QCD-corrections $\Delta^{(\alpha_s)}$ and mixed QCD-electroweak corrections $\Delta^{(\alpha\alpha_s)}$ (6.4), which may be split with regards to the involved electroweak bosons. The contributions containing W-/charged Goldstone bosons and Z-/neutral Goldstone bosons were so far only computed with the help of Padé approximations [45]. We address the mixed QCD-electroweak correction involving W-/charged Goldstone bosons $\Delta_W^{(\alpha\alpha_s)}$, which is the more complicated contribution, due to the presence of W- and top-propagators. We generated all contributing Feynman diagrams (table 6.1 and table 6.2) and translated them to mathematical expressions (table 6.5, table 6.6, (6.34) and (6.35)). Since we utilise the optical theorem (6.41), the required two-point three-loop diagrams correspond to the topologies and top sectors from chapter 5. We simplify the scattering amplitude in (6.19) and (6.23). Finally, the scattering amplitude will be given in terms of the canonical basis of master integrals (6.25).

The master integrals we derived can be helpful in another context as well. On the one hand, they may be transferred directly to other three-loop processes. An example is the analytic calculation of the Higgs boson self-energy at $\mathcal{O}\left(\alpha^2\alpha_s\right)$ involving Z-bosons and accordingly the mixed QCD-electroweak corrections involving Z-/neutral Goldstone bosons to $\Gamma\left(H \to b\bar{b}\right)$. Most of the diagrams involving Z-boson propagators resemble those in fig.5.1, table 6.1 and table 6.2, but contain a neutral weak boson instead of a charged weak boson and consequently only bottom quarks. Hence, those diagrams and corresponding master integrals are a special case of our results, we may obtain them through the shift $m_t \to m_b$. (In addition, Feynman diagrams with closed top quark loops contribute to the Higgs boson self-energy at $\mathcal{O}\left(\alpha^2\alpha_s\right)$ involving Z-boson.) On the other hand, the integrals we found may be utilised as building blocks for even more intrinsic integrals, which are currently still out of reach. We demonstrated this procedure in section 5.4.3. An ansatz for an integral of uniform weight may be composed out of simpler integrals for which a representation of uniform weight is already known (5.43).

We analytically calculated all master integrals relevant to the NNLO Higgs boson self-energy at $\mathcal{O}\left(\alpha^2\alpha_s\right)$ containing W- and top-propagators. We presented a basis of uniform weight expressible through multiple polylogarithms to any order in ϵ. We kept the full

dependence on m_W^2, m_t^2 and p^2. Consequently, we determined all integrals required for the mixed QCD-electroweak corrections to $\Gamma\left(H \to b\bar{b}\right)$ with internal W-/charged Goldstone bosons. Furthermore, the missing integrals of the Higgs boson self-energy at $\mathcal{O}\left(\alpha^2\alpha_s\right)$ with internal Z-propagators are within reach.

ADDENDUM TO CHAPTER 3

A.1 Generalised spherical coordinates

Spherical coordinates in D dimensions are defined as (cf. [50])

$$K_0 = K \cos \Theta_1$$
$$K_1 = K \sin \Theta_1 \cos \Theta_2$$
$$\dots$$
$$K_{D-2} = K \sin \Theta_1 \dots \sin \Theta_{D-2} \cos \Theta_{D-1}$$
$$K_{D-1} = K \sin \Theta_1 \dots \sin \Theta_{D-2} \sin \Theta_{D-1},$$

with K being the radial variable, Θ_j, $1 \leq j \leq D - 2$ being the polar angles and Θ_{D-1} being the azimuthal angle.

A.2 Massive bubble integral

The bubble integral with equal masses is defined as

$$B_{\nu_1 \nu_2}(p^2, m_1^2, m_2^2) \equiv e^{\epsilon \gamma_E} \left(\mu^2 \right)^{\nu - \frac{D}{2}} \int \frac{d^D k}{i \pi^{D/2}} \frac{1}{\left(-k^2 + m_1^2 \right)^{\nu_1} \left(-(k-p)^2 + m_2^2 \right)^{\nu_2}},$$

with

$$\nu = \sum_{j=1}^{2} \nu_j.$$

μ is an arbitrary parameter with mass dimension one, γ_E is Euler's constant,

$$\epsilon = \frac{D_0 - D}{2}, \quad D_0 \in \mathbb{N},$$

is the dimensional regularisation parameter and D the dimension. For $\nu_1 = \nu_2 = 1$, it is given by (cf. [50])

$$I_{11} = B_{11}(p^2, m_q^2, m_q^2) = \frac{1}{2} e^{\epsilon \gamma_E} \left(\frac{m_q^2}{\mu^2} \right)^{-\epsilon} (1-x)^{-\epsilon} \sum_{n=0}^{\infty} \frac{\Gamma(n+\epsilon)}{\Gamma(n+1)} \frac{\chi^n}{\left(n + \frac{1}{2} \right)} \qquad (A.1)$$

$$= \left(\frac{1}{\epsilon} - \ln\left(\frac{m_q^2}{\mu^2} \right) - \ln(1-x) \right) + \sum_{n=1}^{\infty} \left(\frac{1}{n} - \frac{1}{n+\frac{1}{2}} \right) \chi^n + \mathcal{O}(\epsilon),$$

with

$$\chi = \frac{-x}{1-x} = \frac{p^2}{p^2 - 4m_q^2}, \quad \sum_{n=0}^{\infty} \frac{\chi^n}{n} = -\ln(1-\chi),$$

$$\sum_{n=0}^{\infty} \frac{\chi^n}{\left(n+\frac{1}{2}\right)} = -2 - \frac{1}{\sqrt{\chi}} \ln(1-\sqrt{\chi}) + \frac{1}{\sqrt{\chi}} \ln(1+\sqrt{\chi}).$$

ADDENDUM TO CHAPTER 5

B.1 Overview of master integrals

Topology	Sector	Propagators	Master Integrals
A	25	$1, 4, 5$	J_1
	27	$1, 2, 4, 5$	J_2
	30	$2, 3, 4, 5$	J_3, J_4
	85	$1, 3, 5, 7$	J_5, J_6
	86	$2, 3, 5, 7$	J_7, J_8, J_9, J_{10}
	89	$1, 4, 5, 7$	J_{11}
	113	$1, 5, 6, 7$	J_{12}, J_{13}, J_{14}
	201	$1, 4, 7, 8$	J_{15}
	209	$1, 5, 7, 8$	J_{16}
	59	$1, 2, 4, 5, 6$	J_{17}
	87	$1, 2, 3, 5, 7$	J_{18}, J_{19}
	91	$1, 2, 4, 5, 7$	J_{20}

Table B.1: Overview of the set of master integrals; Part 1. The first column denotes the topology, the second column labels consecutively the sectors, the third column gives the sector identity defined in (3.46), the fourth column lists the propagators with positive exponent, the fifth column lists the master integrals in the basis $\vec{J}$.

Topology	Sector	Propagators	Master Integrals
A	94	$2, 3, 4, 5, 7$	J_{21}, J_{22}, J_{23}
	115	$1, 2, 5, 6, 7$	J_{24}, J_{25}, J_{26}
	117	$1, 3, 5, 6, 7$	$J_{27}, J_{28}, J_{29}, J_{30}$
	121	$1, 4, 5, 6, 7$	J_{31}
	203	$1, 2, 4, 7, 8$	J_{32}
	206	$2, 3, 4, 7, 8$	J_{33}, J_{34}
	211	$1, 2, 5, 7, 8$	J_{35}
	213	$1, 3, 5, 7, 8$	J_{36}
	119	$1, 2, 3, 5, 6, 7$	J_{37}, J_{38}
	123	$1, 2, 4, 5, 6, 7$	J_{39}
	215	$1, 2, 3, 5, 7, 8$	J_{40}, J_{41}, J_{42}
	222	$2, 3, 4, 5, 7, 8$	J_{43}, J_{44}
	235	$1, 2, 4, 6, 7, 8$	J_{45}
	249	$1, 4, 5, 6, 7, 8$	J_{46}
	223	$1, 2, 3, 4, 5, 7, 8$	J_{47}, J_{48}, J_{49}
	251	$1, 2, 4, 5, 6, 7, 8$	J_{50}
B	113	$1, 5, 6, 7$	J_{51}
	116	$3, 5, 6, 7$	J_{52}
	115	$1, 2, 5, 6, 7$	J_{53}
	117	$1, 3, 5, 6, 7$	J_{54}, J_{55}, J_{56}
	206	$2, 3, 4, 7, 8$	J_{57}, J_{58}, J_{59}
	233	$1, 4, 6, 7, 8$	J_{60}
	236	$3, 4, 6, 7, 8$	J_{61}
	119	$1, 2, 3, 5, 6, 7$	J_{62}, J_{63}

Table B.2: Overview of the set of master integrals; Part 2. The first column denotes the topology, the second column labels consecutively the sectors, the third column gives the sector identity defined in (3.46), the fourth column lists the propagators with positive exponent, the fifth column lists the master integrals in the basis $\vec{J}$.

Topology	Sector	Propagators	Master Integrals
B	207	$1, 2, 3, 4, 7, 8$	J_{64}
	235	$1, 2, 4, 6, 7, 8$	J_{65}
	223	$1, 2, 3, 4, 5, 7, 8$	J_{66}
	239	$1, 2, 3, 4, 6, 7, 8$	J_{67}
C	101	$1, 3, 6, 7$	J_{68}, J_{69}, J_{70}
	102	$2, 3, 6, 7$	J_{71}
	103	$1, 2, 3, 6, 7$	J_{72}
	117	$1, 3, 5, 6, 7$	J_{73}, J_{74}, J_{75}
	118	$2, 3, 5, 6, 7$	J_{76}, J_{77}, J_{78}
	173	$1, 3, 4, 6, 8$	J_{79}, J_{80}
	181	$1, 3, 5, 6, 8$	J_{81}
	119	$1, 2, 3, 5, 6, 7$	J_{82}, J_{83}, J_{84}
	175	$1, 2, 3, 4, 6, 8$	J_{85}
	183	$1, 2, 3, 5, 6, 8$	J_{86}
	189	$1, 3, 4, 5, 6, 8$	J_{87}, J_{88}
	190	$2, 3, 4, 5, 6, 8$	J_{89}
	231	$1, 2, 3, 6, 7, 8$	J_{90}, J_{91}, J_{92}
	246	$2, 3, 5, 6, 7, 8$	J_{93}, J_{94}
	191	$1, 2, 3, 4, 5, 6, 8$	$J_{95}, J_{96}, J_{97}, J_{98}$
	247	$1, 2, 3, 5, 6, 7, 8$	$J_{99}, J_{100}, J_{101}, J_{102}$
	253	$1, 3, 4, 5, 6, 7, 8$	J_{103}
	255	$1, 2, 3, 4, 5, 6, 7, 8$	J_{104}
D	239	$1, 2, 3, 4, 6, 7, 8$	J_{105}

Table B.3: Overview of the set of master integrals; Part 3. The first column denotes the topology, the second column labels consecutively the sectors, the third column gives the sector identity defined in (3.46), the fourth column lists the propagators with positive exponent, the fifth column lists the master integrals in the basis $\vec{J}$.

B.2 Numerical results

In table B.4 and table B.5 we show numerical results of system 1 as reference value at the kinematic point

$$p^2 = m_H^2,$$

where

$$m_H = 125.2 \text{ GeV}.$$

The other masses are given by

$$m_W = 80.38 \text{ GeV}, \qquad m_t = 173.1 \text{ GeV}.$$

$p^2 > 0$, hence, we are not in the Euclidean region. Due to Feynman's $i\delta$-prescription we have to take a small imaginary part into account: $p^2 \to p^2 + i\delta$, selecting the correct branches for the two square roots.

$$r_1\big|_{p^2=m_H^2} = -i\, 1.3487$$

$$r_2\big|_{p^2=m_H^2} = -i\, 0.6188$$

$$\Rightarrow x\big|_{p^2=m_H^2} = \frac{1}{2}\left(2 - v - r_1\right)\bigg|_{p^2=m_H^2} = 0.7384 + i\, 0.6743$$

$$y\big|_{p^2=m_H^2} = \frac{r_2 - r_1}{1 - w + 2v}\bigg|_{p^2=m_H^2} = i\, 0.3987$$

Table B.4 and table B.5 display the first four orders in ϵ. The first five orders can be viewed in [1].

	ϵ^0	ϵ^1	ϵ^2	ϵ^3	ϵ^4
J_1	1	1.5342081	3.6442984	3.1853184	5.1462966
J_2	0	$-1.4801083i$	$-2.4097495i$	$-5.6149488i$	$-5.2333001i$
J_3	0	$1.4801083i$	$-0.22727279i$	$7.1496293i$	$-6.383137i$
J_4	0	0	-0.54768013	-0.36476197	-2.891637
J_5	0	1.5342081	-2.9983034	19.075365	-53.393746
J_6	0.33333333	1.5342081	-0.088235985	15.450021	-32.95737
J_7	0	$-1.4585842i$	$1.294182i$	$-18.724204i$	$33.200239i$
J_8	0.33333333	0	3.7496407	-3.6797304	30.246157
J_9	0.33333333	1.5342081	1.3128219	16.578415	-17.750719
J_{10}	0	0	-2.2406312	1.0647958	-26.559377
J_{11}	0	-1.5342081	0.91070302	-7.2586694	10.224944
J_{12}	0	$1.4585842i$	$0.050868134i$	$7.6533633i$	$-4.6991476i$
J_{13}	0	1.5342081	-1.7502763	7.0599975	-14.845047
J_{14}	1	1.5342081	5.8849296	4.6861424	17.388435
J_{15}	2	$1.295828 + 6.2831853i$	$-7.8048778 + 4.0709638i$	$-12.450557 - 3.8488956i$	$-11.660945 - 25.721646i$
J_{16}	2	$4.3642443 + 6.2831853i$	$-3.4630132 + 13.710678i$	$-21.696071 + 9.7914742i$	$-38.706617 - 23.053895i$
J_{17}	0	0	2.1907205	3.772359	8.6571337
J_{18}	0	$-1.4801083i$	$0.5445262i$	$-15.995422i$	$23.86858i$
J_{19}	0	0	$-5.2250698i$	$10.295242i$	$-65.298537i$
J_{20}	0	0	$2.2707942i$	$-1.1347528i$	$10.629046i$
J_{21}	0	$1.4801083i$	$-5.4523426i$	$28.891559i$	$-88.331183i$
J_{22}	0	-1.5342081	3.2901965	-18.78899	54.646442
J_{23}	0	1.5342081	-2.1449256	21.075678	-46.255399
J_{24}	0	0	2.1588625	0.27796832	11.346261
J_{25}	0	0	$-2.2707942i$	$2.3774122i$	$-10.218327i$
J_{26}	0	$-1.4801083i$	$-2.4097495i$	$-8.9313256i$	$-7.7660295i$
J_{27}	0	$-1.4585842i$	$1.5911765i$	$-16.821522i$	$38.929474i$
J_{28}	0	$-1.4801083i$	$5.4523426i$	$-27.832513i$	$90.872416i$
J_{29}	0.33333333	0	4.2973208	-7.8296127	39.354989
J_{30}	0	0	0	3.9327313	-9.7902493
J_{31}	0	$-1.4801083i$	$2.8153204i$	$-9.1045495i$	$18.752518i$
J_{32}	0	$-2.9602166i$	$9.2997946 - 2.1958763i$	$6.898549 + 11.35639i$	$-5.0820522 + 19.501961i$
J_{33}	0	$2.9602166i$	$-9.2997946 - 3.0781682i$	$9.6703505 - 3.6126738i$	$-19.245548 - 12.824796i$
J_{34}	0	0	-1.0953603	$0.24128744 - 3.4411758i$	$1.6402683 + 0.75802684i$
J_{35}	0	$-2.9602166i$	$9.2997946 - 6.7374647i$	$21.16637 + 4.5035873i$	$16.446661 + 32.559044i$
J_{36}	0	-1.5342081	$-2.6034827 - 9.6397141i$	$26.9974 - 0.52358996i$	$-27.747558 - 12.210078i$
J_{37}	0	0	0	0	2.4095606
J_{38}	0	0	0	-0.80345343	2.3774716
J_{39}	0	0	2.1907205	-3.9613101	13.09607
J_{40}	0	$2.9602166i$	$-9.2997946 - 3.712675i$	$14.988491 - 6.3598329i$	$-8.0684303 - 1.80014i$
J_{41}	0	0	0	$-1.2199963 - 1.2715067i$	$5.3143264 - 0.86415471i$
J_{42}	0	0	0	0	$4.2051087 + 3.3549988i$
J_{43}	0	0	0	0	$2.6414875 + 2.2409565i$
J_{44}	0	0	0	$-1.2199963 - 1.2715067i$	$4.98217 - 0.70082991i$
J_{45}	0	0	4.381441	$3.6614725 + 13.764703i$	$-16.48045 + 11.502855i$
J_{46}	0	0	0	$-1.2199963 - 1.2715067i$	$3.4643984 - 1.4351478i$
J_{47}	0	0	0	0	0
J_{48}	0	0	0	0	$0.65371112 + 1.0931833i$
J_{49}	0	0	0	0	$1.6251574 + 0.75070903i$
J_{50}	0	0	0	0	$0.94098377 - 0.90286329i$
J_{51}	-3	$-3.887484 - 18.849556i$	$59.166272 - 24.425783i$	$118.51311 + 123.70244i$	$-92.180991 + 423.20939i$
J_{52}	-3	$-8.4901085 - 18.849556i$	$49.671371 - 53.344925i$	$202.90571 + 64.044212i$	$156.24311 + 572.90309i$
J_{53}	0	$4.4403248i$	$-27.899384 + 6.1707632i$	$-38.772048 - 87.008884i$	$179.55177 - 183.60241i$
J_{54}	0	$-2.9171683i$	$9.1645545 - 1.9918105i$	$24.127791 + 5.3212259i$	$-21.804448 + 120.95424i$

Table B.4: Numerical results for the first five terms of the ϵ-expansion of the master integrals J_1-J_{54} at the kinematic point $p^2 = m_H^2$.

	ϵ^0	ϵ^1	ϵ^2	ϵ^3	ϵ^4
J_{55}	0	-1.5342081	$-8.2052687 - 19.279428i$	$79.333963 - 36.244239i$	$118.23648 + 121.5975i$
J_{56}	-0.66666667	-1.5342081	-7.3030938	$-22.007405 - 14.078301i$	$-7.7964625 - 73.29467i$
J_{57}	0	$2.9171683i$	$-9.1645545 + 1.9918105i$	$-6.2574572 - 3.2092524i$	$-20.068012 - 19.446051i$
J_{58}	0	3.0684163	$-1.5124828 + 9.6397141i$	$-7.6933829 - 4.7516047i$	$-18.562293 + 7.543913i$
J_{59}	2	$4.3642443 + 6.2831853i$	$-1.2223821 + 13.710678i$	$-18.743511 + 16.830625i$	$-39.764537 - 13.778153i$
J_{60}	4	$5.1833121 + 25.132741i$	$-78.888363 + 32.56771i$	$-129.16811 - 164.93658i$	$199.25544 - 383.01328i$
J_{61}	4	$11.320145 + 25.132741i$	$-66.228494 + 71.126566i$	$-241.69158 - 85.392283i$	$-87.715765 - 582.60488i$
J_{62}	0	0	0	$-1.2199963 - 1.2715067i$	$5.9914141 - 3.4779304i$
J_{63}	0	$2.9602166i$	$-9.2997946 - 3.712675i$	$-16.248795 - 0.64764184i$	$40.454671 - 155.25155i$
J_{64}	0	$-2.9602166i$	$9.2997946 + 3.712675i$	$-11.663712 + 4.2951778i$	$17.101399 + 9.4430398i$
J_{65}	0	$-5.9204331i$	$37.199178 - 8.2276842i$	$51.696065 + 116.01185i$	$-239.40236 + 202.10303i$
J_{66}	0	0	0	0	0
J_{67}	0	0	0	$1.2199963 + 1.2715067i$	$-6.6685018 + 6.0917061i$
J_{68}	0	$-1.4801083i$	$5.1350892i$	$-25.837256i$	$86.938604i$
J_{69}	0	0	1.0953603	-3.0231166	16.571142
J_{70}	0.33333333	0	1.3701472	1.8283464	-4.959024
J_{71}	1	0	2.4674011	8.4143983	-35.10786
J_{72}	0	$-1.4801083i$	$2.498067i$	$-15.01875i$	$37.560716i$
J_{73}	0	$-1.4585842i$	$1.5911765i$	$-15.779761i$	$37.376156i$
J_{74}	0	1.5342081	-2.1449256	18.664175	-47.494038
J_{75}	0	-1.5342081	-0.2345679	-8.9971424	3.8407769
J_{76}	0	$-1.4585842i$	$1.294182i$	$-16.104568i$	$36.151551i$
J_{77}	0.33333333	1.5342081	0.62627943	18.031643	-37.794484
J_{78}	0	0	0	1.5692999	-6.5217998
J_{79}	0	$2.9602166i$	$-9.2997946 - 3.0781682i$	$-14.67018 - 1.6806018i$	$50.404394 - 150.6488i$
J_{80}	0	0	-0.54768013	$-0.41446154 - 1.7205879i$	$-2.3612249 - 7.5128487i$
J_{81}	0	1.5342081	-2.9983034	17.247662	-52.439144
J_{82}	0	$1.4801083i$	$-5.4523426i$	$23.141893i$	$-87.484869i$
J_{83}	0	0	0	-0.80345343	2.4731997
J_{84}	0	0	0	0	1.6505684
J_{85}	0	0	0	$-0.9800827 - 0.86029394i$	$4.9546534 - 1.9953368i$
J_{86}	0	0	$-0.31725341i$	$-1.4970783i$	$1.498074i$
J_{87}	0	0	-0.13692003	$2.3004984 - 0.43014697i$	$-6.0933617 - 0.63742354i$
J_{88}	0	0	0	$-1.2199963 - 1.2715067i$	$5.1907304 - 3.6242119i$
J_{89}	0	0	0	$-1.3411296 - 1.3187987i$	$5.076922 - 3.9113363i$
J_{90}	0	0	0	$-0.9800827 - 0.86029394i$	$4.8178105 + 0.24314247i$
J_{91}	0	0	0	0	$2.4985099 + 1.7074518i$
J_{92}	0	$1.4801083i$	$-9.2997946 + 2.0569211i$	$2.2589826 - 23.245834i$	$-5.6384268 + 23.974917i$
J_{93}	0	0	0	0	$2.7500878 + 2.2730554i$
J_{94}	0	0	0	$-1.3411296 - 1.3187987i$	$4.9222387 - 0.91431241i$
J_{95}	0	0	0	0	0
J_{96}	0	0	0	0	$0.21789937 + 0.042131655i$
J_{97}	0	0	0	$-0.23991356 - 0.41121273i$	$0.85908359 - 1.5044267i$
J_{98}	0	0	0	0	$0.78680569 - 5.3224605i$
J_{99}	0	0	0	0	0
J_{100}	0	0	0	0	$0.39649658 + 0.58554103i$
J_{101}	0	0	0	$-0.36104693 - 0.45850473i$	$0.35197787 - 1.3297874i$
J_{102}	0	0	0	0	$0.96352362 - 0.98327656i$
J_{103}	0	0	0	0	0
J_{104}	0	0	0	0	0
J_{105}	0	0	0	0	$0.10737705 + 0.15759037i$

Table B.5: Numerical results for the first five terms of the ϵ-expansion of the master integrals J_{55}-J_{105} at the kinematic point $p^2 = m_H^2$.

ADDENDUM TO CHAPTER 6

C.1 Contradictions arising for γ_5 in D dimensions

The four-dimensional γ_5 is defined by

$$\gamma_5^2 = 1, \tag{C.1}$$

$$\{\gamma_5, \gamma^\mu\} = 0, \tag{C.2}$$

$$Tr[\gamma_\mu\gamma_\nu\gamma_\sigma\gamma_\tau\gamma_5] = i4\epsilon_{\mu\nu\sigma\tau}. \tag{C.3}$$

Unfortunately, we can not transport all properties to D dimensions. Contradictions to the property (C.3) arise if we utilise the anticommuting property (C.2) in D dimensions,

$$DTr\left[\gamma_\mu\gamma_\nu\gamma_\sigma\gamma_\rho\gamma_5\right] = Tr\left[\gamma_\tau\gamma^\tau\gamma_\mu\gamma_\nu\gamma_\sigma\gamma_\rho\gamma_5\right] \overset{\text{cyclic}}{\underset{\text{anticom.}}{=}} -Tr\left[\gamma^\tau\gamma_\mu\gamma_\nu\gamma_\sigma\gamma_\rho\gamma_\tau\gamma_5\right]$$

$$\overset{1)}{=} -Tr\left[\gamma^\tau\gamma_\mu\gamma_\nu\gamma_\sigma(2g_{\rho\tau} - \gamma_\tau\gamma_\rho)\gamma_5\right] = -2Tr\left[\gamma_\rho\gamma_\mu\gamma_\nu\gamma_\sigma\gamma_5\right] + Tr\left[\gamma^\tau\gamma_\mu\gamma_\nu\gamma_\sigma\gamma_\tau\gamma_\rho\gamma_5\right]$$

$$\overset{1)}{\underset{\text{cyc.+anticom.}}{=}} 2Tr\left[\gamma_\mu\gamma_\nu\gamma_\sigma\gamma_\rho\gamma_5\right] + Tr\left[\gamma^\tau\gamma_\mu\gamma_\nu(2g_{\sigma\tau} - \gamma_\tau\gamma_\sigma)\gamma_\rho\gamma_5\right]$$

$$\overset{1)}{=} 2Tr\left[\gamma_\mu\gamma_\nu\gamma_\sigma\gamma_\rho\gamma_5\right] + 2Tr\left[\gamma_\sigma\gamma_\mu\gamma_\nu\gamma_\rho\gamma_5\right] - Tr\left[\gamma^\tau\gamma_\mu(2g_{\nu\tau} - \gamma_\tau\gamma_\nu)\gamma_\sigma\gamma_\rho\gamma_5\right]$$

$$= 2Tr\left[\gamma_\mu\gamma_\nu\gamma_\sigma\gamma_\rho\gamma_5\right] + 2Tr\left[\gamma_\sigma\gamma_\mu\gamma_\nu\gamma_\rho\gamma_5\right]$$

$$- 2Tr\left[\gamma_\nu\gamma_\mu\gamma_\sigma\gamma_\rho\gamma_5\right] + 2Tr\left[\gamma_\mu\gamma_\nu\gamma_\sigma\gamma_\rho\gamma_5\right] - Tr\left[D\gamma_\mu\gamma_\nu\gamma_\sigma\gamma_\rho\gamma_5\right]$$

$$\Leftrightarrow 2DTr\left[\gamma_\mu\gamma_\nu\gamma_\sigma\gamma_\rho\gamma_5\right] = 4Tr\left[\gamma_\mu\gamma_\nu\gamma_\sigma\gamma_\rho\gamma_5\right] + 2Tr\left[\gamma_\sigma\gamma_\mu\gamma_\nu\gamma_\rho\gamma_5\right] - 2Tr\left[\gamma_\nu\gamma_\mu\gamma_\sigma\gamma_\rho\gamma_5\right],$$
$$\tag{C.4}$$

where 1) is defined by $\{\gamma_\mu, \gamma_\nu\} = 2g_{\mu\nu} \Leftrightarrow \gamma_\mu\gamma_\nu = 2g_{\mu\nu} - \gamma_\nu\gamma_\mu$.
Contracting equation (C.4) with $\epsilon^{\mu\nu\sigma\rho}$ and dividing by 2, we find

$$D\epsilon^{\mu\nu\sigma\rho}Tr\left[\gamma_\mu\gamma_\nu\gamma_\sigma\gamma_\rho\gamma_5\right] = 2\epsilon^{\mu\nu\sigma\rho}Tr\left[\gamma_\mu\gamma_\nu\gamma_\sigma\gamma_\rho\gamma_5\right] + \underbrace{\epsilon^{\mu\nu\sigma\rho}Tr\left[\gamma_\sigma\gamma_\mu\gamma_\nu\gamma_\rho\gamma_5\right]}_{\substack{\sigma\to\mu,\;\mu\to\nu \\ \nu\to\sigma}\underbrace{\epsilon^{\nu\sigma\mu\rho}}_{=\epsilon^{\mu\nu\sigma\rho}}Tr[\gamma_\mu\gamma_\nu\gamma_\sigma\gamma_\rho\gamma_5]}$$

$$- \underbrace{\epsilon^{\mu\nu\sigma\rho}Tr\left[\gamma_\nu\gamma_\mu\gamma_\sigma\gamma_\rho\gamma_5\right]}_{\substack{\nu\to\mu \\ \mu\to\nu}\underbrace{\epsilon^{\nu\mu\sigma\rho}}_{=-\epsilon^{\mu\nu\sigma\rho}}Tr[\gamma_\mu\gamma_\nu\gamma_\sigma\gamma_\rho\gamma_5]}$$

$$= 4\epsilon^{\mu\nu\sigma\rho} Tr\left[\gamma_\mu \gamma_\nu \gamma_\sigma \gamma_\rho \gamma_5\right],$$
$$\Leftrightarrow (D-4)\epsilon^{\mu\nu\sigma\rho} Tr\left[\gamma_\mu \gamma_\nu \gamma_\sigma \gamma_\rho \gamma_5\right] = 0. \tag{C.5}$$

C.2 Counter term Feynman rules

We described in section 2.3 that we may derive Feynman rules for counterterm insertions from a counterterm Lagrangian $\mathcal{L}_{CT}$. We therefore split the bare Lagrangian,

$$\mathcal{L} \to \mathcal{L}_{bare} = \mathcal{L}_{renormalised} + \mathcal{L}_{CT}. \tag{C.6}$$

In section 2.2, we obtained the Feynman rule of the quark propagator. The quark propagator with counterterm insertion arises in a similar way out of

$$\mathcal{L}_{bare} = Z_2 \bar{q}(i\gamma^\mu \partial_\mu - Z_m m_q)q$$
$$\Rightarrow \mathcal{L}_{CT} = \bar{q}((Z_2 - 1)i\gamma^\mu \partial_\mu - (Z_2 Z_m - 1)m_q)q.$$

It amounts to

$$i\left[(Z_2 - 1)\slashed{k} - (Z_2 Z_m - 1)m_q\right].$$

We require the renormalisation constants Z_2^1 and $Z_{m_q}^1$, which may be constructed from the quark self-energy, at order α_s,

$$Z_2 = 1 + \frac{\alpha_s}{4\pi} Z_2^1 + ...,$$
$$Z_m = 1 + \frac{\alpha_s}{4\pi} Z_m^1 + ..., \tag{C.7}$$

implying for the quark propagator with counterterm insertion

$$i\left[(Z_2 - 1)\slashed{k} - (Z_2 Z_m - 1)m_q\right] = i\frac{\alpha_s}{4\pi}\left[Z_2^1 \slashed{k} - (Z_2^1 + Z_m^1)m_q\right] + \mathcal{O}(\alpha_s^2) + \mathcal{O}(\alpha).$$

The Feynman rule for a $Hq\bar{q}$ vertex with counterterm insertion amounts to

$$-i(Z_{Hqq} - 1)\frac{gm_q}{2m_W}.$$

The renormalisation constant Z_{Hqq} consists of the renormalisation constants of the quark mass and field as well as the W-boson mass and the strong coupling. The Feynman rule for a $W^\pm q\bar{q}$ vertex with counterterm insertion is

---

Feynman diagrams in section C.2 were created with [120]
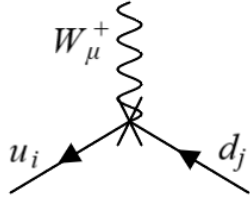
$$i(Z_{Wqq} - 1)\frac{g}{\sqrt{2}}\gamma^\mu\frac{1 - \gamma_5}{2}V_{ij},$$
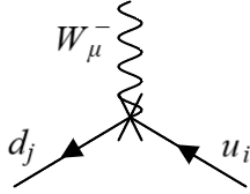
$$i(Z_{Wqq} - 1)\frac{g}{\sqrt{2}}\gamma^\mu\frac{1 - \gamma_5}{2}V_{ij}^*,$$

where the renormalisation constant Z_{Wqq}, which we need at order α_s, is a composition of the renormalisation constants of the quark field, the W-boson field and the strong coupling,

$$Z_{Wqq} = 1 + \frac{\alpha_s}{4\pi}Z_{Wqq}^1 + \mathcal{O}(\alpha_s^2) + \mathcal{O}(\alpha),$$

$$\Rightarrow i(Z_{Wqq} - 1)\frac{g}{\sqrt{2}}\gamma^\mu\frac{1 - \gamma_5}{2}V_{ij} = i\frac{g}{2\sqrt{2}}\gamma^\mu(1 - \gamma_5)V_{ij}\frac{\alpha_s}{4\pi}Z_{Wqq}^1 + \mathcal{O}(\alpha_s^2) + \mathcal{O}(\alpha).$$

The $\Phi^\pm q\bar{q}$ vertex with counterterm insertion
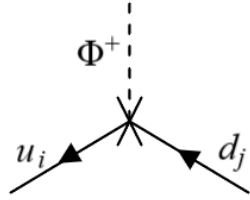
$$i(Z_{Hqq} - 1)\frac{g}{2\sqrt{2}}\left[(1 - \gamma_5)\frac{m_{u_i}}{m_W} - (1 + \gamma_5)\frac{m_{d_j}}{m_W}\right]V_{ij},$$
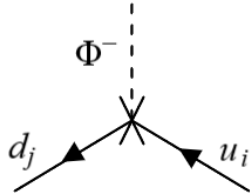
$$i(Z_{Hqq} - 1)\frac{g}{2\sqrt{2}}\left[(1 + \gamma_5)\frac{m_{u_i}}{m_W} - (1 - \gamma_5)\frac{m_{d_j}}{m_W}\right]V_{ij}^*.$$

depends again on Z_{Hqq}. Hence we require Z_{Hqq} at order α and at order α_s,

$$Z_{Hqq} = 1 + \frac{\alpha_s}{4\pi}Z_{Hqq}^{\alpha_s,1} + \frac{\alpha}{4\pi}Z_{Hqq}^{\alpha,1} + \mathcal{O}(\alpha_s^2) + \mathcal{O}(\alpha^2).$$

Z_{Hqq}^1 can be constructed if we consider the α_s correction to the $q\bar{q}$ Higgs vertex. We may obtain Z_{Hqq} at $\mathcal{O}(\alpha)$ from the α correction to the $Hq\bar{q}$ vertex, whereas one contribution arises from flavour changing particles and one from non-flavour changing particles. The latter should be dropped, since we do not consider non-flavour changing electroweak bosons.

[1] Ekta Chaubey, Ina Hönemann, and Stefan Weinzierl.
     "Three-loop master integrals for the Higgs boson self-energy with internal top-
     quarks and W-bosons".
     In: *Journal of High Energy Physics* 2022.11 (2022).
     DOI: 10.1007/jhep11(2022)051.
     URL: https://doi.org/10.1007%2Fjhep11%282022%29051.

[2] G. Zweig.
     "An SU(3) model for strong interaction symmetry and its breaking. Version 2".
     In:
     *DEVELOPMENTS IN THE QUARK THEORY OF HADRONS. VOL. 1. 1964
     - 1978.*
     Ed. by D. B. Lichtenberg and Simon Peter Rosen.
     1964,
     Pp. 22–101.

[3] Murray Gell-Mann.
     "A Schematic Model of Baryons and Mesons".
     In: *Phys. Lett.* 8 (1964), pp. 214–215.
     DOI: 10.1016/S0031-9163(64)92001-3.

[4] E. D. Bloom et al.
     "High-Energy Inelastic $e - p$ Scattering at 6 and 10".
     In: *Phys. Rev. Lett.* 23 (16 1969), pp. 930–934.
     DOI: 10.1103/PhysRevLett.23.930.
     URL: https://link.aps.org/doi/10.1103/PhysRevLett.23.930.

[5] M. Breidenbach et al.
     "Observed Behavior of Highly Inelastic Electron-Proton Scattering".
     In: *Phys. Rev. Lett.* 23 (16 1969), pp. 935–939.
     DOI: 10.1103/PhysRevLett.23.935.
     URL: https://link.aps.org/doi/10.1103/PhysRevLett.23.935.

[6] The Muon $g - 2$ Collaboration.
     "Measurement of the Positive Muon Anomalous Magnetic Moment to 0.46 ppm".
     In: *Physical Review Letters* 126.14 (2021).
     DOI: 10.1103/physrevlett.126.141801.
     URL: https://doi.org/10.1103%2Fphysrevlett.126.141801.

[7]   CDF collaboration.
      "High-precision measurement of the W boson mass with the CDF II detector".
      In: *Science* 376.6589 (2022), pp. 170–176.
      DOI: 10.1126/science.abk1781.
      eprint: https://www.science.org/doi/pdf/10.1126/science.abk1781.
      URL: https://www.science.org/doi/abs/10.1126/science.abk1781.

[8]   Simone Amoroso.
      Status of the W-boson mass averaging project.
      2022.
      DOI: 10.48550/ARXIV.2211.12365.
      URL: https://arxiv.org/abs/2211.12365.

[9]   Peter W. Higgs.
      "Broken Symmetries and the Masses of Gauge Bosons".
      In: *Phys. Rev. Lett.* 13 (1964). Ed. by J. C. Taylor, pp. 508–509.
      DOI: 10.1103/PhysRevLett.13.508.

[10] G. Aad et al.
      "Observation of a new particle in the search for the Standard Model Higgs boson
      with the ATLAS detector at the LHC".
      In: *Physics Letters B* 716.1 (2012), pp. 1–29.
      ISSN: 0370-2693.
      DOI: 10.1016/j.physletb.2012.08.020.
      URL: http://dx.doi.org/10.1016/j.physletb.2012.08.020.

[11] S. Chatrchyan et al.
      "Observation of a new boson at a mass of 125 GeV with the CMS experiment at
      the LHC".
      In: *Physics Letters B* 716.1 (2012), pp. 30–61.
      ISSN: 0370-2693.
      DOI: 10.1016/j.physletb.2012.08.021.
      URL: http://dx.doi.org/10.1016/j.physletb.2012.08.021.

[12] I. Zurbano Fernandez et al.
      "High-Luminosity Large Hadron Collider (HL-LHC): Technical design report".
      In: 10/2020 (2020). Ed. by I. Béjar Alonso et al.
      DOI: 10.23731/CYRM-2020-0010.

[13] Howard Baer et al.
      The International Linear Collider Technical Design Report - Volume 2: Physics.
      2013.
      DOI: 10.48550/ARXIV.1306.6352.
      URL: https://arxiv.org/abs/1306.6352.

[14] T. Barklow et al.
      ILC Operating Scenarios.
      2015.
      DOI: 10.48550/ARXIV.1506.07830.
      URL: https://arxiv.org/abs/1506.07830.

[15] M. Benedikt et al.

Future Circular Hadron Collider FCC-hh: Overview and Status.
2022.
DOI: 10.48550/ARXIV.2203.07804.
URL: https://arxiv.org/abs/2203.07804.

[16] G. Peter Lepage, Paul B. Mackenzie, and Michael E. Peskin.
Expected Precision of Higgs Boson Partial Widths within the Standard Model.
2014.
DOI: 10.48550/ARXIV.1404.0319.
URL: https://arxiv.org/abs/1404.0319.

[17] Michael Spira.
"Higgs Boson Decays: Theoretical Status".
In: *CERN Yellow Reports: Monographs* 3 (2020). Ed. by A. Blondel et al.,
pp. 123–134.
DOI: 10.23731/CYRM-2020-003.123.

[18] Javier Aparisi et al.
"m_b at m_H : The Running Bottom Quark Mass and the Higgs Boson".
In: *Physical Review Letters* 128.12 (2022).
DOI: 10.1103/physrevlett.128.122001.
URL: https://doi.org/10.1103%2Fphysrevlett.128.122001.

[19] Stephen P. Martin.
"Three-loop QCD corrections to the electroweak boson masses".
In: *Physical Review D* 106.1 (2022).
DOI: 10.1103/physrevd.106.013007.
URL: https://doi.org/10.1103%2Fphysrevd.106.013007.

[20] Amlan Chakraborty et al.
The $Hb\bar{b}$ vertex at four loops and hard matching coefficients in SCET for various currents.
2022.
DOI: 10.48550/ARXIV.2204.02422.
URL: https://arxiv.org/abs/2204.02422.

[21] R. P. Feynman.
"Space-Time Approach to Quantum Electrodynamics".
In: *Phys. Rev.* 76 (6 1949), pp. 769–789.
DOI: 10.1103/PhysRev.76.769.
URL: https://link.aps.org/doi/10.1103/PhysRev.76.769.

[22] R. P. Feynman.
"The Theory of Positrons".
In: *Phys. Rev.* 76 (6 1949), pp. 749–759.
DOI: 10.1103/PhysRev.76.749.
URL: https://link.aps.org/doi/10.1103/PhysRev.76.749.

[23] F. J. Dyson.
"The Radiation theories of Tomonaga, Schwinger, and Feynman".
In: *Phys. Rev.* 75 (1949), pp. 486–502.
DOI: 10.1103/PhysRev.75.486.

[24] F. J. Dyson.
"The S Matrix in Quantum Electrodynamics".
In: *Phys. Rev.* 75 (11 1949), pp. 1736–1755.
DOI: 10.1103/PhysRev.75.1736.
URL: https://link.aps.org/doi/10.1103/PhysRev.75.1736.

[25] K.G. Chetyrkin and F.V. Tkachov.
"Integration by parts: The algorithm to calculate β-functions in 4 loops".
In: *Nuclear Physics B* 192.1 (1981), pp. 159–204.
ISSN: 0550-3213.
DOI: https://doi.org/10.1016/0550-3213(81)90199-1.
URL: https://www.sciencedirect.com/science/article/pii/0550321381901991.

[26] F.V. Tkachov.
"A theorem on analytical calculability of 4-loop renormalization group functions".
In: *Physics Letters B* 100.1 (1981), pp. 65–68.
ISSN: 0370-2693.
DOI: https://doi.org/10.1016/0370-2693(81)90288-4.
URL: https://www.sciencedirect.com/science/article/pii/0370269381902884.

[27] A.V. Kotikov.
"Differential equations method. New technique for massive Feynman diagram calculation".
In: *Physics Letters B* 254.1 (1991), pp. 158–164.
ISSN: 0370-2693.
DOI: https://doi.org/10.1016/0370-2693(91)90413-K.
URL: https://www.sciencedirect.com/science/article/pii/037026939190413K.

[28] A.V. Kotikov.
"Differential equation method. The calculation of N-point Feynman diagrams".
In: *Physics Letters B* 267.1 (1991), pp. 123–127.
ISSN: 0370-2693.
DOI: https://doi.org/10.1016/0370-2693(91)90536-Y.
URL: https://www.sciencedirect.com/science/article/pii/037026939190536Y.

[29] E. Remiddi.
"Differential equations for Feynman graph amplitudes".
In: *Il Nuovo Cimento A* 110.12 (1997), pp. 1435–1452.
DOI: 10.1007/bf03185566.
URL: https://doi.org/10.1007%2Fbf03185566.

[30] T. Gehrmann and E. Remiddi.
"Differential equations for two-loop four-point functions".
In: *Nuclear Physics B* 580.1-2 (2000), pp. 485–518.
DOI: 10.1016/s0550-3213(00)00223-6.
URL: https://doi.org/10.1016%2Fs0550-3213%2800%2900223-6.

[31] Johannes M. Henn.
"Multiloop Integrals in Dimensional Regularization Made Simple".
In: *Physical Review Letters* 110.25 (2013).

DOI: 10.1103/physrevlett.110.251601.
URL: https://doi.org/10.1103%2Fphysrevlett.110.251601.

[32] Alexander B. Goncharov.
"Multiple polylogarithms, cyclotomy and modular complexes".
In: *Math. Res. Lett.* 5 (1998), pp. 497–516.
DOI: 10.4310/MRL.1998.v5.n4.a7.
arXiv: 1105.2076 [math.AG].

[33] A. B. Goncharov.
Multiple polylogarithms and mixed Tate motives.
2001.
DOI: 10.48550/ARXIV.MATH/0103059.
URL: https://arxiv.org/abs/math/0103059.

[34] Jonathan M. Borwein et al.
"Special Values of Multiple Polylogarithms".
In: (1999).
DOI: 10.48550/ARXIV.MATH/9910045.
URL: https://arxiv.org/abs/math/9910045.

[35] Afaf Sabry.
"Fourth order spectral functions for the electron propagator".
In: *Nuclear Physics* 33 (1962), pp. 401–430.
ISSN: 0029-5582.
DOI: https://doi.org/10.1016/0029-5582(62)90535-7.
URL: https://www.sciencedirect.com/science/article/pii/0029558262905357.

[36] D. J. Broadhurst, J. Fleischer, and O. V. Tarasov.
"Two-loop two-point functions with masses: asymptotic expansions and Taylor
series, in any dimension".
In: *Zeitschrift für Physik C Particles and Fields* 60.2 (1993), pp. 287–301.
DOI: 10.1007/bf01474625.
URL: https://doi.org/10.1007%2Fbf01474625.

[37] Luise Adams, Christian Bogner, and Stefan Weinzierl.
"The iterated structure of the all-order result for the two-loop sunrise integral".
In: *Journal of Mathematical Physics* 57.3 (2016), p. 032304.
DOI: 10.1063/1.4944722.
URL: https://doi.org/10.1063%2F1.4944722.

[38] Luise Adams and Stefan Weinzierl.
Feynman integrals and iterated integrals of modular forms.
2017.
DOI: 10.48550/ARXIV.1704.08895.
URL: https://arxiv.org/abs/1704.08895.

[39] Johannes Broedel et al.
"Elliptic polylogarithms and iterated integrals on elliptic curves. II. An applica-
tion to the sunrise integral".
In: *Phys. Rev. D* 97 (11 2018), p. 116009.
DOI: 10.1103/PhysRevD.97.116009.

URL: https://link.aps.org/doi/10.1103/PhysRevD.97.116009.

[40]   Luise Adams and Stefan Weinzierl.
       "The $\epsilon-$form of the differential equations for Feynman integrals in the elliptic
       case".
       In: *Physics Letters B* 781 (2018), pp. 270–278.
       ISSN: 0370-2693.
       DOI: https://doi.org/10.1016/j.physletb.2018.04.002.
       URL: https://www.sciencedirect.com/science/article/pii/S0370269318302855.

[41]   Ina Hönemann, Kirsten Tempest, and Stefan Weinzierl.
       "Electron self-energy in QED at two loops revisited".
       In: *Physical Review D* 98.11 (2018).
       DOI: 10.1103/physrevd.98.113008.
       URL: https://doi.org/10.1103%2Fphysrevd.98.113008.

[42]   Jacob L. Bourjaily et al.
       Functions Beyond Multiple Polylogarithms for Precision Collider Physics.
       2022.
       DOI: 10.48550/ARXIV.2203.07088.
       URL: https://arxiv.org/abs/2203.07088.

[43]   Sebastian Pögel, Xing Wang, and Stefan Weinzierl.
       "The three-loop equal-mass banana integral in ϵ-factorised form with meromor-
       phic modular forms".
       In: *Journal of High Energy Physics* 2022.9 (2022).
       DOI: 10.1007/jhep09(2022)062.
       URL: https://doi.org/10.1007%2Fjhep09%282022%29062.

[44]   Sebastian Pögel, Xing Wang, and Stefan Weinzierl.
       *Bananas of equal mass: any loop, any order in the dimensional regularisation
       parameter.*
       2022.
       DOI: 10.48550/ARXIV.2212.08908.
       URL: https://arxiv.org/abs/2212.08908.

[45]   Luminita Mihaila, Barbara Schmidt, and Matthias Steinhauser.
       "$\Gamma(H \to b\bar{b})$ to order $\alpha\alpha_s$".
       In: *Physics Letters B* 751 (2015), pp. 442–447.
       ISSN: 0370-2693.
       DOI: 10.1016/j.physletb.2015.10.078.
       URL: http://dx.doi.org/10.1016/j.physletb.2015.10.078.

[46]   Owe Philipsen.
       Quantenfeldtheorie und das Standardmodell der Teilchenphysik: Eine Einführung.
       2018.
       ISBN: 978-3-662-57819-3.
       DOI: 10.1007/978-3-662-57820-9.

[47]   Michael E. Peskin and Daniel V. Schroeder.
       An Introduction to quantum field theory.
       Reading, USA: Addison-Wesley, 1995.

ISBN: 978-0-201-50397-5.

[48] Matthew D. Schwartz.
Quantum Field Theory and the Standard Model.
Cambridge University Press, 2013.
DOI: [10.1017/9781139540940](10.1017/9781139540940).

[49] Stefan Weinzierl.
Introduction to theoretical particle physics (Relativistic Quantum Field Theory) Part I.
https://particlephysics.uni-mainz.de/weinzierl/download/script_qft1.pdf.
Accessed: 12.12.2022.

[50] Stefan Weinzierl.
Introduction to theoretical particle physics (Relativistic Quantum Field Theory) Part II.
https://particlephysics.uni-mainz.de/weinzierl/download/script_qft2.pdf.
Accessed: 12.12.2022.

[51] Jorge C. Romã o and João P. Silva.
"A resource for signs and Feynman diagrams of the Standard Model".
In: *International Journal of Modern Physics A* 27.26 (2012), p. 1230025.
DOI: [10.1142/s0217751x12300256](10.1142/s0217751x12300256).
URL: https://doi.org/10.1142%2Fs0217751x12300256.

[52] Gerard 't Hooft and M. J. G. Veltman.
"Regularization and Renormalization of Gauge Fields".
In: *Nucl. Phys.* B44 (1972), pp. 189–213.
DOI: [10.1016/0550-3213(72)90279-9](10.1016/0550-3213(72)90279-9).

[53] C. G. Bollini and J. J. Giambiagi.
"Dimensional Renormalization: The Number of Dimensions as a Regularizing Parameter".
In: *Nuovo Cim. B* 12 (1972), pp. 20–26.
DOI: [10.1007/BF02895558](10.1007/BF02895558).

[54] G. M. Cicuta and E. Montaldi.
"Analytic renormalization via continuous space dimension".
In: *Lett. Nuovo Cim.* 4 (1972), pp. 329–332.
DOI: [10.1007/BF02756527](10.1007/BF02756527).

[55] M.Albert et al.
Inkscape, version 1.2.
https://inkscape.org/.
Accessed: 12.12.2022.

[56] G. 't Hooft and M. Veltman.
"Regularization and renormalization of gauge fields".
In: *Nuclear Physics B* 44.1 (1972), pp. 189–213.
ISSN: 0550-3213.
DOI: https://doi.org/10.1016/0550-3213(72)90279-9.

URL: https://www.sciencedirect.com/science/article/pii/0550321372902799.

[57] Stefan Weinzierl.
Feynman Integrals.
2022.
DOI: 10.48550/ARXIV.2201.03593.
URL: https://arxiv.org/abs/2201.03593.

[58] T. Kinoshita.
"Mass singularities of Feynman amplitudes".
In: *J. Math. Phys.* 3 (1962), pp. 650–677.
DOI: 10.1063/1.1724268.

[59] T. D. Lee and M. Nauenberg.
"Degenerate Systems and Mass Singularities".
In: *Phys. Rev.* 133 (6B 1964), B1549–B1562.
DOI: 10.1103/PhysRev.133.B1549.
URL: https://link.aps.org/doi/10.1103/PhysRev.133.B1549.

[60] Johannes M Henn.
"Lectures on differential equations for Feynman integrals".
In: *Journal of Physics A: Mathematical and Theoretical* 48.15 (2015), p. 153001.
DOI: 10.1088/1751-8113/48/15/153001.
URL: https://doi.org/10.1088%2F1751-8113%2F48%2F15%2F153001.

[61] Stefan Weinzierl.
The Art of Computing Loop Integrals.
2006.
DOI: 10.48550/ARXIV.HEP-PH/0604068.
URL: https://arxiv.org/abs/hep-ph/0604068.

[62] Andrey Grozin.
Lectures on QED and QCD.
2005.
DOI: 10.48550/ARXIV.HEP-PH/0508242.
URL: https://arxiv.org/abs/hep-ph/0508242.

[63] G. Passarino and M. Veltman.
"One-loop corrections for $e+e-$ annihilation into $\mu+\mu-$ in the Weinberg model".
In: *Nuclear Physics B* 160.1 (1979), pp. 151–207.
ISSN: 0550-3213.
DOI: https://doi.org/10.1016/0550-3213(79)90234-7.
URL: https://www.sciencedirect.com/science/article/pii/0550321379902347.

[64] G. C. Wick.
"Properties of Bethe-Salpeter Wave Functions".
In: *Phys. Rev.* 96 (4 1954), pp. 1124–1134.
DOI: 10.1103/PhysRev.96.1124.
URL: https://link.aps.org/doi/10.1103/PhysRev.96.1124.

[65] Christian Bogner and Stefan Weinzierl.
"Feynman graph polynomials".
In: *International Journal of Modern Physics A* 25.13 (2010), pp. 2585–2618.

DOI: 10.1142/s0217751x10049438.
URL: https://doi.org/10.1142%2Fs0217751x10049438.

[66] P.A Baikov.
"Explicit solutions of the multi-loop integral recurrence relations and its application".
In: *Nuclear Instruments and Methods in Physics Research Section A: Accelerators, Spectrometers, Detectors and Associated Equipment* 389.1-2 (1997), pp. 347–349.
DOI: 10.1016/s0168-9002(97)00126-5.
URL: https://doi.org/10.1016%2Fs0168-9002%2897%2900126-5.

[67] Laporta.
"High-precision calculation of multi-loop Feynman integrals by difference equations".
In: *International Journal of Modern Physics A* 15 (2000), p. 5087.
DOI: 10.1016/s0217-751x(00)00215-7.
URL: https://doi.org/10.1016%2Fs0217-751x%2800%2900215-7.

[68] Jurgen Moser.
"The order of a singularity in Fuchs' theory".
In: *Mathematische Zeitschrift* 72 (1959), pp. 379–398.

[69] Roman N. Lee.
"Reducing differential equations for multiloop master integrals".
In: *Journal of High Energy Physics* 2015.4 (2015).
DOI: 10.1007/jhep04(2015)108.
URL: https://doi.org/10.1007%2Fjhep04%282015%29108.

[70] Roman N. Lee and Andrei A. Pomeransky.
Normalized Fuchsian form on Riemann sphere and differential equations for multiloop integrals.
2017.
DOI: 10.48550/ARXIV.1707.07856.
URL: https://arxiv.org/abs/1707.07856.

[71] Francis Brown.
"Iterated integrals in quantum field theory".
In: *6th Summer School on Geometric and Topological Methods for Quantum Field Theory.*
2013,
Pp. 188–240.
DOI: 10.1017/CBO9781139208642.006.

[72] Mario Prausa.
"epsilon : A tool to find a canonical basis of master integrals".
In: *Computer Physics Communications* 219 (2017), pp. 361–376.
DOI: 10.1016/j.cpc.2017.05.026.
URL: https://doi.org/10.1016%2Fj.cpc.2017.05.026.

[73] Oleksandr Gituliar and Vitaly Magerya.

"Fuchsia : A tool for reducing differential equations for Feynman master integrals to epsilon form".
In: *Computer Physics Communications* 219 (2017), pp. 329–338.
DOI: 10.1016/j.cpc.2017.05.004.
URL: https://doi.org/10.1016%2Fj.cpc.2017.05.004.

[74] Roman N. Lee.
"Libra: A package for transformation of differential systems for multiloop integrals".
In: *Computer Physics Communications* 267 (2021), p. 108058.
DOI: 10.1016/j.cpc.2021.108058.
URL: https://doi.org/10.1016%2Fj.cpc.2021.108058.

[75] Amedeo Primo and Lorenzo Tancredi.
"On the maximal cut of Feynman integrals and the solution of their differential equations".
In: *Nuclear Physics B* 916 (2017), pp. 94–116.
DOI: 10.1016/j.nuclphysb.2016.12.021.
URL: https://doi.org/10.1016%2Fj.nuclphysb.2016.12.021.

[76] Marco Besier and Dino Festi.
Rationalizability of square roots.
2020.
DOI: 10.48550/ARXIV.2006.07121.
URL: https://arxiv.org/abs/2006.07121.

[77] Matthias Heller, Andreas von Manteuffel, and Robert M. Schabinger.
"Multiple polylogarithms with algebraic arguments and the two-loop EW-QCD Drell-Yan master integrals".
In: *Physical Review D* 102.1 (2020).
DOI: 10.1103/physrevd.102.016025.
URL: https://doi.org/10.1103%2Fphysrevd.102.016025.

[78] Marco Besier, Duco van Straten, and Stefan Weinzierl.
Rationalizing roots: an algorithmic approach.
2018.
DOI: 10.48550/ARXIV.1809.10983.
URL: https://arxiv.org/abs/1809.10983.

[79] Marco Besier, Pascal Wasser, and Stefan Weinzierl.
"RationalizeRoots: Software package for the rationalization of square roots".
In: *Computer Physics Communications* 253 (2020), p. 107197.
DOI: 10.1016/j.cpc.2020.107197.
URL: https://doi.org/10.1016%2Fj.cpc.2020.107197.

[80] O. V. Tarasov.
"Connection between Feynman integrals having different values of the space-time dimension".
In: *Physical Review D* 54.10 (1996), pp. 6479–6490.
DOI: 10.1103/physrevd.54.6479.
URL: https://doi.org/10.1103%2Fphysrevd.54.6479.

[81]   O.V. Tarasov.
       "Generalized recurrence relations for two-loop propagator integrals with arbitrary masses".
       In: *Nuclear Physics B* 502.1-2 (1997), pp. 455–482.
       DOI: 10.1016/s0550-3213(97)00376-3.
       URL: https://doi.org/10.1016%2Fs0550-3213%2897%2900376-3.

[82]   P. Maierhöfer, J. Usovitsch, and P. Uwer.
       "Kira—A Feynman integral reduction program".
       In: *Computer Physics Communications* 230 (2018), pp. 99–112.
       DOI: 10.1016/j.cpc.2018.04.012.
       URL: https://doi.org/10.1016%2Fj.cpc.2018.04.012.

[83]   Jonas Klappert et al.
       "Integral reduction with Kira 2.0 and finite field methods".
       In: *Computer Physics Communications* 266 (2021), p. 108024.
       DOI: 10.1016/j.cpc.2021.108024.
       URL: https://doi.org/10.1016%2Fj.cpc.2021.108024.

[84]   A.V Smirnov.
       "Algorithm FIRE—Feynman Integral REduction".
       In: *Journal of High Energy Physics* 2008.10 (2008), pp. 107–107.
       DOI: 10.1088/1126-6708/2008/10/107.
       URL: https://doi.org/10.1088%2F1126-6708%2F2008%2F10%2F107.

[85]   A.V. Smirnov and F.S. Chukharev.
       "FIRE6: Feynman Integral REduction with modular arithmetic".
       In: *Computer Physics Communications* 247 (2020), p. 106877.
       DOI: 10.1016/j.cpc.2019.106877.
       URL: https://doi.org/10.1016%2Fj.cpc.2019.106877.

[86]   R. N. Lee.
       Presenting LiteRed: a tool for the Loop InTEgrals REDuction.
       2012.
       DOI: 10.48550/ARXIV.1212.2685.
       URL: https://arxiv.org/abs/1212.2685.

[87]   Roman N Lee.
       "LiteRed 1.4: a powerful tool for reduction of multiloop integrals".
       In: *Journal of Physics: Conference Series* 523 (2014), p. 012059.
       DOI: 10.1088/1742-6596/523/1/012059.
       URL: https://doi.org/10.1088%2F1742-6596%2F523%2F1%2F012059.

[88]   C. Studerus.
       "Reduze – Feynman integral reduction in $C++$".
       In: *Computer Physics Communications* 181.7 (2010), pp. 1293–1300.
       DOI: 10.1016/j.cpc.2010.03.012.
       URL: https://doi.org/10.1016%2Fj.cpc.2010.03.012.

[89]   A. von Manteuffel and C. Studerus.
       Reduze 2 - Distributed Feynman Integral Reduction.
       2012.

DOI: `10.48550/ARXIV.1201.4330`.
URL: `https://arxiv.org/abs/1201.4330`.

[90] Hjalte Frellesvig and Costas G. Papadopoulos.
"Cuts of Feynman Integrals in Baikov representation".
In: *Journal of High Energy Physics* 2017.4 (2017).
DOI: `10.1007/jhep04(2017)083`.
URL: `https://doi.org/10.1007%2Fjhep04%282017%29083`.

[91] Freddy Cachazo.
Sharpening The Leading Singularity.
2008.
DOI: `10.48550/ARXIV.0803.1988`.
URL: `https://arxiv.org/abs/0803.1988`.

[92] N. Arkani-Hamed et al.
"Local integrals for planar scattering amplitudes".
In: *Journal of High Energy Physics* 2012.6 (2012).
DOI: `10.1007/jhep06(2012)125`.
URL: `https://doi.org/10.1007%2Fjhep06%282012%29125`.

[93] Johannes Henn et al.
"Constructing d-log integrands and computing master integrals for three-loop
four-particle scattering".
In: *Journal of High Energy Physics* 2020.4 (Apr. 2020).
DOI: `10.1007/jhep04(2020)167`.
URL: `https://doi.org/10.1007%2Fjhep04%282020%29167`.

[94] Ekta Chaubey and Stefan Weinzierl.
"Two-loop master integrals for the mixed QCD-electroweak corrections for $H \to$
$b\bar{b}$ through a $Ht\bar{t}$ -coupling".
In: *Journal of High Energy Physics* 2019.5 (2019).
DOI: `10.1007/jhep05(2019)185`.
URL: `https://doi.org/10.1007%2Fjhep05%282019%29185`.

[95] Luise Adams, Ekta Chaubey, and Stefan Weinzierl.
"Analytic results for the planar double box integral relevant to top-pair produc-
tion with a closed top loop".
In: *Journal of High Energy Physics* 2018.10 (2018).
DOI: `10.1007/jhep10(2018)206`.
URL: `https://doi.org/10.1007%2Fjhep10%282018%29206`.

[96] Tiziano Peraro.
"Scattering amplitudes over finite fields and multivariate functional reconstruc-
tion".
In: *Journal of High Energy Physics* 2016.12 (2016).
DOI: `10.1007/jhep12(2016)030`.
URL: `https://doi.org/10.1007%2Fjhep12%282016%29030`.

[97] Tiziano Peraro.
"FiniteFlow: multivariate functional reconstruction using finite fields and dataflow
graphs".

In: *Journal of High Energy Physics* 2019.7 (2019).
DOI: 10.1007/jhep07(2019)031.
URL: https://doi.org/10.1007%2Fjhep07%282019%29031.

[98] Claude Duhr and Falko Dulat.
"PolyLogTools — polylogs for the masses".
In: *Journal of High Energy Physics* 2019.8 (2019).
DOI: 10.1007/jhep08(2019)135.
URL: https://doi.org/10.1007%2Fjhep08%282019%29135.

[99] Christian W. Bauer, Alexander Frink, and Richard Kreckel.
"Introduction to the GiNaC framework for symbolic computation within the
C++ programming language".
In: *J. Symb. Comput.* 33 (2002), pp. 1–12.
DOI: 10.1006/jsco.2001.0494.
arXiv: cs/0004015.

[100] Jens Vollinga and Stefan Weinzierl.
"Numerical evaluation of multiple polylogarithms".
In: *Computer Physics Communications* 167.3 (2005), pp. 177–194.
DOI: 10.1016/j.cpc.2004.12.009.
URL: https://doi.org/10.1016%2Fj.cpc.2004.12.009.

[101] Xiao Liu, Yan-Qing Ma, and Chen-Yu Wang.
"A systematic and efficient method to compute multi-loop master integrals".
In: *Physics Letters B* 779 (2018), pp. 353–357.
DOI: 10.1016/j.physletb.2018.02.026.
URL: https://doi.org/10.1016%2Fj.physletb.2018.02.026.

[102] Zhi-Feng Liu and Yan-Qing Ma.
"Determining Feynman Integrals with Only Input from Linear Algebra".
In: *Physical Review Letters* 129.22 (2022).
DOI: 10.1103/physrevlett.129.222001.
URL: https://doi.org/10.1103%2Fphysrevlett.129.222001.

[103] Xiao Liu and Yan-Qing Ma.
"AMFlow: A Mathematica package for Feynman integrals computation via aux-
iliary mass flow".
In: *Computer Physics Communications* 283 (2023), p. 108565.
DOI: 10.1016/j.cpc.2022.108565.
URL: https://doi.org/10.1016%2Fj.cpc.2022.108565.

[104] Christian Bogner and Stefan Weinzierl.
"Resolution of singularities for multi-loop integrals".
In: *Computer Physics Communications* 178.8 (2008), pp. 596–610.
DOI: 10.1016/j.cpc.2007.11.012.
URL: https://doi.org/10.1016%2Fj.cpc.2007.11.012.

[105] T. Binoth and G. Heinrich.
"An automatized algorithm to compute infrared divergent multi-loop integrals".
In: *Nuclear Physics B* 585.3 (2000), pp. 741–759.
DOI: 10.1016/s0550-3213(00)00429-6.

URL: https://doi.org/10.1016%2Fs0550-3213%2800%2900429-6.

[106] CERN.
CERN Yellow Reports: Monographs, Vol 2 (2017): Handbook of LHC Higgs cross sections: 4. Deciphering the nature of the Higgs sector. en.
2017.
DOI: 10.23731/CYRM-2017-002.
URL: https://e-publishing.cern.ch/index.php/CYRM/issue/view/32.

[107] R. L. Workman et al.
"Review of Particle Physics".
In: *PTEP* 2022 (2022), p. 083C01.
DOI: 10.1093/ptep/ptac097.

[108] ATLAS Collaboration.
In: *Physics Letters B* (2018).
DOI: 10.1016/j.physletb.2018.09.013.
URL: https://doi.org/10.1016%2Fj.physletb.2018.09.013.

[109] CMS Collaboration.
"Observation of Higgs Boson Decay to Bottom Quarks".
In: *Physical Review Letters* 121.12 (2018).
DOI: 10.1103/physrevlett.121.121801.
URL: https://doi.org/10.1103%2Fphysrevlett.121.121801.

[110] A. Abada et al.
"FCC Physics Opportunities: Future Circular Collider Conceptual Design Report Volume 1".
In: *Eur. Phys. J. C* 79.6 (2019), p. 474.
DOI: 10.1140/epjc/s10052-019-6904-3.

[111] K.G. Chetyrkin and M. Steinhauser.
"Complete QCD corrections of order $O(\alpha_s 3)$ to the hadronic Higgs decay".
In: *Physics Letters B* 408.1-4 (1997), pp. 320–324.
ISSN: 0370-2693.
DOI: 10.1016/s0370-2693(97)00779-x.
URL: http://dx.doi.org/10.1016/S0370-2693(97)00779-X.

[112] Mathias Butenschön, Frank Fugel, and Bernd A. Kniehl.
"two-loop electroweak correction to Higgs-boson decay to bottom quarks".
In: *Nuclear Physics B* 772.1-2 (2007), pp. 25–48.
ISSN: 0550-3213.
DOI: 10.1016/j.nuclphysb.2007.02.027.
URL: http://dx.doi.org/10.1016/j.nuclphysb.2007.02.027.

[113] A. Sirlin.
"Radiative corrections in the $SU(2)_L \times U(1)$ theory: A simple renormalization framework".
In: *Phys. Rev. D* 22 (4 1980), pp. 971–981.
DOI: 10.1103/PhysRevD.22.971.
URL: https://link.aps.org/doi/10.1103/PhysRevD.22.971.

[114] A. L. Kataev.

"Corrections of order $\mathcal{O}(\bar{\alpha}\bar{\alpha}_S)$ and $\mathcal{O}(\bar{\alpha}^2)$ to the $b\bar{b}$ -decay width of the neutral Higgs boson".
In: *Journal of Experimental and Theoretical Physics Letters* 66.5 (1997), pp. 327–330.
DOI: 10.1134/1.567516.
URL: https://doi.org/10.1134%2F1.567516.

[115] Paulo Nogueira.
"Automatic Feynman graph generation".
In: *J. Comput. Phys.* 105 (1993), pp. 279–289.
DOI: 10.1006/jcph.1993.1074.

[116] Thomas Hahn.
"Generating Feynman diagrams and amplitudes with FeynArts 3".
In: *Computer Physics Communications* 140.3 (2001), pp. 418–431.
ISSN: 0010-4655.
DOI: https://doi.org/10.1016/S0010-4655(01)00290-9.
URL: https://www.sciencedirect.com/science/article/pii/S0010465501002909.

[117] Michael S. Chanowitz, M. Furman, and I. Hinchliffe.
"The Axial Current in Dimensional Regularization".
In: *Nucl. Phys.* B159 (1979), pp. 225–243.
DOI: 10.1016/0550-3213(79)90333-X.

[118] Vladyslav Shtabovenko, Rolf Mertig, and Frederik Orellana.
"FeynCalc 9.3: New features and improvements".
In: *Computer Physics Communications* 256 (Nov. 2020), p. 107478.
DOI: 10.1016/j.cpc.2020.107478.
URL: https://doi.org/10.1016%2Fj.cpc.2020.107478.

[119] J. A. M. Vermaseren.
New features of FORM.
2000.
DOI: 10.48550/ARXIV.MATH-PH/0010025.
URL: https://arxiv.org/abs/math-ph/0010025.

[120] *Feynman diagram maker.*
https://www.aidansean.com/feynman/.
Accessed: 12.12.2022.